

MICROWAVE TRANSISTOR AMPLIFIERS

Analysis and Design

Guillermo Gonzalez, Ph.D.

*Professor of Electrical and Computer Engineering
University of Miami*

Library of Congress Cataloging in Publication Data

GONZALEZ, GUILLERMO, 1944-

Microwave transistor amplifiers.

Bibliography: p.

Includes index.

1. Transistor amplifiers. 2. Microwave amplifiers.

I. Title.

TK7871.2.G59 1984 621.381'33 84-2074

ISBN 0-13-581646-7

Editorial/production supervision

and interior design: *Theresa A. Soler*

Manufacturing buyer: *Anthony Caruso*

© 1984 by Prentice-Hall, Inc., Englewood Cliffs, New Jersey 07632

All rights reserved. No part of this book may be reproduced, in any form or by any means, without permission in writing from the publisher.

Printed in the United States of America

10 9 8 7 6 5 4 3

ISBN 0-13-581646-7

Prentice-Hall International, Inc., *London*

Prentice-Hall of Australia Pty. Limited, *Sydney*

Editora Prentice-Hall do Brasil, Ltda., *Rio de Janeiro*

Prentice-Hall Canada Inc., *Toronto*

Prentice-Hall of India Private Limited, *New Delhi*

Prentice-Hall of Japan, Inc., *Tokyo*

Prentice-Hall of Southeast Asia Pte. Ltd., *Singapore*

Whitehall Books Limited, *Wellington, New Zealand*

CONTENTS

PREFACE

vii

— 1 —	REPRESENTATIONS OF TWO-PORT NETWORKS	1
1.1	Introduction	1
1.2	The Impedance, Admittance, Hybrid, and <i>ABCD</i> Matrices	1
1.3	Traveling Waves and Transmission-Line Concepts	4
1.4	The Scattering Matrix and the Chain Scattering Matrix	8
1.5	Shifting Reference Planes	12
1.6	Properties of Scattering Parameters	13
1.7	Generalized Scattering Parameters	19
1.8	Two-Port Network Parameters Conversions	22
1.9	Scattering Parameters of Transistors	23
1.10	Characteristics of Microwave Transistors	31

— 2 —	MATCHING NETWORKS AND SIGNAL FLOW GRAPHS	42
2.1	Introduction	42
2.2	The Smith Chart	43
2.3	The Normalized Impedance and Admittance Smith Chart	51

Appendix

— A —	COMPUTER AIDED DESIGN: COMPACT AND SUPER-COMPACT	217
--------------	---	------------

Appendix

— B —	UM-MAAD	230
--------------	----------------	------------

INDEX	241
--------------	------------

REPRESENTATIONS OF TWO-PORT NETWORKS

1.1 INTRODUCTION

In order to characterize the behavior of a two-port network, measured data of both its transfer and impedance functions must be obtained. At low frequencies, the z , y , h , or $ABCD$ parameters are examples of network functions used in the description of two-port networks. These parameters cannot be measured accurately at higher frequencies because the required short- and open-circuit tests are difficult to achieve over a broadband range of microwave frequencies.

A set of parameters that is very useful in the microwave range are the *scattering parameters* (S parameters). These parameters are defined in terms of traveling waves and completely characterize the behavior of two-port networks at microwave frequencies.

In the 1970s the popularity of S parameters increased because of the appearance of new network analyzers, which performed S -parameter measurements with ease. The S parameters are simple to use in analysis, and flow graph theory is directly applicable. Although the principal use of S parameters in this text is in the characterization of two-port networks, they can also be used in the characterization of n -port networks.

1.2 THE IMPEDANCE, ADMITTANCE, HYBRID, AND $ABCD$ MATRICES

At low frequencies the two-port network shown in Fig. 1.2.1 can be represented in several ways. The most common representations are the impedance

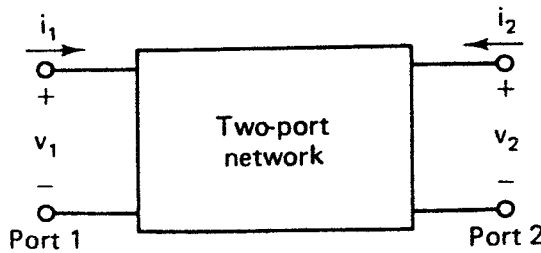


Figure 1.2.1 Two-port network representation.

matrix (z parameters), the admittance matrix (y parameters), the hybrid matrix (h parameters), and the chain or $ABCD$ matrix (chain or $ABCD$ parameters). These parameters are defined as follows:

z Parameters:

$$v_1 = z_{11}i_1 + z_{12}i_2$$

$$v_2 = z_{21}i_1 + z_{22}i_2$$

or in matrix form

$$\begin{bmatrix} v_1 \\ v_2 \end{bmatrix} = \begin{bmatrix} z_{11} & z_{12} \\ z_{21} & z_{22} \end{bmatrix} \begin{bmatrix} i_1 \\ i_2 \end{bmatrix}$$

y Parameters:

$$\begin{bmatrix} i_1 \\ i_2 \end{bmatrix} = \begin{bmatrix} y_{11} & y_{12} \\ y_{21} & y_{22} \end{bmatrix} \begin{bmatrix} v_1 \\ v_2 \end{bmatrix}$$

h Parameters:

$$\begin{bmatrix} v_1 \\ i_2 \end{bmatrix} = \begin{bmatrix} h_{11} & h_{12} \\ h_{21} & h_{22} \end{bmatrix} \begin{bmatrix} i_1 \\ v_2 \end{bmatrix}$$

$ABCD$ Parameters:

$$\begin{bmatrix} v_1 \\ i_1 \end{bmatrix} = \begin{bmatrix} A & B \\ C & D \end{bmatrix} \begin{bmatrix} v_2 \\ -i_2 \end{bmatrix}$$

The previous two-port representations are very useful at low frequencies because the parameters are readily measured using short- and open-circuit tests at the terminals of the two-port network. For example,

$$z_{11} = \left. \frac{v_1}{i_1} \right|_{i_2=0}$$

is measured with an ac open circuit at port 2 (i.e., $i_2 = 0$).

The z , y , and $ABCD$ parameters are also useful in the computer analysis of circuits. When two-port networks are connected in series, as shown in Fig. 1.2.2, we can find the overall z parameters by adding the individual z parame-

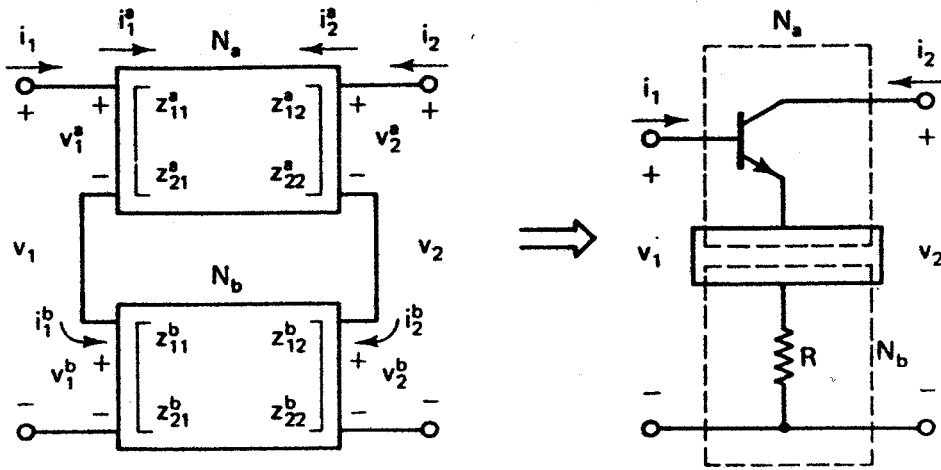


Figure 1.2.2 Series connection using z parameters and a typical application.

ters, namely

$$\begin{bmatrix} v_1 \\ v_2 \end{bmatrix} = \begin{bmatrix} v_1^a + v_1^b \\ v_2^a + v_2^b \end{bmatrix} = \begin{bmatrix} z_{11}^a + z_{11}^b & z_{12}^a + z_{12}^b \\ z_{21}^a + z_{21}^b & z_{22}^a + z_{22}^b \end{bmatrix} \begin{bmatrix} i_1 \\ i_2 \end{bmatrix}$$

When two two-port networks are connected in shunt, as shown in Fig. 1.2.3, we can find the overall y parameters by adding the individual y parameters, namely

$$\begin{bmatrix} i_1 \\ i_2 \end{bmatrix} = \begin{bmatrix} i_1^a + i_1^b \\ i_2^a + i_2^b \end{bmatrix} = \begin{bmatrix} y_{11}^a + y_{11}^b & y_{12}^a + y_{12}^b \\ y_{21}^a + y_{21}^b & y_{22}^a + y_{22}^b \end{bmatrix} \begin{bmatrix} v_1 \\ v_2 \end{bmatrix}$$

When cascading two-port networks the chain or $ABCD$ matrix can be used as follows (see Fig. 1.2.4):

$$\begin{bmatrix} v_1 \\ i_1 \end{bmatrix} = \begin{bmatrix} v_1^a \\ i_1^a \end{bmatrix} = \begin{bmatrix} A^a & B^a \\ C^a & D^a \end{bmatrix} \begin{bmatrix} v_2^a \\ -i_2^a \end{bmatrix} = \begin{bmatrix} A^a & B^a \\ C^a & D^a \end{bmatrix} \begin{bmatrix} A^b & B^b \\ C^b & D^b \end{bmatrix} \begin{bmatrix} v_2^b \\ -i_2^b \end{bmatrix} \quad (1.2.1)$$

because $v_2^a = v_1^b$ and $-i_2^a = i_1^b$. The relation (1.2.1) shows that the overall $ABCD$ matrix is equal to the product (i.e., matrix multiplication) of the individual $ABCD$ matrices.

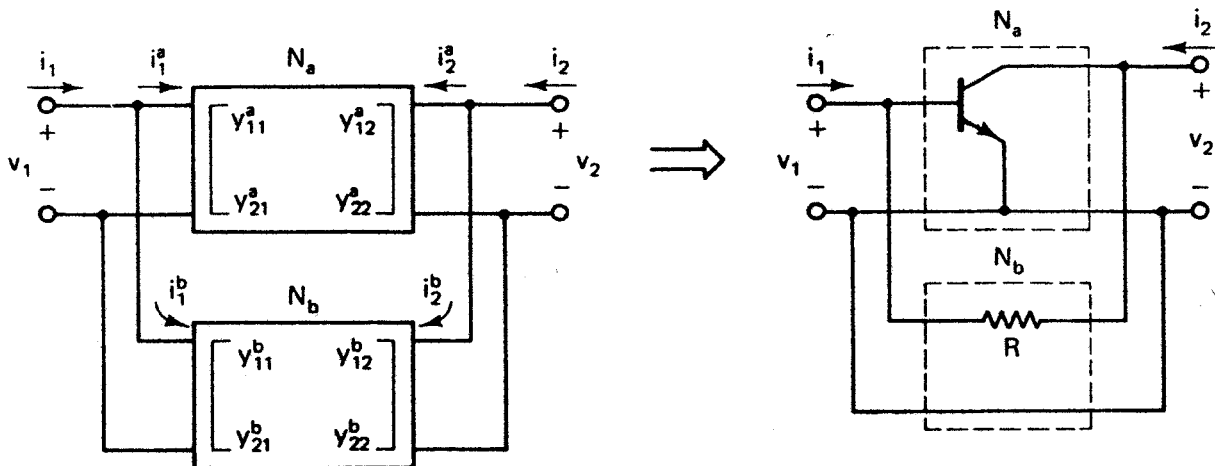


Figure 1.2.3 Shunt connection using y parameters and a typical application.

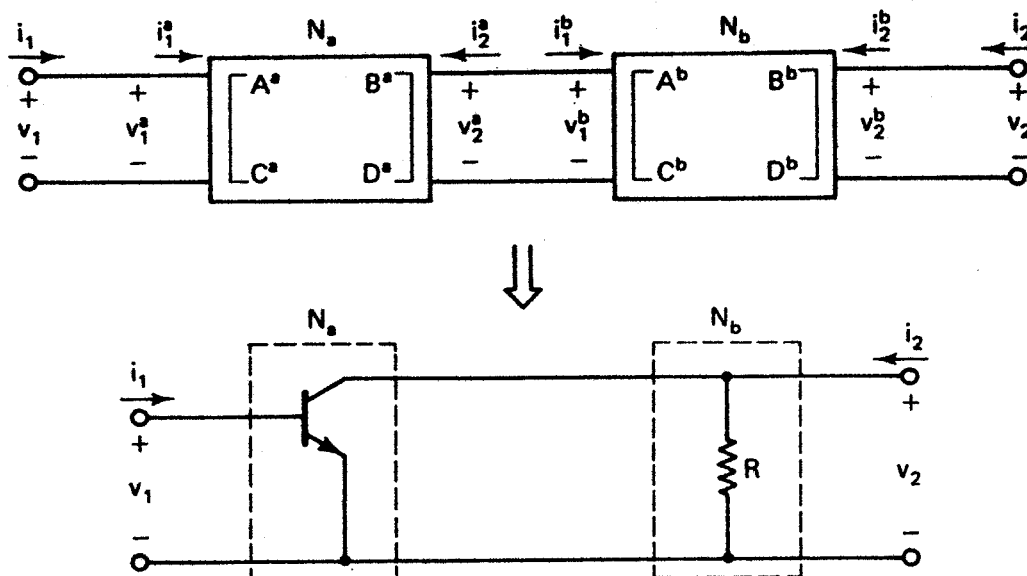


Figure 1.2.4 Cascade connection using $ABCD$ parameters and a typical application.

At microwave frequencies the z , y , h , or $ABCD$ parameters are very difficult (if not impossible) to measure. The reason is that short and open circuits to ac signals are difficult to implement over a broadband, at microwave frequencies. Also, an active two-port (e.g., a microwave transistor) might oscillate under short- or open-circuit conditions. Therefore, a new representation of the two-port network at microwave frequencies is needed. The appropriate representation is called the *scattering matrix* and the scattering parameters are defined in terms of traveling waves.

1.3 TRAVELING WAVES AND TRANSMISSION-LINE CONCEPTS

The voltage and current along a transmission line are functions of position and time. For sinusoidal excitation, the instantaneous voltage and current can be expressed in the form

$$v(x, t) = \text{Re} [V(x)e^{j\omega t}]$$

and

$$i(x, t) = \text{Re} [I(x)e^{j\omega t}]$$

where Re means the real part. The complex quantities $V(x)$ and $I(x)$ are phasors and express the variations of the voltage and current as a function of position along the transmission line. The polar forms of a complex number $re^{j\theta}$ and $r\angle\theta$ are both used in this book.

The differential equations satisfied by the phasors $V(x)$ and $I(x)$ along a

uniform transmission line are (see Problem 1.1)

$$\frac{d^2 V(x)}{dx^2} - \gamma^2 V(x) = 0 \quad (1.3.1)$$

and

$$\frac{d^2 I(x)}{dx^2} - \gamma^2 I(x) = 0 \quad (1.3.2)$$

where the complex propagation constant γ is given by

$$\gamma = \alpha + j\beta = \sqrt{(R + j\omega L)(G + j\omega C)}$$

The attenuation constant α is given in nepers per meter and the propagation constant β in radians per meter. The parameters R , G , L , and C are the resistance, conductance, inductance, and capacitance per unit length of the transmission line. They are assumed to be constant along the transmission line (i.e., the transmission line is uniform).

The general solutions of (1.3.1) and (1.3.2) are

$$V(x) = Ae^{-\gamma x} + Be^{\gamma x} \quad (1.3.3)$$

and

$$I(x) = \frac{A}{Z_o} e^{-\gamma x} - \frac{B}{Z_o} e^{\gamma x} \quad (1.3.4)$$

where

$$Z_o = \sqrt{\frac{R + j\omega L}{G + j\omega C}}$$

is known as the *complex characteristic impedance* of the transmission line. The constants A and B are, in general, complex quantities.

Equations (1.3.3) and (1.3.4) represent the voltage and current along the transmission line as a pair of waves traveling in opposite directions, with phase velocity $v_p = \omega/\beta$ and decreasing in amplitude according to $e^{-\alpha x}$ or $e^{\alpha x}$. The wave $e^{-\gamma x} = e^{-\alpha x}e^{-j\beta x}$ is called the *incident wave* (outgoing wave) and the wave $e^{\gamma x} = e^{\alpha x}e^{j\beta x}$ is called the *reflected wave* (incoming wave). The quantity βx is known as the *electrical length* of the line.

A transmission line of characteristic impedance Z_o terminated in a load Z_L is shown in Fig. 1.3.1. The reflection coefficient $\Gamma(x)$ is defined as

$$\Gamma(x) = \frac{Be^{\gamma x}}{Ae^{-\gamma x}} = \frac{B}{A} e^{2\gamma x} = \Gamma_0 e^{2\gamma x} \quad (1.3.5)$$

where Γ_0 is the load reflection coefficient, namely

$$\Gamma_0 = \Gamma(0) = \frac{B}{A}$$

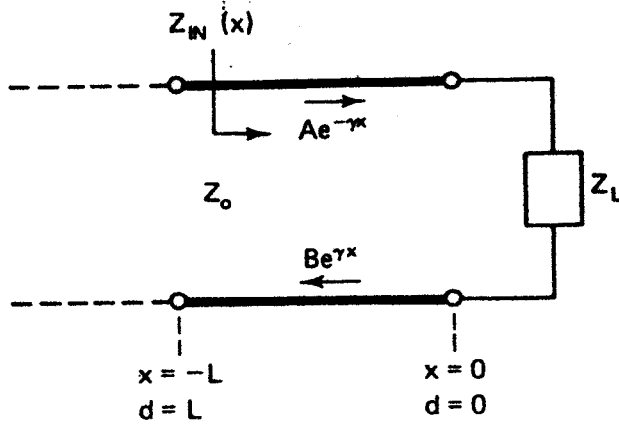


Figure 1.3.1 Transmission line terminated in the load Z_L .

Therefore, the reflected wave can be written as $A\Gamma_0 e^{\gamma x}$ and (1.3.3) and (1.3.4) can be expressed in the form

$$V(x) = A(e^{-\gamma x} + \Gamma_0 e^{\gamma x}) \quad (1.3.6)$$

$$I(x) = \frac{A}{Z_o} (e^{-\gamma x} - \Gamma_0 e^{\gamma x})$$

The input impedance of the transmission line at any position x is defined as

$$Z_{IN}(x) = \frac{V(x)}{I(x)} = Z_o \frac{e^{-\gamma x} + \Gamma_0 e^{\gamma x}}{e^{-\gamma x} - \Gamma_0 e^{\gamma x}} \quad (1.3.7)$$

where the constant Γ_0 can be evaluated using the condition

$$Z_{IN}(0) = Z_L$$

Then

$$Z_L = Z_o \frac{1 + \Gamma_0}{1 - \Gamma_0}$$

or

$$\Gamma_0 = \frac{Z_L - Z_o}{Z_L + Z_o} \quad (1.3.8)$$

Equation (1.3.8) shows that $\Gamma_0 = 0$ when $Z_L = Z_o$. That is, there is no reflection in a properly terminated or matched (i.e., $Z_L = Z_o$) transmission line. Substituting (1.3.8) into (1.3.7) and letting $x = -d$ gives

$$Z_{IN}(d) = Z_o \frac{Z_L + Z_o \tanh \gamma d}{Z_o + Z_L \tanh \gamma d} \quad (1.3.9)$$

The change $x = -d$ is normally done in transmission-line problems in order to measure positive distances as one moves from the load toward the source.

At microwave frequencies R and G are usually negligible and the trans-

mission line is said to be lossless. In a lossless transmission line

$$\alpha = 0$$

$$\gamma = j\beta$$

$$\beta = \omega\sqrt{LC}$$

$$v_p = \frac{1}{\sqrt{LC}}$$

$$\lambda = \frac{v_p}{f}$$

$$V(x) = Ae^{-j\beta x} + Be^{j\beta x}$$

$$I(x) = \frac{A}{Z_o} e^{-j\beta x} - \frac{B}{Z_o} e^{j\beta x}$$

and

$$Z_o = \sqrt{\frac{L}{C}}$$

Observe that Z_o is real. Also, from (1.3.9) the input impedance in a lossless transmission line can be expressed in the form

$$Z_{IN}(d) = Z_o \frac{Z_L + jZ_o \tan \beta d}{Z_o + jZ_L \tan \beta d} \quad (1.3.10)$$

Unless otherwise specified, all transmission lines in this book are assumed to be lossless and uniform.

The two waves traveling in opposite directions in a transmission line produce a standing-wave pattern. From (1.3.6), the maximum value of the voltage along the line has the value

$$|V(x)|_{\max} = |A|(1 + |\Gamma_o|)$$

and the minimum value of the voltage is

$$|V(x)|_{\min} = |A|(1 - |\Gamma_o|)$$

These values are used to define the *voltage standing-wave ratio* (VSWR), namely

$$\text{VSWR} = \frac{|V(x)|_{\max}}{|V(x)|_{\min}} = \frac{1 + |\Gamma_o|}{1 - |\Gamma_o|} \quad (1.3.11)$$

or

$$|\Gamma_o| = \frac{\text{VSWR} - 1}{\text{VSWR} + 1}$$

In a properly terminated or matched transmission line we obtain from (1.3.8), (1.3.10), and (1.3.11) that $\Gamma_0 = 0$, $Z_{IN}(d) = Z_o$, and $VSWR = 1$.

In a shorted transmission line ($Z_L = 0$) it follows that $\Gamma_0 = -1$, $VSWR = \infty$, and the input impedance, called $Z_{sc}(d)$, is given by

$$Z_{sc}(d) = jZ_o \tan \beta d$$

In an open-circuited transmission line ($Z_L = \infty$) it follows that $\Gamma_0 = 1$, $VSWR = \infty$, and the input impedance, called $Z_{oc}(d)$, is given by

$$Z_{oc}(d) = -jZ_o \cot \beta d$$

Another important case is the quarter-wave transmission line (also known as the quarter-wave transformer). With $d = \lambda/4$, (1.3.10) gives

$$Z_{IN}\left(\frac{\lambda}{4}\right) = \frac{Z_o^2}{Z_L} \quad (1.3.12)$$

Equation (1.3.12) shows that in order to transform a real impedance Z_L to another real impedance given by $Z_{IN}(\lambda/4)$, a line with characteristic impedance

$$Z_o = \sqrt{Z_{IN}\left(\frac{\lambda}{4}\right)Z_L}$$

can be used.

1.4 THE SCATTERING MATRIX AND THE CHAIN SCATTERING MATRIX

Introducing the notation

$$V^+(x) = Ae^{-\gamma x}$$

and

$$V^-(x) = Be^{\gamma x}$$

where $\gamma = j\beta$ for a lossless transmission line, we can write (1.3.3) and (1.3.4) in the form

$$V(x) = V^+(x) + V^-(x) \quad (1.4.1)$$

and

$$I(x) = I^+(x) - I^-(x) = \frac{V^+(x)}{Z_o} - \frac{V^-(x)}{Z_o} \quad (1.4.2)$$

Also, the reflection coefficient between the incident and reflected wave can be

written as

$$\Gamma(x) = \frac{V^-(x)}{V^+(x)} \quad (1.4.3)$$

where $\Gamma_0 = \Gamma(0) = V^-(0)/V^+(0)$ is the load reflection coefficient.

Introducing the normalized notation

$$v(x) = \frac{V(x)}{\sqrt{Z_0}}$$

$$i(x) = \sqrt{Z_0} I(x)$$

$$a(x) = \frac{V^+(x)}{\sqrt{Z_0}}$$

and

$$b(x) = \frac{V^-(x)}{\sqrt{Z_0}}$$

we can write (1.4.1), (1.4.2), and (1.4.3) in the form

$$v(x) = a(x) + b(x)$$

$$i(x) = a(x) - b(x)$$

and

$$b(x) = \Gamma(x)a(x) \quad (1.4.4)$$

If instead of a one-port transmission line we have the two-port network shown in Fig. 1.4.1 with incident wave a_1 and reflected wave b_1 at port 1, and incident wave a_2 and reflected wave b_2 at port 2, we can generalize (1.4.4) and write

$$b_1 = S_{11}a_1 + S_{12}a_2$$

and

$$b_2 = S_{21}a_1 + S_{22}a_2$$

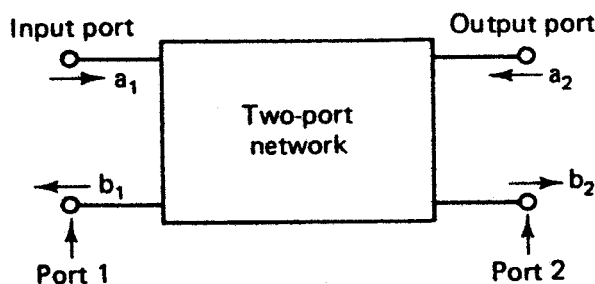


Figure 1.4.1 Incident and reflected waves in a two-port network.

or in matrix form,

$$\begin{bmatrix} b_1 \\ b_2 \end{bmatrix} = \begin{bmatrix} S_{11} & S_{12} \\ S_{21} & S_{22} \end{bmatrix} \begin{bmatrix} a_1 \\ a_2 \end{bmatrix} \quad (1.4.5)$$

Observe that a_1 , a_2 , b_1 , and b_2 are values of the incident and reflected waves at the specific locations denoted as port 1 and port 2 in Fig. 1.4.1. The term $S_{11}a_1$ represents the contribution to the reflected wave b_1 due to the incident wave a_1 at port 1. Similarly, $S_{12}a_2$ represents the contribution to the reflected wave b_1 due to the incident wave a_2 at port 2, and so on. The parameters S_{11} , S_{12} , S_{21} , and S_{22} , which represent reflection and transmission coefficients, are called the *scattering parameters* of the two-port network. The matrix

$$[S] = \begin{bmatrix} S_{11} & S_{12} \\ S_{21} & S_{22} \end{bmatrix}$$

is called the *scattering matrix*.

The S parameters are seen to represent reflection or transmission coefficients. From (1.4.5), they are defined as follows:

$$\begin{aligned} S_{11} &= \left. \frac{b_1}{a_1} \right|_{a_2=0} && \text{(input reflection coefficient with} \\ &&& \text{output properly terminated)} \\ S_{21} &= \left. \frac{b_2}{a_1} \right|_{a_2=0} && \text{(forward transmission coefficient} \\ &&& \text{with output properly terminated)} \\ S_{22} &= \left. \frac{b_2}{a_2} \right|_{a_1=0} && \text{(output reflection coefficient} \\ &&& \text{with input properly terminated)} \\ S_{12} &= \left. \frac{b_1}{a_2} \right|_{a_1=0} && \text{(reverse transmission coefficient} \\ &&& \text{with input properly terminated)} \end{aligned}$$

The advantage of using S parameters is clear from their definitions. They are measured using a matched termination (i.e., making $a_1 = 0$ or $a_2 = 0$). For example, to measure S_{11} we measure the ratio b_1/a_1 at the input port with the output port properly terminated, that is, with $a_2 = 0$. Terminating the output port with an impedance equal to the characteristic impedance of the transmission line produces $a_2 = 0$, because a traveling wave incident on the load will be totally absorbed and no energy will be returned to the output port. This situation is illustrated in Fig. 1.4.2.

Observe that the network output impedance Z_{OUT} does not have to be matched to Z_{o2} . In fact, it is rare that $Z_{OUT} = Z_{o2}$, but with $Z_L = Z_{o2}$ the condition $a_2 = 0$ is satisfied. Similar considerations apply to measurements at the input port. Also, the characteristic impedances of the transmission lines are usually identical (i.e., $Z_{o1} = Z_{o2}$).

Using matched resistive terminations to measure the S parameters of a transistor has the advantage that the transistor does not oscillate. In contrast, if we were to use a short- or open-circuit test, the transistor could become unstable.

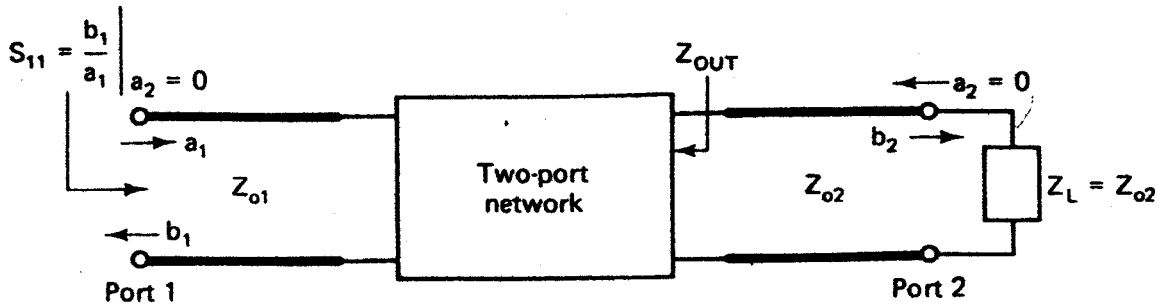


Figure 1.4.2 Procedure for measuring S_{11} . The characteristic impedances of the transmission lines are Z_{01} and Z_{02} .

The *chain scattering parameters*, also called the *scattering transfer parameters* or T parameters, are used when cascading networks. They are defined in such a way that the input waves a_1 and b_1 in Fig. 1.4.1 are the dependent variables and the output waves a_2 and b_2 are the independent variables. That is,

$$\begin{bmatrix} a_1 \\ b_1 \end{bmatrix} = \begin{bmatrix} T_{11} & T_{12} \\ T_{21} & T_{22} \end{bmatrix} \begin{bmatrix} b_2 \\ a_2 \end{bmatrix} \quad (1.4.6)$$

The relationship between the S and T parameters can be developed from (1.4.5) and (1.4.6), namely

$$\begin{bmatrix} T_{11} & T_{12} \\ T_{21} & T_{22} \end{bmatrix} = \begin{bmatrix} \frac{1}{S_{21}} & -\frac{S_{22}}{S_{21}} \\ \frac{S_{11}}{S_{21}} & S_{12} - \frac{S_{11}S_{22}}{S_{21}} \end{bmatrix} \quad (1.4.7)$$

and

$$\begin{bmatrix} S_{11} & S_{12} \\ S_{21} & S_{22} \end{bmatrix} = \begin{bmatrix} \frac{T_{21}}{T_{11}} & T_{22} - \frac{T_{21}T_{12}}{T_{11}} \\ \frac{1}{T_{11}} & -\frac{T_{12}}{T_{11}} \end{bmatrix} \quad (1.4.8)$$

The T parameters are useful in the analysis of cascade connections of two-port networks. Figure 1.4.3 shows that the output waves of the first network are identical to the input waves of the second network, namely

$$\begin{bmatrix} b_2 \\ a_2 \end{bmatrix} = \begin{bmatrix} a'_1 \\ b'_1 \end{bmatrix}$$

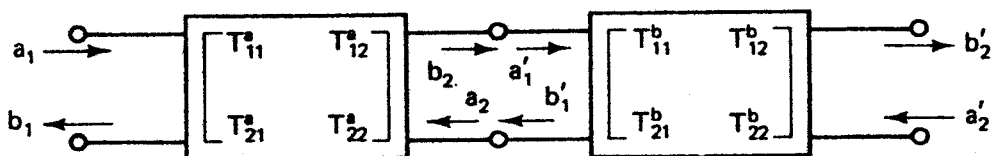


Figure 1.4.3 Cascade connection of two-port networks.

Therefore, the chain scattering matrix of the cascade connection can be written in terms of the individual chain scattering matrix as follows:

$$\begin{bmatrix} a_1 \\ b_1 \end{bmatrix} = \begin{bmatrix} T_{11}^a & T_{12}^a \\ T_{21}^a & T_{22}^a \end{bmatrix} \begin{bmatrix} b_2 \\ a_2 \end{bmatrix}$$

$$\begin{bmatrix} a'_1 \\ b'_1 \end{bmatrix} = \begin{bmatrix} T_{11}^b & T_{12}^b \\ T_{21}^b & T_{22}^b \end{bmatrix} \begin{bmatrix} b'_2 \\ a'_2 \end{bmatrix}$$

and

$$\begin{bmatrix} a_1 \\ b_1 \end{bmatrix} = \begin{bmatrix} T_{11}^a & T_{12}^a \\ T_{21}^a & T_{22}^a \end{bmatrix} \begin{bmatrix} T_{11}^b & T_{12}^b \\ T_{21}^b & T_{22}^b \end{bmatrix} \begin{bmatrix} b'_2 \\ a'_2 \end{bmatrix} \quad (1.4.9)$$

Equation (1.4.9) is useful in the analysis and design of microwave amplifiers using computer-aided design techniques.

1.5 SHIFTING REFERENCE PLANES

In practice we often need to attach transmission lines to the two-port network. Since the S parameters are measured using traveling waves, we need to specify the positions where the measurements are made. The positions are called *reference planes*. For example, in Fig. 1.5.1 we can measure the S parameters at the reference planes located at port 1' and port 2' and relate them to the S parameters at port 1 and port 2 of the two-port network.

At the reference planes at port 1 and port 2 in Fig. 1.5.1, we write the scattering matrix as

$$\begin{bmatrix} b_1 \\ b_2 \end{bmatrix} = \begin{bmatrix} S_{11} & S_{12} \\ S_{21} & S_{22} \end{bmatrix} \begin{bmatrix} a_1 \\ a_2 \end{bmatrix} \quad (1.5.1)$$

and at port 1' and port 2' as

$$\begin{bmatrix} b'_1 \\ b'_2 \end{bmatrix} = \begin{bmatrix} S'_{11} & S'_{12} \\ S'_{21} & S'_{22} \end{bmatrix} \begin{bmatrix} a'_1 \\ a'_2 \end{bmatrix} \quad (1.5.2)$$

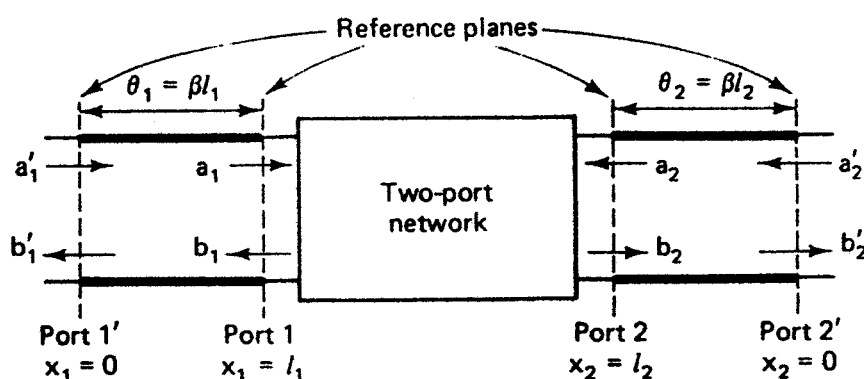


Figure 1.5.1 Model for shifting reference planes.

The angles θ_1 and θ_2 are the electrical lengths of the transmission lines between the primed and unprimed reference planes.

From our knowledge of traveling waves on a lossless transmission line we can write

$$\begin{aligned} b_1 &= b'_1 e^{j\theta_1} \\ a_1 &= a'_1 e^{-j\theta_1} \\ b_2 &= b'_2 e^{j\theta_2} \end{aligned}$$

and

$$a_2 = a'_2 e^{-j\theta_2}$$

where the factor $e^{\pm j\theta}$ accounts for the phase difference of the waves at the different reference planes. Substituting the previous relations into (1.5.1) gives

$$\begin{bmatrix} b'_1 \\ b'_2 \end{bmatrix} = \begin{bmatrix} S_{11} e^{-j2\theta_1} & S_{12} e^{-j(\theta_1 + \theta_2)} \\ S_{21} e^{-j(\theta_1 + \theta_2)} & S_{22} e^{-j2\theta_2} \end{bmatrix} \begin{bmatrix} a'_1 \\ a'_2 \end{bmatrix} \quad (1.5.3)$$

Comparing (1.5.3) with (1.5.2) gives the relations

$$\begin{bmatrix} S'_{11} & S'_{12} \\ S'_{21} & S'_{22} \end{bmatrix} = \begin{bmatrix} S_{11} e^{-j2\theta_1} & S_{12} e^{-j(\theta_1 + \theta_2)} \\ S_{21} e^{-j(\theta_1 + \theta_2)} & S_{22} e^{-j2\theta_2} \end{bmatrix} \quad (1.5.4)$$

and

$$\begin{bmatrix} S_{11} & S_{12} \\ S_{21} & S_{22} \end{bmatrix} = \begin{bmatrix} S'_{11} e^{j2\theta_1} & S'_{12} e^{j(\theta_1 + \theta_2)} \\ S'_{21} e^{j(\theta_1 + \theta_2)} & S'_{22} e^{j2\theta_2} \end{bmatrix} \quad (1.5.5)$$

Equations (1.5.4) and (1.5.5) provide the relationship between S parameters at two sets of reference planes.

1.6 PROPERTIES OF SCATTERING PARAMETERS

Consider the two-port network shown in Fig. 1.6.1, where the transmission lines are assumed to be lossless and the characteristic impedances are *real*. This is the typical situation at microwave frequencies where 50- Ω transmission lines and 50- Ω terminations are commonly used. From (1.4.1) and (1.4.2) the

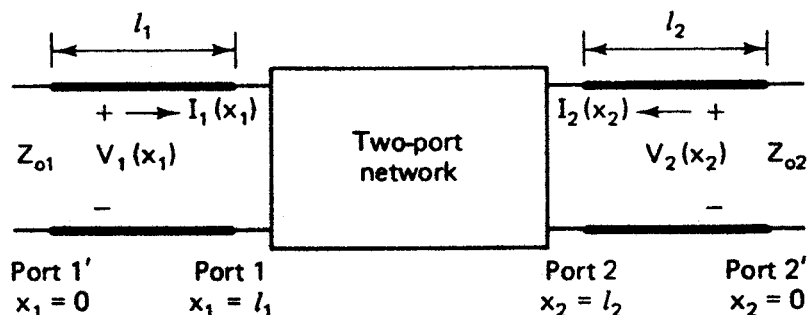


Figure 1.6.1 Two-port network.

voltages and currents in the two-port network can be written as

$$V_i(x_i) = V_i^+(x_i) + V_i^-(x_i) \quad (1.6.1)$$

and

$$I_i(x_i) = I_i^+(x_i) - I_i^-(x_i) = \frac{V_i^+(x_i)}{Z_{oi}} - \frac{V_i^-(x_i)}{Z_{oi}} \quad (1.6.2)$$

where $i = 1$ or 2 , and the voltages and currents are assumed to be scaled to root-mean-square (rms) values.

From (1.6.1) and (1.6.2) we can express the normalized incident and reflected voltages at the i th port in the form

$$a_i(x_i) = \frac{V_i^+(x_i)}{\sqrt{Z_{oi}}} = \sqrt{Z_{oi}} I_i^+(x_i) = \frac{1}{2\sqrt{Z_{oi}}} [V_i(x_i) + Z_{oi} I_i(x_i)] \quad (1.6.3)$$

and

$$b_i(x_i) = \frac{V_i^-(x_i)}{\sqrt{Z_{oi}}} = \sqrt{Z_{oi}} I_i^-(x_i) = \frac{1}{2\sqrt{Z_{oi}}} [V_i(x_i) - Z_{oi} I_i(x_i)] \quad (1.6.4)$$

The average power associated with the incident waves on the primed i th port (i.e., at $x_1 = 0$ and $x_2 = 0$) is

$$P_i^+(0) = \frac{|V_i^+(0)|^2}{Z_{oi}} = a_i(0)a_i^*(0) = |a_i(0)|^2 \quad (1.6.5)$$

and the average reflected power is

$$P_i^-(0) = \frac{|V_i^-(0)|^2}{Z_{oi}} = b_i(0)b_i^*(0) = |b_i(0)|^2 \quad (1.6.6)$$

Since the line is lossless [i.e., $P_i^+(0) = P_i^+(l_i)$ and $P_i^-(0) = P_i^-(l_i)$], (1.6.5) and (1.6.6) show that the quantities $|a_i(x)|^2$ and $|b_i(x)|^2$ represent the power associated with the incident and reflected waves, respectively.

Now consider the network in Fig. 1.6.2, in which port 1' is excited by the generator $E_1 \angle 0^\circ$ V rms having impedance Z_{o1} , and port 2' is terminated in its

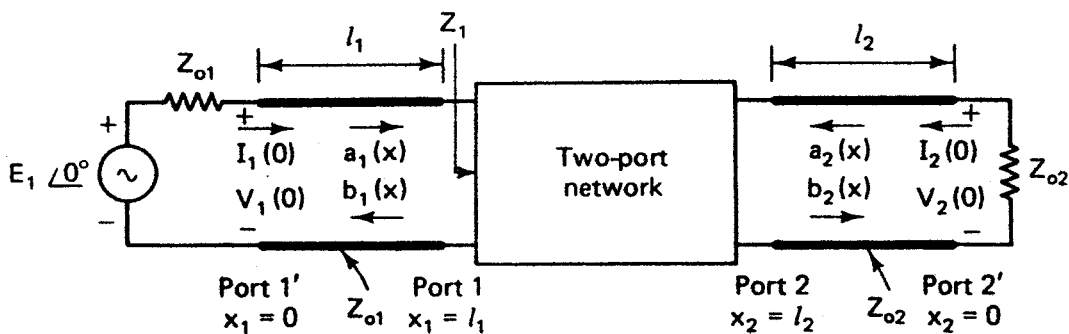


Figure 1.6.2 Two-port network excited by the generator $E_1 \angle 0^\circ$ V rms with internal impedance Z_{o1} and terminated in the impedance Z_{o2} .

normalizing impedance Z_{o2} (i.e., matched impedance). Again, we point out that in practice Z_{o1} and Z_{o2} are pure resistors (usually 50 Ω). Since port 2 is terminated in its normalizing impedance, we can write

$$V_2(0) = -Z_{o2} I_2(0) \quad (1.6.7)$$

and from (1.6.3) it follows that $a_2(0) = 0$.

At $x_1 = 0$, we have

$$V_1(0) = E_1 - Z_{o1} I_1(0) \quad (1.6.8)$$

Substituting (1.6.8) into (1.6.3) gives

$$a_1(0) = \frac{E_1}{2\sqrt{Z_{o1}}}$$

or

$$|a_1(0)|^2 = \frac{|E_1|^2}{4Z_{o1}} \quad (1.6.9)$$

Equation (1.6.9) shows that $|a_1(0)|^2$ represents the power available from the source E_1 with internal resistance Z_{o1} . We call this quantity P_{AVS} . Since the line is lossless ($|a_1(0)|^2 = |a_1(l_1)|^2$) $|a_1(0)|^2$ represents the power available at port 1. The power available from the source E_1 is independent of the input impedance of the two-port network.

Substituting (1.6.8) into (1.6.9) gives

$$\begin{aligned} |a_1(0)|^2 &= \frac{E_1 E_1^*}{4Z_{o1}} = \frac{[V_1(0) + Z_{o1} I_1(0)][V_1(0) + Z_{o1} I_1(0)]^*}{4Z_{o1}} \\ &= \frac{1}{4Z_{o1}} [|V_1(0)|^2 + Z_{o1} I_1(0) V_1^*(0) + Z_{o1} V_1(0) I_1^*(0) \\ &\quad + Z_{o1}^2 |I_1(0)|^2] \end{aligned} \quad (1.6.10)$$

Similarly, from (1.6.4) we obtain

$$|b_1(0)|^2 = \frac{1}{4Z_{o1}} [|V_1(0)|^2 - Z_{o1} I_1(0) V_1^*(0) - Z_{o1} I_1^*(0) V_1(0) + Z_{o1}^2 |I_1(0)|^2] \quad (1.6.11)$$

Subtracting (1.6.11) from (1.6.10) gives

$$\begin{aligned} |a_1(0)|^2 - |b_1(0)|^2 &= \frac{1}{2} [I_1(0) V_1^*(0) + I_1^*(0) V_1(0)] \\ &= \text{Re} [I_1(0) V_1^*(0)] \end{aligned}$$

which represents the power delivered to port 1', or to port 1 since the line is lossless. We call this quantity P_1 [i.e., $P_1 = |a_1(0)|^2 - |b_1(0)|^2$]. Therefore, it follows that

$$|b_1(0)|^2 = P_{AVS} - P_1 \quad (1.6.12)$$

The quantity $|b_1(0)|^2$ represents the reflected power from port 1 or port 1'.

From (1.6.7) and (1.6.4) we obtain

$$b_2(0) = -\sqrt{Z_{o2}} I_2(0)$$

Therefore,

$$|b_2(0)|^2 = Z_{o2} |I_2(0)|^2$$

represents the power delivered to the load Z_{o2} , called P_L [i.e., $P_L = |b_2(0)|^2$].

Equations (1.6.9) and (1.6.12) show that the generator sends the available power $|a_1(0)|^2$ toward the input port 1. This power is independent of the input impedance Z_1 . If the input impedance Z_1 is matched to the transmission line (i.e., if $Z_1 = Z_{o1}$), then the reflected power is zero. However, if $Z_1 \neq Z_{o1}$, part of the incident power $|a_1(0)|^2$ is reflected back to the generator. The reflected power is given by $|b_1(0)|^2$ and the net power delivered to port 1 is $|a_1(0)|^2 - |b_1(0)|^2$.

In order to calculate the S parameters of the two-port network at the unprimed reference plane (i.e., at ports 1 and 2) we replace the network in Fig. 1.6.2 by the equivalent network shown in Fig. 1.6.3. The equivalent network was obtained by finding the Thévenin's equivalent at ports 1 and 2. The Thévenin's voltage is called $E_{1,TH}$.

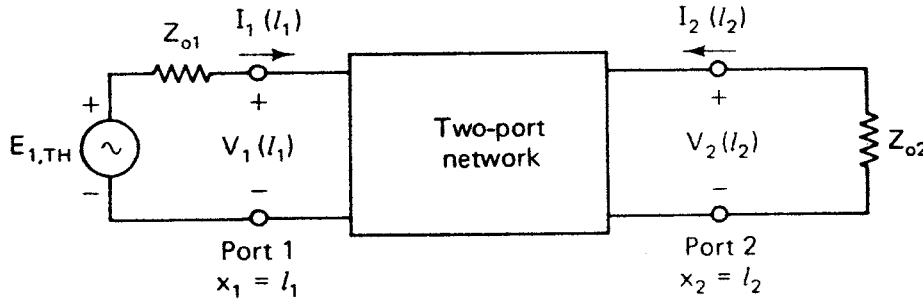


Figure 1.6.3 Two-port network with Thévenin's equivalent at ports 1 and 2.

The scattering parameter S_{11} is given by

$$S_{11} = \left. \frac{b_1(l_1)}{a_1(l_1)} \right|_{a_2(l_2)=0} = \left. \frac{V_1^-(l_1)}{V_1^+(l_1)} \right|_{V_2^-(l_2)=0} \quad (1.6.13)$$

which from (1.3.8) it can be expressed as

$$S_{11} = \frac{Z_1 - Z_{o1}}{Z_1 + Z_{o1}} \quad (1.6.14)$$

Equation (1.6.13) or (1.6.14) shows that S_{11} is the reflection coefficient of port 1 with port 2 terminated in its normalizing impedance Z_{o2} (i.e., $a_2 = 0$).

If we consider the quantity $|S_{11}|^2$ we find from (1.6.9) and (1.6.12) that

$$|S_{11}|^2 = \left. \frac{|b_1(l_1)|^2}{|a_1(l_1)|^2} \right|_{a_2(l_2)=0} = \frac{P_{AVS} - P_1}{P_{AVS}} \quad (1.6.15)$$

Equation (1.6.15) shows that $|S_{11}|^2$ represents the ratio of the power reflected from port 1 to the power available at port 1. If $|S_{11}| > 1$, the power reflected is larger than the power available at port 1. Therefore, in this case port 1 acts as a source of power and oscillations can occur.

The evaluation of S_{21} is as follows:

$$\begin{aligned} S_{21} &= \left. \frac{b_2(l_2)}{a_1(l_1)} \right|_{a_2(l_2)=0} = \frac{\sqrt{Z_{o2}} I_2^-(l_2)}{\sqrt{Z_{o1}} I_1^+(l_1)} \Big|_{I_2^+(l_2)=0} \\ &= \frac{-\sqrt{Z_{o2}} I_2(l_2)}{\sqrt{Z_{o1}} I_1^+(l_1)} \Big|_{I_2^+(l_2)=0} \end{aligned} \quad (1.6.16)$$

because $I_2(l_2) = -I_2^-(l_2)$ [i.e., $a_2(l_2) = I_2^+(l_2) = 0$]. Since

$$I_1^+(l_1) = \frac{E_{1,TH}}{2Z_{o1}}$$

and

$$V_2(l_2) = -Z_{o2} I_2(l_2)$$

we can write (1.6.16) in the form

$$S_{21} = \frac{2\sqrt{Z_{o1}}}{\sqrt{Z_{o2}}} \frac{V_2(l_2)}{E_{1,TH}} \quad (1.6.17)$$

Equation (1.6.17) shows that S_{21} represents a forward voltage transmission coefficient from port 1 to port 2.

The analysis of $|S_{21}|^2$ gives

$$|S_{21}|^2 = \frac{|I_2(l_2)|^2 Z_{o2}}{|E_{1,TH}|^2 / 4Z_{o1}} \quad (1.6.18)$$

Equation (1.6.18) shows that $|S_{21}|^2$ represents the ratio of the power delivered to the load Z_{o2} (i.e., P_L) to the power available from the source (i.e., P_{AVS}). The ratio P_L/P_{AVS} is known as the *transducer power gain*.

If we analyze the network shown in Fig. 1.6.4 in which the excitation $E_2 \angle 0^\circ$ V rms is placed in port 2', and port 1' is terminated in its normalizing impedance Z_{o1} , we find that

$$S_{22} = \left. \frac{b_2(l_2)}{a_2(l_2)} \right|_{a_1(l_1)=0} = \frac{Z_2 - Z_{o2}}{Z_2 + Z_{o2}} \quad (1.6.19)$$

and

$$S_{12} = \left. \frac{b_1(l_1)}{a_2(l_2)} \right|_{a_1(l_1)=0} = \frac{2\sqrt{Z_{o2}}}{\sqrt{Z_{o1}}} \frac{V_1(l_1)}{E_{2,TH}}$$

where $E_{2,TH}$ is the Thévenin's voltage at port 2. Equation (1.6.19) shows that S_{22} is the reflection coefficient of port 2 with port 1 terminated in its normal-

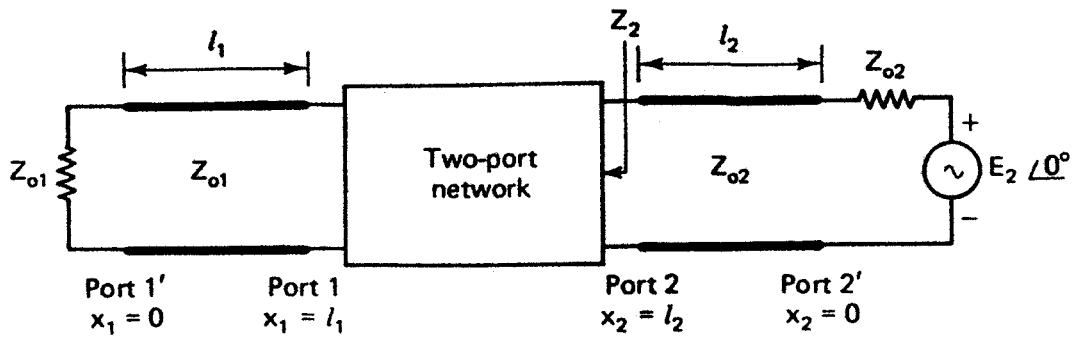


Figure 1.6.4 Two-port network excited by the generator $E_2 \angle 0^\circ$ V rms with internal impedance Z_{o2} and terminated in the impedance Z_{o1} .

izing impedance Z_{o1} (i.e., $a_1 = 0$), and S_{12} represents a reverse voltage transmission coefficient from port 2 to port 1.

The quantity $|S_{22}|^2$ represents the ratio of the power reflected from port 2 to the power available at port 2. If $|S_{22}| > 1$, the power reflected is larger than the power available at port 2 and oscillation can occur. The quantity $|S_{12}|^2$ represents a reverse transducer power gain. In fact,

$$|S_{12}|^2 = \frac{|I_1(l_1)|^2 Z_{o1}}{|E_{2,TH}|^2 / 4Z_{o2}}$$

Example 1.6.1

Evaluate the S parameters of a series impedance Z and a shunt admittance Y .

Solution. The two-port network of a series impedance is shown in Fig. 1.6.5a, and the network excited by a source and terminated in its normalizing impedance Z_o is shown in Fig. 1.6.5b.

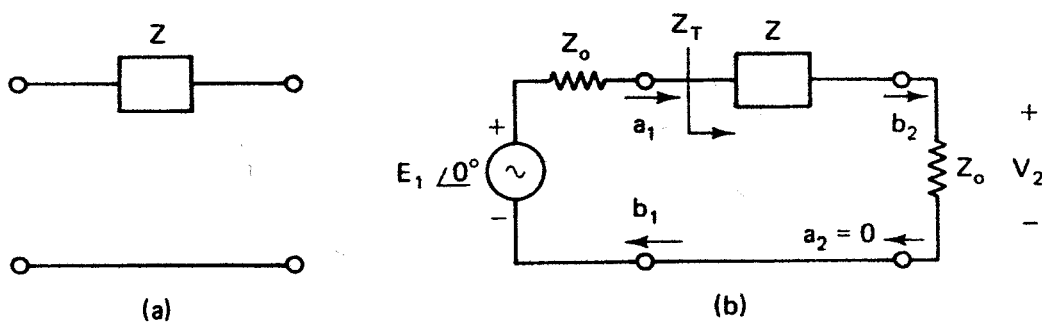


Figure 1.6.5 Two-port network of a series impedance Z .

From (1.6.14) we find that

$$S_{11} = \left. \frac{b_1}{a_1} \right|_{a_2=0} = \frac{Z_T - Z_o}{Z_T + Z_o}$$

where $Z_T = Z + Z_o$. Therefore,

$$S_{11} = \frac{Z}{Z + 2Z_o}$$

Since

$$V_2 = \frac{E_1 Z_o}{Z + 2Z_o}$$

we find from (1.6.17) that

$$S_{21} = \frac{2Z_o}{Z + 2Z_o}$$

From symmetry, we observe that $S_{22} = S_{11}$ and $S_{12} = S_{21}$.

The two-port network of a shunt admittance is shown in Fig. 1.6.6a, and the terminated network is shown in Fig. 1.6.6b. In this case

$$Z_T = \frac{Z_o}{1 + Z_o Y}$$

and from (1.6.14)

$$S_{11} = \frac{Z_T - Z_o}{Z_T + Z_o} = \frac{-Z_o Y}{2 + Z_o Y}$$

Since

$$V_2 = \frac{E_1}{2 + Z_o Y}$$

we obtain from (1.6.17)

$$S_{21} = \frac{2}{2 + Z_o Y}$$

Again, from symmetry we observe that $S_{22} = S_{11}$ and $S_{12} = S_{21}$.

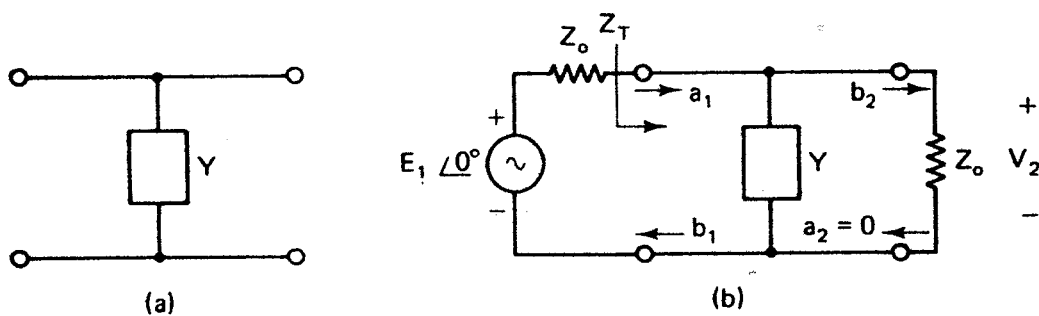
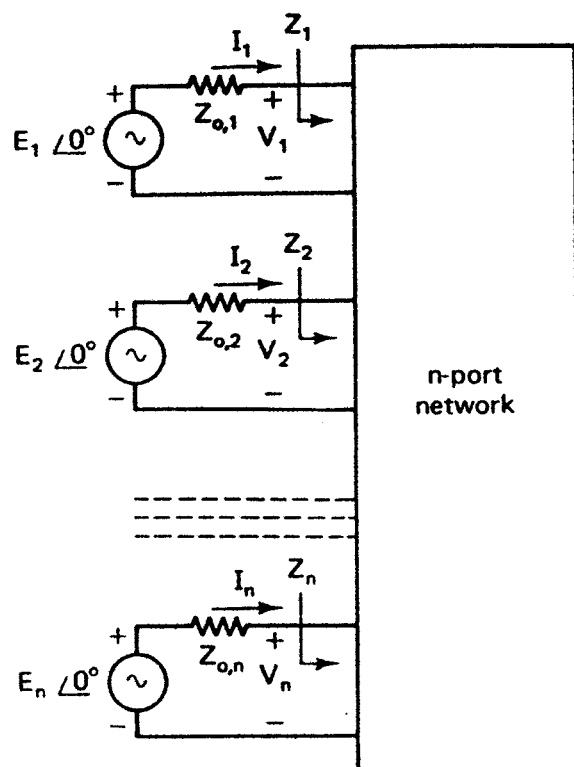


Figure 1.6.6 Two-port network of a shunt admittance Y .

1.7. GENERALIZED SCATTERING PARAMETERS

The typical situation that occurs at microwave frequencies, where 50- Ω transmission lines and 50- Ω terminations are commonly used to measure the S parameters of a two-port network, was analyzed in the preceding section. In this section we consider the case of the n -port network shown in Fig. 1.7.1. The

Figure 1.7.1 An n -port network.

generators $E_i \angle 0^\circ$ and the impedances $Z_{o,i}$ represent the Thévenin equivalent circuits seen by the i th ports. The impedances $Z_{o,i}$ (also called normalizing impedances) are assumed to have a positive real part.

In the n -port network the normalized incident and reflected waves are defined as

$$[a] = \frac{1}{2} [R_{o,i}^{-1/2}] ([V] + [Z_{o,i}] [I]) \quad (1.7.1)$$

and

$$[b] = \frac{1}{2} [R_{o,i}^{-1/2}] ([V] - [Z_{o,i}]^* [I]) \quad (1.7.2)$$

where

$$[Z_{o,i}] = \begin{bmatrix} Z_{o,1} & 0 & \cdots & 0 \\ 0 & Z_{o,2} & \cdots & 0 \\ \vdots & \vdots & \ddots & \vdots \\ 0 & 0 & \cdots & Z_{o,n} \end{bmatrix}$$

and

$$[R_{o,i}^{-1/2}] = \begin{bmatrix} (\text{Re } Z_{o,1})^{-1/2} & 0 & \cdots & 0 \\ 0 & (\text{Re } Z_{o,2})^{-1/2} & \cdots & 0 \\ \vdots & \vdots & \ddots & \vdots \\ 0 & \cdots & \cdots & (\text{Re } Z_{o,n})^{-1/2} \end{bmatrix}$$

$[a]$, $[b]$, $[V]$, and $[I]$ are column matrices.

The definitions (1.7.1) and (1.7.2) are generalizations of (1.6.3) and (1.6.4).

In fact, at port 1 we can write

$$a_1 = \frac{1}{2} R_{o,1}^{-1/2} (V_1 + Z_{o,1} I_1) \quad (1.7.3)$$

and

$$b_1 = \frac{1}{2} R_{o,1}^{-1/2} (V_1 - Z_{o,1}^* I_1) \quad (1.7.4)$$

and the relation between V_1 and I_1 is

$$V_1 = E_1 - Z_{o,1} I_1 \quad (1.7.5)$$

Substituting (1.7.5) into (1.7.3) gives

$$a_1 = \frac{E_1}{2R_{o,1}^{1/2}}$$

or

$$|a_1|^2 = \frac{|E_1|^2}{4R_{o,1}} \quad (1.7.6)$$

which is recognized as the power available from E_1 at port 1. Also, from (1.7.3) and (1.7.4) we obtain

$$\begin{aligned} |a_1|^2 - |b_1|^2 &= \frac{1}{4R_{o,1}} (V_1 + Z_{o,1} I_1)(V_1^* + Z_{o,1}^* I_1^*) \\ &\quad - \frac{1}{4R_{o,1}} (V_1 - Z_{o,1}^* I_1)(V_1^* - Z_{o,1} I_1^*) \\ &= \operatorname{Re} (V_1^* I_1) \end{aligned} \quad (1.7.7)$$

which is recognized as the power delivered to port 1.

Equations (1.7.4), (1.7.6), and (1.7.7) show that the generator E_1 sends the available power $|a_1|^2$ toward port 1. When port 1 is matched [i.e., when $Z_1 = V_1/I_1 = (Z_{o,1})^*$] the power $|a_1|^2$ is completely absorbed by Z_1 . When port 1 is not matched, the power absorbed by the port 1 is $|a_1|^2 - |b_1|^2$, where $|b_1|^2$ is the reflected power.

Solving (1.7.1) and (1.7.2) for $[V]$ and $[I]$ results in

$$\begin{aligned} [V] &= [V^+] + [V^-] \\ [I] &= [I^+] - [I^-] \end{aligned}$$

where

$$\begin{aligned} [V^+] &= [Z_{o,i}^*][I^+] \\ [V^-] &= [Z_{o,i}][I^-] \\ [a] &= [R_{o,i}^{1/2}][I^+] \end{aligned}$$

and

$$[b] = [R_{o,i}^{1/2}][I^-]$$

The generalized scattering matrix of the n -port network is defined as

$$[b] = [S][a] \quad (1.7.8)$$

The definition (1.7.8) of the scattering matrix shows that different normalizing impedances $Z_{o,i}$ produce different values of the generalized scattering parameters. Therefore, the generalized scattering parameters are defined in terms of specific normalizing impedances. If the normalizing impedances are pure resistances, the results in Section 1.6 for the two-port network follow.

From (1.7.8), the elements of $[S]$ are given by

$$S_{ii} = \left. \frac{b_i}{a_i} \right|_{a_k=0, k \neq i (k=0, 1, \dots, n)}$$

and

$$S_{ki} = \left. \frac{b_k}{a_i} \right|_{a_k=0, k \neq i (k=0, 1, \dots, n)}$$

S_{ii} is recognized as the input reflection coefficient at port 1 with all other ports matched (i.e., $a_k = 0$ when $V_k = -Z_{o,k} I_k$, $k \neq i$). Observing that

$$V_i = Z_i I_i$$

then from the i th equation in (1.7.1) and (1.7.2), we obtain

$$S_{ii} = \left. \frac{b_i}{a_i} \right|_{a_k=0, k \neq i} = \frac{V_i - Z_{o,i}^* I_i}{V_i + Z_{o,i} I_i} = \frac{Z_i - Z_{o,i}^*}{Z_i + Z_{o,i}}$$

The quantity $|S_{ki}|^2$ can be shown to be the transducer power gain from port i to port k with $a_k = 0$, $k \neq i$.

1.8 TWO-PORT NETWORK PARAMETERS CONVERSIONS

At a given frequency a two-port network can be described in terms of several parameters. Therefore, it is desirable to have relations to convert from one set of parameters to another. For example, the z parameters of a two-port network are defined by

$$[V] = [z][I] \quad (1.8.1)$$

where

$$[V] = \begin{bmatrix} v_1 \\ v_2 \end{bmatrix}$$

$$[I] = \begin{bmatrix} i_1 \\ i_2 \end{bmatrix}$$

and

$$[z] = \begin{bmatrix} z_{11} & z_{12} \\ z_{21} & z_{22} \end{bmatrix}$$

In terms of incident and reflected waves, we obtain from (1.8.1)

$$[V^+] + [V^-] = [z]([I^+] - [I^-])$$

or

$$([z] + [Z_o])[I^-] = ([z] - [Z_o])[I^+]$$

where Z_o is assumed to be real and

$$[Z_o] = \begin{bmatrix} Z_o & 0 \\ 0 & Z_o \end{bmatrix}$$

Therefore, the scattering matrix [i.e., (1.7.8)] in terms of z parameters is given by

$$[S] = \frac{[I^-]}{[I^+]} = ([z] + [Z_o])^{-1}([z] - [Z_o]) \quad (1.8.2)$$

and solving for $[z]$, we obtain

$$[z] = [Z_o]([1] + [S])([1] - [S])^{-1} \quad (1.8.3)$$

where $[1]$ is the unit diagonal matrix. Equations (1.8.2) and (1.8.3) give the conversion relations between the S and z parameters. These conversions, as well as others among the z , y , h , $ABCD$, and S parameters, are tabulated in Fig. 1.8.1.

1.9 SCATTERING PARAMETERS OF TRANSISTORS

The S parameters of microwave transistors are usually available for the transistor in chip and packaged form. Transistors in chip form are used when the best performance in gain, bandwidth, and noise is desired. Packaged transistors are very popular because they come in sealed enclosures and are easy to work with. The parasitic elements introduced by the package produce a degradation in the transistor ac performance.

Manufacturers usually measure and provide common-emitter or common-source S parameters of transistors as a function of frequency at a given dc bias. Since the minimum noise figure, linear output power, and maximum gain require different dc bias settings, the manufacturers usually provide two or three sets of S parameters.

Conversions from common-emitter to common-base S parameters can be done using the conversion relations in Fig. 1.8.1. For example, to convert from common-emitter to common-base S parameters, we first convert the common-

ABCD

h

y

z

S

S	z	y	h	ABCD	
				$\frac{A' + B' - C' - D'}{\Delta_4}$	$\frac{\lambda(A'D' - B'C')}{\Delta_4}$
S_{11} S_{12} S_{21} S_{22}	$S_{11} = \frac{(z'_{11} - 1)(z'_{22} + 1) - z'_{12}z'_{21}}{\Delta_1}$ $S_{12} = \frac{2z'_{12}}{\Delta_1}$ $S_{21} = \frac{2z'_{21}}{\Delta_1}$ $S_{22} = \frac{(z'_{11} + 1)(z'_{22} - 1) - z'_{12}z'_{21}}{\Delta_1}$	$S_{11} = \frac{(1 - y'_{11})(1 + y'_{22}) + y'_{12}y'_{21}}{\Delta_2}$ $S_{12} = \frac{-2y'_{12}}{\Delta_2}$ $S_{21} = \frac{-2y'_{21}}{\Delta_2}$ $S_{22} = \frac{(1 + y'_{11})(1 - y'_{22}) + y'_{12}y'_{21}}{\Delta_2}$	$S_{11} = \frac{(h'_{11} - 1)(h'_{22} + 1) - h'_{12}h'_{21}}{\Delta_3}$ $S_{12} = \frac{2h'_{12}}{\Delta_3}$ $S_{21} = \frac{-2h'_{21}}{\Delta_3}$ $S_{22} = \frac{(1 + h'_{11})(1 - h'_{22}) + h'_{12}h'_{21}}{\Delta_3}$	$\frac{2}{\Delta_4}$ $\frac{-A' + B' - C' + D'}{\Delta_4}$	
$z'_{11} = \frac{(1 + S_{11})(1 - S_{22}) + S_{12}S_{21}}{\Delta_5}$ $z'_{12} = \frac{2S_{12}}{\Delta_5}$ $z'_{21} = \frac{2S_{21}}{\Delta_5}$ $z'_{22} = \frac{(1 - S_{11})(1 + S_{22}) + S_{12}S_{21}}{\Delta_5}$	z_{11} z_{12} z_{21} z_{22}	$y_{22} = \frac{y_{22}}{ y }$ $y_{21} = \frac{-y_{21}}{ y }$ $y_{12} = \frac{-y_{12}}{ y }$ $y_{11} = \frac{y_{11}}{ y }$	$\frac{ h }{h_{22}} \frac{h_{12}}{h_{22}}$ $\frac{-h_{21}}{h_{22}} \frac{1}{h_{22}}$	$\frac{A}{C} \frac{\Delta_2}{C}$ $\frac{1}{C} \frac{D}{C}$	
$y'_{11} = \frac{(1 - S_{11})(1 + S_{22}) + S_{12}S_{21}}{\Delta_6}$ $y'_{12} = \frac{-2S_{12}}{\Delta_6}$ $y'_{21} = \frac{-2S_{21}}{\Delta_6}$ $y'_{22} = \frac{(1 + S_{11})(1 - S_{22}) + S_{12}S_{21}}{\Delta_6}$	$\frac{z_{22}}{ z } \frac{-z_{12}}{ z }$ $\frac{-z_{21}}{ z } \frac{z_{11}}{ z }$	y_{11} y_{12} y_{21} y_{22}	$\frac{1}{h_{11}} \frac{-h_{12}}{h_{11}}$ $\frac{h_{21}}{h_{11}} \frac{ h }{h_{11}}$	$\frac{D}{B} \frac{-\Delta_2}{B}$ $\frac{-1}{B} \frac{A}{B}$	

S

z

y

$h_{11} = \frac{(1 + S_{11}X(1 + S_{22}) - S_{12}S_{21})}{\Delta_7}$ $h_{12} = \frac{2S_{12}}{\Delta_7}$ $h_{21} = \frac{-2S_{21}}{\Delta_7}$ $h_{22} = \frac{(1 - S_{22}X(1 - S_{11}) - S_{12}S_{21})}{\Delta_7}$	$\frac{ z }{z_{22}} \frac{z_{12}}{z_{22}}$ $\frac{-z_{21}}{z_{22}} \frac{1}{z_{22}}$	$\frac{1}{y_{11}} \frac{-y_{12}}{y_{11}}$ $\frac{y_{21}}{y_{11}} \frac{ y }{y_{11}}$	$h_{11} \quad h_{12}$ $h_{21} \quad h_{22}$	$\frac{B}{D} \quad \frac{\Delta_2}{D}$ $-\frac{1}{D} \quad \frac{C}{D}$
$A' = \frac{(1 + S_{11}X(1 - S_{22}) + S_{12}S_{21})}{2S_{21}}$ $B' = \frac{(1 + S_{11}X(1 + S_{22}) - S_{12}S_{21})}{2S_{21}}$ $C' = \frac{(1 - S_{11}X(1 - S_{22}) - S_{12}S_{21})}{2S_{21}}$ $D' = \frac{(1 - S_{11}X(1 + S_{22}) + S_{12}S_{21})}{2S_{21}}$	$\frac{z_{11}}{z_{21}} \frac{ z }{z_{21}}$ $\frac{1}{z_{21}} \frac{z_{22}}{z_{21}}$	$\frac{-y_{22}}{y_{21}} \frac{-1}{y_{21}}$ $\frac{- y }{y_{21}} \frac{-y_{11}}{y_{21}}$	$-\frac{ h }{h_{21}} \frac{-h_{11}}{h_{21}}$ $-\frac{h_{22}}{h_{21}} \frac{-1}{h_{21}}$	$A \quad B$ $C \quad D$

h

ABCD

$$\begin{aligned} \Delta_1 &= (x'_{11} + 1)(x'_{22} + 1) - z'_{12}z'_{21} \\ \Delta_2 &= (1 + y'_{11}X(1 + y'_{22}) - y'_{12}y'_{21}) \\ \Delta_3 &= (h'_{11} + 1)(h'_{22} + 1) - h'_{12}h'_{21} \\ \Delta_4 &= A' + B' + C' + D' \\ \Delta_5 &= (1 - S_{11}X(1 - S_{22}) - S_{12}S_{21}) \\ \Delta_6 &= (1 + S_{11}X(1 + S_{22}) - S_{12}S_{21}) \\ \Delta_7 &= (1 - S_{11}X(1 + S_{22}) + S_{12}S_{21}) \\ \Delta_8 &= AD - BC \end{aligned}$$

$$\begin{aligned} z'_{11} &= z_{11}/Z_0, \quad z'_{12} = z_{12}/Z_0, \quad z'_{21} = z_{21}/Z_0, \quad z'_{22} = z_{22}/Z_0 \\ y'_{11} &= y_{11}Z_0, \quad y'_{12} = y_{12}Z_0, \quad y'_{21} = y_{21}Z_0, \quad y'_{22} = y_{22}Z_0 \\ h'_{11} &= h_{11}/Z_0, \quad h'_{12} = h_{12}, \quad h'_{21} = h_{21}, \quad h'_{22} = h_{22}Z_0 \\ A' &= A, \quad B' = B/Z_0, \quad C' = CZ_0, \quad D' = D \\ |z| &= z_{11}z_{22} - z_{12}z_{21} \\ |y| &= y_{11}y_{22} - y_{12}y_{21} \\ |h| &= h_{11}h_{22} - h_{12}h_{21} \end{aligned}$$

(a)

Conversion Between Common-Base, Common-Emitter, and Common-Collector y Parameters

$$\begin{aligned}
 y_{11,e} &= y_{11,b} + y_{12,b} + y_{21,b} + y_{22,b} = y_{11,c} \\
 y_{12,e} &= -(y_{12,b} + y_{22,b}) = -(y_{11,c} + y_{12,c}) \\
 y_{21,e} &= -(y_{21,b} + y_{22,b}) = -(y_{11,c} + y_{21,c}) \\
 y_{22,e} &= y_{22,b} = y_{11,c} + y_{12,c} + y_{21,c} + y_{22,c} \\
 y_{11,b} &= y_{11,e} + y_{12,e} + y_{21,e} + y_{22,e} = y_{22,c} \\
 y_{12,b} &= -(y_{12,e} + y_{22,e}) = -(y_{21,c} + y_{22,c}) \\
 y_{21,b} &= -(y_{21,e} + y_{22,e}) = -(y_{12,c} + y_{22,c}) \\
 y_{22,b} &= y_{22,e} = y_{11,c} + y_{12,c} + y_{21,c} + y_{22,c} \\
 y_{11,c} &= y_{11,e} = y_{11,b} + y_{12,b} + y_{21,b} + y_{22,b} \\
 y_{11,c} &= -(y_{11,e} + y_{12,e}) = -(y_{11,b} + y_{21,b}) \\
 y_{21,c} &= -(y_{11,e} + y_{21,e}) = -(y_{11,b} + y_{12,b}) \\
 y_{22,c} &= y_{11,e} + y_{12,e} + y_{21,e} + y_{22,e} = y_{11,b}
 \end{aligned}$$

(b)

Figure 1.8.1 (a) Conversions among the z , y , h , $ABCD$, and S parameters; (b) conversions between y parameters.

emitter S parameters to common-emitter y parameters, then convert the common-emitter y parameters to common-base y parameters, and then convert the common-base y parameters to common-base S parameters.

The frequency characteristics of a network can be represented as a continuous impedance or reflection coefficient plot in the Smith chart (see Sections 2.2 and 2.3). For example, the series RC network shown in Fig. 1.9.1a has the impedance or reflection coefficient plot shown in Fig. 1.9.1b. As the frequency increases, the capacitive reactance decreases, and the impedance plot moves clockwise along a constant-resistance circle.

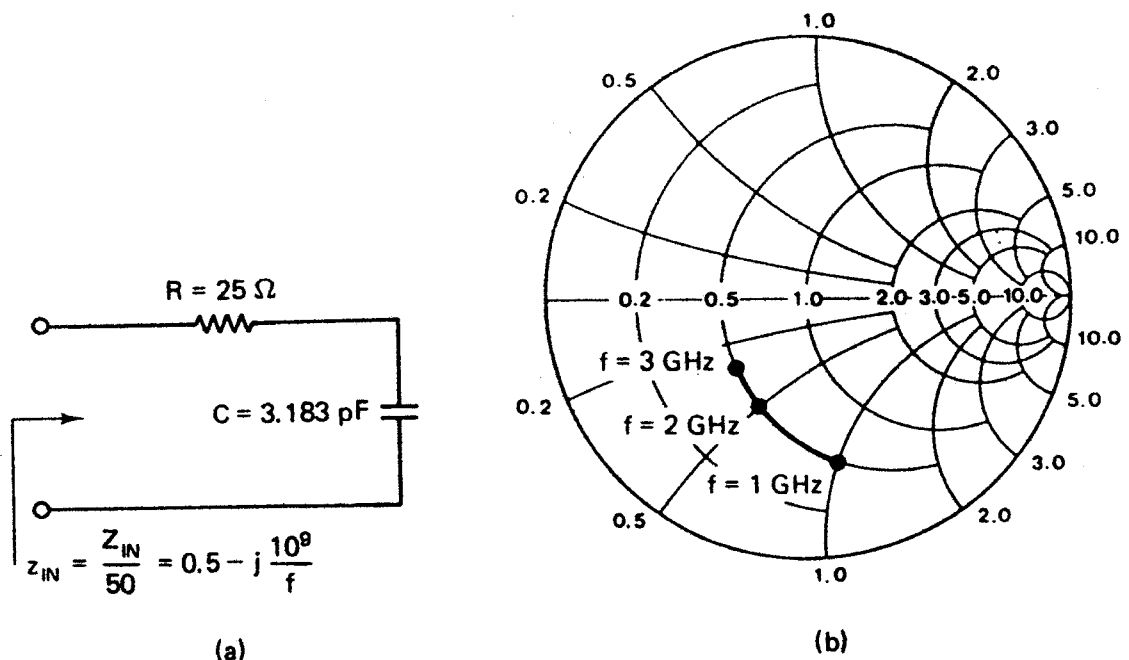


Figure 1.9.1 Frequency response of a series RC network.

A typical plot of S_{11} for a transistor in the common-emitter configuration is shown in Fig. 1.9.2. The plot of S_{11} is given for the transistor in chip form and in packaged form. The bias conditions are also shown. It is observed that S_{11} for this transistor in chip form follows a constant-resistance circle, with a capacitive reactance at the lower frequencies and an inductive reactance at the higher frequencies. The equivalent circuit for this transistor in chip form which exhibits the behavior of S_{11} is shown in Fig. 1.9.3a. The resistance R represents the base-to-emitter resistance plus any contact resistance. The capacitance C is due to the junction capacitance from base to emitter. The inductance L is due to the reflection properties of a transistor where the emitter resistance, when $h_{fe}(\omega)$ is complex, produces an inductive reactance across the base-to-emitter terminals.

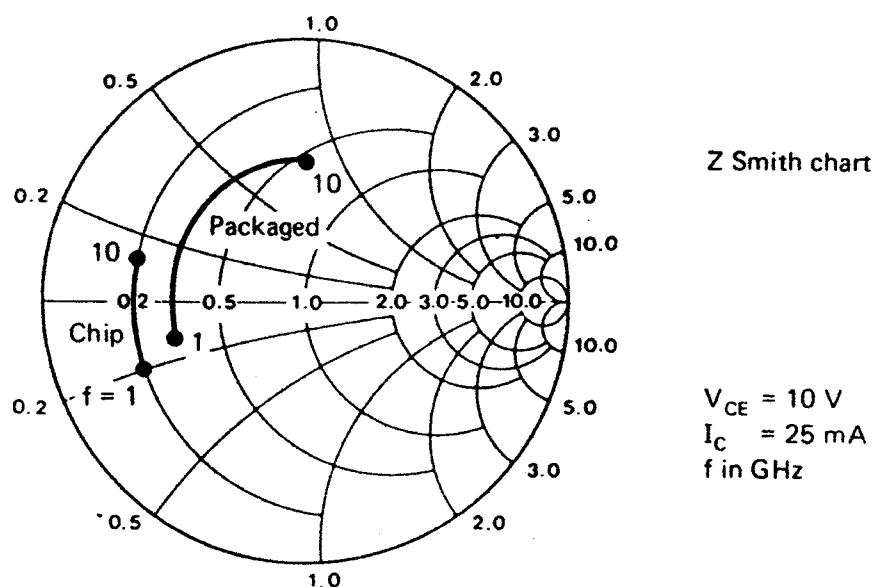


Figure 1.9.2 S_{11} of a common-emitter transistor in chip and packaged form.

The equivalent circuit for the transistor in packaged form is shown in Fig. 1.9.3b. In this case, the package inductance (L_{pkg}) and the package capacitance (C_{pkg}) contribute to the reflection coefficient variations at the higher frequencies.

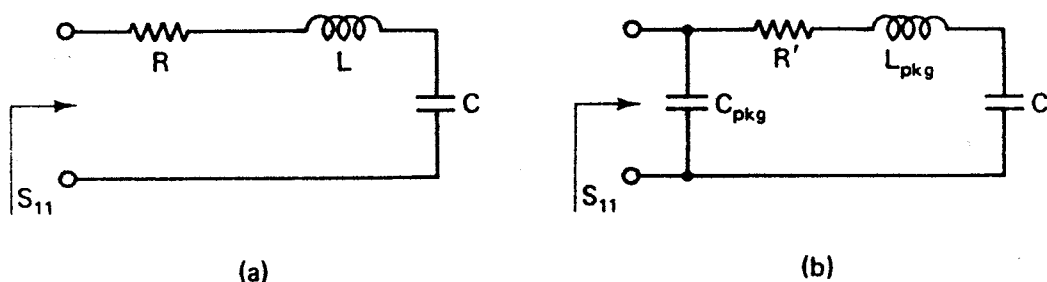


Figure 1.9.3 (a) Input equivalent circuit for a transistor in chip form; (b) input equivalent circuit for a packaged transistor.

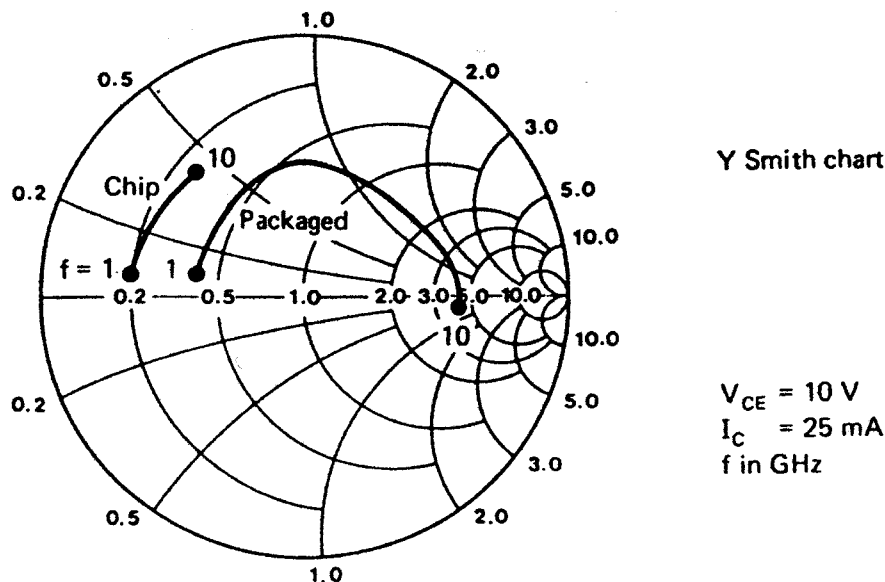


Figure 1.9.4 S_{22} of a common-emitter transistor in chip and packaged form.

A typical S_{22} plot for a chip and packaged transistor in the common-emitter configuration is shown in Fig. 1.9.4. For this transistor the chip characteristic follows a constant conductance curve (i.e., a shunt RC equivalent network).

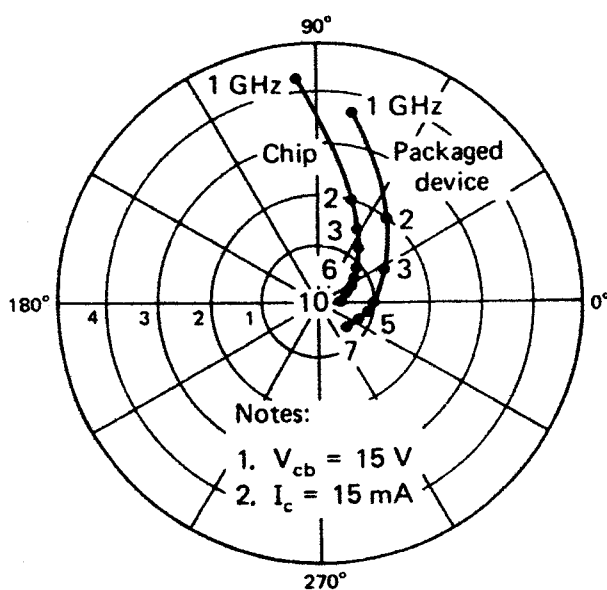


Figure 1.9.5 S_{21} of a common-emitter transistor in chip and packaged form. (From Ref. [1.1]; courtesy of Hewlett-Packard.)

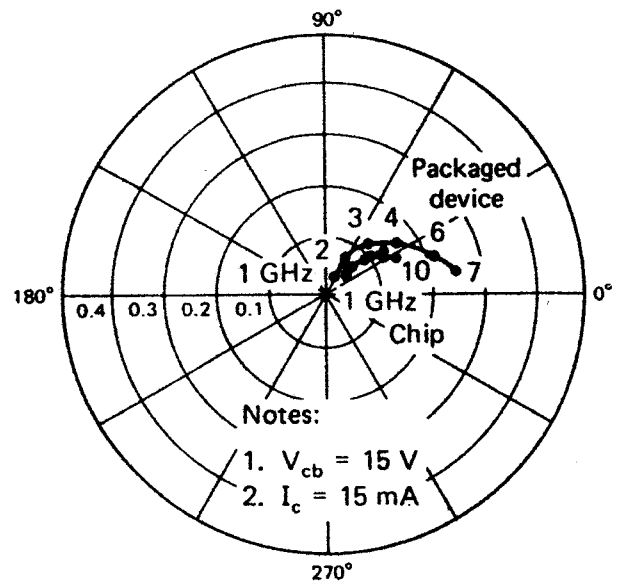


Figure 1.9.6 S_{12} of a common-emitter transistor in chip and packaged form. (From Ref. [1.1]; courtesy of Hewlett-Packard.)

The forward and reverse transmission coefficients S_{21} and S_{12} are usually given in a polar plot as shown in Figs. 1.9.5 and 1.9.6.

The parameter $|S_{21}|$ is constant for frequencies below the beta cutoff frequency (i.e., f_β) and then decays at 6 dB/octave. The transducer cutoff frequency (f_s) is the frequency where $|S_{21}|$ is equal to 1. The parameter $|S_{12}|$

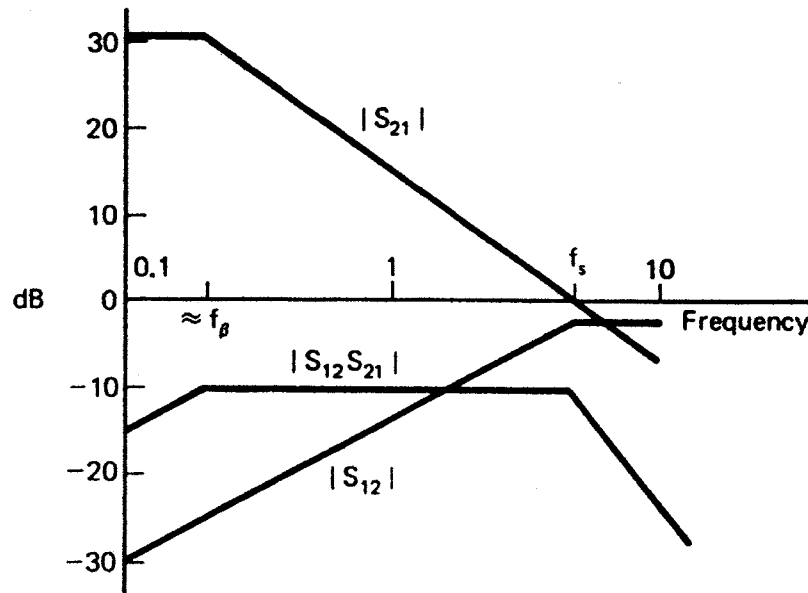


Figure 1.9.7 Frequency behavior of $|S_{21}|$, $|S_{12}|$, and $|S_{12}S_{21}|$. (From Ref. [1.1]; courtesy of Hewlett-Packard.)

increases at approximately 6 dB/octave, levels off around f_s , and decays at higher frequencies. A typical Bode plot of $|S_{21}|$, $|S_{12}|$, and the product $|S_{12}S_{21}|$ is shown in Fig. 1.9.7.

The common-emitter S parameters of a transistor are shown in Fig. 1.9.8. This figure illustrates some of the information typically provided by manufacturers.

A transistor can be considered to be a three-port device as shown in Fig. 1.9.9. In this case the scattering matrix, also called the *indefinite scattering matrix*, is

$$\begin{bmatrix} b_1 \\ b_2 \\ b_3 \end{bmatrix} = \begin{bmatrix} S_{11} & S_{12} & S_{13} \\ S_{21} & S_{22} & S_{23} \\ S_{31} & S_{32} & S_{33} \end{bmatrix} \begin{bmatrix} a_1 \\ a_2 \\ a_3 \end{bmatrix} \quad (1.9.1)$$

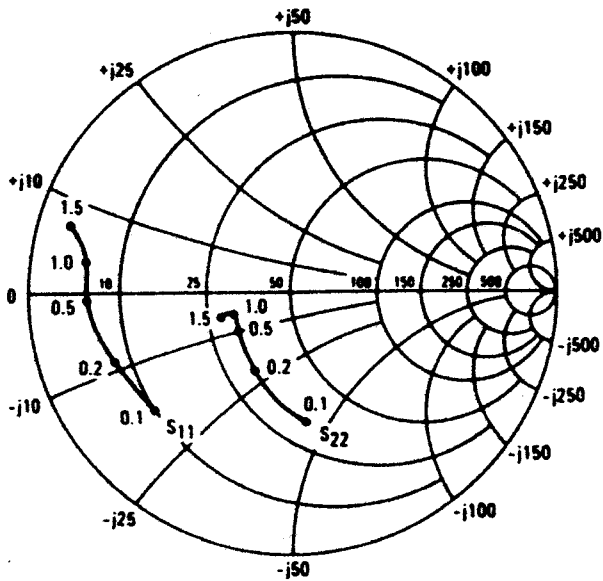
The name “indefinite scattering matrix” is used because no definite choice is made to ground a particular port. The meaning of S_{11} in (1.9.1) is

$$S_{11} = \left. \frac{b_1}{a_1} \right|_{a_2=0, a_3=0} \quad (1.9.2)$$

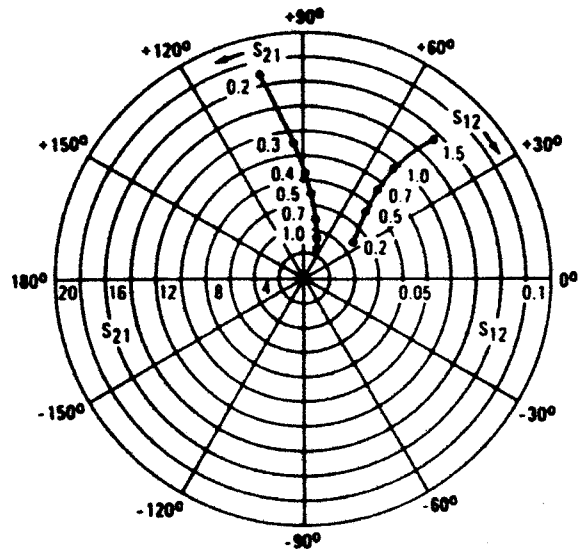
That is, to measure S_{11} reference resistances of 50Ω are used at ports 2 and 3. In a two-port common-emitter configuration, S_{11} is measured with the emitter grounded. Therefore, the value of S_{11} in (1.9.2) will be different from the value of S_{11} in a two-port common-emitter configuration. Similarly, the parameter S_{12} , S_{21} , and S_{22} in (1.9.1) will be different from the S_{12} , S_{21} , and S_{22} in a two-port common-emitter configuration.

MRF962 COMMON-EMITTER S-PARAMETERS

INPUT/OUTPUT REFLECTION
COEFFICIENTS versus FREQUENCY
($V_{CE} = 10\text{ V}$, $I_C = 50\text{ mA}$)



FORWARD/REVERSE TRANSMISSION
COEFFICIENTS versus FREQUENCY
($V_{CE} = 10\text{ V}$, $I_C = 50\text{ mA}$)



V_{CE} (Volts)	I_C (mA)	f (MHz)	S_{11}		S_{21}		S_{12}		S_{22}	
			$ S_{11} $	$\angle\phi$	$ S_{21} $	$\angle\phi$	$ S_{12} $	$\angle\phi$	$ S_{22} $	$\angle\phi$
5.0	10	100	0.70	-102	17.42	128	0.044	43	0.65	-57
		300	0.75	-156	7.11	98	0.058	24	0.32	-97
		500	0.78	-170	4.36	86	0.064	25	0.26	-110
		700	0.78	-176	3.16	77	0.071	26	0.23	-117
		1000	0.78	176	2.26	67	0.078	27	0.24	-126
		1500	0.79	167	1.51	54	0.092	29	0.31	-133
	25	100	0.69	-131	24.24	118	0.029	38	0.56	-87
		300	0.77	-167	8.76	95	0.039	32	0.35	-137
		500	0.79	-176	5.26	85	0.046	36	0.32	-150
		700	0.80	178	3.82	78	0.055	40	0.31	-158
		1000	0.79	173	2.72	70	0.067	42	0.32	-164
		1500	0.81	164	1.82	59	0.086	42	0.34	-167
	50	100	0.71	-147	27.72	113	0.021	37	0.53	-107
		300	0.78	-173	9.59	94	0.030	40	0.41	-152
		500	0.81	179	5.72	85	0.038	46	0.39	-163
		700	0.81	176	4.09	78	0.048	50	0.38	-169
		1000	0.81	171	2.89	71	0.061	51	0.38	-175
		1500	0.82	163	1.96	62	0.082	49	0.40	-177
10	10	100	0.71	-92	18.77	131	0.037	47	0.70	-44
		300	0.74	-150	8.09	100	0.051	28	0.34	-69
		500	0.75	-166	5.01	87	0.056	28	0.27	-75
		700	0.76	-174	3.62	78	0.064	28	0.24	-79
		1000	0.76	179	2.58	69	0.071	30	0.24	-88
		1500	0.77	168	1.72	55	0.085	31	0.31	-104
	25	100	0.67	-120	27.10	122	0.027	42	0.57	-68
		300	0.73	-163	10.27	97	0.035	36	0.27	-110
		500	0.76	-174	6.21	86	0.043	39	0.22	-124
		700	0.77	-179	4.48	78	0.051	41	0.20	-132
		1000	0.77	175	3.19	71	0.062	43	0.20	-139
		1500	0.78	166	2.13	59	0.080	42	0.25	-142
	50	100	0.68	-137	31.53	116	0.020	37	0.49	-85
		300	0.74	-169	11.17	95	0.028	40	0.27	-131
		500	0.77	-177	6.69	85	0.037	46	0.24	-144
		700	0.77	178	4.82	78	0.047	48	0.23	-152
		1000	0.77	173	3.42	71	0.059	50	0.23	-158
		1500	0.79	165	2.30	61	0.078	47	0.27	-159

Figure 1.9.8 S-parameter data for the Motorola MRF962 transistor. (From Motorola RF Data Manual; reproduced with permission of Motorola, Inc.)

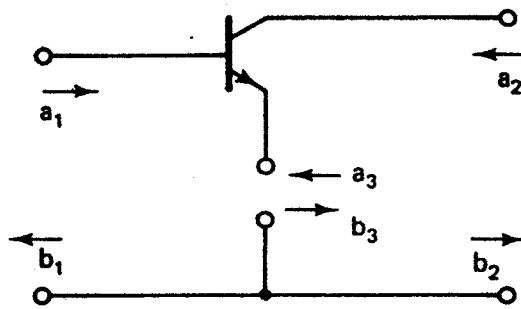


Figure 1.9.9 A transistor as a three-port network.

1.10 CHARACTERISTICS OF MICROWAVE TRANSISTORS

Most microwave bipolar junction transistors (BJTs) are planar in form and made from silicon in the *npn* type. Their dimensions are very small to permit operation at microwave frequencies. For example, the base thickness is of the order of a tenth of a micron.

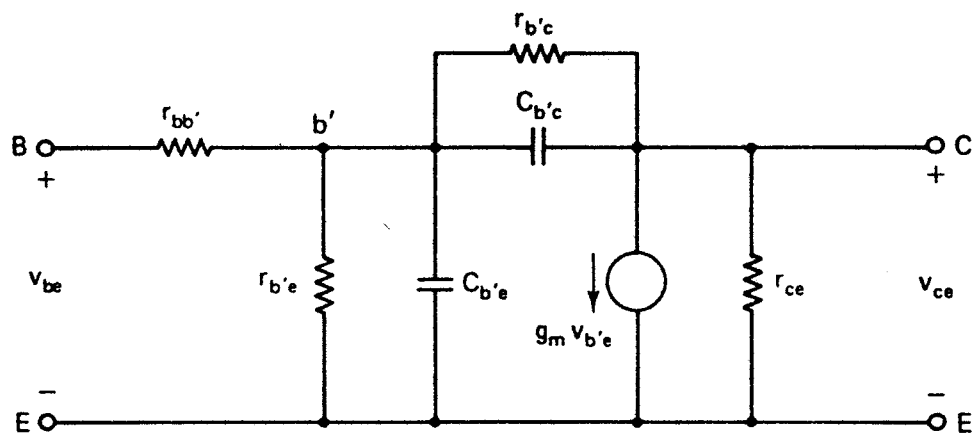


Figure 1.10.1 Hybrid- π model of a common-emitter BJT.

The equivalent hybrid- π model of the intrinsic BJT is shown in Fig. 1.10.1. In the microwave range, the reactance of $C_{b'c}$ is very small in comparison to the resistance of $r_{b'c}$, and the resistor r_{ce} is very large. Also, the reactance of $C_{b'e}$ is usually smaller than the resistance $r_{b'e}$. Therefore, the simplified model shown in Fig. 1.10.2 follows.

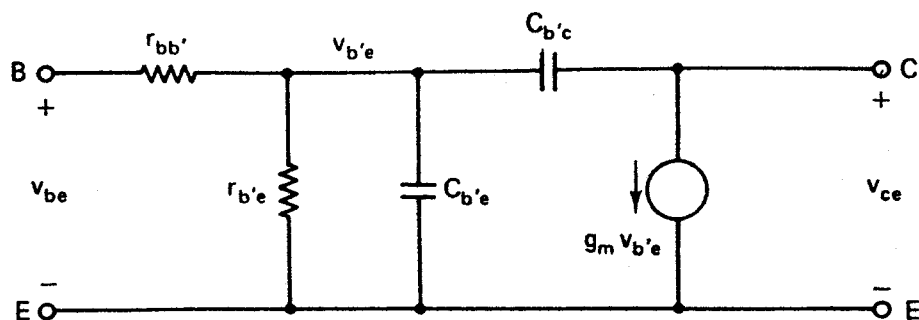


Figure 1.10.2 Simplified hybrid- π model of a microwave BJT in the common-emitter configuration.

In the actual (or extrinsic) microwave transistor, additional parasitic resistances, inductances, and capacitances appear (as well as other distributed elements) and must be included in the model. One such model is shown in Fig. 1.10.3. The meaning of the parasitic elements R_e , L_b , L_e , L_c , C_{be} , and C_{ce} is self-explanatory.

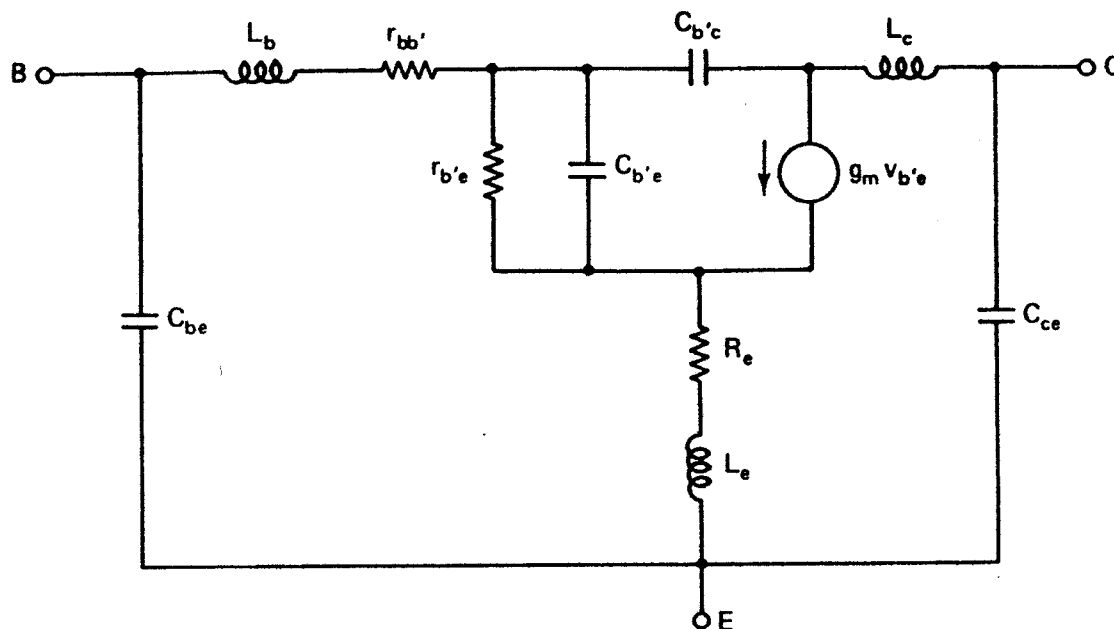


Figure 1.10.3 A microwave BJT common-emitter model that includes parasitics.

There are two figures of merit that are commonly used by manufacturers of microwave BJTs to describe the transistor performance. These are:

1. f_T : the gain-bandwidth frequency. It is the frequency where the short-circuit gain $|h_{fe}(\omega)|$ approximates unity.
2. f_{max} : the maximum frequency of oscillation. It is the frequency where the maximum available power gain of the transistor (called $G_{A,max}$) is equal to 1.

$G_{A,max}$ and f_{max} can be measured by conjugately matching the source impedance to the transistor input impedance, and the load to the transistor output impedance. Of course, the transistor must be unconditionally stable (i.e., no oscillations). $G_{A,max}$ is higher than the transducer gain $|S_{21}|^2$ because of the matching conditions. These concepts are discussed in detail in Chapter 3.

The frequency dependence of $h_{fe}(\omega)$ is given by

$$h_{fe}(\omega) = \frac{h_{fe}}{1 + jf/f_\beta}$$

where h_{fe} is the low-frequency short-circuit current gain and f_β is the beta

cutoff frequency, namely

$$f_{\beta} = \frac{1}{2\pi r_{b'e}(C_{b'e} + C_{b'c})} \approx \frac{1}{2\pi r_{b'e} C_{b'e}}$$

The frequencies f_T and f_{\max} for the intrinsic BJT model, shown in Fig. 1.10.2, are given by

$$f_T \approx \frac{g_m}{2\pi C_{b'e}} \quad (1.10.1)$$

and

$$f_{\max} = \sqrt{\frac{f_T}{8\pi r_{b'e} C_{b'c}}} \quad (1.10.2)$$

Also, f_{β} and f_T are related by

$$f_{\beta} = \frac{f_T}{h_{fe}} \quad (1.10.3)$$

The frequency f_T can also be expressed in terms of the total signal time delay from emitter to collector as [1.2]

$$f_T = \frac{1}{2\pi\tau_{ec}}$$

where τ_{ec} is the emitter-to-collector time delay, namely

$$\tau_{ec} \approx \tau_b + \tau_c$$

The parameter τ_b represents the base delay time and τ_c the base-to-collector depletion-layer delay time.

Figure 1.10.4 illustrates the meaning of f_T , f_s , and f_{\max} . Observe the gain rolloff at the rate of 6 dB/octave.

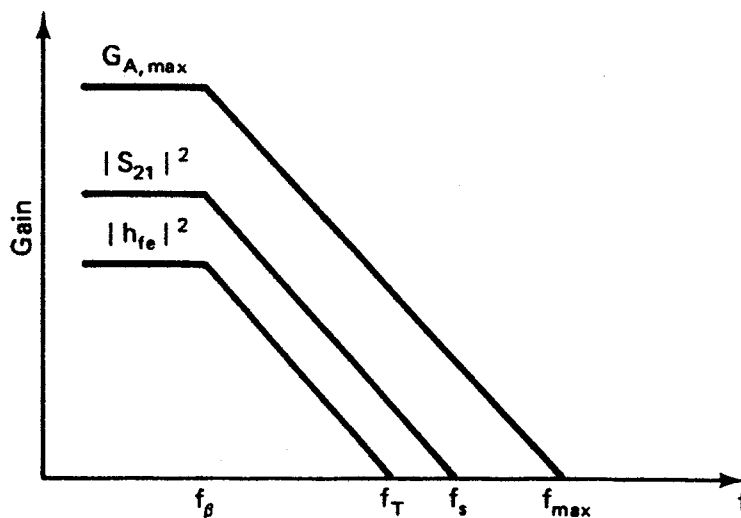


Figure 1.10.4 Frequency characteristics of $G_{A,\max}$, $|S_{21}|^2$ and $|h_{fe}|^2$.

Two sources of noise in a microwave BJT are thermal noise and shot noise. *Thermal noise* is caused by the thermal agitation of the carriers in the ohmic resistance of the emitter, base, and collector. *Shot noise* is a current dependent effect caused by fluctuations in the electron and hole currents due to bias conditions.

The gallium arsenide (GaAs) field-effect transistors (FETs) are commonly made in the metal semiconductor field-effect transistor structure (MESFET). That is, the gate terminal is constructed using a Schottky barrier gate. However, the other FET structures, such as the junction field-effect transistor (JFET), the metal-oxide semiconductor field-effect transistor (MOSFET), and the insulated-gate field-effect transistor (IGFET), have also been used.

The microwave FETs are made with GaAs because the electron mobility is greater than that of silicon. The high electron mobility results in excellent frequency response and noise performance, especially above 4 GHz.

The high-frequency model of the intrinsic GaAs FET in a common-source configuration is shown in Fig. 1.10.5. The capacitor C_i represents the gate-to-source capacitance and the resistor r_i is the small gate-to-source channel resistance. An extrinsic GaAs FET high-frequency model which includes parasitic elements is shown in Fig. 1.10.6. The meaning of the parasitic elements R_g , R_s , R_d , L_g , L_s , and L_d is self-explanatory.

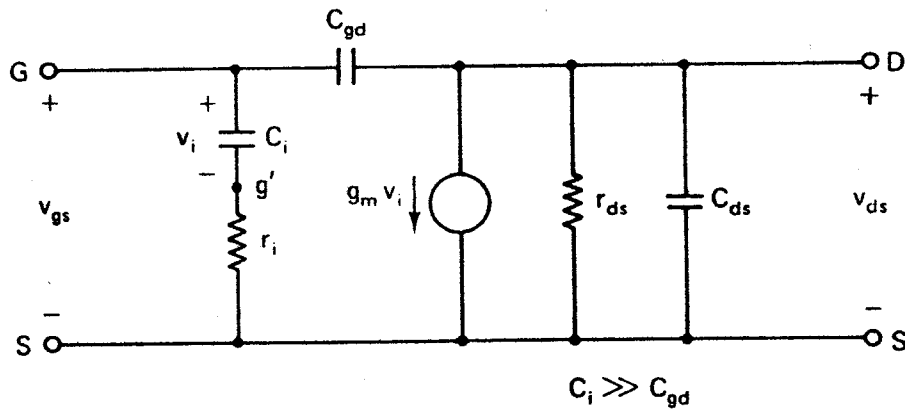


Figure 1.10.5 GaAs FET high-frequency model for the common-source configuration.

When the GaAs FET is unconditionally stable in the frequency range of interest, the feedback capacitance is very small and can be neglected. That is, there is no reverse transmission from the output to the input port of the transistor and the transistor becomes unilateral (i.e., $S_{12} = 0$). The simplified unilateral high-frequency model for the intrinsic GaAs FET is shown in Fig. 1.10.7.

The short length of the gate determines the frequency response of the GaAs FET. For the model shown in Fig. 1.10.7, the frequencies f_T and f_{\max} are given by

$$f_T = \frac{g_m}{2\pi C_i} \quad (1.10.4)$$

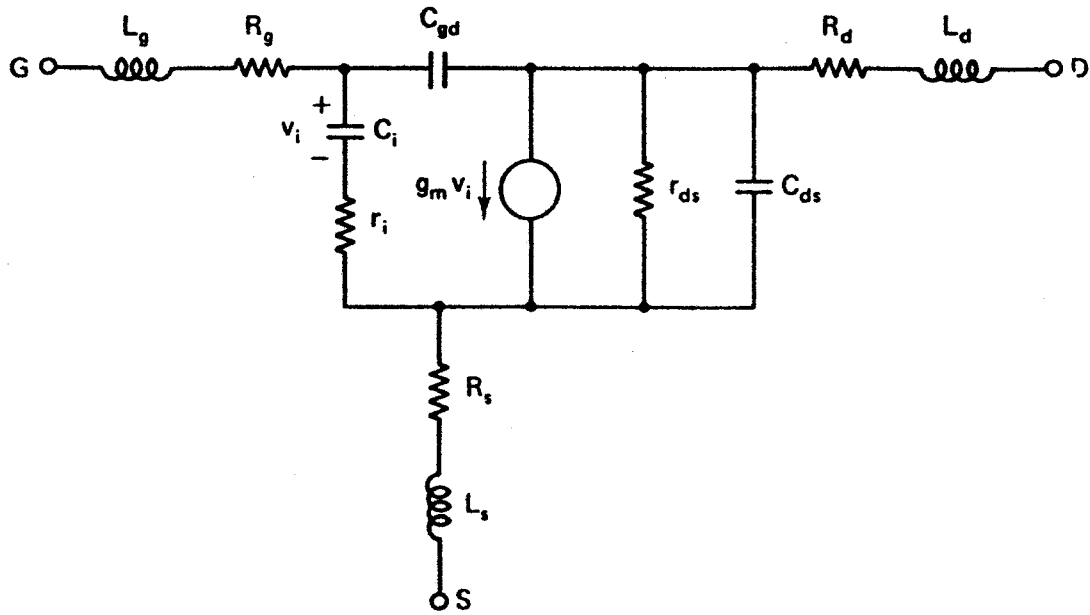


Figure 1.10.6 A microwave GaAs FET common-source model that includes parasitic elements.

and

$$f_{\max} = \frac{f_T}{2} \sqrt{\frac{r_{ds}}{r_i}} \quad (1.10.5)$$

Since f_T is limited by the electron transit time (τ_c) through the channel, f_T can be expressed in the form [1.2]

$$f_T = \frac{1}{2\pi\tau_c}$$

where

$$\tau_c = \frac{L}{v_s}$$

Here L is the gate length and v_s is the electron saturation drift velocity. Another expression for f_{\max} , found experimentally, is [1.2]

$$f_{\max} = \frac{33 \times 10^3}{L}$$

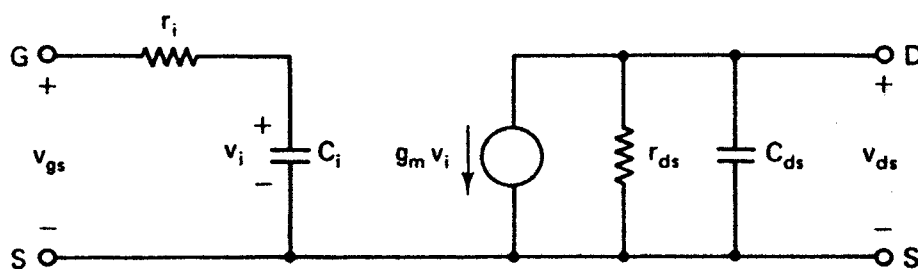


Figure 1.10.7 Simplified unilateral high-frequency model for a common-source GaAs FET.

The intrinsic noise sources in a GaAs FET are the thermal-generated channel noise and the induced noise at the gate. The induced noise at the gate is produced by the channel noise voltage. The extrinsic noise sources (see Fig. 1.10.6) are associated with the resistances R_g and R_s , and the gate bonding pad resistance. In addition, the GaAs FET exhibits intervalley scattering noise produced by scattering of electrons between energy bands.

PROBLEMS

1.1. A section Δx of a uniform transmission line is shown in Fig. P1.1.

(a) Using Kirchhoff's voltage and current laws, show that as $\Delta x \rightarrow 0$

$$-\frac{\partial v(x, t)}{\partial x} = Ri(x, t) + L \frac{\partial i(x, t)}{\partial t}$$

and

$$-\frac{\partial i(x, t)}{\partial x} = Gv(x, t) + C \frac{\partial v(x, t)}{\partial t}$$

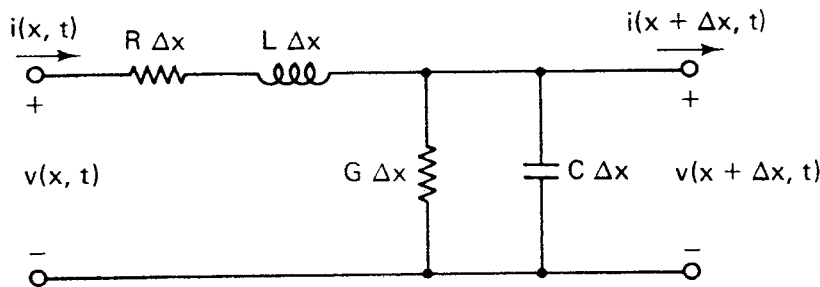


Figure P1.1

(b) Show that $v(x, t)$ and $i(x, t)$ satisfy the equations

$$\frac{\partial^2 v(x, t)}{\partial x^2} = LC \frac{\partial^2 v(x, t)}{\partial t^2} + (RC + LG) \frac{\partial v(x, t)}{\partial t} + RGv(x, t)$$

and

$$\frac{\partial^2 i(x, t)}{\partial x^2} = LC \frac{\partial^2 i(x, t)}{\partial t^2} + (RC + LG) \frac{\partial i(x, t)}{\partial t} + RGi(x, t)$$

(c) Assuming a sinusoidal excitation, show that the phasors $V(x)$ and $I(x)$ satisfy (1.3.1) and (1.3.2), respectively.

(d) Verify the general solution for $V(x)$ and $I(x)$ in (1.3.3) and (1.3.4).

(e) Show that in a lossless transmission line the voltage $V(x)$ satisfies

$$\frac{d^2 V(x)}{dx^2} + \beta^2 V(x) = 0$$

where $\beta = \omega \sqrt{LC}$. Write the general solution for $V(x)$.

1.2. Verify the equations for $Z_{IN}(d)$ in (1.3.9) and (1.3.10).

1.3. Verify the S - and T -parameter conversions given in (1.4.7) and (1.4.8).

- 1.4. (a) Find the $ABCD$ matrix of the series impedance Z and shunt admittance Y of Example 1.6.1.
 (b) Use Fig. 1.8.1 to convert the $ABCD$ parameters obtained in part (a) to S parameters. Compare the answers with the results in Example 1.6.1.
- 1.5. Find the scattering matrix and the chain scattering matrix of a transmission line of length l and characteristic impedance Z_o .
- 1.6. Find the scattering matrix and the chain scattering matrix of
 (a) A short-circuited shunt stub of length l and characteristic impedance Z_o .
 (b) An open-circuited shunt stub of length l and characteristic impedance Z_o .
- 1.7. Find the S parameters of the 1-to- n turns ratio transformer shown in Fig. P1.7 at ports 1–2 and 1'–2'.

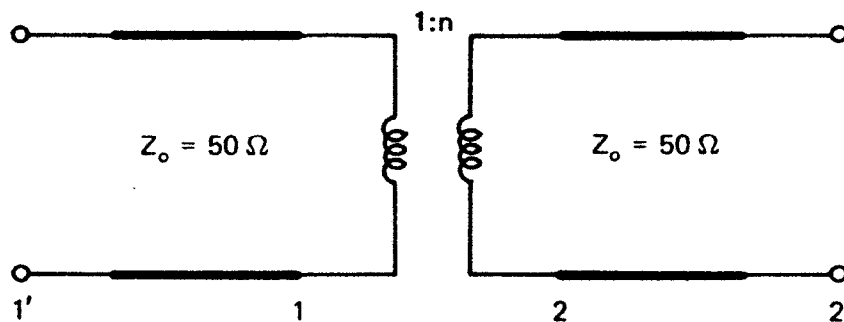


Figure P1.7

- 1.8. Show that the overall S_{21} parameter of two cascade two-port networks with scattering matrices $[S_A]$ and $[S_B]$, respectively, is given by

$$S_{21} = \frac{S_{21,A} S_{21,B}}{1 - S_{22,A} S_{11,B}}$$

- 1.9. In the two-port network shown in Fig. P1.9:

- (a) Find $Z_{IN}(0)$.
 (b) Find $a_1(0)$, $b_1(0)$, $a_1(\lambda/8)$, $b_1(\lambda/8)$, and $a_2(0)$.
 (c) Evaluate $V_1(0)$, $V_1(\lambda/8)$, $I_1(0)$, and $I_1(\lambda/8)$.
 (d) Evaluate the average input power at $x_1 = 0$ and the average input power at $x_1 = \lambda/8$.
 (e) Show that $P_1(0) = P_1(\lambda/8)$.
 (f) Evaluate $S_{11}(0)$ and $S_{11}(\lambda/8)$.
 (g) Find the electrical length and the length in centimeters of the $\lambda/8$ transmission line at $f = 1$ GHz.

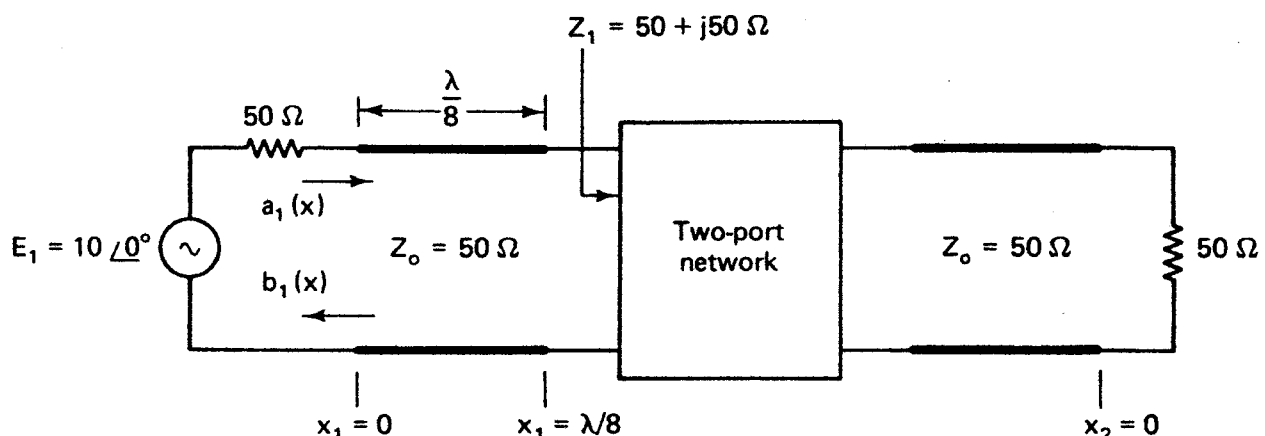


Figure P1.9

- 1.10. (a) Find the value of the source impedance that results in maximum power delivered to the load in Fig. P1.10. Evaluate the maximum power delivered to the load.
- (b) Using the value of Z_s from part (a), find the Thévenin's equivalent circuit at the load end and evaluate the power delivered to the load.

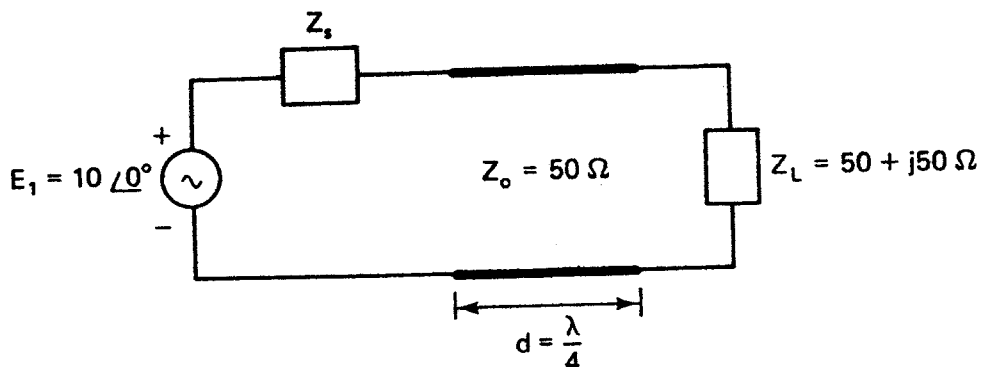


Figure P1.10

- 1.11. Show that in the n -port network of Fig. 1.7.1, the transducer power gain from port i to port k , $|S_{ki}|^2$, is given by

$$|S_{ki}|^2 = \frac{\operatorname{Re}(Z_{o,k})|I_k|^2}{|E_i|^2/4\operatorname{Re}(Z_{o,i})} = \frac{P_k}{(P_{AVS})_i}$$

where $(P_{AVS})_i$ is the maximum available power at port i and P_k is the power delivered to $Z_{o,k}$.

- 1.12. In Fig. 1.8.1, verify the conversions between

- (a) z and y parameters
 (b) z and $ABCD$ parameters

- 1.13. (a) Show that

$$[S] = -([y] + [Y_o])^{-1}([y] - [Y_o])$$

and

$$[y] = [Y_o]([1] - [S])([1] + [S])^{-1}$$

where

$$[Y_o] = \begin{bmatrix} Y_o & 0 \\ 0 & Y_o \end{bmatrix}$$

- (b) Verify the conversion between S and y parameters in Fig. 1.8.1.

- 1.14. In the network shown in Fig. P1.14, the S parameters of the BJT and the value of L are known. Explain how the overall S parameters of the two-port can be calculated.

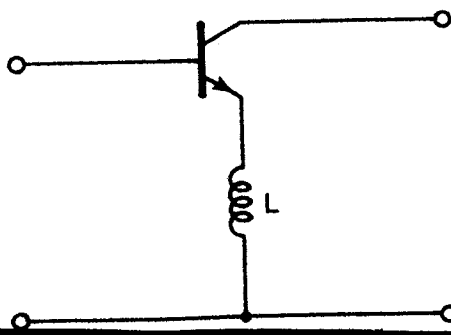


Figure P1.14

1.15. The common-emitter S -parameters of a GaAs FET at $f = 10$ GHz are

$$S_{11} = 0.73 \angle -128^\circ$$

$$S_{21} = 1.73 \angle 73^\circ$$

$$S_{12} = 0.045 \angle 114^\circ$$

$$S_{22} = 0.75 \angle -52^\circ$$

Determine the common-base and common-collector S -parameters.

- 1.16. Find equivalent circuits that exhibit the S_{22} characteristics (chip and packaged form) shown in Fig. 1.9.4.
- 1.17. (a) Derive the equations for f_T , f_{\max} , and f_β , for a BJT, given in (1.10.1), (1.10.2), and (1.10.3).
 (b) Derive the equations for f_T and f_{\max} , for a GaAs FET, given in (1.10.4) and (1.10.5).
- 1.18. Show that for equal reference resistance ($Z_{o1} = Z_{o2}$), the scattering matrix in (1.4.5) can be written in the form

$$V_1^- = S_{11}V_1^+ + S_{12}V_2^+$$

$$V_2^- = S_{21}V_1^+ + S_{22}V_2^+$$

and

$$I_1^- = S_{11}I_1^+ + S_{12}I_2^+$$

$$I_2^- = S_{21}I_1^+ + S_{22}I_2^+$$

- 1.19. Show that in the indefinite scattering matrix given in (1.9.1), the sum of the coefficient of any row is equal to 1 and the sum of the coefficient of any column is equal to 1.

Hint: Since (1.9.1) is valid for any values of a_1 , a_2 , and a_3 , consider the case where $a_2 = a_3 = 0$ as shown in Fig. P1.19a. Then $b_1 = S_{11}a_1$, $b_2 = S_{21}a_1$, and $b_3 = S_{31}a_1$, and at P we can write

$$I_1^+ = I_1^- + I_2^- + I_3^-$$

Therefore, it follows that

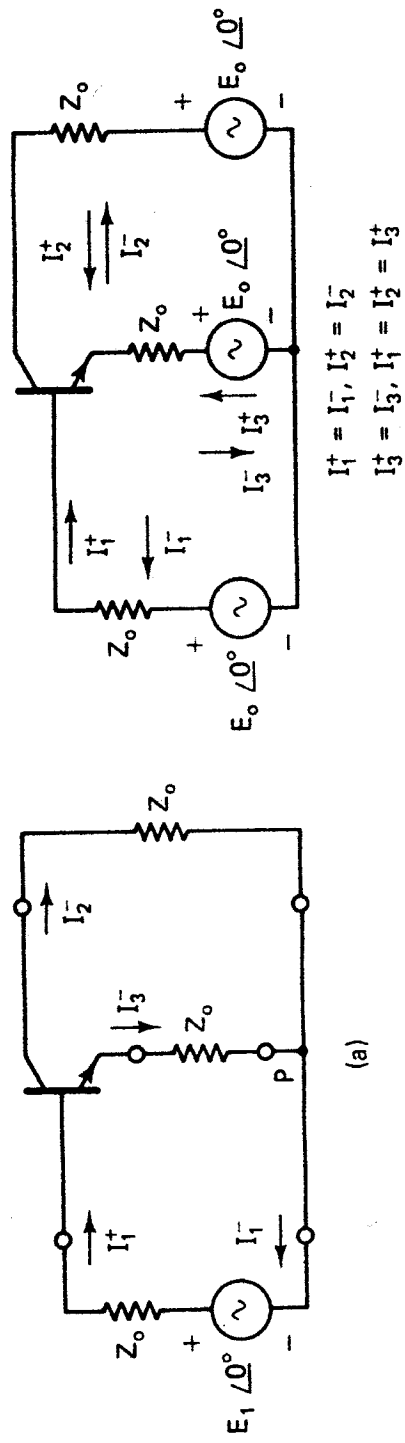
$$S_{11} + S_{21} + S_{31} = 1$$

The circuit shown in Fig. P1.19b can be used to show that the sum of the coefficients in any row is equal to 1.

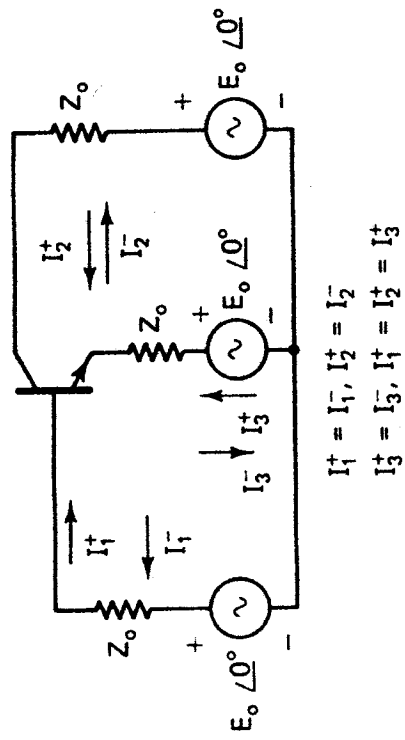
- 1.20. Show that the generalized scattering parameters for a two-port network in terms of arbitrary source (Z_s) and load (Z_L) impedances are given by

$$S'_{11} = \frac{A_1^* (1 - \Gamma_L S_{22})(S_{11} - \Gamma_s^*) + \Gamma_L S_{12} S_{21}}{D}$$

$$S'_{12} = \frac{A_2^* S_{12} [1 - |\Gamma_s|^2]}{D}$$



(a)



$$I_1^+ = I_1^-, I_2^+ = I_2^-$$

$$I_3^+ = I_3^-, I_1^+ = I_2^+ = I_3^+$$

(b)

Figure P1.19

$$S'_{21} = \frac{A_1^*}{A_1} \frac{S_{21}[1 - |\Gamma_L|^2]}{D}$$

$$S'_{22} = \frac{A_2^*}{A_2} \frac{(1 - \Gamma_s S_{22})(S_{22} - \Gamma_L^*) + \Gamma_s S_{12} S_{22}}{D}$$

where

$$D = [(1 - \Gamma_s S_{11})(1 - \Gamma_L S_{22}) - \Gamma_s \Gamma_L S_{12} S_{21}]$$

$$A_1 = \frac{1 - \Gamma_s^*}{|1 - \Gamma_s|} \sqrt{1 - |\Gamma_s|^2}, \quad A_2 = \frac{(1 - \Gamma_L^*)}{|1 - \Gamma_L|} \sqrt{1 - |\Gamma_L|^2}$$

$$\Gamma_s = \frac{Z_s - Z_o}{Z_s + Z_o}, \quad \Gamma_L = \frac{Z_L - Z_o}{Z_L + Z_o}$$

The S parameters are normalized to a real Z_o .

Note: This is a difficult problem that involves some matrix manipulations to obtain $[S']$ as a function of $[S]$.

REFERENCES

- [1.1] "S Parameter Design," Hewlett-Packard Application Note 154, April 1972.
- [1.2] D. V. Morgan and M. J. Howes, editors, *Microwave Solid State Devices and Applications*, Peter Peregrinus Ltd., New York, 1980.

MATCHING NETWORKS AND SIGNAL FLOW GRAPHS

2.1 INTRODUCTION

The analysis of transmission-line problems and of matching circuits at microwave frequencies can be cumbersome in analytical form. The Smith chart provides a very useful graphical aid to the analysis of these problems. The Smith chart is basically a plot of all passive impedances in a reflection coefficient chart of unit radius. The reading accuracy from the Smith chart is sufficient for most practical microwave transistor amplifier design problems.

Matching circuits that provide optimum performance in a microwave amplifier can be easily and quickly designed using the normalized impedance and admittance Smith chart. The Smith chart is also used to present the frequency dependence of scattering parameters and other amplifier characteristics.

The characteristics of microstrip transmission lines are presented in this chapter. The mode of propagation in a microstrip line is assumed to be quasi-transverse electromagnetic. Although radiation losses in a microstrip line can be severe, the use of a thin material, having a high dielectric constant, between the top strip conductor and the ground plane of a microstrip line reduces the radiation losses to a minimum.

Microstrip lines find extensive use as passive circuit elements and as a medium in which the complete microwave amplifier can be built. The interconnection features of the microstrip line are unsurpassed. Transistors in chip or packaged form can be easily attached to the strip conductors of the microstrip line. Some practical circuit construction techniques using microstrips are presented.

The description of two-port networks in terms of S parameters permits the use of signal flow graph in the analysis of microwave transistor amplifiers.

2.2 THE SMITH CHART

The Smith chart is the representation in the reflection coefficient plane, called the Γ plane, of the relation

$$\Gamma = \frac{Z - Z_o}{Z + Z_o} \quad (2.2.1)$$

for all values of Z , such that $\text{Re}[Z] \geq 0$. Z_o is the characteristic impedance of the transmission line or a reference impedance value. Defining the normalized impedance z as $z = Z/Z_o$, we can write (2.2.1) in the form

$$\Gamma = \frac{z - 1}{z + 1} \quad (2.2.2)$$

Figure 2.2.1 illustrates the properties of the transformation (2.2.2) for some values of z . For example, if $Z = 50 \Omega$ and $Z_o = 50 \Omega$, then $z = 1$ and $\Gamma = 0$. That is, the point $z = 1$ in the normalized z plane maps into the origin of the Γ plane. Next, we consider the mapping of normalized impedances having constant real and imaginary parts. For example, for $z = 1 + jx$ the corresponding values of Γ will be shown to lie in a circle of radius $1/2$, centered at $U = 1/2$, $V = 0$. Also, for $z = r + j1$ ($r \geq 0$) it follows that the corresponding values of Γ lie in a circle of radius 1 , centered at $U = 1$, $V = 1$. All passive impedances, that is, impedances having $r \geq 0$ map inside the unit circle (i.e. $|\Gamma| \leq 1$) in the Γ plane. Observe that the imaginary axis (i.e., $r = 0$) maps into the unit circle, $|\Gamma| = 1$.

The transformation (2.2.2) can be analyzed in general as follows. Let

$$\Gamma = U + jV = \frac{(r - 1) + jx}{(r + 1) + jx}$$

Then rationalize and separate the real and imaginary parts to obtain

$$U = \frac{r^2 - 1 + x^2}{(r + 1)^2 + x^2} \quad (2.2.3)$$

and

$$V = \frac{2x}{(r + 1)^2 + x^2} \quad (2.2.4)$$

Eliminating x from (2.2.3) and (2.2.4) results in

$$\left(U - \frac{r}{r + 1}\right)^2 + V^2 = \left(\frac{1}{r + 1}\right)^2$$

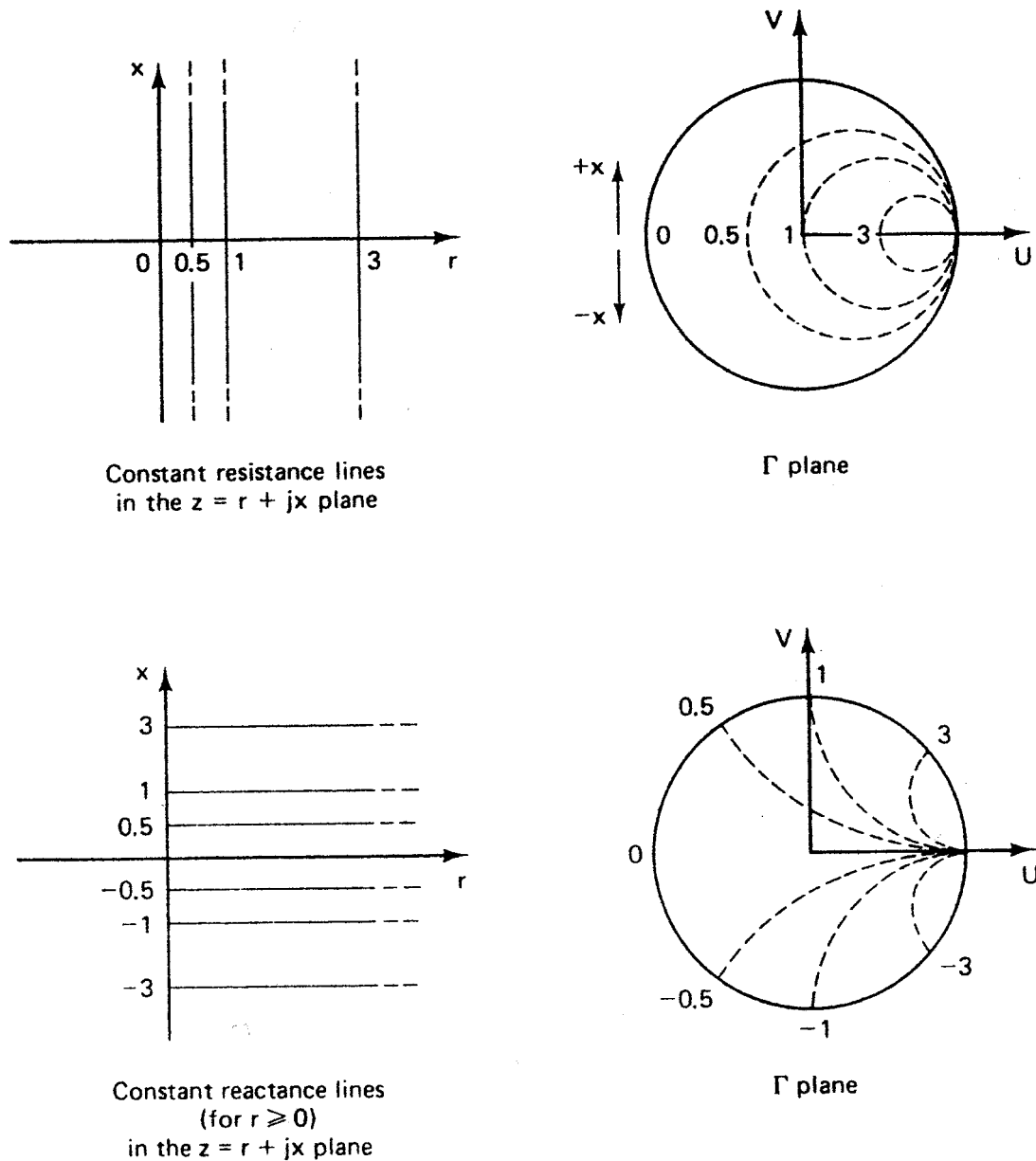


Figure 2.2.1 Development of the Smith chart.

which is the equation of a family of circles centered at $U = r/(r + 1)$, $V = 0$ with radii $1/(r + 1)$. The circles for $r = 0, 0.5, 1$, and 3 are shown in Fig. 2.2.1. Eliminating r from (2.2.3) and (2.2.4) results in

$$(U - 1)^2 + \left(V - \frac{1}{x}\right)^2 = \left(\frac{1}{x}\right)^2$$

which is the equation of a family of circles centered at $U = 1$, $V = 1/x$, with radii $1/x$. The circles for $x = -3, -1, -0.5, 0, 1, 0.5$, and 3 (with $r \geq 0$) are shown in Fig. 2.2.1.

There is a one-to-one correspondence between points in the z plane and points in the Γ plane. The plot of the constant-resistance and constant-reactance circles in a graph is known as the *Smith chart*. The Smith chart is shown in Fig. 2.2.2. Observe that the upper half of the chart represents normalized impedances having a positive reactance (i.e., $+jx$), and the lower half represents negative reactances (i.e., $-jx$). The distance around the chart is $\lambda/2$.

NAME	TITLE	DWG. NO.
SMITH CHART FORM 82-BSPR (9-66)		DATE
KAY ELECTRIC COMPANY, PINE BROOK, N.J. © 1966. PRINTED IN U.S.A.		

IMPEDANCE OR ADMITTANCE COORDINATES

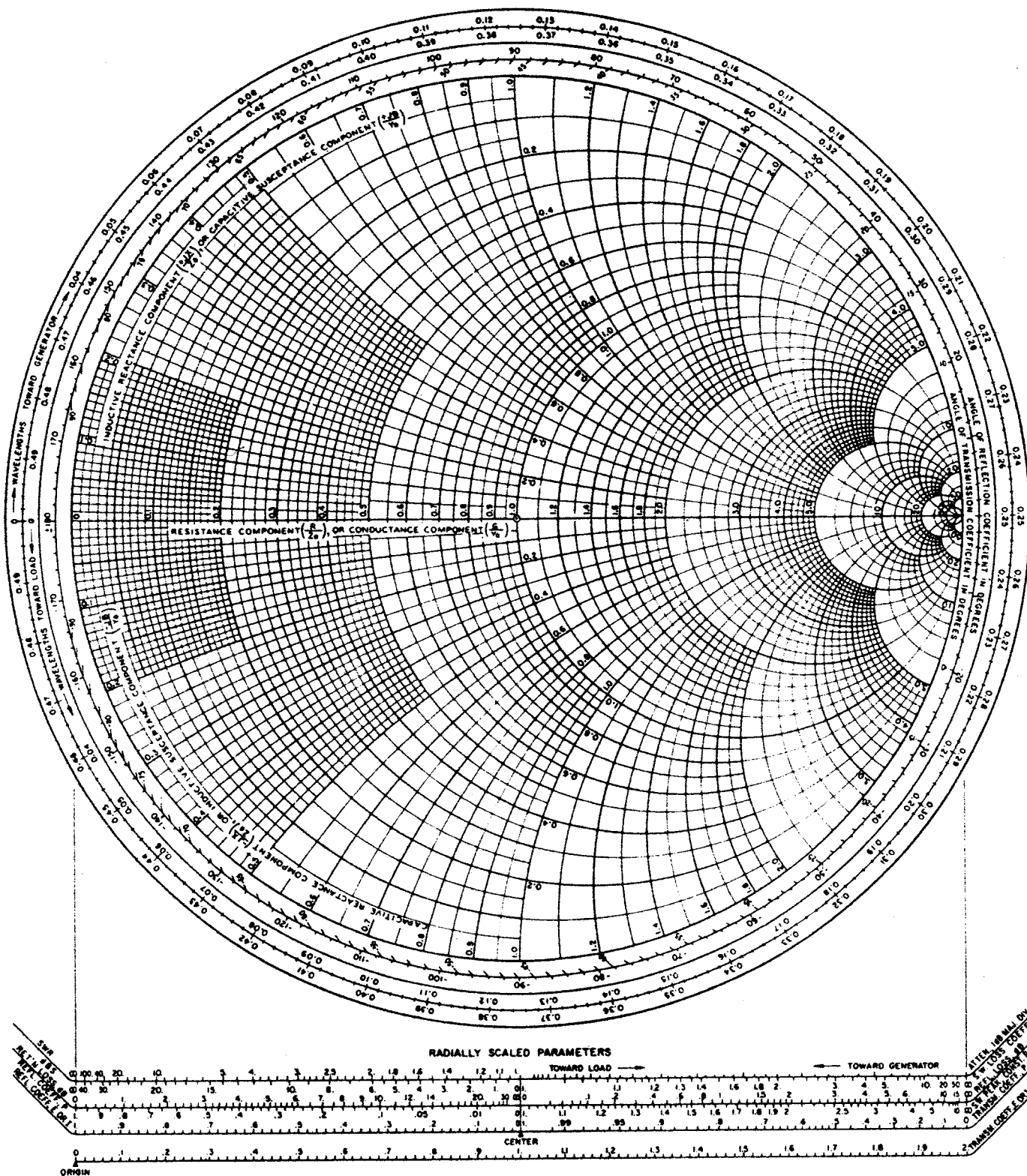


Figure 2.2.2 The Smith chart. (Reproduced with permission of Kay Electric Co., Pine Brook, N.J.)

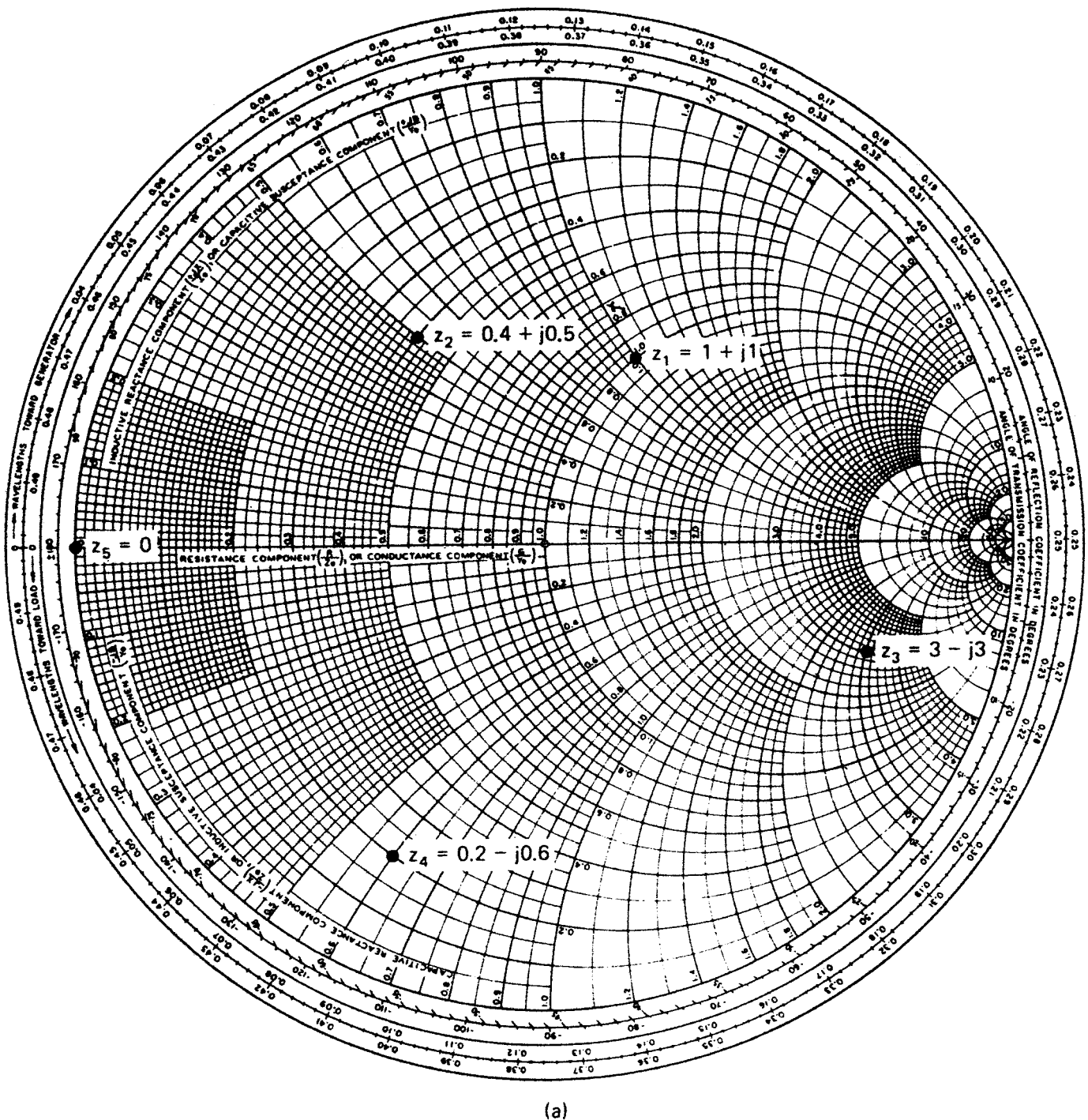


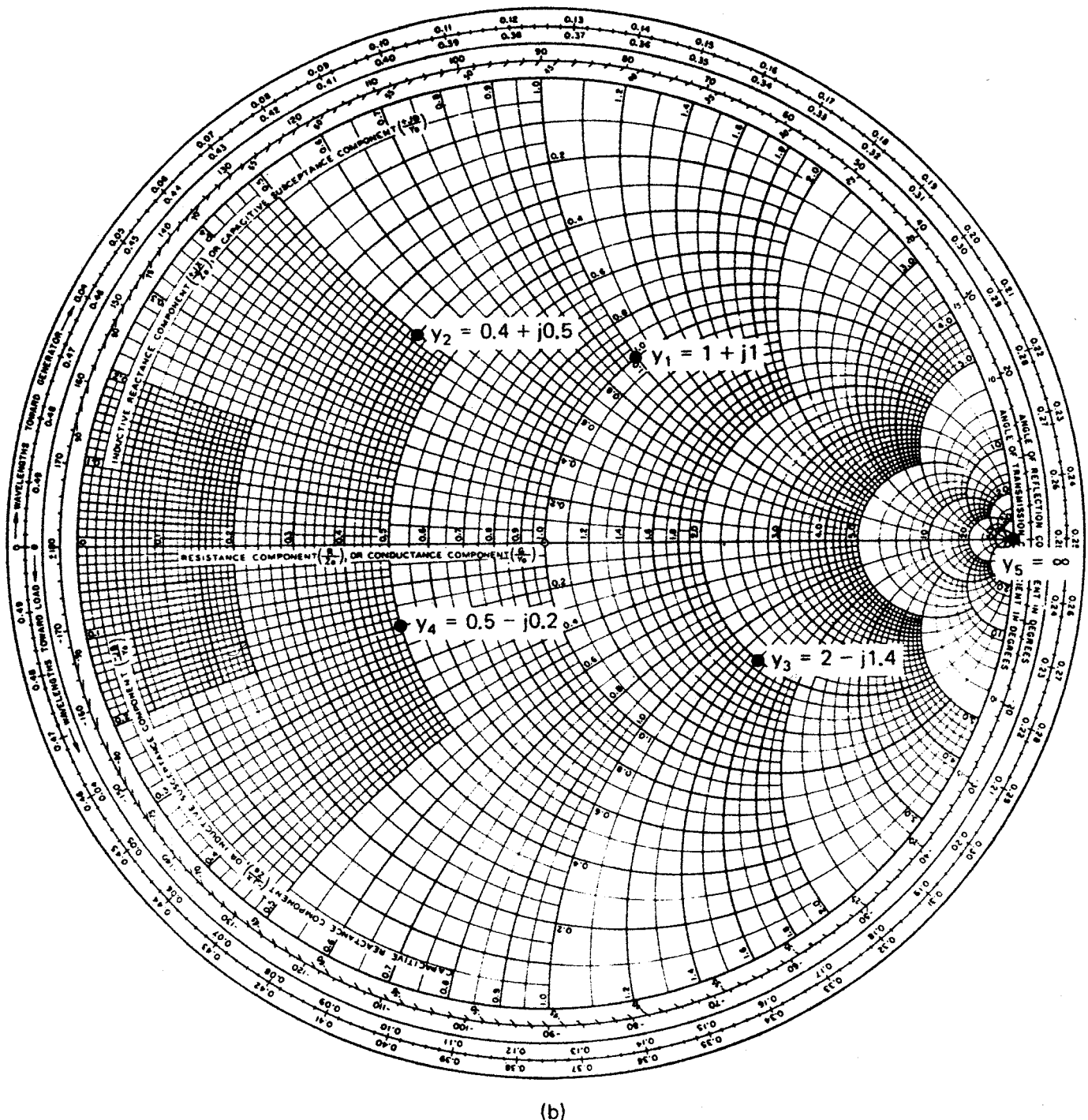
Figure 2.2.3 (a) Values of z in the Z Smith chart; (b) values of y in the Y Smith chart.

The Smith chart can also be used as an admittance chart. The appropriate transformation in this case is

$$\Gamma = \frac{y - 1}{y + 1}$$

where the normalized admittance is $y = Y/Y_0$. Y_0 is the characteristic admittance of the transmission line or a reference admittance value.

In the admittance chart, since $y = g + jb$, the previous constant-resistance (r) circles become constant-conductance (g) circles and the constant-reactance (x) circles become constant-susceptance (b) circles. Observe that the upper half of the chart represents normalized admittances having a positive



(b)

Figure 2.2.3 (continued)

susceptance (i.e., $+jb$) and the lower half represents negative susceptances (i.e., $-jb$).

When needed for clarity, we will call a Smith chart used as an impedance chart a “Z Smith chart,” and a Smith chart used as an admittance chart a “Y Smith chart.”

Example 2.2.1

Locate in the Smith chart the following normalized impedances and admittances:

$$z_1 = 1 + j1, \quad z_2 = 0.4 + j0.5, \quad z_3 = 3 - j3, \quad z_4 = 0.2 - j0.6, \quad z_5 = 0$$

$$y_1 = 1 + j1, \quad y_2 = 0.4 + j0.5, \quad y_3 = 2 - j1.4, \quad y_4 = 0.5 - j0.2, \quad y_5 = \infty$$

Solution. The values of z 's and y 's are shown in Fig. 2.2.3. The Smith chart in Fig. 2.2.3a is obviously used as a Z Smith chart, and that in Fig. 2.2.3b as a Y Smith chart.

Impedances having a negative real part will have a reflection coefficient whose magnitude is greater than 1. These impedances, therefore, map outside the Smith chart. Figure 2.2.4 shows a chart (known as the *compressed Smith chart*) that includes the Smith chart (i.e., $|\Gamma| \leq 1$) plus a portion of the negative impedance region.

An alternative way of handling negative resistances (i.e., $|\Gamma| > 1$) is to plot in the Smith chart $1/\Gamma^*$ and take the values of the resistance circles as being negative and the reactance circles as labeled.

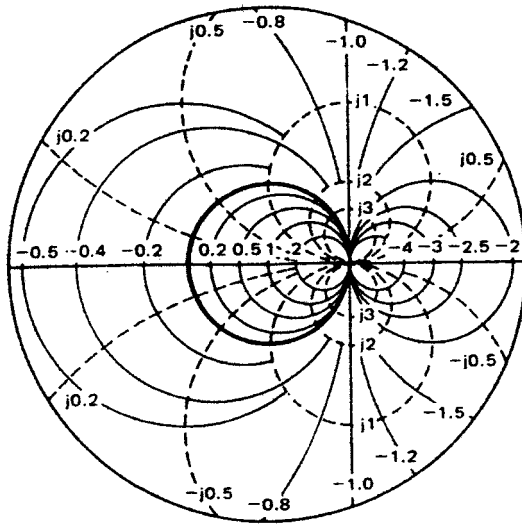


Figure 2.2.4 The compressed Smith chart. (From Ref. [1.1]; courtesy of Hewlett-Packard.)

Example 2.2.2

Find the impedance whose reflection coefficient is $2.236e^{j26.56^\circ}$.

Solution. If we plot in the Smith chart shown in Fig. 2.2.5, the quantity

$$\frac{1}{\Gamma^*} = 0.447e^{j26.56^\circ}$$

the resulting z is $-2 + j1$. Of course, from (2.2.2),

$$\Gamma = \frac{-2 + j1 - 1}{-2 + j1 + 1} = 2.236e^{j26.56^\circ}$$

The use of the Smith chart in a transmission-line calculation follows from (1.3.5), (1.3.7), and (1.3.8). For a lossless transmission line, we can conveniently write (1.3.5), (1.3.7), and (1.3.8) in the form

$$\Gamma_0 = \frac{z - 1}{z + 1} \quad (2.2.5)$$

$$\Gamma_{IN}(d) = \Gamma_0 e^{-j2\beta d} \quad (2.2.6)$$

$$z_{IN}(d) = \frac{1 + \Gamma_{IN}(d)}{1 - \Gamma_{IN}(d)} \quad (2.2.7)$$

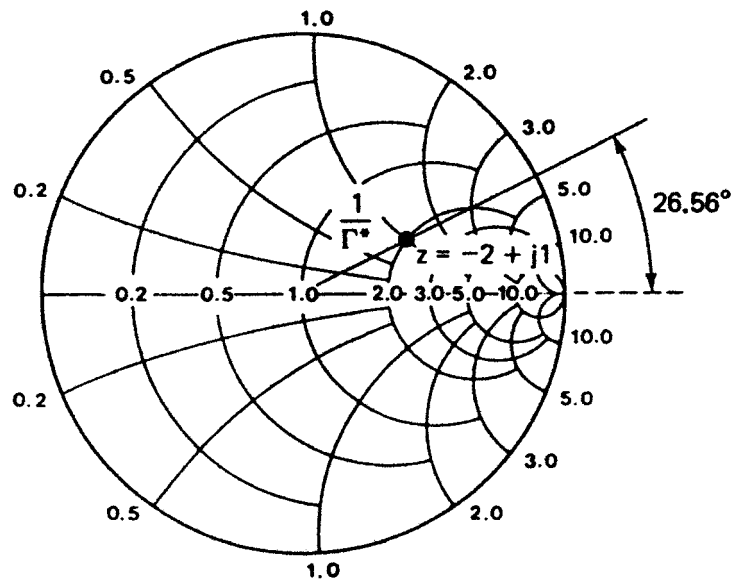


Figure 2.2.5 Negative resistances in the Smith chart.

A typical transmission-line input impedance calculation involves the following steps:

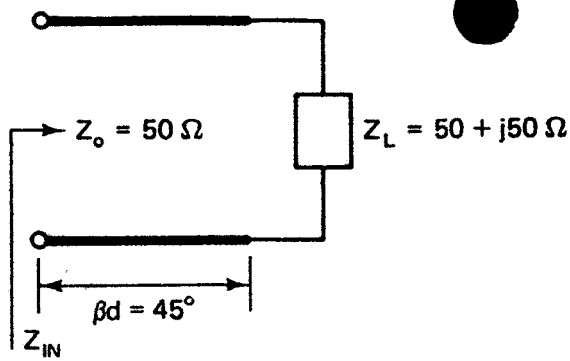
1. Locate Γ_0 in the Z Smith chart for a given $z = Z_L/Z_o$ [i.e., (2.2.5)].
2. Rotate Γ_0 by $-2\beta d$ to obtain $\Gamma_{IN}(d)$ [i.e., (2.2.6)]. Observe that the rotation is along a vector of constant magnitude, namely $|\Gamma_0| = |\Gamma_{IN}(d)|$.
3. Read the value of the normalized $z_{IN}(d)$ associated with $\Gamma_{IN}(d)$ [i.e., (2.2.7)].

Example 2.2.3

Find the input impedance, the reflection coefficient, and the VSWR in a transmission line having an electrical length of 45° , characteristic impedance of 50Ω , and terminated in a load $Z_L = 50 + j50 \Omega$.

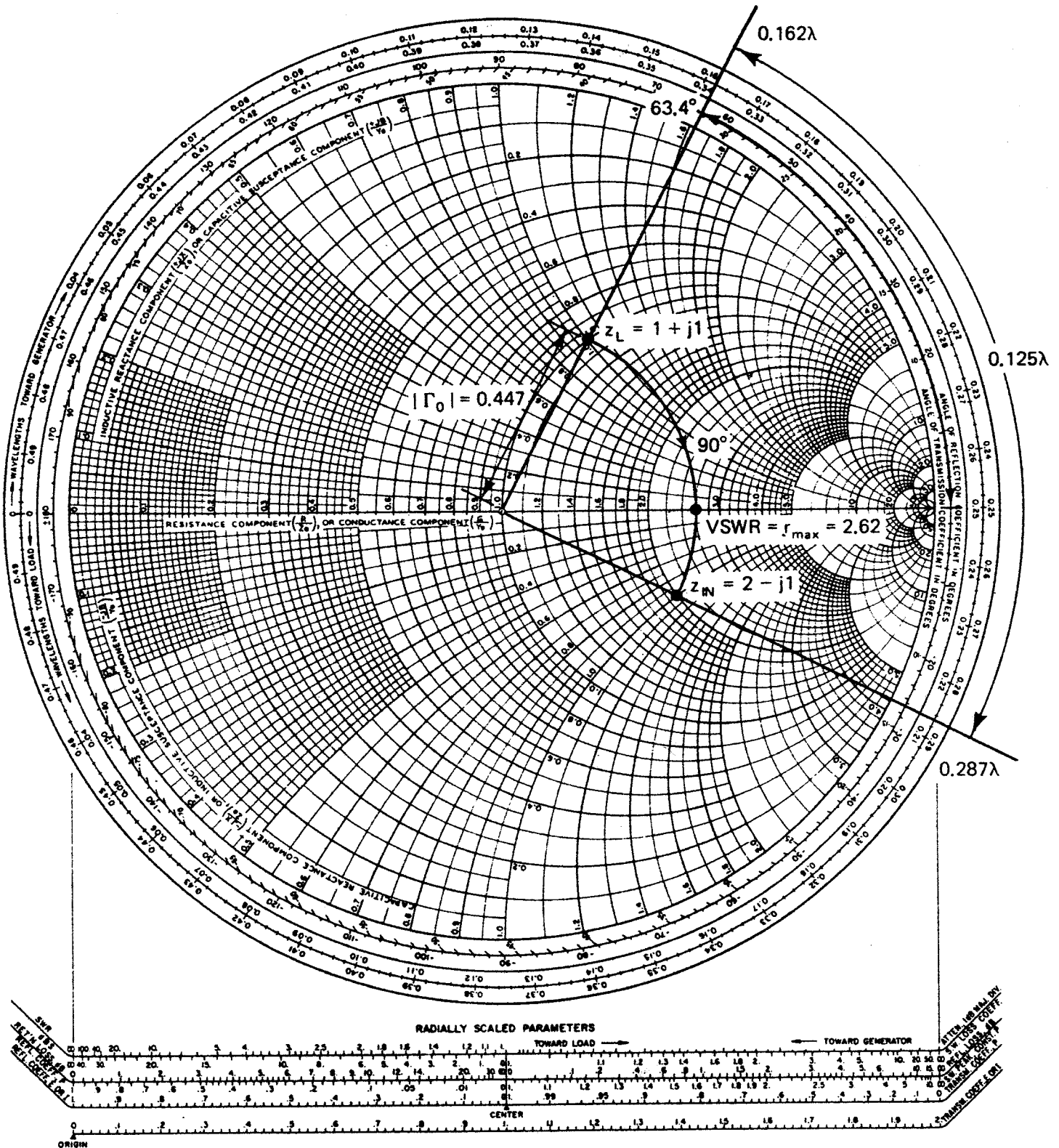
Solution. The transmission line is shown in Fig. 2.2.6a, where $z_L = Z_L/Z_o = 1 + j1$ and $\beta d = 2\pi d/\lambda = \pi/4$ or $d = \lambda/8 = 0.125\lambda$. In Fig. 2.2.6b the point $z_L = 1 + j1$ is located and the vector representing Γ_0 drawn. To find Z_{IN} , we rotate along a constant Γ radius a distance of -90° (i.e., $-2\beta d$). Observe that the Smith chart already has a wavelength scale. Therefore, if we rotate toward the generator a distance $d = 0.125\lambda$ along the wavelength scale, it is equivalent to a rotation of -90° . The procedure is illustrated in Fig. 2.2.6b. That is, at $z = 1 + j1$, we read the value of 0.162λ from the wavelength scale; next, we add 0.125λ and rotate along a constant $|\Gamma_0|$ radius until we reach the value of $0.162\lambda + 0.125\lambda = 0.287\lambda$. At 0.287λ the input impedance is read directly from the Smith chart as $z_{IN} = 2 - j1$ or $Z_{IN} = 100 - j50 \Omega$.

The magnitude and phase of Γ_0 are read as indicated in Fig. 2.2.6b. Observe the linear scale for the magnitude of the reflection coefficient. The distance from the origin to z_L can be measured with a ruler or compass and superimposed on the linear scale. The reading of Γ_0 can be done quite accurately, namely $\Gamma_0 = 0.447 \angle 63.4^\circ$.



(a)

IMPEDANCE OR ADMITTANCE COORDINATES



(b)

Figure 2.2.6 Typical transmission-line calculation using the Smith chart.

Finally, the VSWR can be calculated from (1.3.11) or the distance from the origin to z_L can be measured and superimposed on the VSWR scale. The value obtained is 2.62. It can also be shown that the value of the maximum resistance in the line is numerically equal to the VSWR. This value is indicated in Fig. 2.2.6b as $\text{VSWR} = r_{\max} = 2.62$.

2.3 THE NORMALIZED IMPEDANCE AND ADMITTANCE SMITH CHART

The conversion of a normalized impedance to a normalized admittance can be done easily in the Smith chart. Since

$$z = \frac{1 + \Gamma}{1 - \Gamma}$$

and

$$y = \frac{1}{z} = \frac{1 - \Gamma}{1 + \Gamma}$$

we observe that rotating Γ by $e^{j\pi}$, namely

$$z = \frac{1 + \Gamma e^{j\pi}}{1 - \Gamma e^{j\pi}} = \frac{1 - \Gamma}{1 + \Gamma}$$

results in the value $(1 - \Gamma)/(1 + \Gamma)$, which is identical to the value of the admittance y .

Example 2.3.1

Find y for $z = 1 + j1$ using the Smith chart.

Solution. The graphical solution is illustrated in Fig. 2.3.1. The value of y is read as $0.5 - j0.5$, which of course agrees with

$$y = \frac{1}{z} = \frac{1}{1 + j1} = 0.5 - j0.5$$

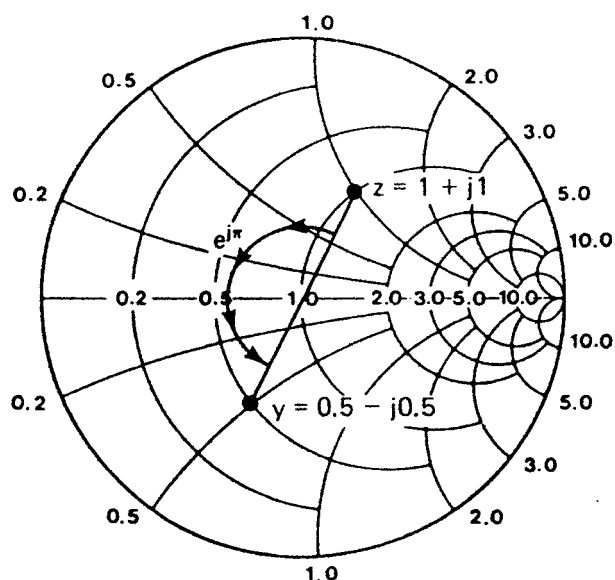


Figure 2.3.1 Conversion of z to y in the Smith chart.

NAME	TITLE	DWG. NO.
SMITH CHART FORM ZY-81-N	ANALOG INSTRUMENTS COMPANY, NEW PROVIDENCE, N.J. 07974	DATE

NORMALIZED IMPEDANCE AND ADMITTANCE COORDINATES

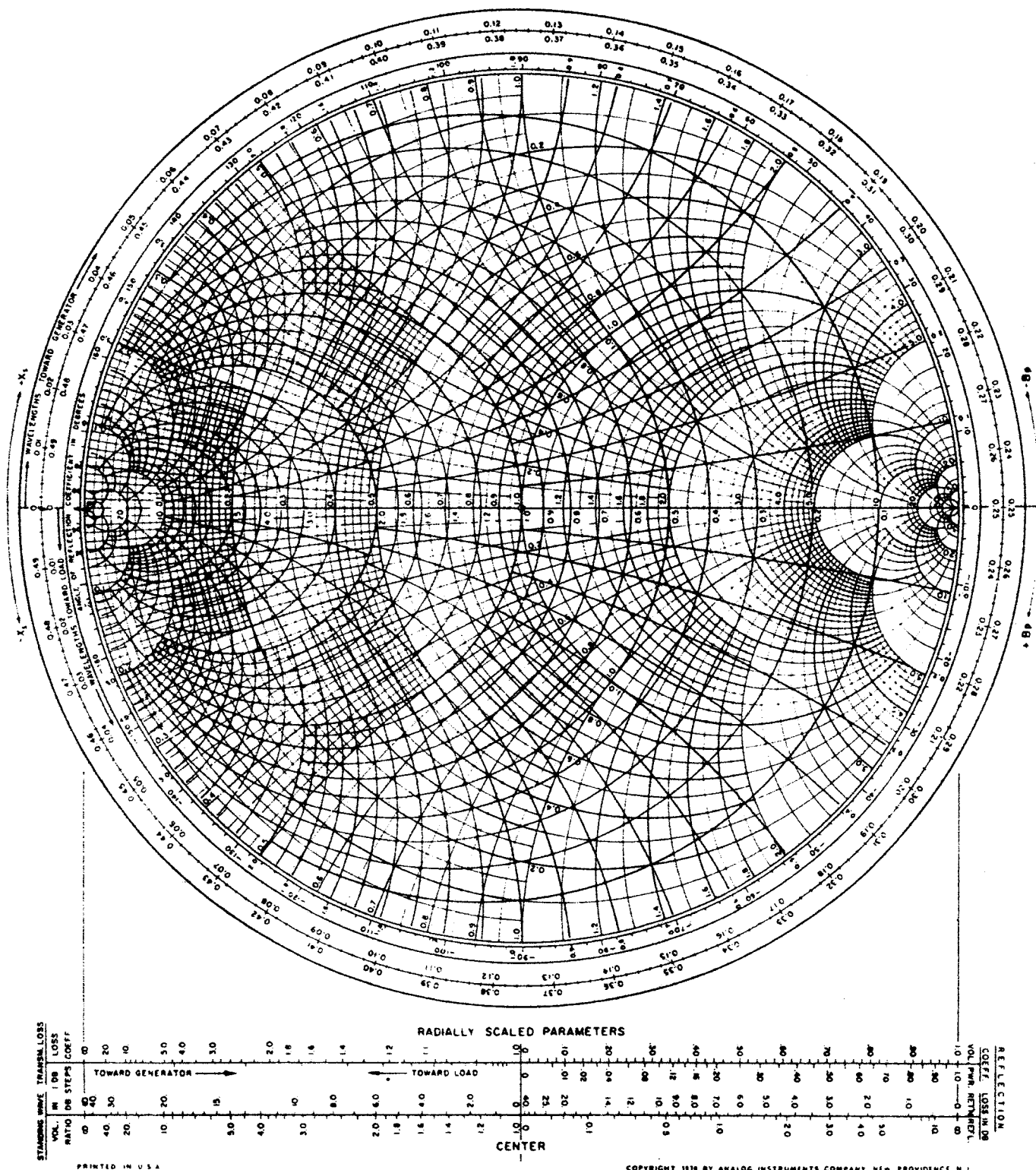


Figure 2.3.2 The normalized impedance and admittance coordinates Smith chart. (Reproduced with permission of Analog Instruments Co., New Providence, N.J.)

The impedance-to-admittance conversion can also be obtained by rotating the Smith chart by 180° and calling the rotated chart an *admittance chart*. The superposition of the original and the rotated chart is known as the *normal-*

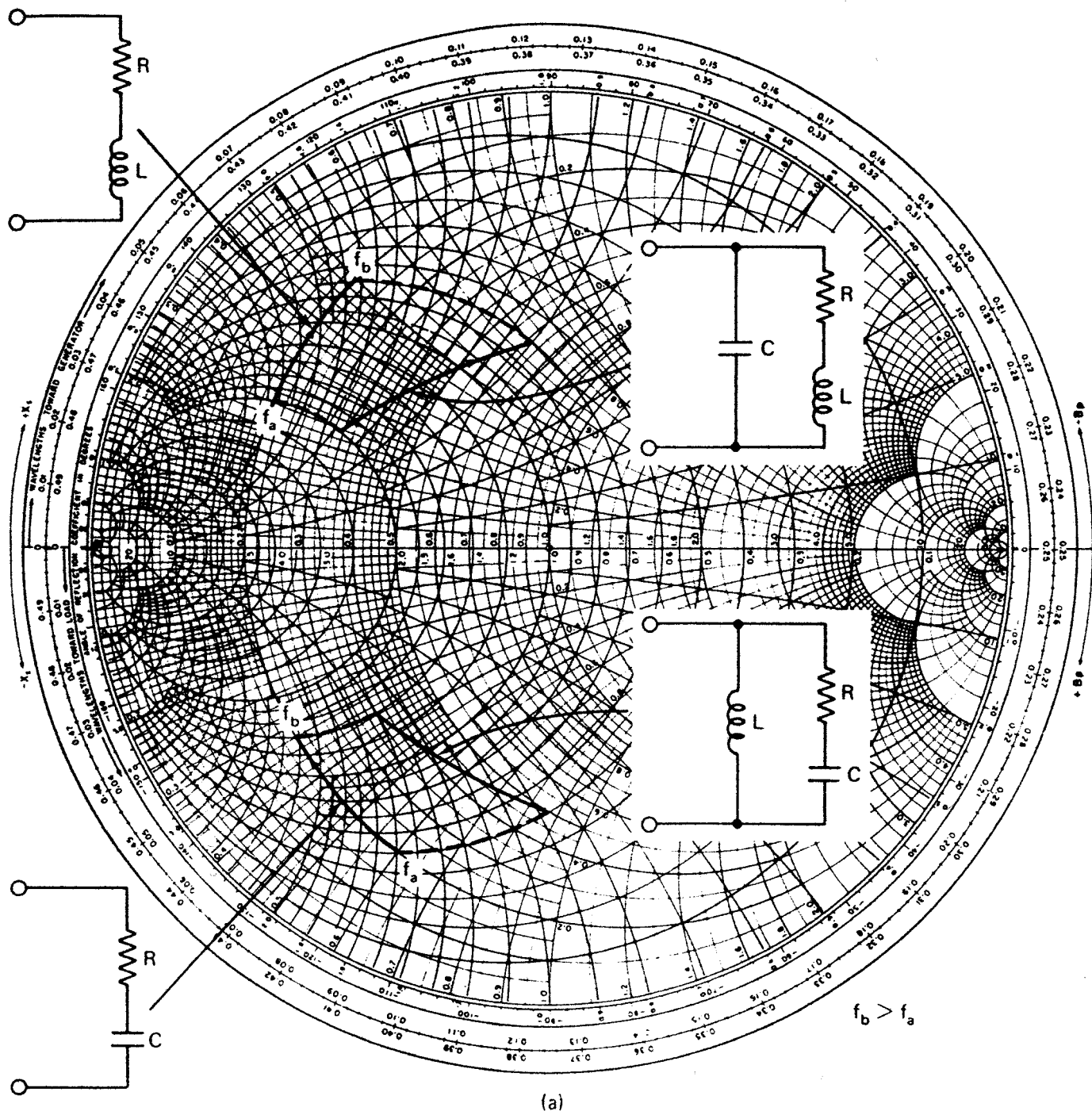


Figure 2.3.3 Characteristics of some networks in the ZY Smith chart.

ized impedance and admittance coordinates Smith chart. We will refer to this Smith chart as the “ZY Smith chart.” The ZY Smith chart is shown in Fig. 2.3.2, where the impedance values are shown in red color and the admittance values in green. (See Figure 2.3.2 on inside cover.)

Observe that the upper half of the chart for the admittance coordinates (i.e., green curves) represents normalized admittances having negative susceptances (i.e., $-jb$) and the lower half represents positive susceptances (i.e., $+jb$). The impedance coordinates (i.e., red curves) are the same as in the Z Smith chart.

Example 2.3.2

Find y for $z = 1 + j1$ using the ZY Smith chart.

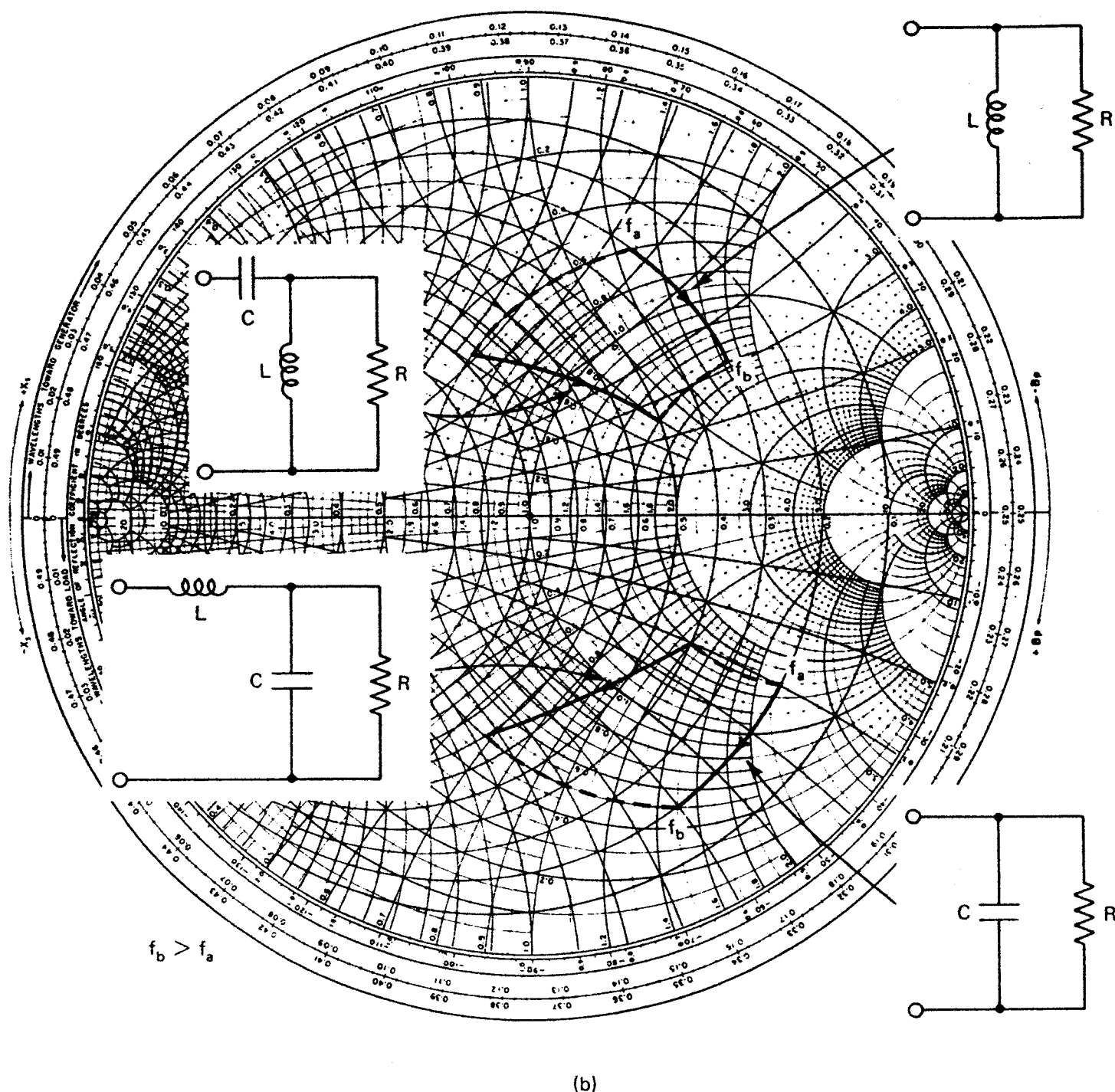


Figure 2.3.3 (continued)

Solution. We can locate in the ZY Smith chart in Fig. 2.3.2 the point $z = 1 + j1$ (red curves), and read directly from the green curves the value $y = 0.5 - j0.5$.

In Section 1.9 some equivalent circuits were obtained from the Smith chart impedance plot of the S parameters. Some practical equivalent circuits are shown in Fig. 2.3.3. Some of these circuits can be used to represent equivalent input and output models of transistors.

2.4 IMPEDANCE MATCHING NETWORKS

The need for matching networks arises because amplifiers, in order to deliver maximum power to a load, or to perform in a certain desired way, must be properly terminated at both the input and the output ports. Figure 2.4.1 illustrates a typical situation in which a transistor, in order to deliver maximum power to the 50- Ω load, must have the terminations Z_s and Z_L . Although many different types of matching networks can be designed, the eight *ell* sections shown in Fig. 2.4.2 are not only simple to design, but quite practical.

The ZY Smith chart can be used conveniently in the design of matching networks. The effect of adding a series reactance element to an impedance or a parallel susceptance element to an admittance, in the ZY Smith chart, is illustrated in the following example.

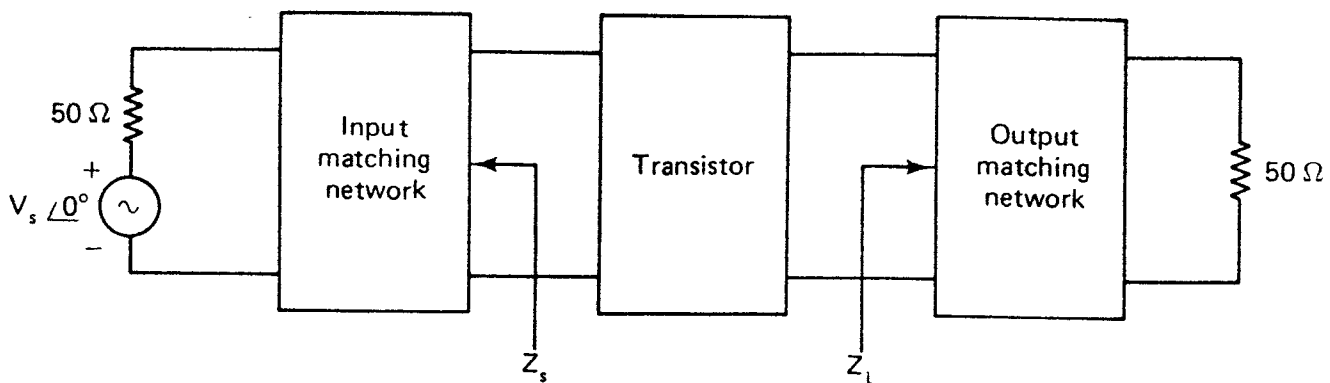


Figure 2.4.1 Block diagram of a microwave amplifier.

Example 2.4.1

(a) Illustrate the effect of adding a series inductor L ($z_L = j0.8$) to an impedance z ($z = 0.3 - j0.3$) in the ZY Smith chart.

Solution. Figure 2.4.3 shows that the effect of adding a series inductance with $z_L = j0.8$ is to move along a constant-resistance circle from a reactance value of -0.3 to a reactance of 0.5 . In other words, the motion is in a clockwise direction along a constant-resistance circle.

(b) Illustrate the effect of adding a series capacitor C ($z_C = -j0.8$) to an impedance z ($z = 0.3 - j0.3$) in the ZY Smith chart.

Solution. Figure 2.4.4 shows that the effect of adding a series capacitor with $z_C = -j0.8$ is to move along a constant-resistance circle from a reactance value of -0.3 to a reactance of -1.1 . In other words, the motion is in a counterclockwise direction along a constant-resistance circle.

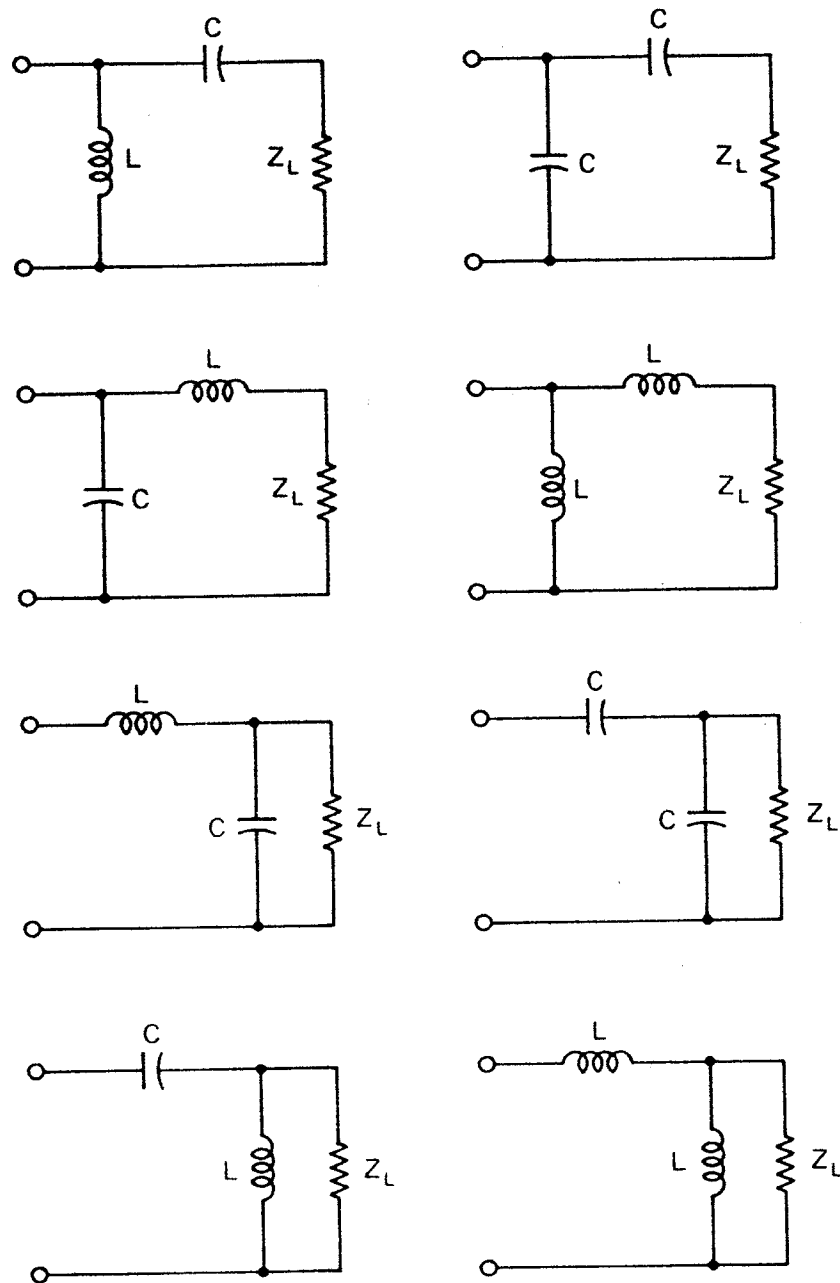
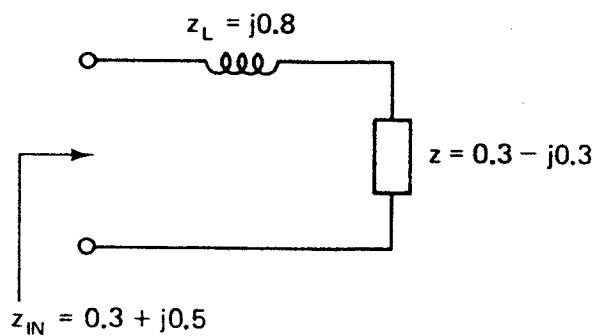


Figure 2.4.2 Matching networks.

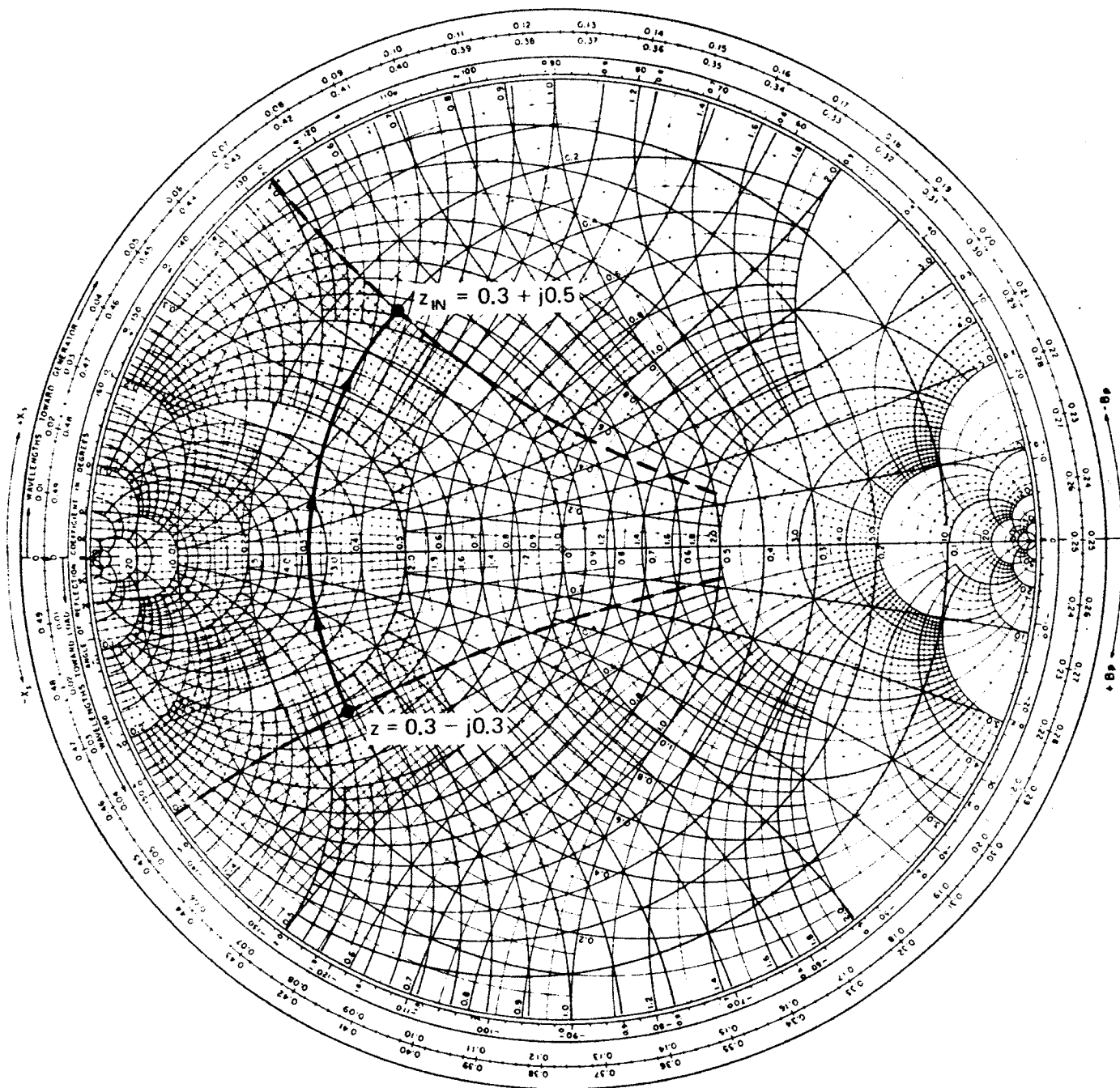
(c) Illustrate the effect of adding a shunt inductor L ($y_L = -j2.4$) to an admittance y ($y = 1.6 + j1.6$) in the ZY Smith chart.

Solution. Figure 2.4.5 shows that the effect of adding a shunt inductor with $y_L = -j2.4$ is to move along a constant-conductance circle from a susceptance of 1.6 to a susceptance of -0.8 . In other words, the motion is in a counterclockwise direction along a constant-conductance circle.

(d) Illustrate the effect of adding a shunt capacitor C ($y_C = j3.4$) to an admittance y ($y = 1.6 + j1.6$) in the ZY Smith chart.

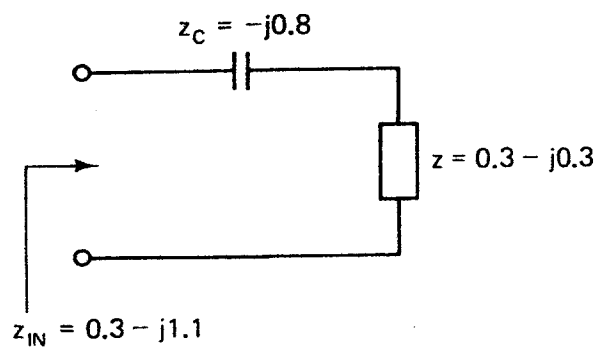


(a)

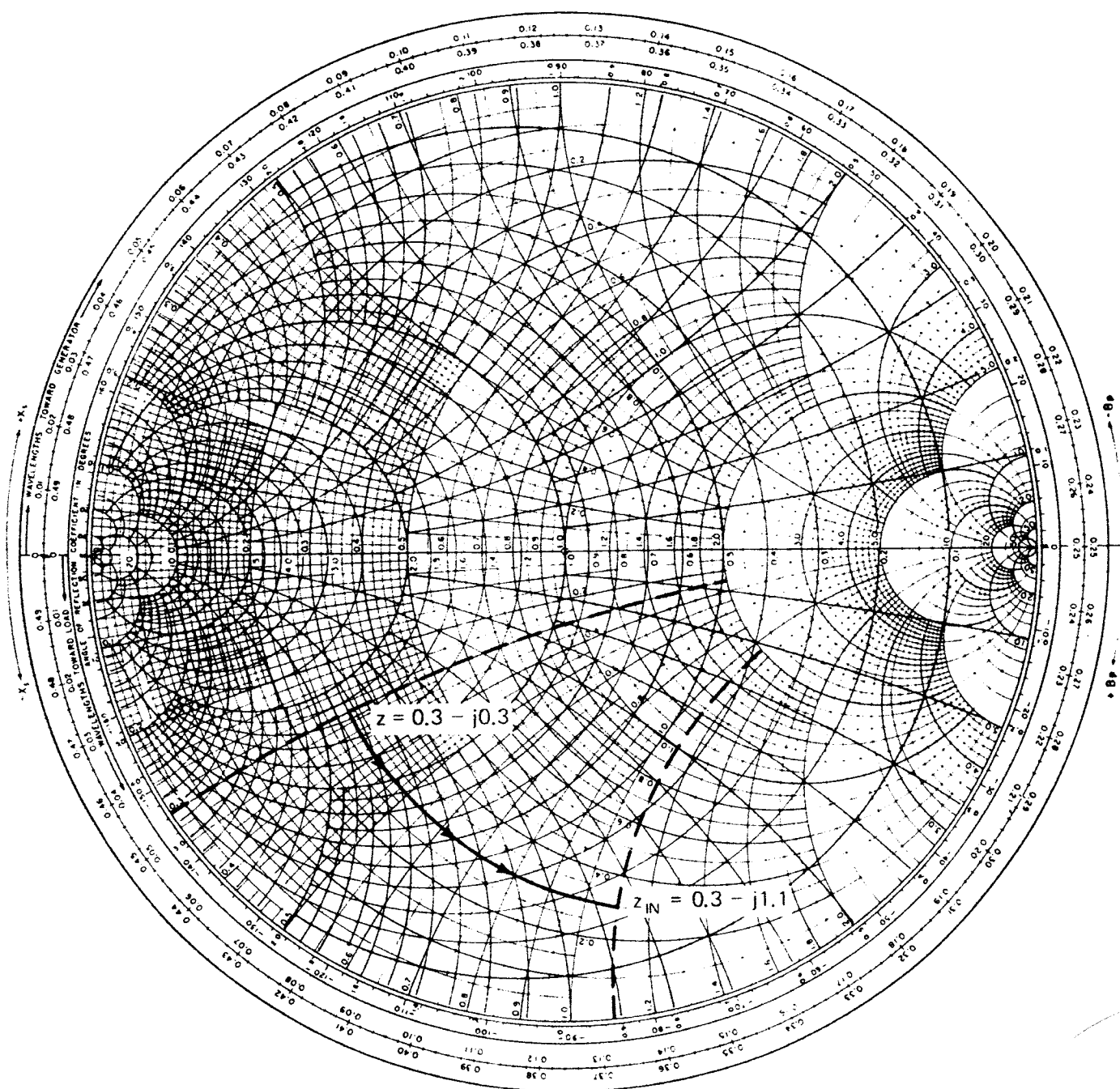


(b)

Figure 2.4.3 Effect of adding a series inductor to an impedance in the ZY Smith chart.

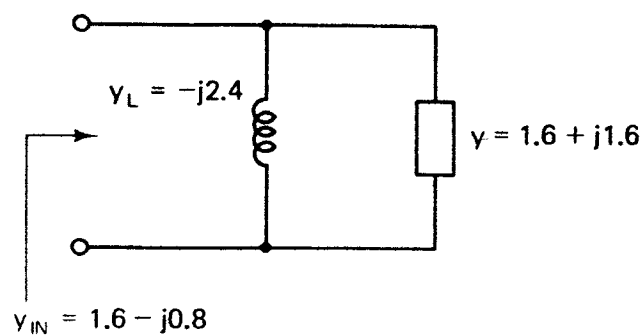


(a)

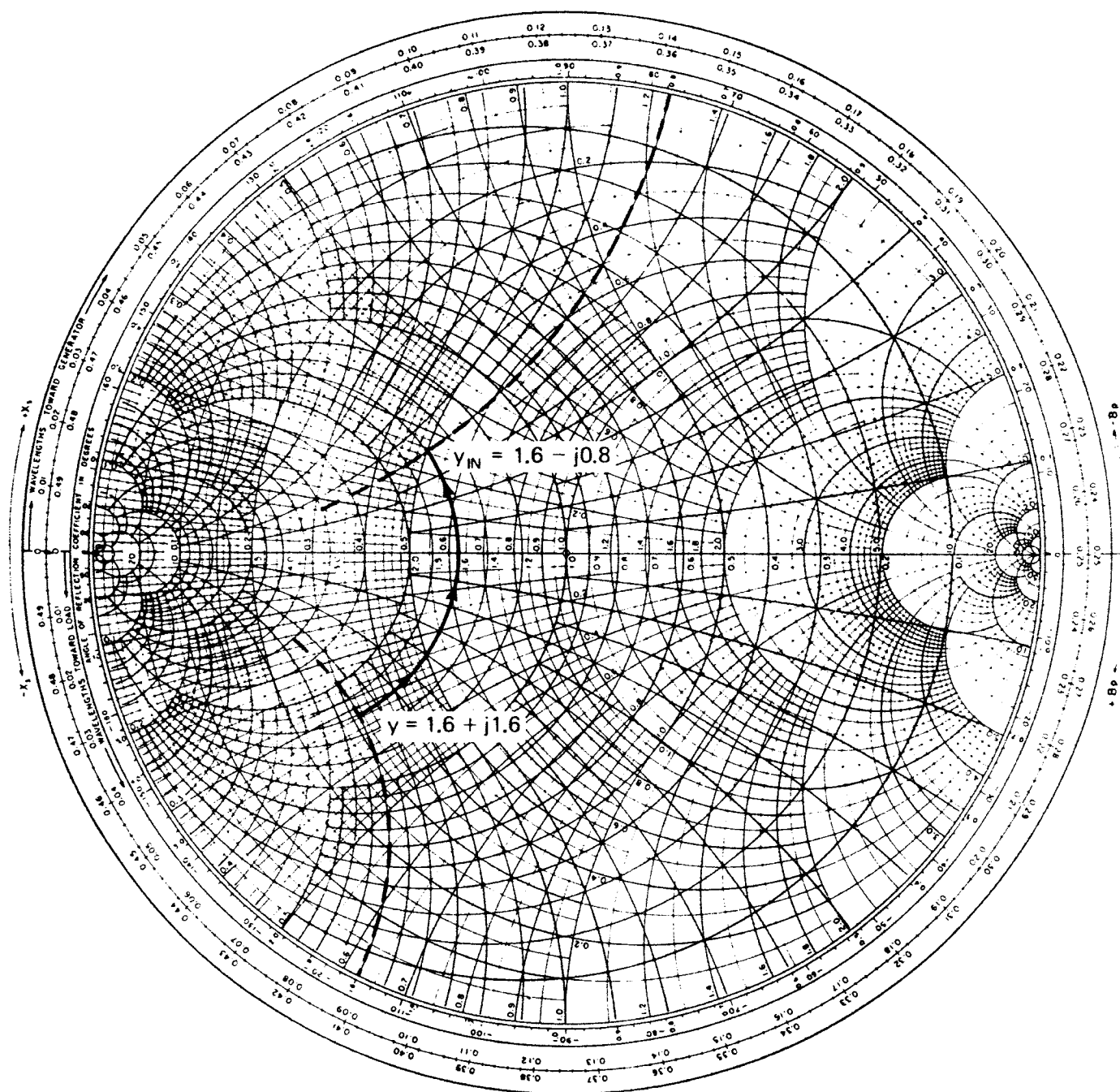


(b)

Figure 2.4.4 Effect of adding a series capacitor to an impedance in the ZY Smith chart.

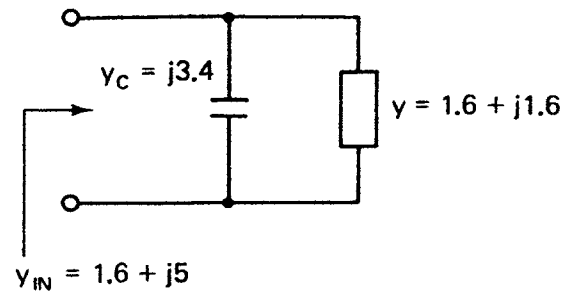


(a)

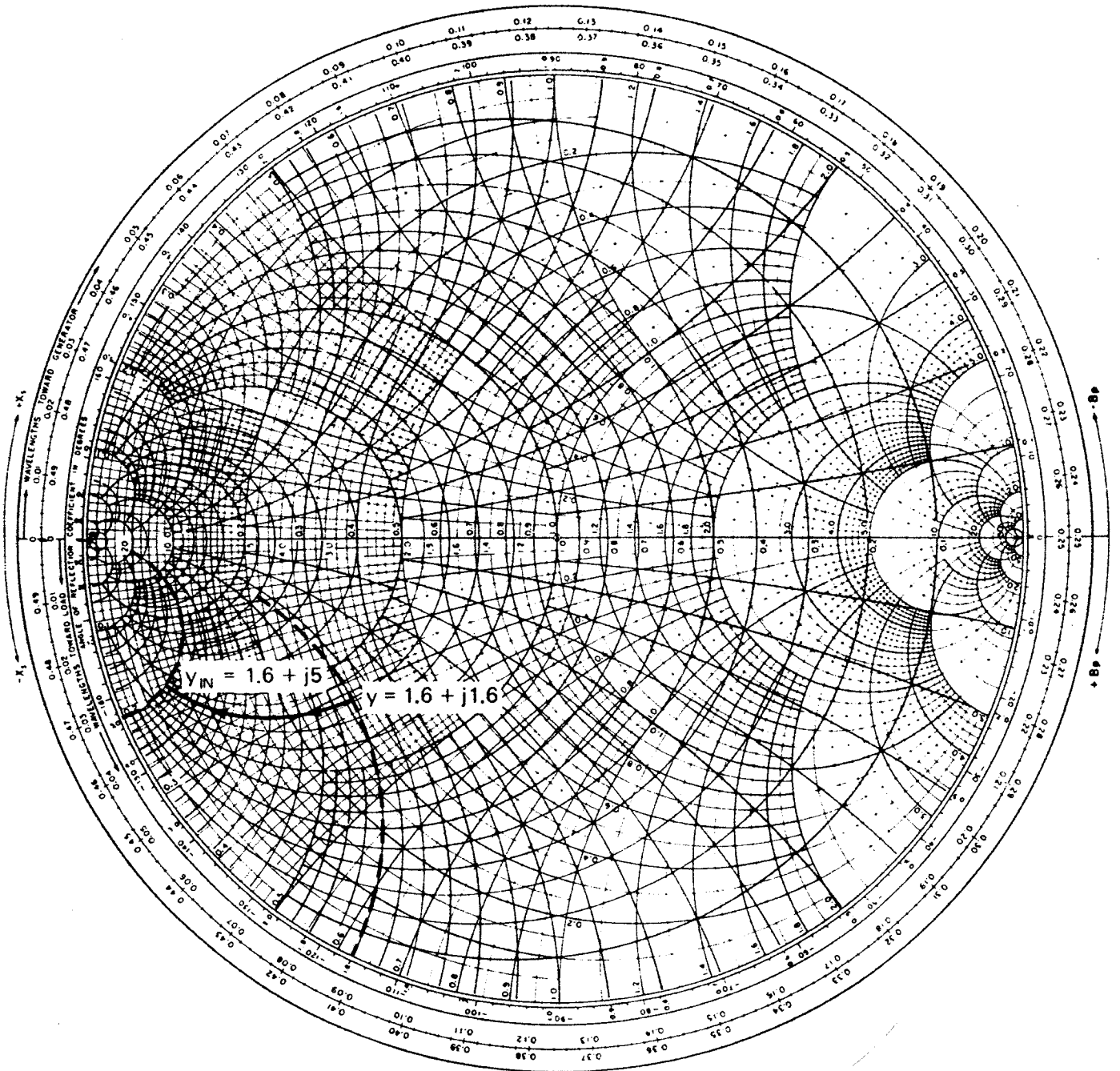


(b)

Figure 2.4.5 Effect of adding a shunt inductor to an admittance in the ZY Smith chart.



(a)



(b)

Figure 2.4.6 Effect of adding a shunt capacitor to an admittance in the ZY Smith chart.

Solution. Figure 2.4.6 shows that the effect of adding a shunt capacitor with $y_C = j3.4$ is to move along a constant-conductance circle from a susceptance of 1.6 to a susceptance of 5. In other words, the motion is in a clockwise direction along a constant-conductance circle.

In conclusion, adding a series reactance produces a motion along a constant-resistance circle in the ZY Smith chart, and adding shunt susceptance produces a motion along a constant-conductance circle in the ZY Smith chart. The four types of motions are illustrated in Fig. 2.4.7.

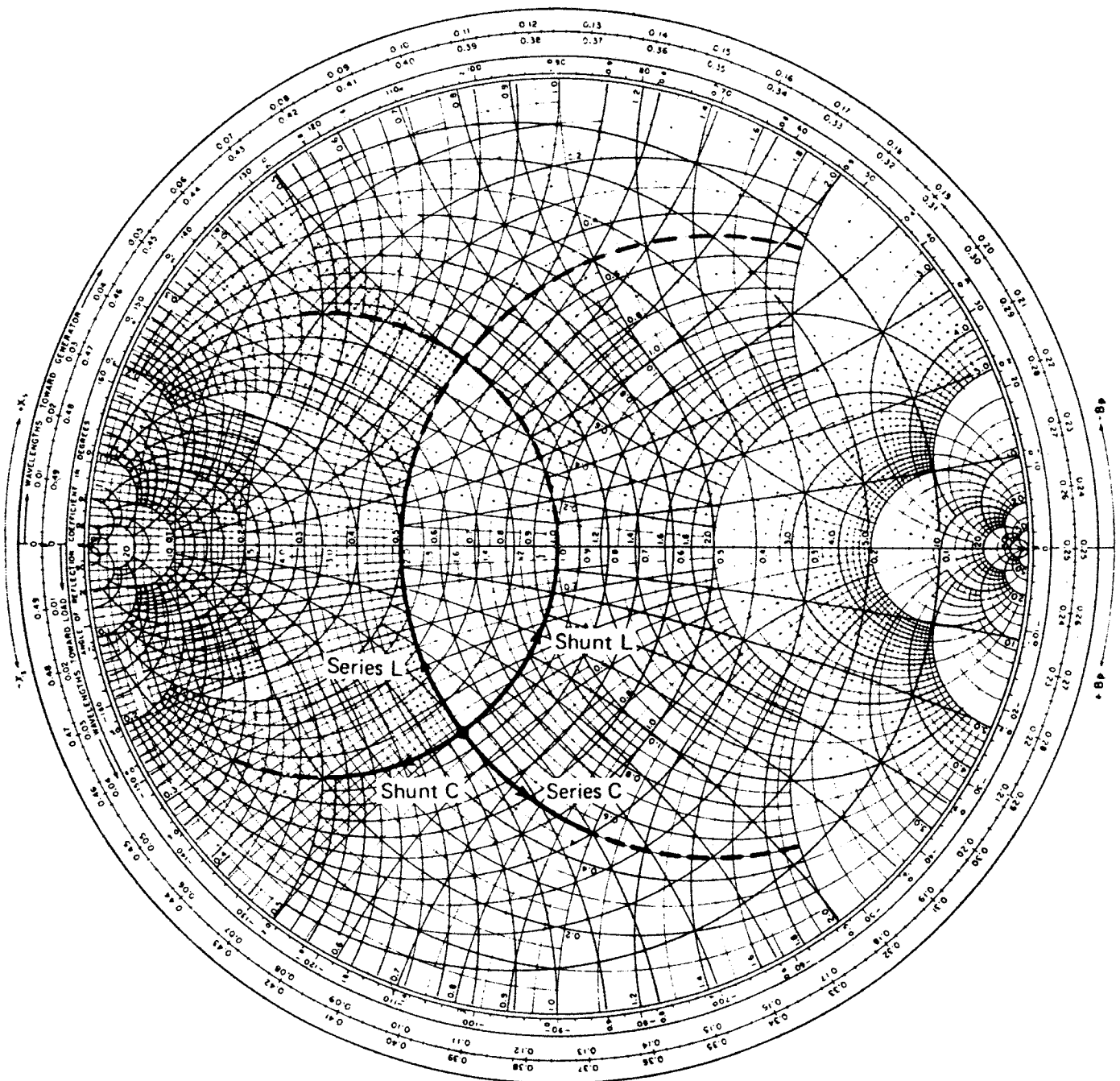


Figure 2.4.7 Effect of adding series and shunt elements in the ZY Smith chart.

Designing a matching network in the ZY Smith chart consists of moving along a constant-resistance or constant-conductance circle from one value of impedance or admittance to another. Each motion along a constant-resistance or constant-conductance circle gives the value of an appropriate element. The following examples illustrate the use of the ZY Smith chart in the design of matching networks.

Example 2.4.2

A load $Z_{\text{LOAD}} = 10 + j10 \, \Omega$ is to be matched to a $50\text{-}\Omega$ line. Design two matching networks and specify the values of L and C at a frequency of 500 MHz.

Solution. Selecting the series L –shunt C network shown in Fig. 2.4.8a, the matching network is designed as shown in Fig. 2.4.8b. (See Figure 2.4.8b on inside cover.) The motion from point A [i.e., $z_{\text{LOAD}} = (10 + j10)/50 = 0.2 + j0.2$] to point B is along a constant-resistance circle, and we obtain for the inductor impedance $z_L = j0.4 - j0.2 = j0.2$. Observe that point B is along the unit constant-conductance circle. The admittance at point B is $y_B = 1 - j2$. The motion from point B to point C (i.e., the origin) is along a constant-conductance circle, and we obtain the capacitor admittance $y_C = 0 - (-j2) = j2$ (or $z_C = 1/j2 = -j0.5$). Therefore, at point C , $y_{\text{IN}} = z_{\text{IN}} = 1$ (or $Z_{\text{IN}} = 50 \, \Omega$) and the network is matched to a $50\text{-}\Omega$ line. At 500 MHz, the value of L is

$$L = \frac{10}{2\pi(500 \times 10^6)} = 3.18 \, \text{nH}$$

and the value of C is

$$C = \frac{1}{25(2\pi)500 \times 10^6} = 12.74 \, \text{pF}$$

The matching network at 500 MHz is shown in Fig. 2.4.8c.

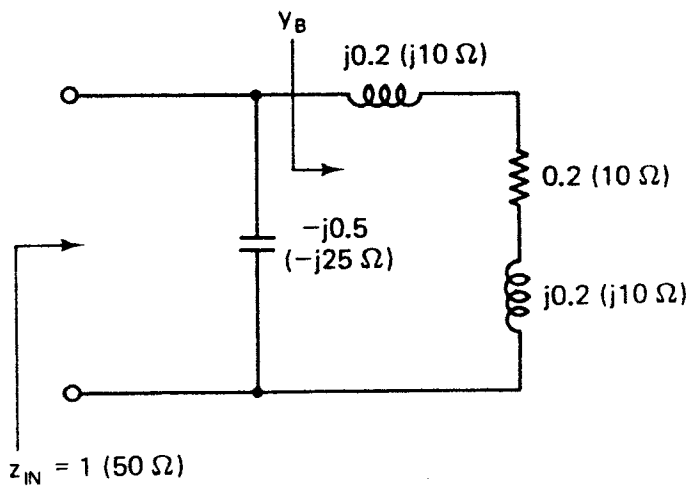
The second matching network is shown in Fig. 2.4.9a and the ZY Smith chart design in Fig. 2.4.9b. (See Figure 2.4.9b on inside cover.) The motion from A to B in Fig. 2.4.9b is along a constant-resistance circle; therefore, the impedance of the series capacitor is $z_C = -j0.4 - j0.2 = -j0.6$. The motion from B to C is along a constant-conductance circle; therefore, the admittance of the shunt inductor is $y_L = 0 - j2 = -j2$ (or $z_L = 1/-j2 = j0.5$). The design at 500 MHz is shown in Fig. 2.4.9c.

Example 2.4.3

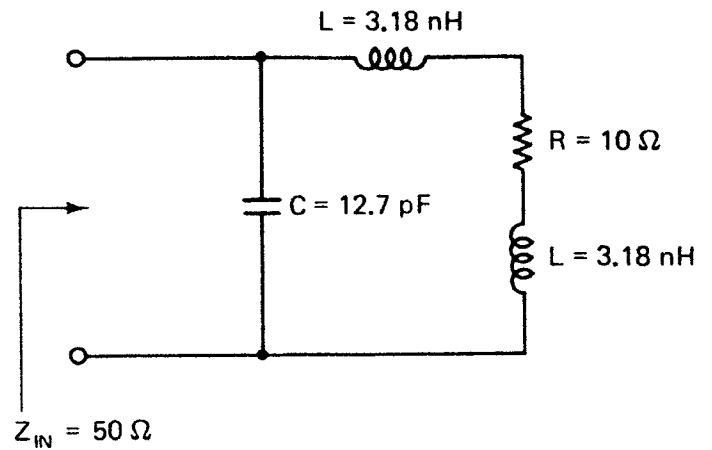
Design a matching network to transform a $50\text{-}\Omega$ load to the admittance $Y_{\text{OUT}} = (8 - j12) \times 10^{-3} \, \text{S}$.

Solution. Figure 2.4.10a illustrates a motion in the ZY Smith chart from the origin (i.e., $z_{\text{LOAD}} = 50/50 = 1$) to $y_{\text{OUT}} = 50(8 - j12) \times 10^{-3} = 0.4 - j0.6$. (See Figure 2.4.10a on inside cover.) The motion from A to B produces a series capacitor having an impedance of $z_C = -j1.21$. The motion from B to C produces a shunt inductor having an admittance of $y_L = -j0.6 - j0.49 = -j1.09$ (or $z_L = 1/-j1.09 = j0.917$). The matching network is shown in Fig. 2.4.10b.

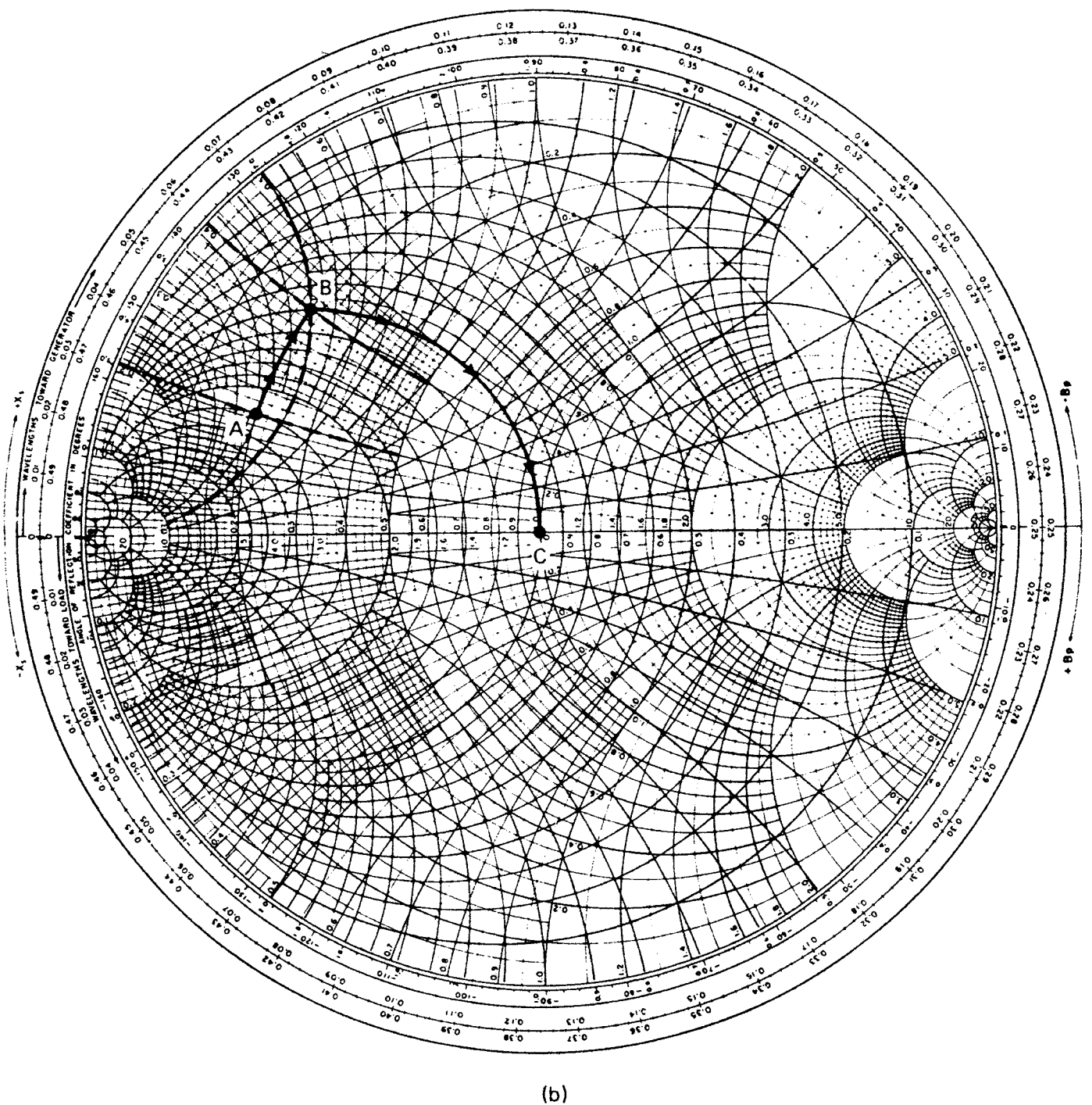
Sometimes a specific matching network cannot be used to accomplish a given match. For example, any load impedance falling in the marked region in



(a)

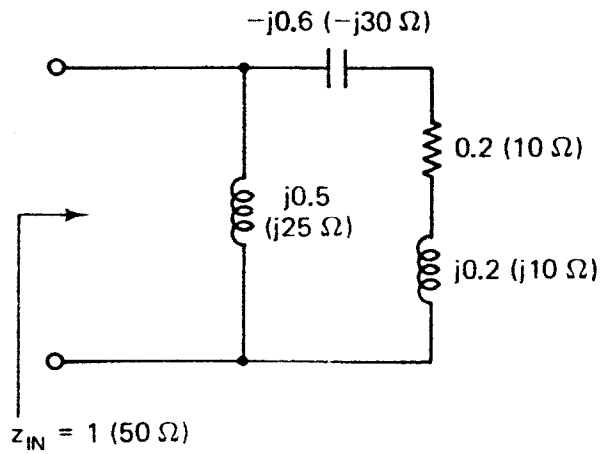


(c)

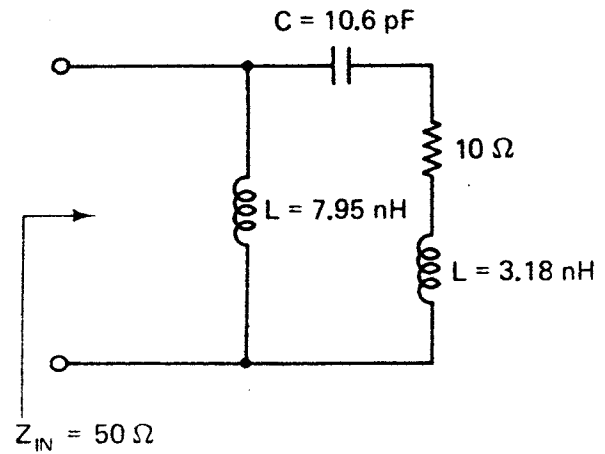


(b)

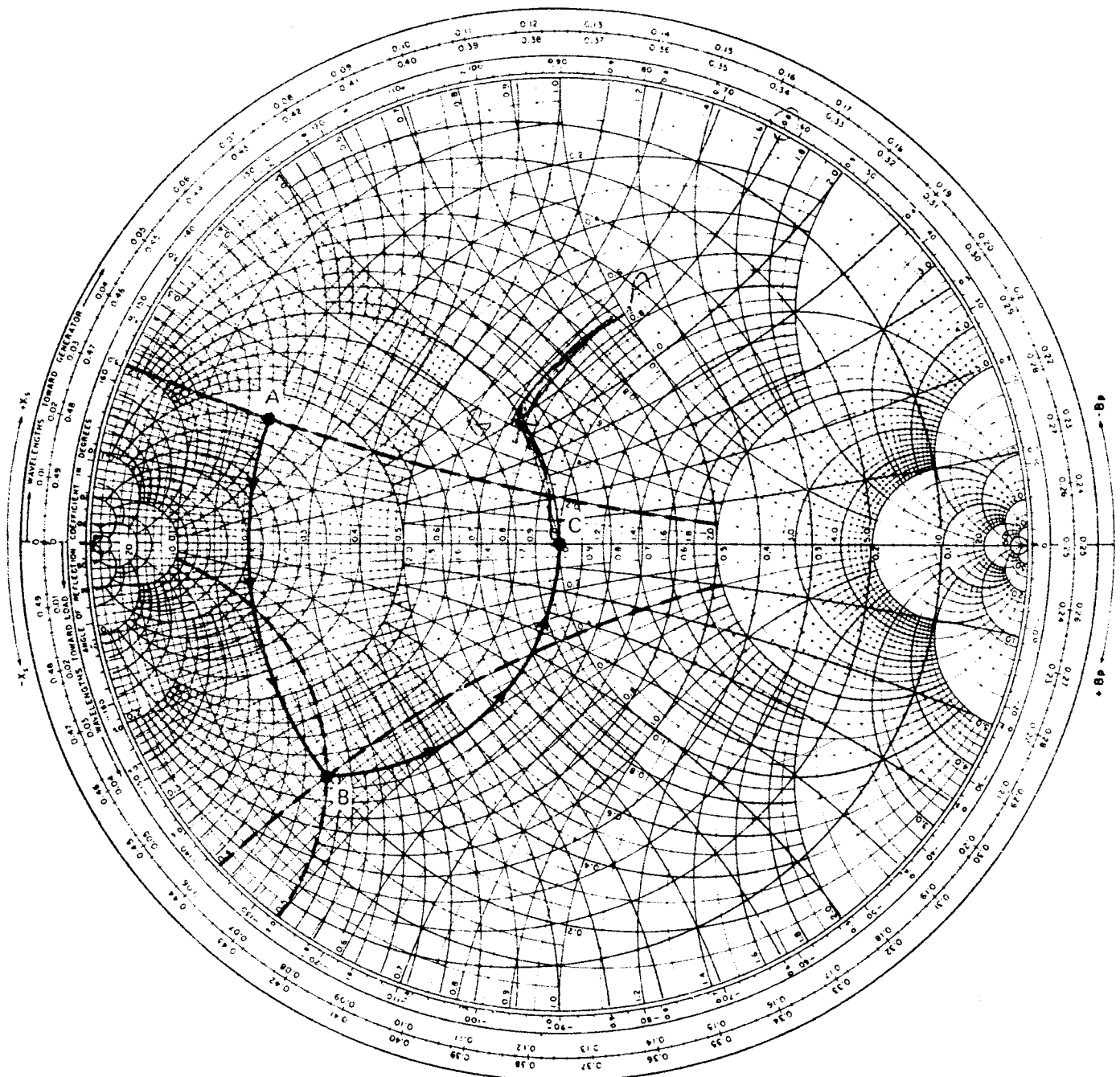
Figure 2.4.8 Design of a series L-shunt C matching network.



(a)

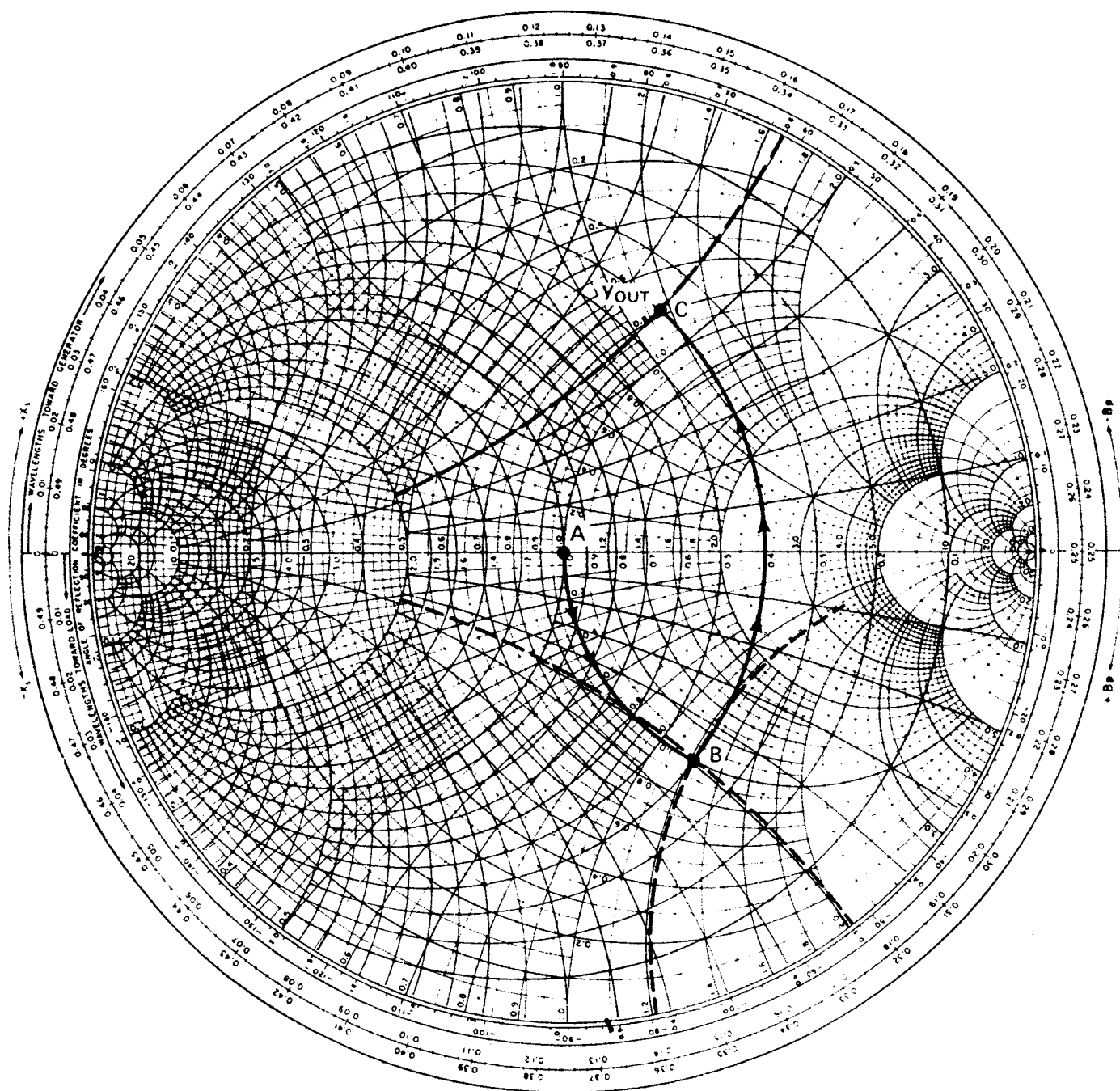


(c)

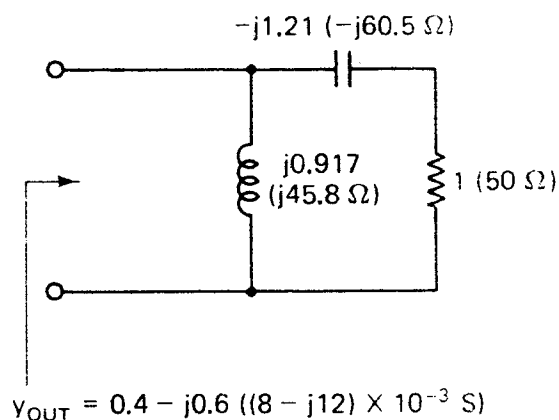


(b)

Figure 2.4.9 Design of a series C-shunt L matching network.

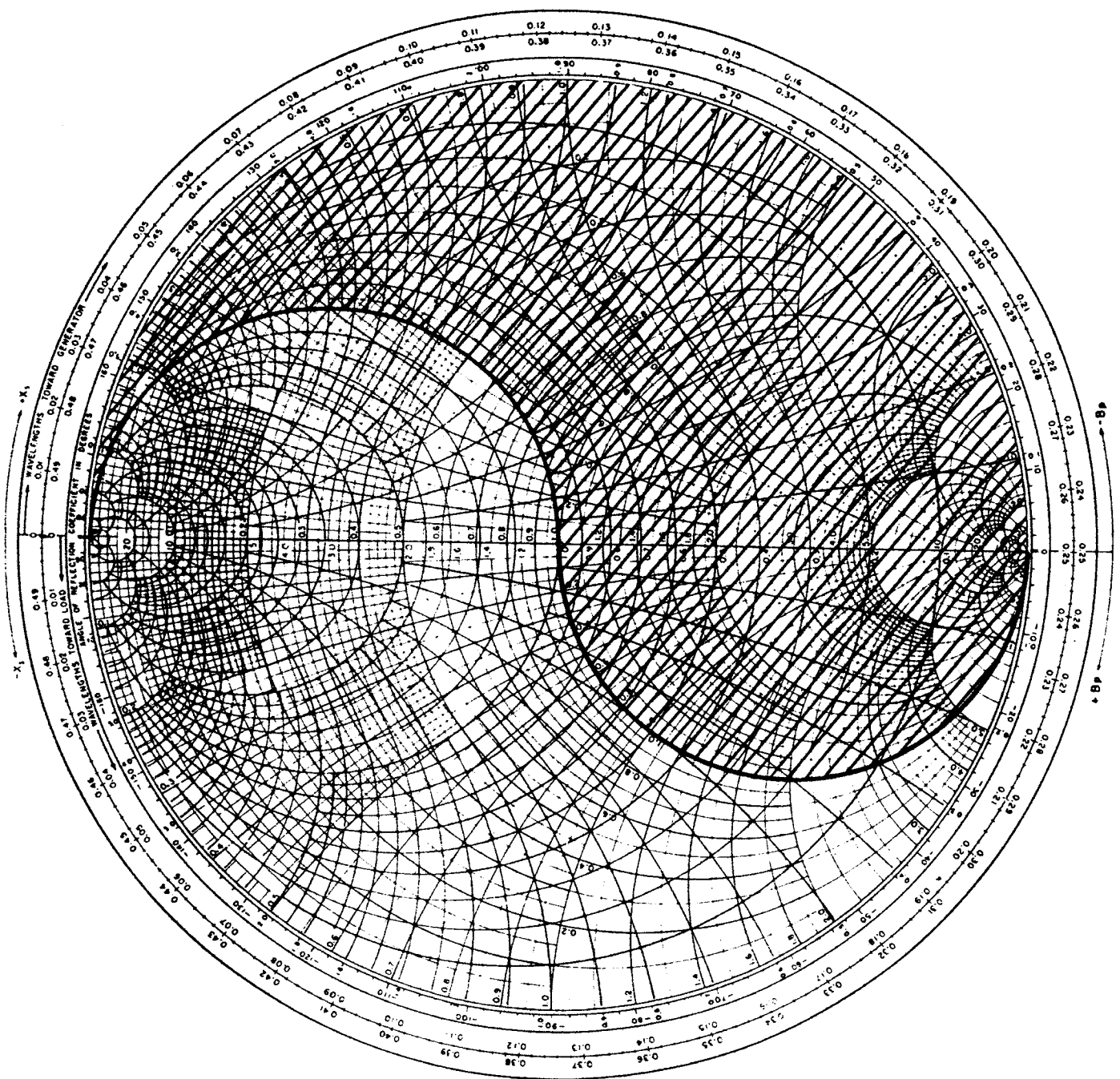


(a)

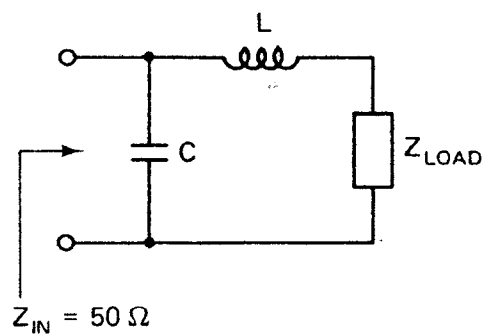


(b)

Figure 2.4.10 Matching a 50-Ω load to a given y_{OUT} using a series C -shunt L matching network.



(a)



(b)

Figure 2.4.11 Forbidden region in the ZY Smith chart to match a given Z_{LOAD} to $50\ \Omega$ using a series L -shunt C matching network.

Fig. 2.4.11a cannot be matched to $50\ \Omega$ with the network in Fig. 2.4.11b because adding a series L produces motion, in a clockwise direction, away from any constant-conductance circle that passes through the origin.

2.5 MICROSTRIP MATCHING NETWORKS

Microstrip lines are used extensively in building microwave transistor amplifiers because they are easily fabricated using printed-circuit techniques. Network interconnections and the placement of lumped and transistor devices are easily made on its metal surface. The superior performance characteristics of the microstrip line makes it one of the most important medium of transmission in microwave transistor amplifiers and in microwave integrated-circuit technology.

A microstrip line is by definition a transmission line consisting of a strip conductor and a ground plane separated by a dielectric medium. Figure 2.5.1 illustrates the microstrip geometry. The dielectric material serves as a substrate and it is sandwiched between the strip conductor and the ground plane. Some typical dielectric substrates are: Duroid, a trademark of Rogers Corporation (Chandler, Arizona), ($\epsilon = 2.56\epsilon_0$), quartz ($\epsilon = 3.78\epsilon_0$), alumina ($\epsilon = 9.7\epsilon_0$), and silicon ($\epsilon = 11.7\epsilon_0$). The relative dielectric constant of the substrate, ϵ_r , follows from $\epsilon = \epsilon_r \epsilon_0$, where $\epsilon_0 = 8.854 \times 10^{-12}\ \text{F/m}$.

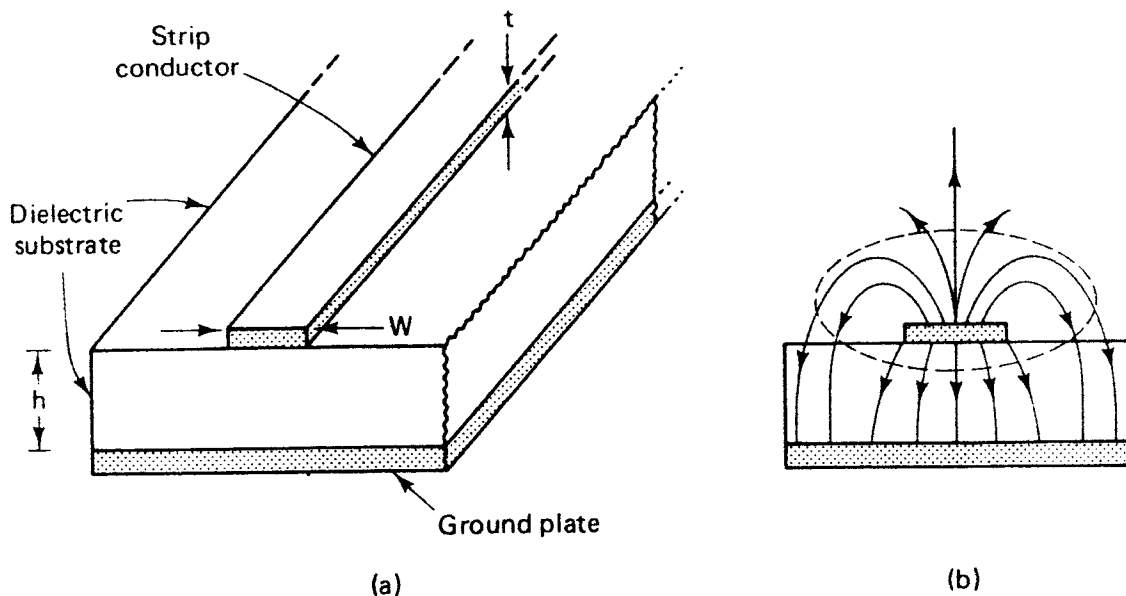


Figure 2.5.1 Microstrip geometry and field configuration. In (b), the solid lines represent electric field lines and the dashed line represents a magnetic field line.

The electromagnetic field lines in the microstrip are not contained entirely in the substrate. Therefore, the propagating mode in the microstrip is not a pure transverse electromagnetic mode (TEM mode) but a quasi-TEM. As-

suming a quasi-TEM mode of propagation in the microstrip line, the phase velocity is given by

$$v_p = \frac{c}{\sqrt{\epsilon_{ff}}} \quad (2.5.1)$$

where c is the speed of light (i.e., 3×10^8 m/s) and ϵ_{ff} is the effective relative dielectric constant of the dielectric substrate. The effective relative dielectric constant of the microstrip is related to the relative dielectric constant of the dielectric substrate, and also takes into account the effect of the external electromagnetic fields.

The characteristic impedance of the microstrip line is given by

$$Z_o = \frac{1}{v_p C} \quad (2.5.2)$$

where C is the capacitance per unit length of the microstrip. The wavelength in the microstrip line is given by

$$\lambda = \frac{v_p}{f} = \frac{c}{f \sqrt{\epsilon_{ff}}} = \frac{\lambda_0}{\sqrt{\epsilon_{ff}}} \quad (2.5.3)$$

where λ_0 is the free-space wavelength.

As seen from (2.5.1), (2.5.2), and (2.5.3), the evaluation of v_p , Z_o , and λ in a microstrip line requires the evaluation of ϵ_{ff} and C . There are different methods for determining ϵ_{ff} and C and, of course, closed-form expressions are of great importance in microstrip-line design. The evaluation of ϵ_{ff} and C based on a quasi-TEM mode is accurate for design purposes at lower microwave frequencies. However, at higher microwave frequencies the longitudinal components of the electromagnetic fields are significant and the quasi-TEM assumption is no longer valid.

A useful set of relations for the characteristic impedance, assuming zero or negligible thickness of the strip conductor (i.e., $t/h < 0.005$), are [2.1]:

For $W/h \leq 1$:

$$Z_o = \frac{60}{\sqrt{\epsilon_{ff}}} \ln \left(8 \frac{h}{W} + 0.25 \frac{W}{h} \right) \quad (2.5.4)$$

where

$$\epsilon_{ff} = \frac{\epsilon_r + 1}{2} + \frac{\epsilon_r - 1}{2} \left[\left(1 + 12 \frac{h}{W} \right)^{-1/2} + 0.04 \left(1 - \frac{W}{h} \right)^2 \right] \quad (2.5.5)$$

For $W/h \geq 1$:

$$Z_o = \frac{120\pi/\sqrt{\epsilon_{ff}}}{W/h + 1.393 + 0.667 \ln(W/h + 1.444)} \quad (2.5.6)$$

where

$$\epsilon_{eff} = \frac{\epsilon_r + 1}{2} + \frac{\epsilon_r - 1}{2} \left(1 + 12 \frac{h}{W} \right)^{-1/2} \quad (2.5.7)$$

Plots of the characteristic impedance, as well as the normalized wavelength, as a function of W/h are shown in Figs. 2.5.2 and 2.5.3.

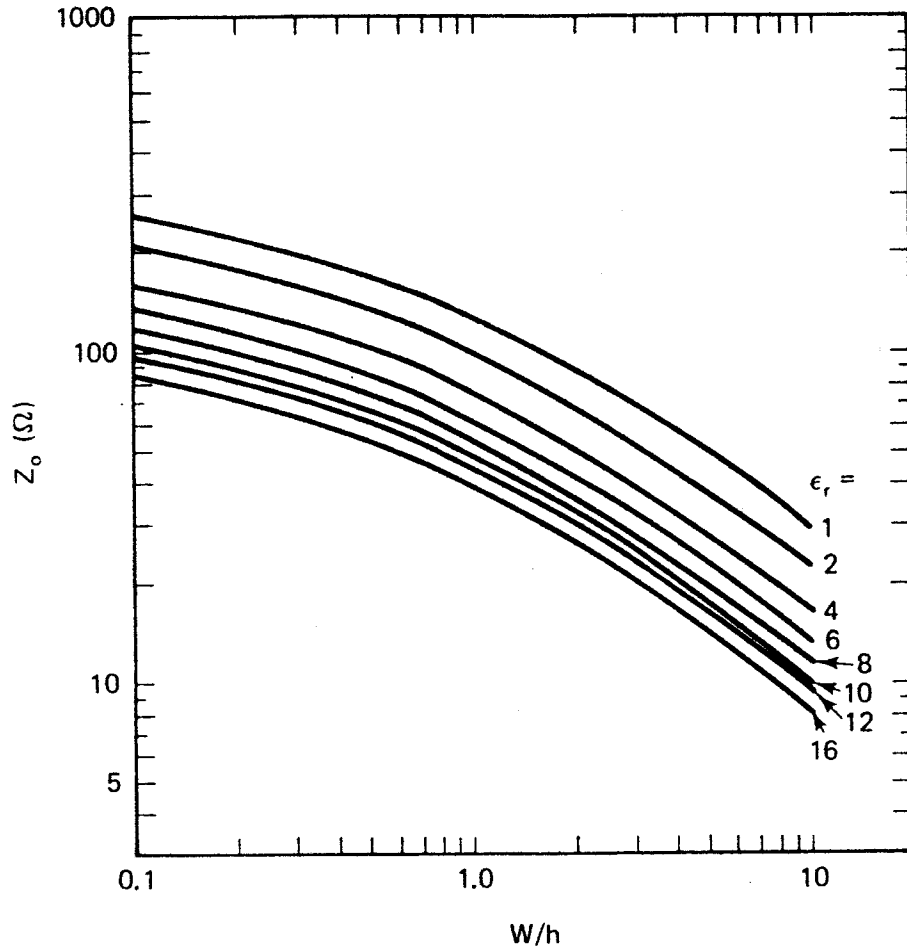


Figure 2.5.2 Characteristic impedance of the microstrip line versus W/h . (From H. Sobol [2.2]; copyright 1971, IEEE; reproduced with permission of IEEE.)

Based on the results in (2.5.3), (2.5.5), and (2.5.7) and/or in experimental data, the wavelength in the microstrip line, assuming zero or negligible thickness (i.e., $t/h \leq 0.005$) for the strip conductor, is given by the relations [2.3]:

For $W/h \geq 0.6$:

$$\lambda = \frac{\lambda_0}{\sqrt{\epsilon_r}} \left[\frac{\epsilon_r}{1 + 0.63(\epsilon_r - 1)(W/h)^{0.1255}} \right]^{1/2} \quad (2.5.8)$$

For $W/h < 0.6$:

$$\lambda = \frac{\lambda_0}{\sqrt{\epsilon_r}} \left[\frac{\epsilon_r}{1 + 0.6(\epsilon_r - 1)(W/h)^{0.0297}} \right]^{1/2} \quad (2.5.9)$$

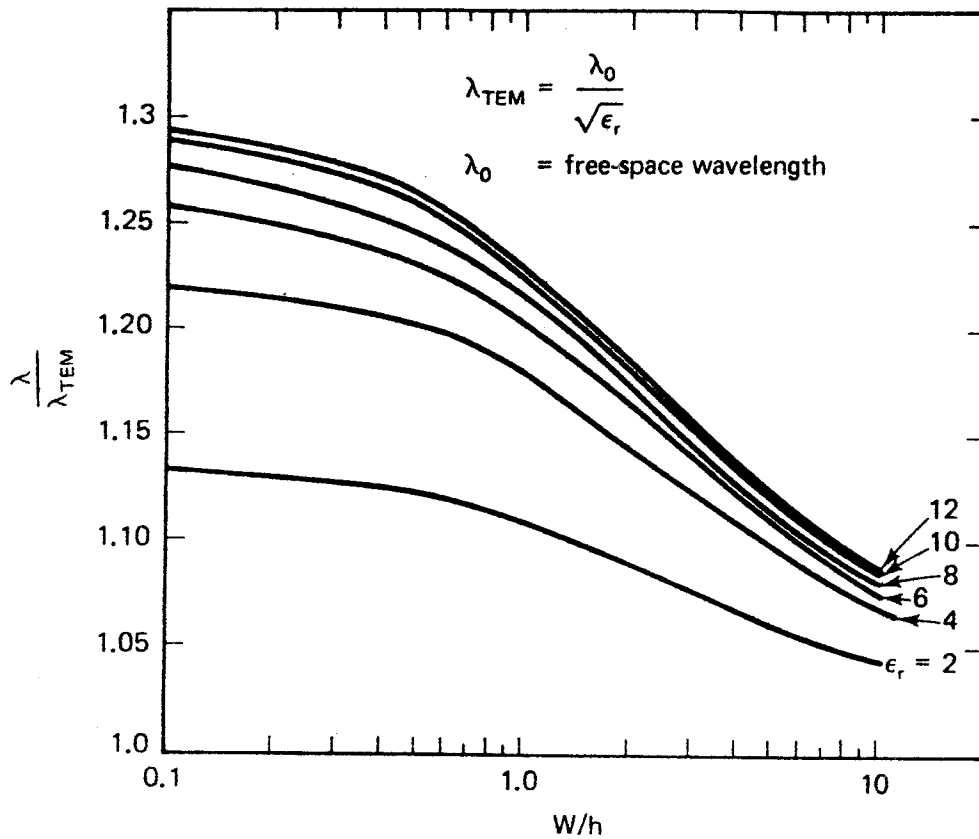


Figure 2.5.3 Normalized wavelength of the microstrip line versus W/h . (From H. Sobol [2.2]; copyright 1971, IEEE; reproduced with permission of IEEE.)

For design purposes a set of equations relating Z_o and ϵ_r to the ratio W/h of the microstrip line is desirable. Assuming zero or negligible thickness of the strip conductor (i.e., $t/h \leq 0.005$), the expressions are [2.2]:

For $W/h \leq 2$:

$$\frac{W}{h} = \frac{8e^A}{e^{2A} - 2} \quad (2.5.10)$$

For $W/h \geq 2$:

$$\frac{W}{h} = \frac{2}{\pi} \left\{ B - 1 - \ln(2B - 1) + \frac{\epsilon_r - 1}{2\epsilon_r} \left[\ln(B - 1) + 0.39 - \frac{0.61}{\epsilon_r} \right] \right\} \quad (2.5.11)$$

where

$$A = \frac{Z_o}{60} \sqrt{\frac{\epsilon_r + 1}{2}} + \frac{\epsilon_r - 1}{\epsilon_r + 1} \left(0.23 + \frac{0.11}{\epsilon_r} \right)$$

and

$$B = \frac{377\pi}{2Z_o\sqrt{\epsilon_r}}$$

The zero or negligible thickness formulas given in (2.5.4) to (2.5.11) can be modified to include the thickness of the strip conductor. The first-order effect of a strip conductor of finite thickness t is to increase the capacitance. Therefore, an approximate correction is made by replacing the strip width W by the effective width W_{eff} . The following relation for W_{eff}/h are useful when $t < h$ and $t < W/2$:

For $W/h \geq 1/2\pi$:

$$\frac{W_{\text{eff}}}{h} = \frac{W}{h} + \frac{t}{\pi h} \left(1 + \ln \frac{2h}{t} \right)$$

For $W/h \leq 1/2\pi$:

$$\frac{W_{\text{eff}}}{h} = \frac{W}{h} + \frac{t}{\pi h} \left(1 + \ln \frac{4\pi W}{t} \right)$$

The restrictions $t < h$ and $t < W/2$ are usually satisfied since for dielectric substrates a typical thickness is $t = 0.002$ in.

The formulas presented thus far are valid at frequencies where the quasi-TEM assumption can be made. When the quasi-TEM assumption is not valid, ϵ_{ff} and Z_o are functions of frequency and, therefore, the microstrip line becomes dispersive. The phase velocity of the microstrip line decreases with increasing frequency. Therefore, $\epsilon_{ff}(f)$ increases with frequency. Also, the characteristic impedance of the microstrip line increases with frequency, and it follows that the effective width $W_{\text{eff}}(f)$ decreases.

The frequency below which dispersion may be neglected is given by

$$f_o(\text{GHz}) = 0.3 \sqrt{\frac{Z_o}{h\sqrt{\epsilon_r} - 1}}$$

where h must be expressed in centimeters.

An analytical expression that shows the effect of dispersion in $\epsilon_{ff}(f)$ is [2.1]

$$\epsilon_{ff}(f) = \epsilon_r - \frac{\epsilon_r - \epsilon_{ff}}{1 + G(f/f_p)^2} \quad (f \text{ in GHz})$$

where

$$f_p = \frac{Z_o}{8\pi h} \quad (h \text{ in cm})$$

and

$$G = 0.6 + 0.009Z_o$$

Observe that when $f_p \gg f$, then $\epsilon_{ff}(f) \simeq \epsilon_{ff}$. In other words, high-impedance lines on thin substrates are less dispersive.

The expression for the dispersion in Z_o is [2.1]

$$Z_o(f) = \frac{377h}{W_{\text{eff}}(f)\sqrt{\epsilon_{ff}}}$$

where

$$W_{\text{eff}}(f) = W + \frac{W_{\text{eff}}(0) - W}{1 + (f/f_p)^2}$$

and

$$W_{\text{eff}}(0) = \frac{377h}{Z_o(0)\sqrt{\epsilon_{ff}(0)}}$$

Another characteristic of the microstrip line is its attenuation. The attenuation constant is a function of the microstrip geometry, the electrical properties of the dielectric substrate and the conductors, and the frequency.

There are two types of losses in a microstrip line: a dielectric substrate loss and the ohmic skin loss in the conductors. The losses can be expressed as a loss per unit length along the microstrip line in terms of the attenuation factor α . Since the power carried by a wave traveling in the positive direction in a quasi-TEM mode is given by

$$\begin{aligned} P^+(z) &= \frac{1}{2} (V^+ e^{-\alpha z} I^+ e^{-\alpha z}) = \frac{1}{2} \frac{|V^+|^2}{Z_o} e^{-2\alpha z} \\ &= P_0 e^{-2\alpha z} \end{aligned} \quad (2.5.12)$$

where $P_0 = |V^+|^2/2Z_o$ is the power at $z = 0$. Then, from (2.5.12) we can write

$$\alpha = \frac{-dP(z)/dz}{2P(z)} = \alpha_d + \alpha_c$$

where α_d is the dielectric loss factor and α_c the conduction loss factor.

A useful set of expressions for calculating α_d is [2.1]:

For a dielectric with low losses:

$$\alpha_d = 27.3 \frac{\epsilon_r}{\sqrt{\epsilon_{ff}}} \frac{\epsilon_{ff} - 1}{\epsilon_r - 1} \frac{\tan \delta}{\lambda_0} \quad \frac{\text{dB}}{\text{cm}} \quad (2.5.13)$$

where the loss tangent δ is given by

$$\tan \delta = \frac{\sigma}{\omega \epsilon}$$

For a dielectric with $\sigma \neq 0$:

$$\alpha_d = 4.34 \frac{\epsilon_{ff} - 1}{\sqrt{\epsilon_{ff}} (\epsilon_r - 1)} \left(\frac{\mu_0}{\epsilon_0} \right)^{1/2} \sigma \quad \frac{\text{dB}}{\text{cm}} \quad (2.5.14)$$

In (2.5.13) and (2.5.14), σ is the conductivity of the dielectric and $\mu_0 = 4\pi \times 10^{-7}$ H/m.

A set of expressions for calculating α_c is [2.1]:

For $W/h \rightarrow \infty$:

$$\alpha_c = \frac{8.68}{Z_o W} R_s$$

where

$$R_s = \sqrt{\frac{\pi f \mu_0}{\sigma}}$$

For $W/h \leq 1/2\pi$:

$$\alpha_c = \frac{8.68 R_s P}{2\pi Z_o h} \left[1 + \frac{h}{W_{\text{eff}}} + \frac{h}{\pi W_{\text{eff}}} \left(\ln \frac{4\pi W}{t} + \frac{t}{W} \right) \right]$$

For $\frac{1}{2}\pi < W/h \leq 2$:

$$\alpha_c = \frac{8.68 R_s}{2\pi Z_o h} P Q$$

For $W/h \geq 2$:

$$\alpha_c = \frac{8.68 R_s Q}{Z_o h} \left\{ \frac{W_{\text{eff}}}{h} + \frac{2}{\pi} \ln \left[2\pi e \left(\frac{W_{\text{eff}}}{2h} + 0.94 \right) \right] \right\}^{-2} \left[\frac{W_{\text{eff}}}{h} + \frac{W_{\text{eff}}/\pi h}{(W_{\text{eff}}/2h) + 0.94} \right]$$

where

$$P = 1 - \left(\frac{W_{\text{eff}}}{4h} \right)^2$$

and

$$Q = 1 + \frac{h}{W_{\text{eff}}} + \frac{h}{\pi W_{\text{eff}}} \left(\ln \frac{2h}{t} - \frac{t}{h} \right)$$

In dielectric substrates, the dielectric losses are normally smaller than conductor losses. However, dielectric losses in silicon substrates can be of the same order or larger than conductor losses.

The quality factor Q of a microstrip line is calculated from

$$Q = \frac{\beta}{2\alpha}$$

where

$$\beta = \frac{2\pi}{\lambda}$$

and α is the total loss. Therefore,

$$Q = \frac{\pi}{\lambda\alpha}$$

or in decibels we can write

$$\begin{aligned} Q &= \frac{8.686\pi}{\lambda\alpha} \quad \text{dB} \\ &= \frac{27.3}{\alpha} \quad \frac{\text{dB}}{\lambda} \end{aligned}$$

where we used the fact that 1 dB = 8.686 nepers.

A microstrip line also has radiation losses. The effect of radiation losses can be accounted for in terms of the radiation quality factor Q_r , given by [2.1]

$$Q_r = \frac{Z_o}{480\pi(h/\lambda_o)F}$$

where

$$F = \frac{\epsilon_{ff}(f) + 1}{\epsilon_{ff}(f)} - \frac{(\epsilon_{ff}(f) - 1)^2}{2[\epsilon_{ff}(f)]^{2/3}} \ln \frac{\sqrt{\epsilon_{ff}(f) + 1}}{\sqrt{\epsilon_{ff}(f) - 1}}$$

is known as the *radiation factor*.

The total Q , called Q_T , of a microstrip resonator can be expressed as

$$\frac{1}{Q_T} = \frac{1}{Q_c} + \frac{1}{Q_d} + \frac{1}{Q_r}$$

where Q_d and Q_c are the quality factors of the dielectric (i.e., $Q_d = \pi/\lambda\alpha_d$) and conductor (i.e., $Q_c = \pi/\lambda\alpha_c$), respectively.

The impedance transforming properties of transmission lines can be used in the design of matching networks. A microstrip line can be used as a series transmission line, as an open-circuited stub or as a short-circuited stub. In fact, a series microstrip line together with a short- or open-circuited shunt stub can transform a 50- Ω resistor into any value of impedance. Also, a quarter-wave microstrip line can be used to change a 50- Ω resistor to any value of resistance. This line, together with a short- or open-circuited shunt stub, can be used to transform 50 Ω to any value of impedance. The following example illustrates the use of microstrip lines in matching networks.

Example 2.5.1

Design two microstrip matching networks for the amplifier shown in Fig. 2.5.4, whose reflection coefficients for a good match, in a 50- Ω system, are $\Gamma_s = 0.614 \angle 160^\circ$ and $\Gamma_L = 0.682 \angle 97^\circ$.

Solution. *Design 1:* The amplifier block diagram is shown in Fig. 2.5.4. The normalized impedances and admittances associated with Γ_s and Γ_L can be read, to reasonable

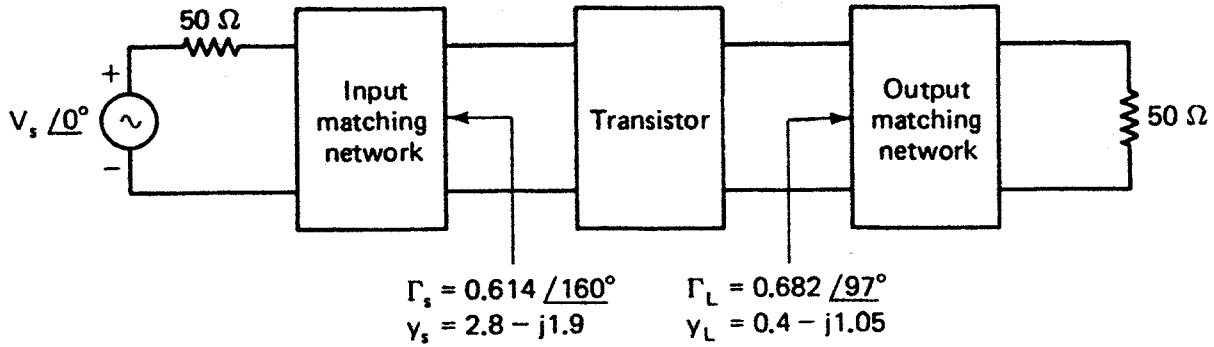


Figure 2.5.4 Amplifier block diagram.

accuracy, from the ZY Smith chart, namely

$$y_s = \frac{1}{z_s} = \frac{1}{0.245 + j0.165} = 2.8 - j1.9$$

and

$$y_L = \frac{1}{z_L} = \frac{1}{0.325 + j0.83} = 0.4 - j1.05$$

In order to design the input matching network, we locate y_s in the Y Smith chart shown in Fig. 2.5.5a. The shortest length of microstrip line plus stub is obtained by using an open-circuited shunt stub of length 0.159λ to move from the origin (i.e., $50\ \Omega$) to point A on the Smith chart, and then using a transmission line length of 0.099λ to move from A to y_s .

Next, we locate y_L in Fig. 2.5.5b and follow a similar procedure. In this case, the shortest length of microstrip line plus stub is obtained by using a short-circuited shunt stub of length 0.077λ to move from the origin to point B. Then a series transmission line of length 0.051λ to move from B to y_L .

The complete design showing the transistor, the microstrip matching network, and the dc supply is shown in Fig. 2.5.6. The characteristic impedance of all microstrip lines is $50\ \Omega$.

The capacitors C_A are coupling capacitors. Typical values for the chip capacitors C_A are 200 to 1000 pF, high-Q capacitor. The bypass capacitors C_B (i.e., chip capacitors, 50 to 500 pF) provide the ac short circuits for the 0.077λ and $\lambda/4$ short-circuited stubs. The $\lambda/4$ short-circuited stub, high-impedance line (denoted by $Z_o \gg$), provides the dc path for the base supply voltage V_{BB} . It also presents an open circuit to the ac signal at the base of the transistor. The narrowest practical line (i.e., large Z_o) should be used for the $\lambda/4$ short-circuited stub to avoid unwanted ac coupling.

To minimize transition interaction between the shunt stubs and the series transmission lines, the shunt stubs are usually balanced along the series transmission line. A schematic of the amplifier using balanced shunt stubs is shown in Fig. 2.5.7. The schematic also shows that $50\text{-}\Omega$ lines were added on both sides of C_A to provide a soldering area.

In Fig. 2.5.7 two parallel shunt stubs must provide the same admittance as the single stub in Fig. 2.5.6. Therefore, the admittance of each side of the balanced stub must be equal to half of the total admittance. For example, each side of the input

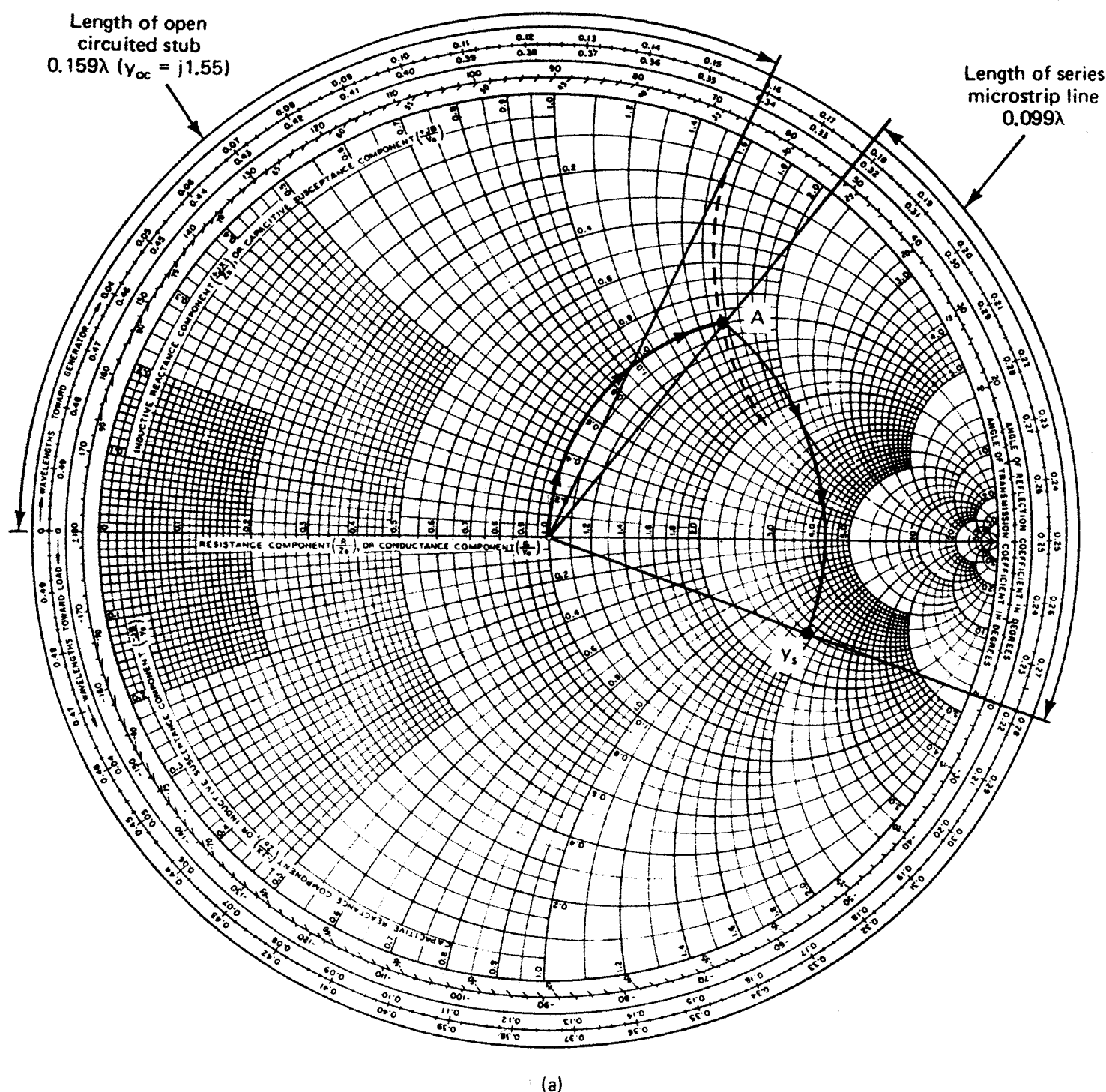


Figure 2.5.5 (a) Input matching network design; (b) output matching network design.

balanced shunt stubs must have an admittance of $y = j1.55/2 = j0.775$. Using the Smith chart, we obtain that the length of each side must be 0.105λ . Observe that the length of the shunt stubs in Fig. 2.5.7 is not equal to the total length of the balance stubs in Fig. 2.5.6. Of course, a simple check will show that the admittance seen by the series transmission line is the same in both cases.

If we use Duroid ($\epsilon_r = 2.23$, $h = 0.7874$ mm) to build the amplifier, we find from the results in Section 2.5 that a characteristic impedance of 50Ω is obtained with $W = 2.42$ mm and $\epsilon_{ff} = 1.91$. The microstrip wavelength in the $50\text{-}\Omega$ Duroid microstrip line is $\lambda = \lambda_0/\sqrt{1.91} = 0.7236\lambda_0$, where $\lambda_0 = 30$ cm at $f = 1$ GHz. For a

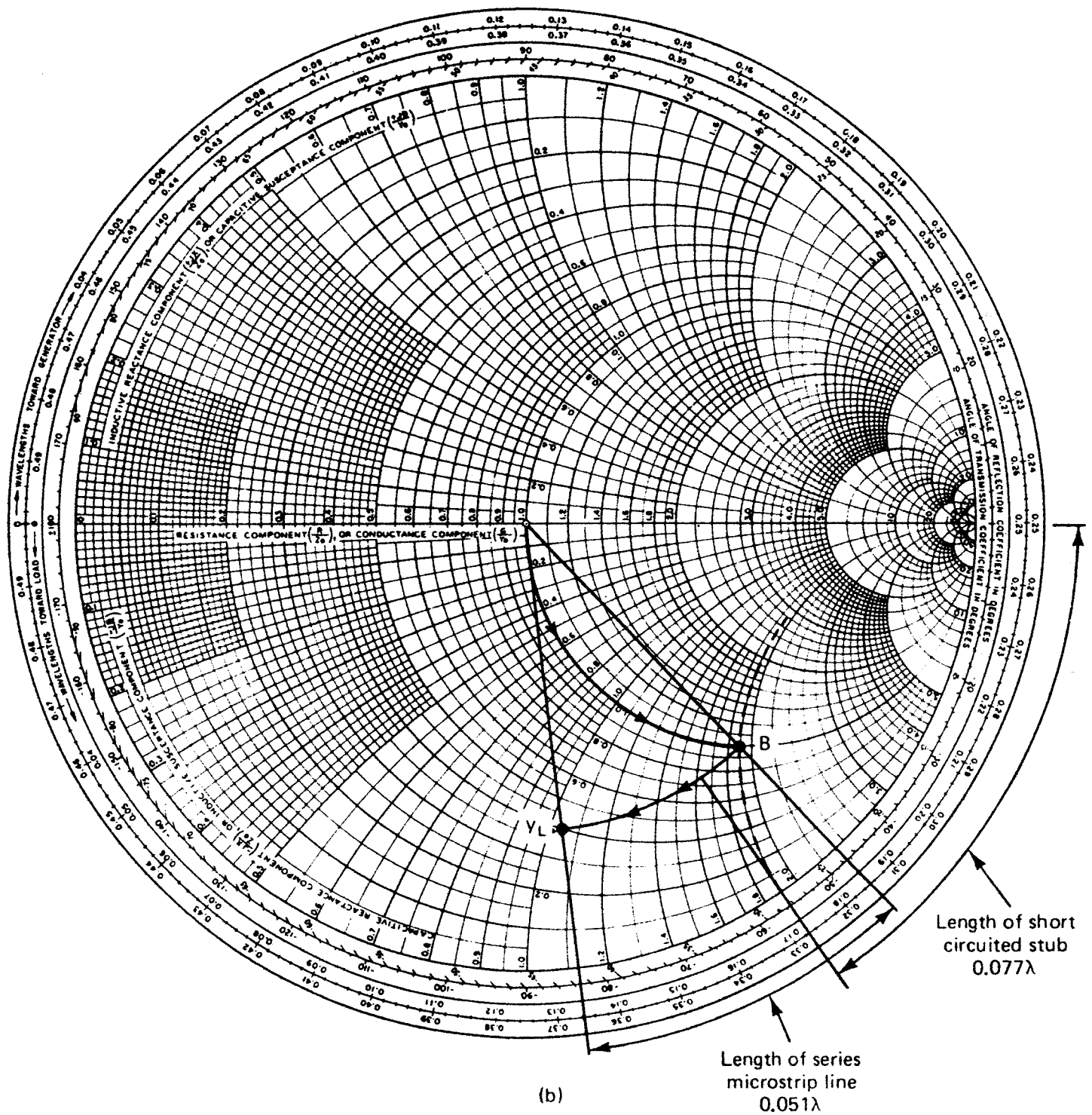


Figure 2.5.5 (continued)

characteristic impedance of 100Ω in the $\lambda/4$ line, the width must be $W = 0.7$ mm. The line lengths in Fig. 2.5.7 are

$$0.105\lambda = 2.28 \text{ cm}$$

$$0.099\lambda = 2.15 \text{ cm}$$

$$0.051\lambda = 1.10 \text{ cm}$$

$$0.129\lambda = 2.80 \text{ cm}$$

$$\lambda/4 = 5.43 \text{ cm}$$

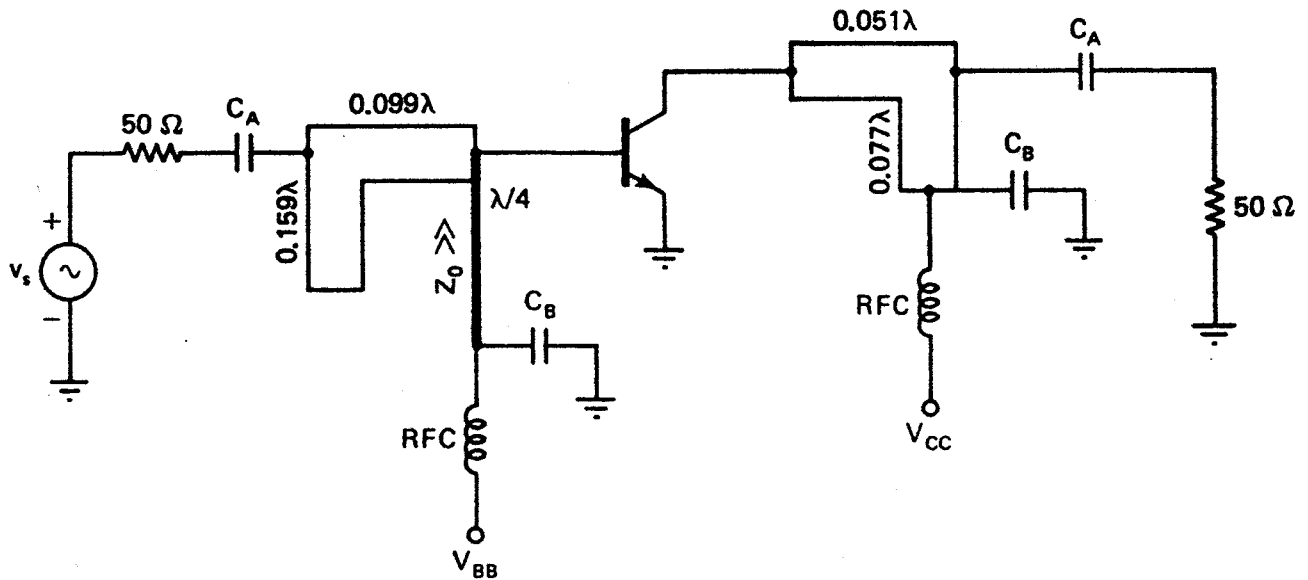


Figure 2.5.6 Complete amplifier schematic. The characteristic impedance of the microstrip lines is $50\ \Omega$.

Design 2: This method uses microstrip lines with different characteristic impedances. The design requires the transformation of $50\ \Omega$ to $Y_s = (2.8 - j1.9)/50 = 0.056 - j0.038\ \text{S}$. A quarter-wave transformer can be used to transform the source impedance of $50\ \Omega$ to the resistance $1/0.056 = 17.86\ \Omega$. The characteristic impedance of the quarter-wave transformer is

$$Z_o = \sqrt{50(17.86)} = 29.9\ \Omega$$

An open-circuited stub provides an admittance of $Y_{oc} = jY_o \tan \beta l$. Therefore, an open-circuited shunt stub of length $3\lambda/8$, or a short-circuited shunt stub of length $\lambda/8$, looks like a shunt inductor having the admittance $-jY_o$. Using an open-circuited shunt stub of length $3\lambda/8$, we find its characteristic impedance to be $Z_o = 1/Y_o = 1/0.038 = 26.32\ \Omega$.

Similarly, for the output matching network [$Y_L = (0.4 - j1.05)/50 = 0.008 - j0.021\ \text{S}$] a quarter-wave line of characteristic impedance

$$Z_o = \sqrt{50(125)} = 79.1\ \Omega$$

transforms the $50\text{-}\Omega$ load to a resistance of value $1/0.008 = 125\ \Omega$. An open-circuited shunt stub of length $3\lambda/8$ and characteristic impedance $Z_o = 1/Y_o = 1/0.021 = 47.6\ \Omega$ produces the required admittance of $-j0.021$.

The complete amplifier is shown in Fig. 2.5.8a. Figure 2.5.8b shows the amplifier using balanced shunt stubs of length $3\lambda/8$ to minimize the microstrip transition interaction. Observe that in the balance stubs the lengths were kept at $3\lambda/8$, but the characteristic impedance was doubled so that the parallel combinations produce the required $26.32\ \Omega$ and $47.6\ \Omega$.

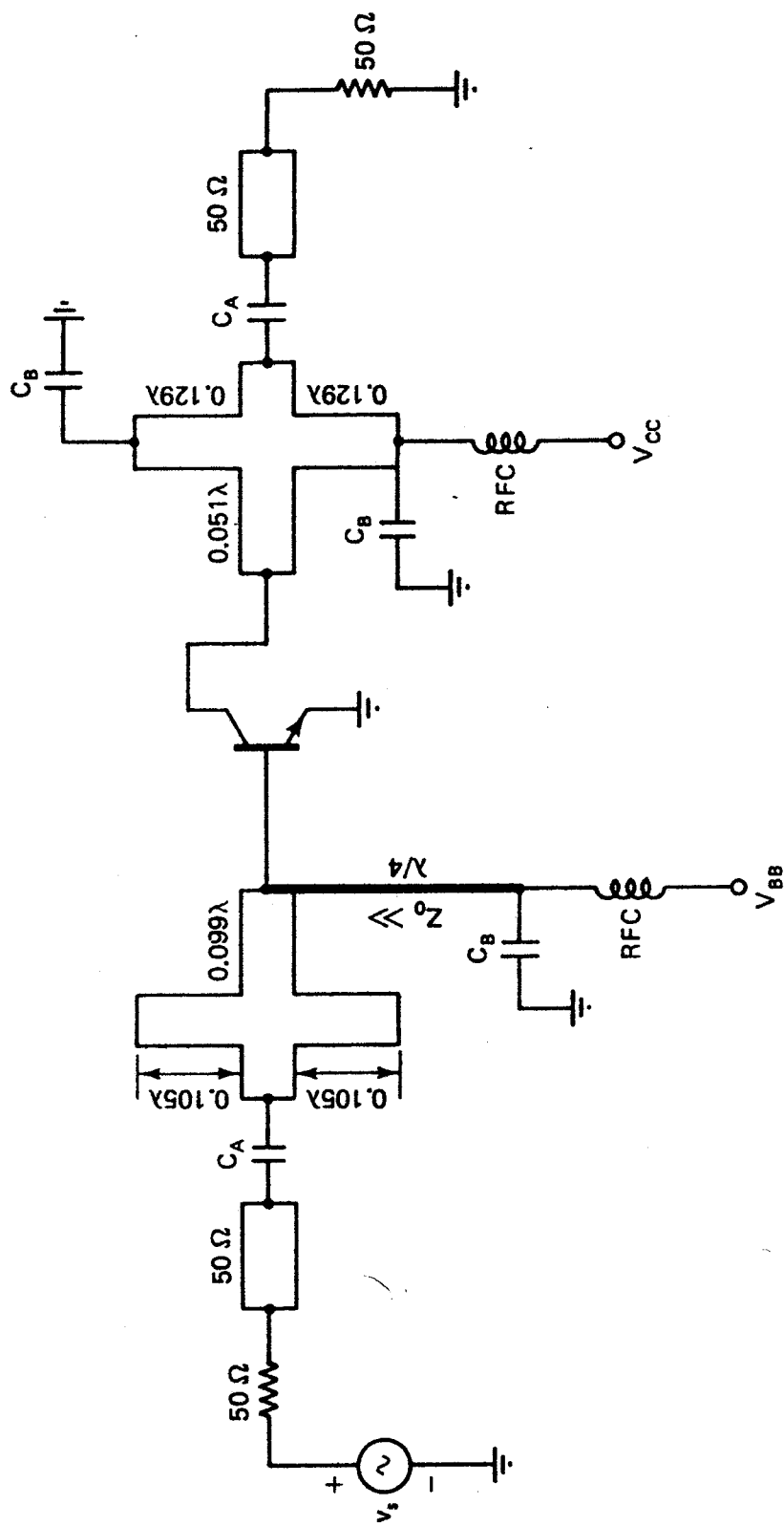


Figure 2.5.7 Complete amplifier schematic using balanced shunt stubs. The characteristic impedance of the microstrip lines is $50\ \Omega$.

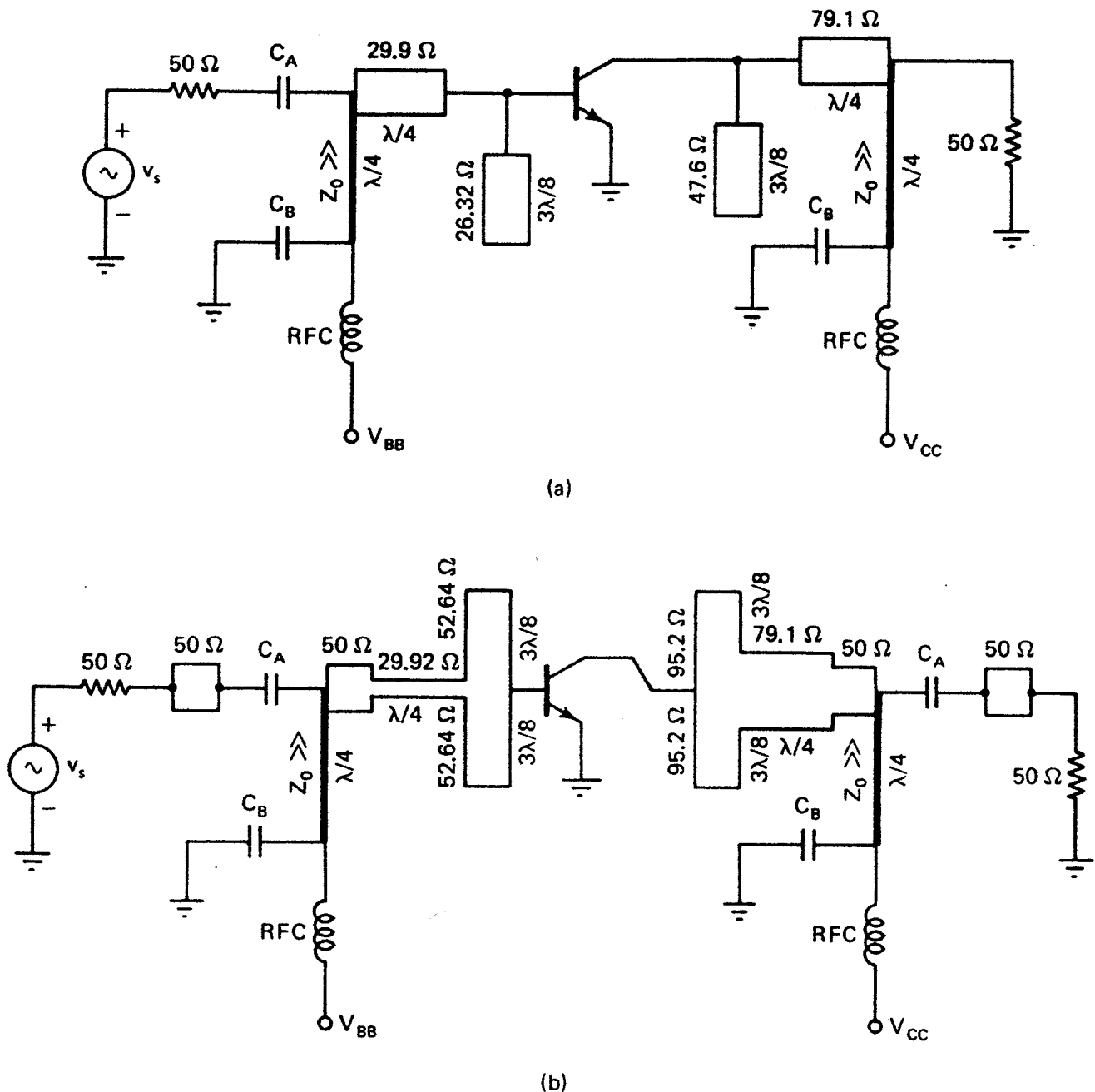


Figure 2.5.8 Matching network design using microstrip lines with different characteristic impedances.

2.6 SIGNAL FLOW GRAPH

A signal flow graph is a convenient technique to represent and analyze the transmission and reflection of waves in a microwave amplifier. Once the signal flow graph is developed, relations between the variables can be obtained using Mason's rule. The flow graph technique permits expressions, such as power gains and voltage gains of complex microwave amplifiers, to be easily derived. Certain rules are followed in constructing a signal flow graph:

1. Each variable is designated as a node.
2. The S parameters and reflection coefficients are represented by branches.

3. Branches enter dependent variable nodes and emanate from independent variable nodes. The independent variable nodes are the incident waves and the reflected waves are dependent variable nodes.
4. A node is equal to the sum of the branches entering it.

The signal flow graph of the S parameters of a two-port network is shown in Fig. 2.6.1. Observe that b_1 and b_2 are the dependent nodes and a_1 and a_2 the independent nodes. The complete signal flow graph of the two-port network is shown in Fig. 2.6.2.

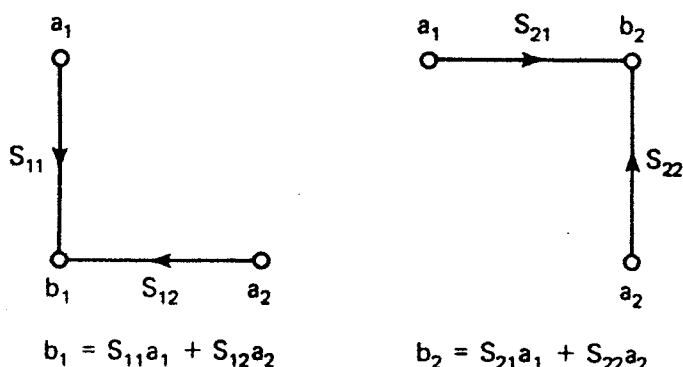


Figure 2.6.1 Signal flow graph for the scattering parameter equations.

The signal flow graph in Fig. 2.6.2 shows the relationship between the traveling waves. The incident wave a_1 at port 1 gets partly transmitted (i.e., $S_{21}a_1$) to become part of b_2 , and partly reflected (i.e., $S_{11}a_1$) to become part of b_1 . Similarly, the incident wave a_2 at port 2 gets partly transmitted (i.e., $S_{12}a_2$) to become part of b_1 and partly reflected (i.e., $S_{22}a_2$) to become part of b_2 .

In order to obtain the signal flow graph of a microwave amplifier we need to obtain the signal flow graph of a signal generator with some internal impedance, and the signal flow graph of a load impedance.

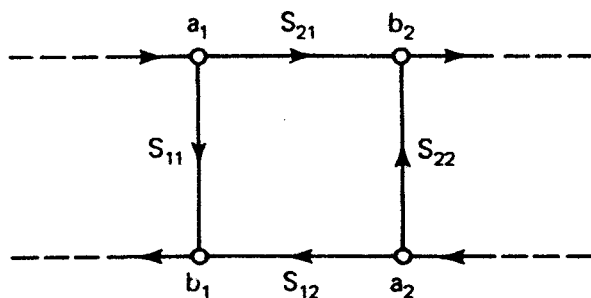


Figure 2.6.2 Signal flow graph of a two-port network.

Figure 2.6.3a shows a voltage-source generator with impedance Z_s . At the terminals we can write

$$V_g = E_s + I_g Z_s \quad (2.6.1)$$

Using (1.4.1) and (1.4.2), we can express (2.6.1) in terms of traveling waves, namely

$$V_g^+ + V_g^- = E_s + \left(\frac{V_g^+}{Z_o} - \frac{V_g^-}{Z_o} \right) Z_s$$

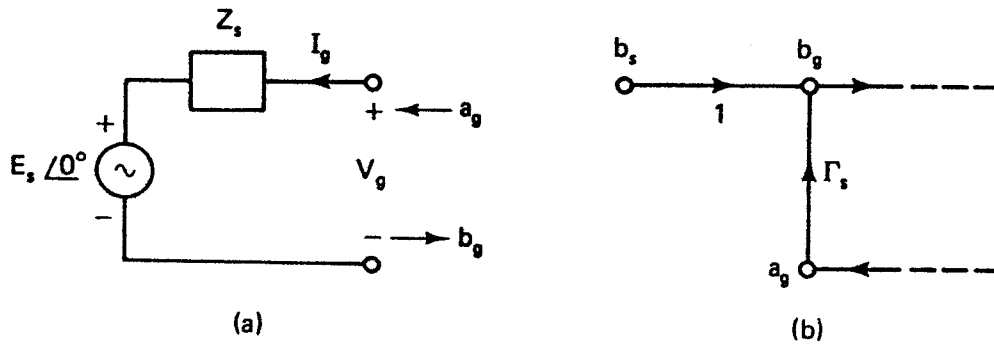


Figure 2.6.3 Signal flow graph of a voltage-source generator.

Solving for V_g^- , we obtain

$$b_g = b_s + \Gamma_s a_g \quad (2.6.2)$$

where

$$b_g = \frac{V_g^-}{\sqrt{Z_o}}$$

$$a_g = \frac{V_g^+}{\sqrt{Z_o}}$$

$$b_s = \frac{E_s \sqrt{Z_o}}{Z_s + Z_o}$$

and

$$\Gamma_s = \frac{Z_s - Z_o}{Z_s + Z_o}$$

From (2.6.2) the signal flow graph in Fig. 2.6.3b follows.

For the load impedance shown in Fig. 2.6.4a we can write

$$V_L = Z_L I_L$$

In terms of traveling waves, we obtain

$$V_L^+ + V_L^- = Z_L \left(\frac{V_L^+}{Z_o} - \frac{V_L^-}{Z_o} \right)$$

or

$$b_L = \Gamma_L a_L \quad (2.6.3)$$

where

$$b_L = \frac{V_L^-}{\sqrt{Z_o}}$$

$$a_L = \frac{V_L^+}{\sqrt{Z_o}}$$

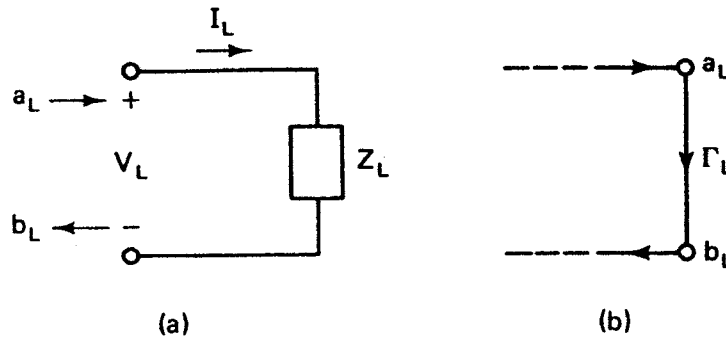


Figure 2.6.4 Signal flow graph of a load impedance.

and

$$\Gamma_L = \frac{Z_L - Z_o}{Z_L + Z_o}$$

The signal flow graph follows from (2.6.3) and it is shown in Fig. 2.6.4b.

We can now combine the signal flow graph for the two-port network in Fig. 2.6.2 with the signal flow graphs of the signal generator (i.e., Fig. 2.6.3b) and the load (i.e., Fig. 2.6.4b). Observe that the nodes b_g , a_g , b_L , and a_L are identical to a_1 , b_1 , a_2 , and b_2 , respectively. The resulting signal flow graph of a microwave amplifier is shown in Fig. 2.6.5.

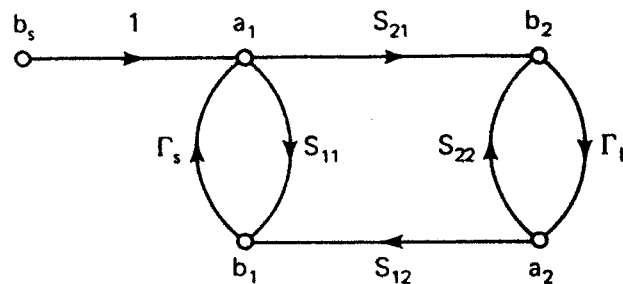


Figure 2.6.5 Signal flow graph of a microwave amplifier.

To determine the ratio or transfer function T of a dependent to an independent variable, we apply Mason's rule, namely

$$T = \frac{P_1[1 - \sum L(1)^{(1)} + \sum L(2)^{(1)} - \cdots] + P_2[1 - \sum L(1)^{(2)} + \cdots] + \cdots}{1 - \sum L(1) + \sum L(2) - \sum L(3) + \cdots}$$

where the different terms are defined as follows.

The terms P_1 , P_2 , and so on, are the different paths connecting the dependent and independent variables whose transfer function T is to be determined. A path is defined as a set of consecutive, codirectional branches along which no node is encountered more than once as we move in the graph from the independent to the dependent node. The value of the path is the product of all branch coefficients along the path. For example, in Fig. 2.6.5 b_s is the only

independent variable. To determine the ratio b_1/b_s , we identify two paths, $P_1 = S_{11}$ and $P_2 = S_{21}\Gamma_L S_{12}$.

The term $\sum L(1)$ is the sum of all first-order loops. A first-order loop is defined as the product of the branches encountered in a round trip as we move from a node in the direction of the arrows back to that original node. In Fig. 2.6.5, $S_{11}\Gamma_s$, $S_{21}\Gamma_L S_{12}\Gamma_s$, and $S_{22}\Gamma_L$ are first-order loops.

The term $\sum L(2)$ is the sum of all second-order loops. A second-order loop is defined as the product of any two nontouching first-order loops. In Fig. 2.6.5, $S_{11}\Gamma_s$ and $S_{22}\Gamma_L$ do not touch; therefore, the product $S_{11}\Gamma_s S_{22}\Gamma_L$ is a second-order loop.

The term $\sum L(3)$ is the sum of all third-order loops. A third-order loop is defined as the product of three nontouching first-order loops. In Fig. 2.6.5 there are no third-order loops. Of course, the terms $\sum L(4)$, $\sum L(5)$, and so on, represent fourth-, fifth-, and higher-order loops.

The terms $\sum L(1)^{(P)}$ is the sum of all first-order loops that do not touch the path P between the independent and dependent variables. In Fig. 2.6.5, for the path $P_1 = S_{11}$ we find that $\sum L(1)^{(1)} = \Gamma_L S_{22}$, and for the path $P_2 = S_{21}\Gamma_L S_{12}$ we find that $\sum L(1)^{(2)} = 0$.

The term $\sum L(2)^{(P)}$ is the sum of all second-order loops that do not touch the path P between the independent and dependent variables. In Fig. 2.6.5, we find that $\sum L(2)^{(P)} = 0$. Of course, $\sum L(3)^{(P)}$, $\sum L(4)^{(P)}$, and so on, represent higher-order loops that do not touch the path P .

For the transfer function b_1/b_s in Fig. 2.6.5 we have found that $P_1 = S_{11}$, $P_2 = S_{21}\Gamma_L S_{12}$, $\sum L(1) = S_{11}\Gamma_s + S_{22}\Gamma_L + S_{21}\Gamma_L S_{12}\Gamma_s$, $\sum L(2) = S_{11}\Gamma_s S_{22}\Gamma_L$, and $\sum L(1)^{(1)} = \Gamma_L S_{22}$. Therefore, using Mason's rule, we obtain

$$\frac{b_1}{b_s} = \frac{S_{11}(1 - \Gamma_L S_{22}) + S_{21}\Gamma_L S_{12}}{1 - (S_{11}\Gamma_s + S_{22}\Gamma_L + S_{21}\Gamma_L S_{12}\Gamma_s) + S_{11}\Gamma_s S_{22}\Gamma_L}$$

2.7 APPLICATIONS OF SIGNAL FLOW GRAPHS

The first application of signal flow graph analysis is in the calculation of the input reflection coefficient, called Γ_{IN} , when a load is connected to the output of a two-port network. The signal flow graph is shown in Fig. 2.7.1.

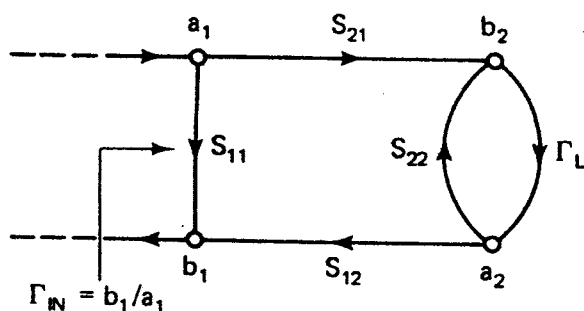


Figure 2.7.1 Signal flow graph for the input reflection coefficient Γ_{IN} .

The input reflection coefficient Γ_{IN} is defined as

$$\Gamma_{IN} = \frac{b_1}{a_1}$$

Observing that $P_1 = S_{11}$, $P_2 = S_{21}\Gamma_L S_{12}$, $\sum L(1) = S_{22}\Gamma_L$, and $\sum L(1)^{(1)} = S_{22}\Gamma_L$, we can use Mason's rule to obtain

$$\begin{aligned} \Gamma_{IN} &= \frac{S_{11}(1 - S_{22}\Gamma_L) + S_{21}\Gamma_L S_{12}}{1 - S_{22}\Gamma_L} \\ &= S_{11} + \frac{S_{12}S_{21}\Gamma_L}{1 - S_{22}\Gamma_L} \end{aligned} \quad (2.7.1)$$

If $\Gamma_L = 0$, it follows from (2.7.1) that $\Gamma_{IN} = S_{11}$. Also, when there is no transmission from the output to the input (i.e., when $S_{12} = 0$), it follows that $\Gamma_{IN} = S_{11}$. When $S_{12} = 0$, we call the device represented by the two-port a unilateral device.

Similarly, we can calculate the output reflection coefficient $\Gamma_{OUT} = b_2/a_2$ with $b_s = 0$ from the signal flow graph shown in Fig. 2.7.2. The expression for Γ_{OUT} is

$$\Gamma_{OUT} = S_{22} + \frac{S_{12}S_{21}\Gamma_s}{1 - S_{11}\Gamma_s} \quad (2.7.2)$$

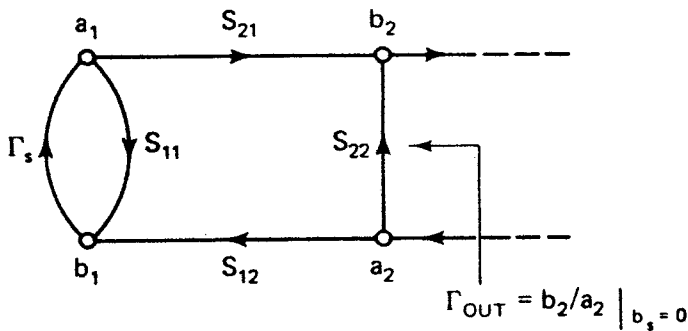


Figure 2.7.2 Signal flow graph for the output reflection coefficient Γ_{OUT} .

Next, we use signal flow graphs to calculate power gain and voltage gain. The square of the magnitude of the incident and reflected waves represent power. Therefore, the power delivered to the load in Fig. 2.6.5 is given by the difference between the incident and reflected power, namely

$$P_L = |b_2|^2 - |a_2|^2 = |b_2|^2(1 - |\Gamma_L|^2) \quad (2.7.3)$$

The power available from a source is defined as the power delivered by the source to a conjugately matched load. Figure 2.7.3 shows the signal flow graph of a source connected to a conjugate match load (i.e., $\Gamma_L = \Gamma_s^*$). Therefore, the power available from the source, in Fig. 2.7.3, is given by

$$P_{AVS} = |b_g|^2 - |a_g|^2 \quad (2.7.4)$$

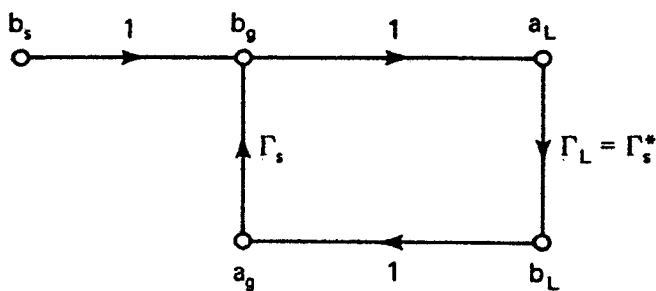


Figure 2.7.3 Signal flow graph of a voltage source connected to a conjugate matched load.

Observing that $b_g = b_s + b_g \Gamma_s \Gamma_s^*$ and $a_g = b_g \Gamma_s^*$, we obtain

$$b_g = \frac{b_s}{1 - |\Gamma_s|^2} \quad (2.7.5)$$

and

$$a_g = \frac{b_s \Gamma_s^*}{1 - |\Gamma_s|^2} \quad (2.7.6)$$

Substituting (2.7.5) and (2.7.6) into (2.7.4) gives

$$P_{\text{AVS}} = \frac{|b_s|^2}{1 - |\Gamma_s|^2} \quad (2.7.7)$$

The previous results could have also been obtained as follows. Observe that the power delivered to the load Γ_L in Fig. 2.7.3 is given by

$$P_L = |a_L|^2 (1 - |\Gamma_L|^2) = \frac{|b_s|^2 (1 - |\Gamma_L|^2)}{|1 - \Gamma_s \Gamma_L|^2}$$

Therefore, with $\Gamma_L = \Gamma_s^*$ the power delivered to the load is equal to the available power from the source, and (2.7.7) follows.

The transducer power gain, called G_T , is defined as the ratio of the power delivered to a load to the power available from the source. From (2.7.3) and (2.7.7) we obtain

$$G_T = \frac{P_L}{P_{\text{AVS}}} = \frac{|b_2|^2}{|b_s|^2} (1 - |\Gamma_L|^2)(1 - |\Gamma_s|^2) \quad (2.7.8)$$

The ratio b_2/b_s can be obtained using Mason's rule, namely

$$\frac{b_2}{b_s} = \frac{S_{21}}{1 - (S_{11}\Gamma_s + S_{22}\Gamma_L + S_{21}\Gamma_L S_{12}\Gamma_s) + S_{11}\Gamma_s S_{22}\Gamma_L} \quad (2.7.9)$$

Substituting (2.7.9) into (2.7.8) results in

$$G_T = \frac{|S_{21}|^2 (1 - |\Gamma_s|^2)(1 - |\Gamma_L|^2)}{|(1 - S_{11}\Gamma_s)(1 - S_{22}\Gamma_L) - S_{21}S_{12}\Gamma_L\Gamma_s|^2} \quad (2.7.10)$$

The denominator of (2.7.10) can be further manipulated and G_T can be expressed in the form

$$G_T = \frac{1 - |\Gamma_s|^2}{|1 - \Gamma_{\text{IN}}\Gamma_s|^2} |S_{21}|^2 \frac{1 - |\Gamma_L|^2}{|1 - S_{22}\Gamma_L|^2} \quad (2.7.11)$$

or

$$G_T = \frac{1 - |\Gamma_s|^2}{|1 - S_{11}\Gamma_s|^2} |S_{21}|^2 \frac{1 - |\Gamma_L|^2}{|1 - \Gamma_{OUT}\Gamma_L|^2} \quad (2.7.12)$$

where Γ_{IN} and Γ_{OUT} are given by (2.7.1) and (2.7.2), respectively.

The voltage gain of the amplifier is defined as the ratio of the output voltage to the input voltage. That is,

$$A_v = \frac{a_2 + b_2}{a_1 + b_1}$$

and dividing by b_s gives

$$A_v = \frac{a_2/b_s + b_2/b_s}{a_1/b_s + b_1/b_s}$$

Therefore, we need to calculate the ratios a_2/b_s , b_2/b_s , a_1/b_s , and b_1/b_s using Mason's rule. The expression for A_v can be shown to be

$$A_v = \frac{S_{21}(1 + \Gamma_L)}{(1 - S_{22}\Gamma_L) + S_{11}(1 - S_{22}\Gamma_L) + S_{21}\Gamma_L S_{12}} \quad (2.7.13)$$

PROBLEMS

- 2.1. (a) Show that impedances having a negative real part (i.e., $z = -r + jx$) have a reflection coefficient whose magnitude is greater than 1.
- (b) Prove that negative resistances can be handled in the Smith chart by plotting $1/\Gamma^*$ and interpreting the resistance circles as being negative and the reactance circles as marked.
- (c) Locate in the Smith chart the impedances $Z_1 = -20 + j16 \, \Omega$ and $Z_2 = -200 + j25 \, \Omega$ and find the associated reflection coefficient. Normalize the impedances to $50 \, \Omega$.
- (d) Work the problem in part (c) in the compressed Smith chart.
- 2.2. (a) Prove that the maximum normalized resistance in a transmission line is numerically equal to the VSWR.
- (b) Prove that the minimum normalized resistance in a transmission line is numerically equal to $1/\text{VSWR}$.
- 2.3 Show that the impedance along a transmission line repeats itself at every $\lambda/2$ distance. That is,

$$Z(d) = Z\left(d + \frac{n\lambda}{2}\right), \quad n = 1, 2, 3, \dots$$

- 2.4. Show that the impedance along a transmission line can be expressed in the form

$$Z(d) = R(d) + jX(d) = |Z(d)|e^{j\theta_d}$$

where

$$R(d) = Z_o \frac{1 - |\Gamma|^2}{1 - 2|\Gamma| \cos \phi + |\Gamma|^2}$$

$$X(d) = Z_o \frac{2|\Gamma| \sin \phi}{1 - 2|\Gamma| \cos \phi + |\Gamma|^2}$$

$$|Z(d)| = Z_o \sqrt{\frac{1 + 2|\Gamma| \cos \phi + |\Gamma|^2}{1 - 2|\Gamma| \cos \phi + |\Gamma|^2}}$$

$$\theta_d = \tan^{-1} \frac{X(d)}{R(d)} = \tan^{-1} \left(\frac{2|\Gamma| \sin \phi}{1 - |\Gamma|^2} \right)$$

$$\Gamma = |\Gamma_o| e^{j\phi}, \quad \Gamma_o = |\Gamma_o| e^{j\phi_o}, \quad \phi = \phi_o - 2\beta d$$

- 2.5. Find the input impedance, the load reflection coefficient, and the VSWR in a transmission line having an electrical length of 90° , $Z_o = 50 \Omega$, and terminated in the load $Z_L = 50 + j100 \Omega$. Work the problem in both the Z and Y Smith charts.
- 2.6. (a) Design a single-stub matching system (see Fig. P2.6) to match the load $Z_L = 15 + j25 \Omega$ to a $50\text{-}\Omega$ transmission line. The characteristic impedance of the short-circuited stub is 50Ω .
- (b) Design the single-stub matching system in Fig. P2.6 assuming that the characteristic impedance of the stub is 100Ω .

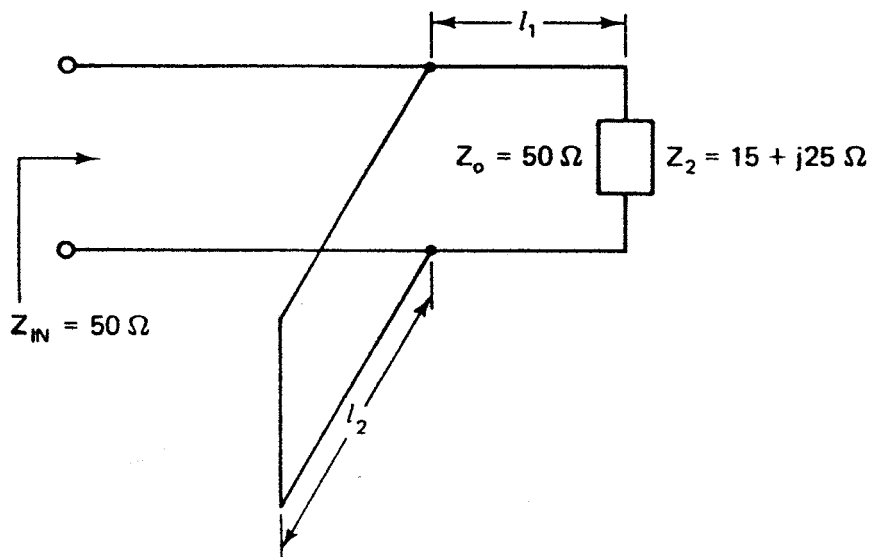


Figure P2.6

- 2.7. Two types of ell matching networks are shown in Fig. P2.7. Select one that can match the load $Y_L = (8 - j12) \times 10^{-3} \text{ S}$ to a $50\text{-}\Omega$ transmission line. Find the element values at $f = 1 \text{ GHz}$.
- 2.8. Design four different ell matching networks to match the load $Z_L = 10 + j40 \Omega$ to a $50\text{-}\Omega$ transmission line.
- 2.9. Design the matching network in Fig. P2.9 that provides $Y_L = (4 - j4) \times 10^{-3} \text{ S}$ to the transistor. Find the element values at 700 MHz .
- 2.10. Use (2.5.8) to (2.5.11) to show that for Duroid, ($\epsilon_r = 2.23$, $h = 0.7874 \text{ mm}$), a $50\text{-}\Omega$ characteristic impedance is obtained with $W/h = 3.073$. Also, $\epsilon_{ff} = 1.91$ and $\lambda = 0.7236\lambda_0$.

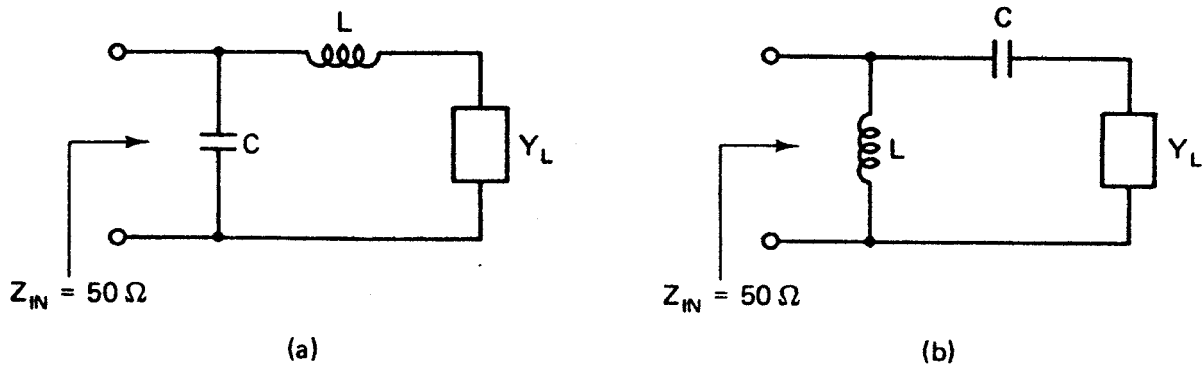


Figure P2.7

- 2.11. In the amplifier shown in Fig. 2.5.8b, calculate the width and the length of the lines at $f = 1$ GHz.
- 2.12. Design two microstrip matching networks for an amplifier whose reflection coefficients at $f = 800$ MHz, in a $50\text{-}\Omega$ system, are $\Gamma_s = 0.8 \angle 160^\circ$ and $\Gamma_L = 0.7 \angle 20^\circ$. Show the diagram for the complete amplifier using balanced shunt stubs.

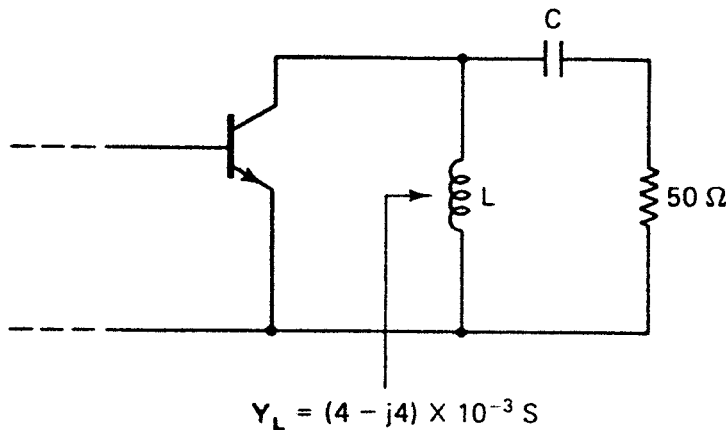


Figure P2.9

- 2.13. Design the matching networks in Fig. P2.13 to match the load $Z_L = 100 + j100 \Omega$ to a $50\text{-}\Omega$ transmission line.
- 2.14. Design the matching network in Fig. P2.14 to match a $50\text{-}\Omega$ load to the impedance $Z_{IN} = 25 - j25 \Omega$.
- 2.15. Verify the expressions for G_T in (2.7.11) and (2.7.12).
- 2.16. Verify the expression for A_p in (2.7.13).

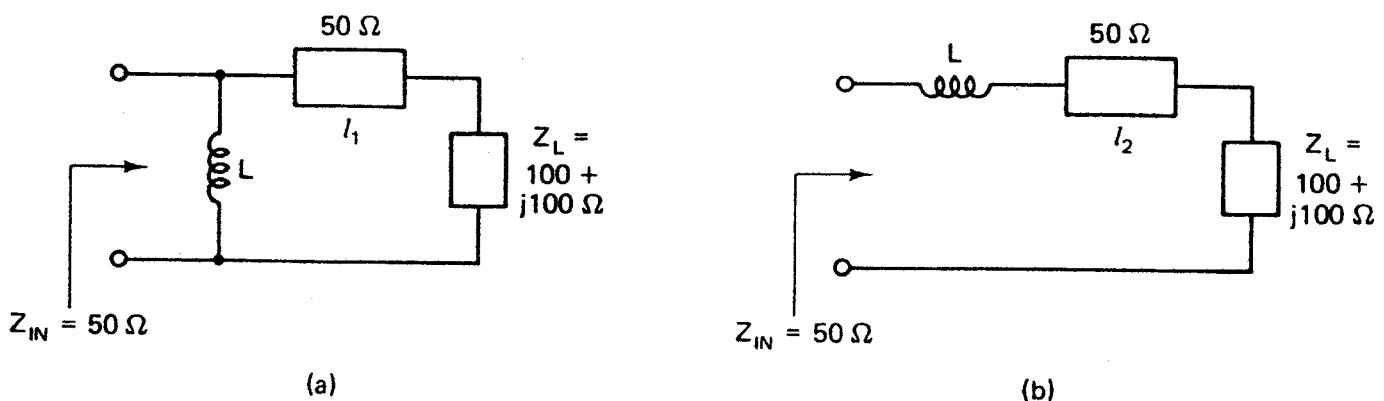


Figure P2.13

MICROWAVE TRANSISTOR AMPLIFIER DESIGN

3.1 INTRODUCTION

This chapter develops some basic principles used in the analysis and design of microwave transistor amplifiers. Based on the S parameters of the transistor and certain performance requirements, a systematic procedure is developed for the design of a microwave transistor amplifier. Of course, some errors are expected in the final implementation of the design resulting from parameter variations, stray capacitances, and other random causes.

The most important design considerations in a microwave transistor amplifier are stability, power gain, bandwidth, noise, and dc requirements. This chapter deals with the problems of stability, power gain, and the dc bias design.

A design usually starts with a set of specifications and the selection of the proper transistor. Then a systematic mathematical solution, aided by graphical methods, is developed to determine the transistor loading (i.e., the source and load reflection coefficients) for a particular stability and gain criteria. An unconditionally stable transistor will not oscillate with any passive termination. On the other hand, a design using a potentially unstable transistor requires some analysis and careful considerations so that the passive terminations produce a stable amplifier.

Design procedures for both unilateral and bilateral transistors, based on stability and gain requirements, are described. Both passive and active dc bias networks for BJTs and GaAs FETs are analyzed. It is important to select the correct dc operating point and the proper dc network topology in order to obtain the desired ac performance.

3.2 POWER GAIN EQUATIONS

Several power gain equations appear in the literature and are used in the design of microwave amplifiers. Figure 3.2.1 illustrates a microwave amplifier signal flow graph and the different powers used in gain equations are indicated. The transducer power gain G_T , the power gain G_p (also called the *operating power gain*), and the available power gain G_A are defined as follows:

$$G_T = \frac{P_L}{P_{AVS}} = \frac{\text{power delivered to the load}}{\text{power available from the source}}$$

$$G_p = \frac{P_L}{P_{IN}} = \frac{\text{power delivered to the load}}{\text{power input to the network}}$$

and

$$G_A = \frac{P_{AVN}}{P_{AVS}} = \frac{\text{power available from the network}}{\text{power available from the source}}$$

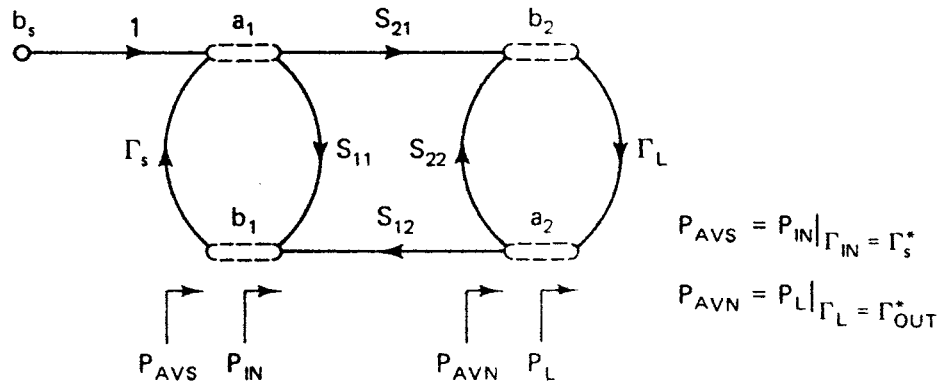


Figure 3.2.1 Different power definitions.

The expressions for G_T were already derived in (2.7.11) and (2.7.12). Observing that $P_{IN} = |a_1|^2 - |b_1|^2$ and that the power available from the network, P_{AVN} , is that power delivered by the network to a conjugately matched load, we can write the power gain equations in the form

$$G_T = \frac{1 - |\Gamma_s|^2}{|1 - \Gamma_{IN} \Gamma_s|^2} |S_{21}|^2 \frac{1 - |\Gamma_L|^2}{|1 - S_{22} \Gamma_L|^2} \quad (3.2.1)$$

$$G_T = \frac{1 - |\Gamma_s|^2}{|1 - S_{11} \Gamma_s|^2} |S_{21}|^2 \frac{1 - |\Gamma_L|^2}{|1 - \Gamma_{OUT} \Gamma_L|^2} \quad (3.2.2)$$

$$G_p = \frac{1}{1 - |\Gamma_{IN}|^2} |S_{21}|^2 \frac{1 - |\Gamma_L|^2}{|1 - S_{22} \Gamma_L|^2} \quad (3.2.3)$$

$$G_A = \frac{1 - |\Gamma_s|^2}{|1 - S_{11} \Gamma_s|^2} |S_{21}|^2 \frac{1}{1 - |\Gamma_{OUT}|^2} \quad (3.2.4)$$

$$\Gamma_{IN} = S_{11} + \frac{S_{12} S_{21} \Gamma_L}{1 - S_{22} \Gamma_L} \quad (3.2.5)$$

$$\Gamma_{OUT} = S_{22} + \frac{S_{12} S_{21} \Gamma_s}{1 - S_{11} \Gamma_s} \quad (3.2.6)$$

G_T is a $f(\Gamma_s, \Gamma_L, [S])$ (i.e., a function of Γ_s , Γ_L , and the S parameters of the transistor), $G_p = f(\Gamma_L, [S])$, and $G_A = f(\Gamma_s, [S])$.

If we assume the network to be unilateral, that is, when $S_{12} = 0$, then $\Gamma_{IN} = S_{11}$, $\Gamma_{OUT} = S_{22}$, and the unilateral transducer power gain from (3.2.1) and (3.2.2), called G_{TU} , is given by

$$G_{TU} = \frac{1 - |\Gamma_s|^2}{|1 - S_{11} \Gamma_s|^2} |S_{21}|^2 \frac{1 - |\Gamma_L|^2}{|1 - S_{22} \Gamma_L|^2} \quad (3.2.7)$$

The first term in (3.2.7) depends on the S_{11} parameter of the transistor and the source reflection coefficient. The second term, $|S_{21}|^2$, depends on the transistor scattering parameter S_{21} ; and the third term depends on the S_{22} parameter of the transistor and the load reflection coefficient. We can think of (3.2.7) as being composed of three distinct and independent gain terms. Therefore, we can write (3.2.7) in the form

$$G_{TU} = G_s G_o G_L \quad (3.2.8)$$

where

$$G_s = \frac{1 - |\Gamma_s|^2}{|1 - S_{11} \Gamma_s|^2} \quad (3.2.9)$$

$$G_o = |S_{21}|^2 \quad (3.2.10)$$

$$G_L = \frac{1 - |\Gamma_L|^2}{|1 - S_{22} \Gamma_L|^2} \quad (3.2.11)$$

and the microwave amplifier can be represented by three different gain (or loss) blocks, as shown in Fig. 3.2.2.

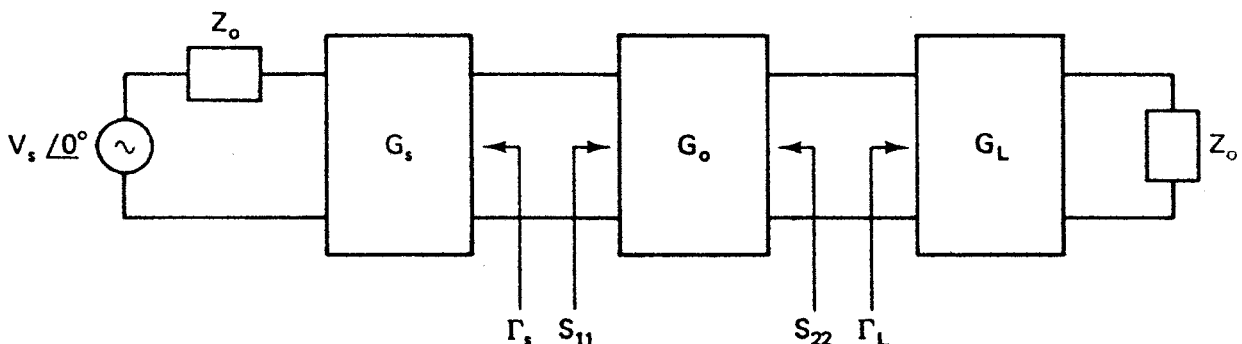


Figure 3.2.2 Unilateral transducer power gain block diagram.

The terms G_s and G_L represent the gain or loss produced by the matching or mismatching of the input or output circuits, respectively. The term G_s affects the degree of matching or mismatching between Γ_s and S_{11} . Although the G_s block is made up of passive components, it can either have a gain contribution greater than unity or a loss. The reason we usually refer to G_s as a gain block is that there is an intrinsic mismatch loss between Z_o , the matching network, and S_{11} (i.e., between Γ_s and S_{11}). Therefore, decreasing the mismatch loss can be thought of as providing a gain. Similarly, the term G_L affects the output matching and can be thought of as the output gain block. The term G_o is related to the device and is equal to $|S_{21}|^2$. In terms of decibels we can write from (3.2.8) to (3.2.11)

$$G_{TU} \text{ (dB)} = G_s \text{ (dB)} + G_o \text{ (dB)} + G_L \text{ (dB)}$$

If we optimize Γ_s and Γ_L to provide maximum gain in G_s and G_L , we refer to the gain as the maximum unilateral transducer power gain, called $G_{TU,\max}$. The maximum gain of G_s and G_L , with $|S_{11}| < 1$ and $|S_{22}| < 1$, is obtained when

$$\Gamma_s = S_{11}^*$$

and

$$\Gamma_L = S_{22}^*$$

Therefore, from (3.2.9) and (3.2.11) we obtain

$$G_{s,\max} = \frac{1}{1 - |S_{11}|^2}$$

$$G_{L,\max} = \frac{1}{1 - |S_{22}|^2}$$

and (3.2.8) gives

$$\begin{aligned} G_{TU,\max} &= G_{s,\max} G_o G_{L,\max} \\ &= \frac{1}{1 - |S_{11}|^2} |S_{21}|^2 \frac{1}{1 - |S_{22}|^2} \end{aligned} \quad (3.2.12)$$

The appropriate block diagram for (3.2.12) is shown in Fig. 3.2.3.

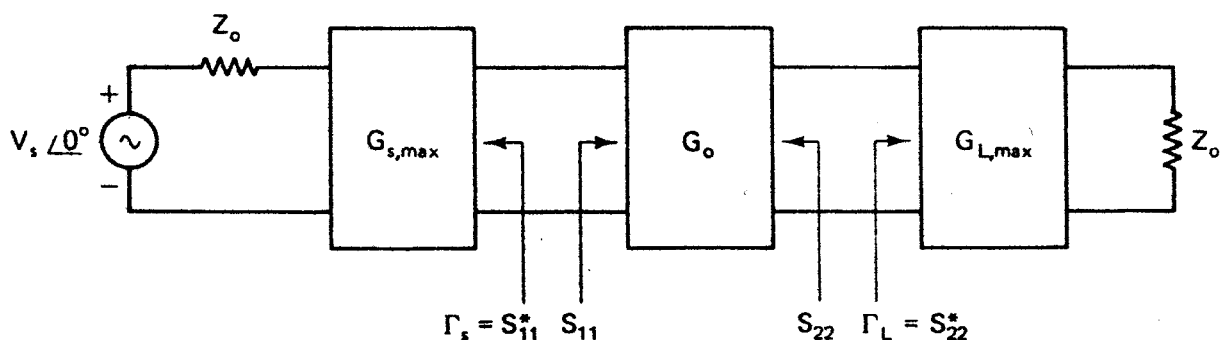


Figure 3.2.3 Maximum unilateral transducer power gain block diagram.

3.3 STABILITY CONSIDERATIONS

The stability of an amplifier, or its resistance to oscillate, is a very important consideration in a design and can be determined from the S parameters, the matching networks, and the terminations. In a two-port network, oscillations are possible when either the input or output port presents a negative resistance. This occurs when $|\Gamma_{IN}| > 1$ or $|\Gamma_{OUT}| > 1$, which for a unilateral device occurs when $|S_{11}| > 1$ or $|S_{22}| > 1$.

The two-port network shown in Fig. 3.3.1 is said to be unconditionally stable at a given frequency if the real parts of Z_{IN} and Z_{OUT} are greater than zero for all passive load and source impedances. If the two-port is not unconditionally stable, it is potentially unstable. That is, some passive load and source terminations can produce input and output impedances having a negative real part.

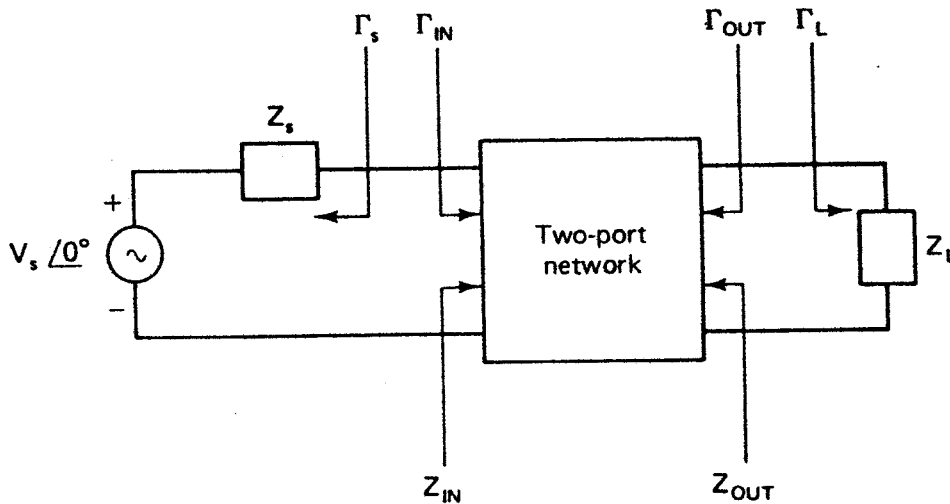


Figure 3.3.1 Stability of two-port networks.

In terms of reflection coefficients, the conditions for unconditional stability at a given frequency are

$$|\Gamma_s| < 1 \quad (3.3.1)$$

$$|\Gamma_L| < 1 \quad (3.3.2)$$

$$|\Gamma_{IN}| = \left| S_{11} + \frac{S_{12} S_{21} \Gamma_L}{1 - S_{22} \Gamma_L} \right| < 1 \quad (3.3.3)$$

and

$$|\Gamma_{OUT}| = \left| S_{22} + \frac{S_{12} S_{21} \Gamma_s}{1 - S_{11} \Gamma_s} \right| < 1 \quad (3.3.4)$$

where, of course, all coefficients are normalized to the same characteristic impedance Z_0 .

The solutions of (3.3.1) to (3.3.4) give the required conditions for the two-port network to be unconditionally stable. However, before we discuss the intricacies of the necessary and sufficient conditions for unconditional stability, a graphical analysis of (3.3.1) to (3.3.4) is presented. The graphical analysis is especially useful in the analysis of potentially unstable transistors.

When the two-port in Fig. 3.3.1 is potentially unstable, there may be values of Γ_s and Γ_L (i.e., source and load impedances) for which the real parts of Z_{IN} and Z_{OUT} are positive. These values of Γ_s and Γ_L (i.e., regions in the Smith chart) can be determined using the following graphical procedure.

First, the regions where values of Γ_L and Γ_s produce $|\Gamma_{IN}| = 1$ and $|\Gamma_{OUT}| = 1$ are determined, respectively. Setting the magnitude of (3.3.3) and (3.3.4) equal to 1 and solving for the values of Γ_L and Γ_s shows that the solutions for Γ_L and Γ_s lie on circles (called *stability circles*) whose equations are given by

$$\left| \Gamma_L - \frac{(S_{22} - \Delta S_{11}^*)^*}{|S_{22}|^2 - |\Delta|^2} \right| = \left| \frac{S_{12} S_{21}}{|S_{22}|^2 - |\Delta|^2} \right| \quad (3.3.5)$$

and

$$\left| \Gamma_s - \frac{(S_{11} - \Delta S_{22}^*)^*}{|S_{11}|^2 - |\Delta|^2} \right| = \left| \frac{S_{12} S_{21}}{|S_{11}|^2 - |\Delta|^2} \right| \quad (3.3.6)$$

where

$$\Delta = S_{11} S_{22} - S_{12} S_{21}$$

The radii and centers of the circles where $|\Gamma_{IN}| = 1$ and $|\Gamma_{OUT}| = 1$ in the Γ_L plane and Γ_s plane, respectively, are obtained from (3.3.5) and (3.3.6), namely:

Γ_L values for $|\Gamma_{IN}| = 1$ (*Output Stability Circle*):

$$r_L = \left| \frac{S_{12} S_{21}}{|S_{22}|^2 - |\Delta|^2} \right| \quad (\text{radius}) \quad (3.3.7)$$

$$C_L = \frac{(S_{22} - \Delta S_{11}^*)^*}{|S_{22}|^2 - |\Delta|^2} \quad (\text{center}) \quad (3.3.8)$$

Γ_s values for $|\Gamma_{OUT}| = 1$ (*Input Stability Circle*):

$$r_s = \left| \frac{S_{12} S_{21}}{|S_{11}|^2 - |\Delta|^2} \right| \quad (\text{radius}) \quad (3.3.9)$$

$$C_s = \frac{(S_{11} - \Delta S_{22}^*)^*}{|S_{11}|^2 - |\Delta|^2} \quad (\text{center}) \quad (3.3.10)$$

With the S parameters of a two-port device at one frequency, the expressions (3.3.7) to (3.3.10) can be calculated, plotted on a Smith chart, and the set of values of Γ_L and Γ_s that produce $|\Gamma_{IN}| = 1$ and $|\Gamma_{OUT}| = 1$ easily observed. Figure 3.3.2 illustrates the graphical construction of the stability circles

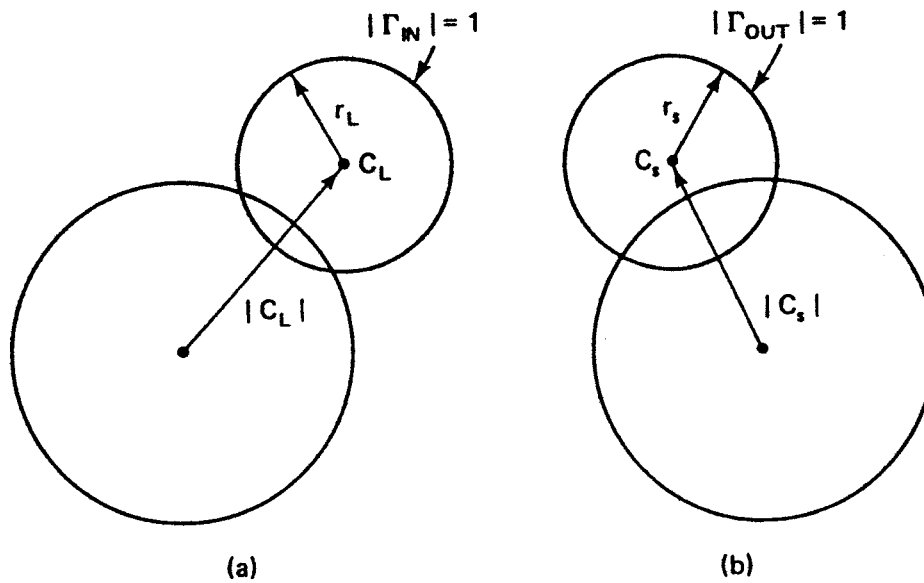


Figure 3.3.2 Stability circle construction in the Smith chart: (a) Γ_L plane; (b) Γ_s plane.

where $|\Gamma_{IN}| = 1$ and $|\Gamma_{OUT}| = 1$. On one side of the stability circle boundary, in the Γ_L plane, we will have $|\Gamma_{IN}| < 1$ and on the other side $|\Gamma_{IN}| > 1$. Similarly, in the Γ_s plane on one side of the stability circle boundary, we will have $|\Gamma_{OUT}| < 1$ and on the other side $|\Gamma_{OUT}| > 1$.

Next, we need to determine which area in the Smith chart represents the stable region. In other words, the region where values of Γ_L (where $|\Gamma_L| < 1$) produce $|\Gamma_{IN}| < 1$, and where values of Γ_s (where $|\Gamma_s| < 1$) produce $|\Gamma_{OUT}| < 1$. To this end, we observe that if $Z_L = Z_o$, then $\Gamma_L = 0$ and from (3.2.5) $|\Gamma_{IN}| = |S_{11}|$. If the magnitude of S_{11} is less than 1, then $|\Gamma_{IN}| < 1$ when $\Gamma_L = 0$. That is, the center of the Smith chart in Fig. 3.3.2a represents a stable operating point, because for $\Gamma_L = 0$ it follows that $|\Gamma_{IN}| < 1$. On the other hand, if $|S_{11}| > 1$ when $Z_L = Z_o$, then $|\Gamma_{IN}| > 1$ when $\Gamma_L = 0$ and the center of the Smith chart represents an unstable operating point. Figure 3.3.3 illus-

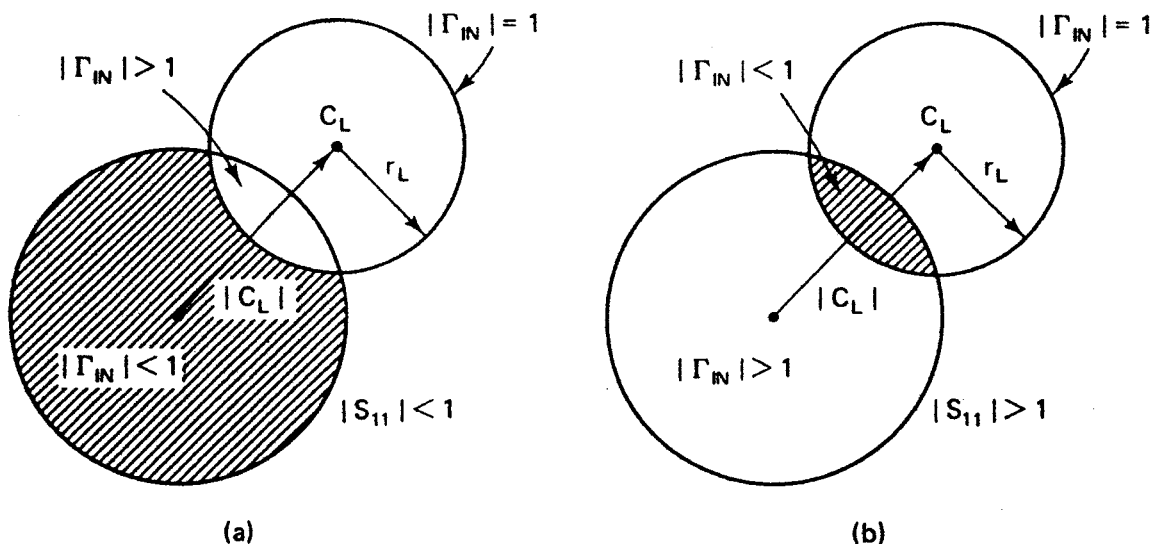


Figure 3.3.3 Smith chart illustrating stable and unstable regions in the Γ_L plane.

In fact, the input and output stability circles, from (3.3.7) to (3.3.10), are located at $C_s = 0.1 \angle 107.4^\circ$, $r_s = 0.44$, $C_L = 0.26 \angle -36.3^\circ$, and $r_L = 0.41$, which can be drawn inside the Smith chart to show the unstable regions. Also, a calculation of B_1 from (3.3.16) produces a negative value (i.e., $B_1 = -3.34$). Since $K > 1$ and $B_1 < 0$, we conclude again that the transistor is potentially unstable.

In the unilateral amplifier $K = \infty$ and we have unconditional stability if $|S_{11}| < 1$ and $|S_{22}| < 1$ for all passive load and source terminations.

In the potentially unstable situation illustrated in Figs. 3.3.3 and 3.3.4, the real part of the input and output impedances can be negative for some source and load reflection coefficients. In this case, selecting Γ_s and Γ_L in the stable region produces a stable operation.

Even when the selection of Γ_L and Γ_s produces $|\Gamma_{IN}| > 1$ or $|\Gamma_{OUT}| > 1$, the circuit can be made stable if the total input and output loop resistance in Fig. 3.3.1 is positive. In other words, the circuit is stable if

$$\operatorname{Re}(Z_s + Z_{IN}) > 0$$

and

$$\operatorname{Re}(Z_L + Z_{OUT}) > 0$$

A potentially unstable transistor can be made unconditionally stable by either resistively loading the transistor or by adding negative feedback. These techniques are not recommended in narrowband amplifiers because of the resulting degradation in power gain, noise figure, and so on. Narrowband amplifier design with potentially unstable transistors is best done by the proper selection of Γ_s and Γ_L to ensure stability. On the other hand, the techniques are popular in the design of some broadband amplifiers where the transistor is potentially unstable.

The following example illustrates how resistive loading can stabilize a potentially unstable transistor.

Example 3.3.1

The S parameters of a transistor at $f = 800$ MHz are

$$S_{11} = 0.65 \angle -95^\circ$$

$$S_{12} = 0.035 \angle 40^\circ$$

$$S_{21} = 5 \angle 115^\circ$$

$$S_{22} = 0.8 \angle -35^\circ$$

Determine the stability and show how resistive loading can stabilize the transistor.

Solution. From (3.3.13) and (3.3.17) we find that $K = 0.547$ and $\Delta = 0.504 \angle 249.6^\circ$. Since $K < 1$, the transistor is potentially unstable at $f = 800$ MHz.

The input and output stability circles are calculated using (3.3.7) to (3.3.10):

$$C_s = 1.79 \angle 122^\circ \quad C_L = 1.3 \angle 48^\circ$$

$$r_s = 1.04 \quad r_L = 0.45$$

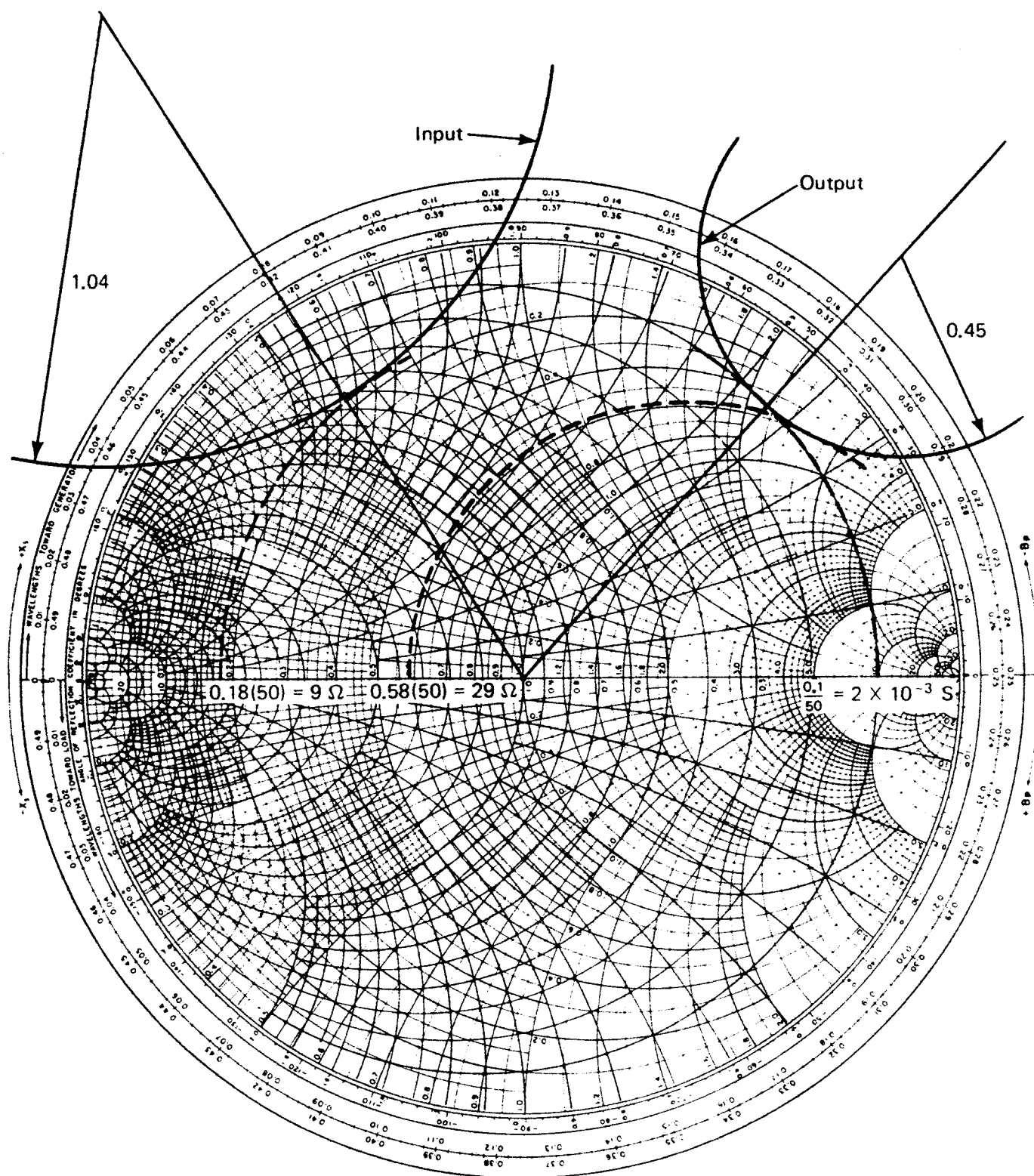


Figure 3.3.6 Input and output stability circles.

Figure 3.3.6 shows the plot of the stability circles, together with the stable region. It can be seen that a series resistor with the input, of approximately $9\ \Omega$, assures stability at the input. Also, a series resistor of approximately $29\ \Omega$, or a shunt resistor of approximately $500\ \Omega$ at the output, produces stability at the output. The three choices of resistive loading are shown in Fig. 3.3.7. The most popular is the shunt resistor configuration in Fig. 3.3.7c.

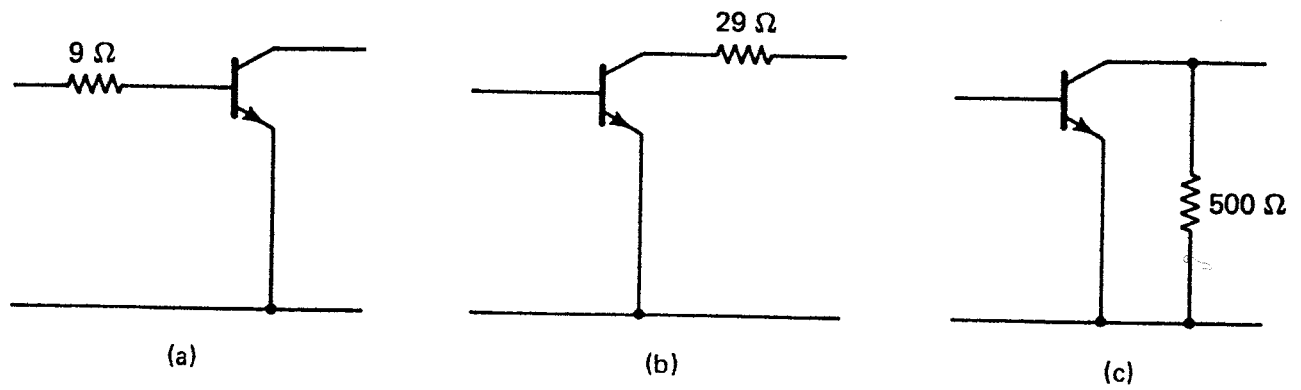


Figure 3.3.7 Three types of resistive loading to improve stability.

For the stabilized shunt resistor configuration in Fig. 3.3.7c (i.e., with a 500-Ω shunt resistor), the resulting S parameters are

$$S_{11} = 0.65 \angle -94^\circ$$

$$S_{12} = 0.032 \angle 41.2^\circ$$

$$S_{21} = 4.62 \angle 116.2^\circ$$

$$S_{22} = 0.66 \angle -36^\circ$$

and from (3.3.13) and (3.3.17) $K = 1.04$ and $\Delta = 0.409 \angle 250.13^\circ$, which show that the stabilized network in Fig. 3.3.7c is unconditionally stable at $f = 800$ MHz.

Negative feedback can be used to stabilize a transistor by neutralizing S_{12} , that is, by making $S_{12} = 0$. However, this is not commonly done. In a broadband amplifier design using a potentially unstable transistor, a common procedure is to use resistive loading to stabilize the transistor and negative feedback to provide the proper ac performance, that is, to provide constant gain and low input and output VSWR.

3.4 CONSTANT-GAIN CIRCLES—UNILATERAL CASE

The unilateral transducer power gain is given by (3.2.7) or (3.2.8), and the maximum unilateral transducer power gain, obtained when $\Gamma_s = S_{11}^*$ and $\Gamma_L = S_{22}^*$, is given by (3.2.12). The expressions for G_s and G_L in (3.2.9) and (3.2.11) are similar in form and they can be written in the general form

$$G_i = \frac{1 - |\Gamma_i|^2}{|1 - S_{ii}\Gamma_i|^2} \quad (3.4.1)$$

where $i = s$ ($ii = 11$) or $i = L$ ($ii = 22$). The design for a specific gain is based on (3.4.1).

Two cases must be considered in the analysis of (3.4.1), the unconditionally stable case where $|S_{ii}| < 1$ and the potentially unstable case where $|S_{ii}| > 1$.

Unconditionally Stable Case, $|S_{ii}| < 1$

The maximum value of (3.4.1) is obtained when $\Gamma_i = S_{ii}^*$, and it is given by

$$G_{i,\max} = \frac{1}{1 - |S_{ii}|^2} \quad (3.4.2)$$

The terminations that produce $G_{i,\max}$ are called the *optimum terminations*.

From (3.4.1), G_i has a minimum value of zero when $|\Gamma_i| = 1$. Other values of Γ_i produce values of G_i between zero and $G_{i,\max}$, that is,

$$0 \leq G_i \leq G_{i,\max}$$

The values of Γ_i that produce a constant gain G_i will be shown to lie in a circle in the Smith chart. These circles are called *constant-gain circles*.

Define the normalized gain factor as

$$g_i = \frac{G_i}{G_{i,\max}} = G_i(1 - |S_{ii}|^2) \quad (3.4.3)$$

such that

$$0 \leq g_i \leq 1$$

In order to set g_i equal to a constant and solve for the values of Γ_i , we let

$$\Gamma_i = U_i + jV_i \quad (3.4.4)$$

and

$$S_{ii} = A_{ii} + jB_{ii} \quad (3.4.5)$$

Substitute (3.4.4) and (3.4.5) into (3.4.3); after some manipulations we obtain

$$\begin{aligned} \left[U_i - \frac{g_i A_{ii}}{1 - |S_{ii}|^2(1 - g_i)} \right]^2 + \left[V_i + \frac{g_i B_{ii}}{1 - |S_{ii}|^2(1 - g_i)} \right]^2 \\ = \left[\frac{\sqrt{1 - g_i(1 - |S_{ii}|^2)}}{1 - |S_{ii}|^2(1 - g_i)} \right]^2 \end{aligned} \quad (3.4.6)$$

Equation (3.4.6) is recognized as a family of circles with g_i as a parameter. The centers of the circles are located at

$$U_c = \frac{g_i A_{ii}}{1 - |S_{ii}|^2(1 - g_i)}$$

and

$$V_c = \frac{-g_i B_{ii}}{1 - |S_{ii}|^2(1 - g_i)}$$

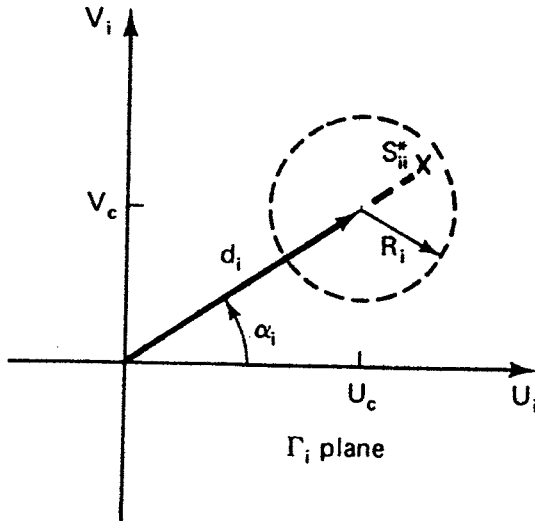


Figure 3.4.1 Constant-gain circles in the Smith chart.

and the radii of the circles are given by

$$R_i = \frac{\sqrt{1 - g_i (1 - |S_{ii}|^2)}}{1 - |S_{ii}|^2(1 - g_i)} \quad (3.4.7)$$

Figure 3.4.1 illustrates the location of a constant-gain circle. The distance from the origin to the center of a constant-gain circle is given by

$$d_i = \sqrt{U_c^2 + V_c^2} = \frac{g_i |S_{ii}|}{1 - |S_{ii}|^2(1 - g_i)} \quad (3.4.8)$$

and the angle of inclination, α_i , is

$$\tan \alpha_i = \frac{V_c}{U_c}$$

or

$$\alpha_i = \tan^{-1} \frac{-B_{ii}}{A_{ii}} \quad (3.4.9)$$

Equation (3.4.9) shows that the constant-gain circles are located, at a distance d_i given by (3.4.8), along the line drawn from the origin to the point S_{ii}^* (i.e., $S_{ii}^* = A_{ii} - jB_{ii}$).

It is observed that when $g_i = 1$ (i.e., when $G_i = G_{i,\max}$) (3.4.7) gives $R_i = 0$ and (3.4.8) gives $d_i = |S_{ii}|$. Therefore, the constant-gain circle for maximum gain is represented by a point, located at S_{ii}^* .

In conclusion, the procedure for drawing the constant-gain circles in the Z Smith chart is:

1. Locate S_{ii}^* and draw a line from the origin to S_{ii}^* . At S_{ii}^* , the gain is $G_{i,\max}$ and given by (3.4.2).
2. Determine the values of G_i , where $0 \leq G_i \leq G_{i,\max}$, for which the constant-gain circles are to be drawn, and calculate the corresponding values of $g_i = G_i/G_{i,\max}$.

3. From (3.4.8), determine the values of d_i for each g_i .
4. From (3.4.7), determine the values of R_i for each g_i .

The 0-dB circle ($G_i = 1$) always passes through the origin of the Smith chart. This is not a coincidence. In fact, $G_i = 1$ occurs when $\Gamma_i = 0$ and from (3.4.3)

$$g_{i,0dB} = 1 - |S_{ii}|^2$$

then, from (3.4.7) and (3.4.8),

$$R_{i,0dB} = d_{i,0dB} = \frac{|S_{ii}|}{1 + |S_{ii}|^2}$$

which shows that the radius and the distance from the origin to the center of the 0-dB constant-gain circle are identical.

A typical set of constant-gain circles for G_s are calculated in the following example and shown in Fig. 3.4.2.

Example 3.4.1

The S parameters of a BJT measured at $V_{CE} = 10$ V, $I_C = 30$ mA, and $f = 1$ GHz, in a 50- Ω system are

$$S_{11} = 0.73 \angle 175^\circ$$

$$S_{12} = 0$$

$$S_{21} = 4.45 \angle 65^\circ$$

$$S_{22} = 0.21 \angle -80^\circ$$

- (a) Calculate the optimum terminations.
- (b) Calculate $G_{s,max}$, $G_{L,max}$, and $G_{TU,max}$ in decibels.
- (c) Draw several G_s constant-gain circles.
- (d) Design the input matching network for $G_s = 2$ dB.

Solution. (a) The optimum terminations are

$$\Gamma_s = S_{11}^* = 0.73 \angle -175^\circ$$

and

$$\Gamma_L = S_{22}^* = 0.21 \angle 80^\circ$$

Using the Smith chart, the impedances associated with Γ_s and Γ_L are $Z_s = 50(0.152 - j0.047) = 7.6 - j2.35 \Omega$ and $Z_L = 50(0.97 + j0.43) = 48.5 + j21.5 \Omega$.

(b) From (3.4.2) we find that

$$G_{s,max} = \frac{1}{1 - |S_{11}|^2} = 2.141 \quad \text{or} \quad 3.31 \text{ dB}$$

$$G_{L,max} = \frac{1}{1 - |S_{22}|^2} = 1.046 \quad \text{or} \quad 0.196 \text{ dB}$$

Since

$$G_o = |S_{21}|^2 = 19.8 \quad \text{or} \quad 12.97 \text{ dB}$$

then

$$G_{TU,\max} (\text{dB}) = 3.31 + 0.196 + 12.97 = 16.47 \text{ dB}$$

(c) The output network provides little gain (i.e., $G_{L,\max} = 0.195 \text{ dB}$); therefore, the output matching network is designed to present the optimum termination $\Gamma_L = 0.21 \angle 80^\circ$. Since $G_{s,\max} = 3.31 \text{ dB}$, constant-gain circles at 2, 1, 0, and -1 dB are drawn in Fig. 3.4.2a. The necessary calculations are given in Fig. 3.4.2b.

(d) Any Γ_s along the $G_s = 2 \text{ dB}$ circle provides the constant gain. Selecting Γ_s at point A (i.e., $z_s = 0.42 + j0.1$) in Fig. 3.4.2a results in the input matching network shown in Fig. 3.4.3a. The details of the matching network design are shown in Fig. 3.4.3b.

Potentially Unstable Case, $|S_{ii}| > 1$

In this case $|S_{ii}| > 1$ and it is possible for a passive termination to produce an infinite value of G_i . The infinite value of G_i in (3.4.1) is produced by the critical value of Γ_i , called $\Gamma_{i,c}$, given by

$$\Gamma_{i,c} = \frac{1}{S_{ii}} \quad (3.4.10)$$

Equation (3.4.10) basically states that the real part of the impedance associated with $\Gamma_{i,c}$ is equal to the magnitude of the negative resistance associated with S_{ii} . Therefore, the total input or output loop resistance is zero, and oscillations will occur.

As discussed in Section 2.2, in the case of negative resistances we can locate $1/S_{ii}^*$ in the Smith chart and interpret the resistance circles as being negative and the reactance circles as labeled.

With g_i defined as in (3.4.3), namely

$$g_i = G_i(1 - |S_{ii}|^2)$$

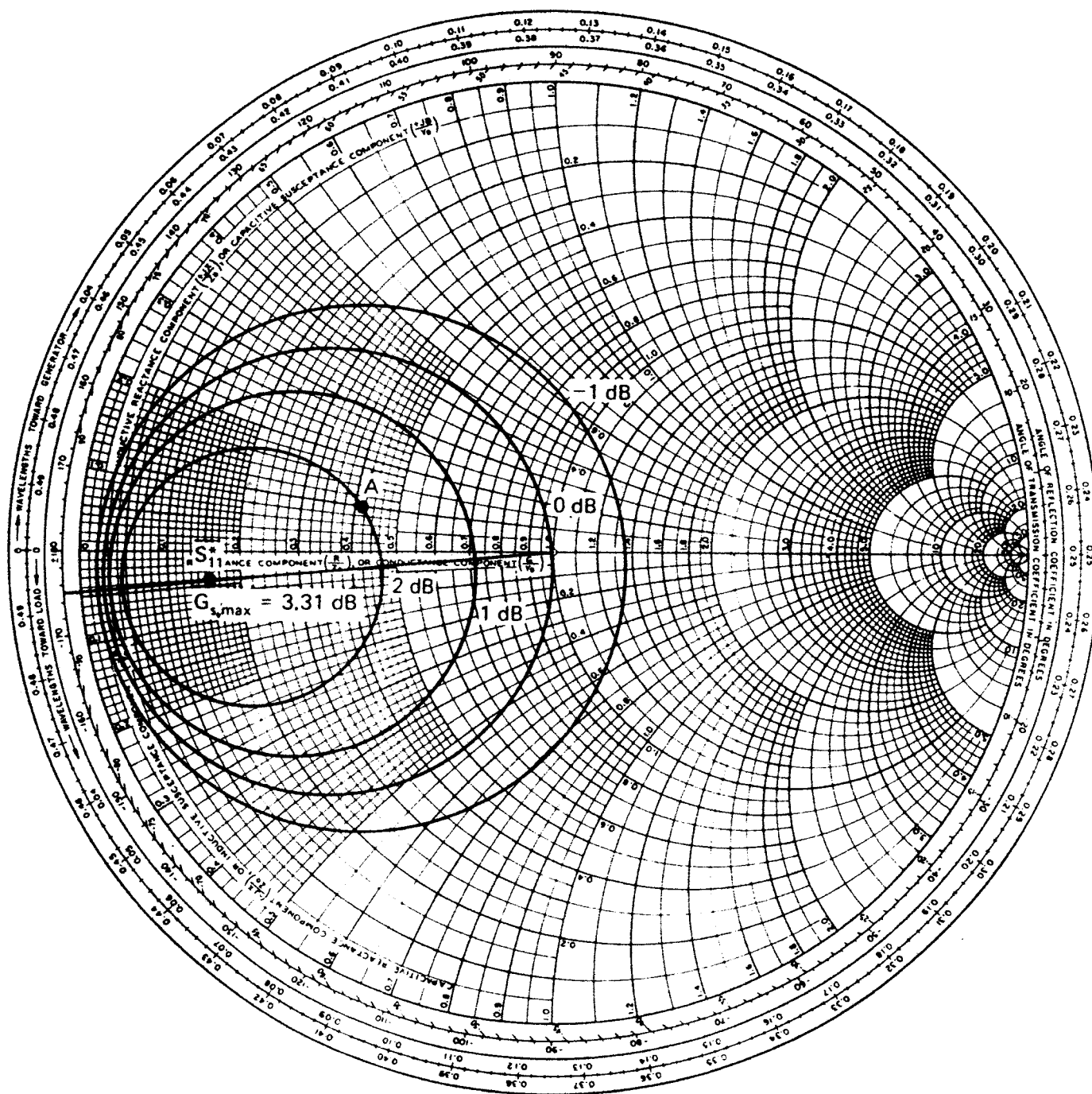
where now g_i can attain negative values because $|S_{ii}| > 1$, it is not difficult to show that the centers of the constant-gain circles are located at the distance d_i given by (3.4.8) and the radii of the circles R_i given by (3.4.7). The centers of the constant-gain circles are located, at the distance d_i , along a line drawn from the origin to the point $1/S_{ii}$.

To prevent oscillations in the input or output port, Γ_i must be selected such that the real part of the termination impedance is larger than the magnitude of the negative resistance associated with the point $1/S_{ii}^*$. The stable region is that region where values of Γ_i produce a termination such that

$$\text{Re}(Z_s) > |\text{Re}(Z_{\text{IN}})|$$

and

$$\text{Re}(Z_L) > |\text{Re}(Z_{\text{OUT}})|$$

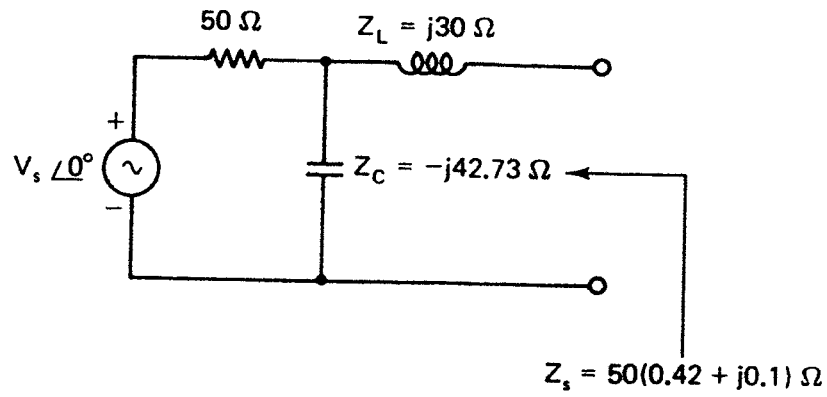


(a)

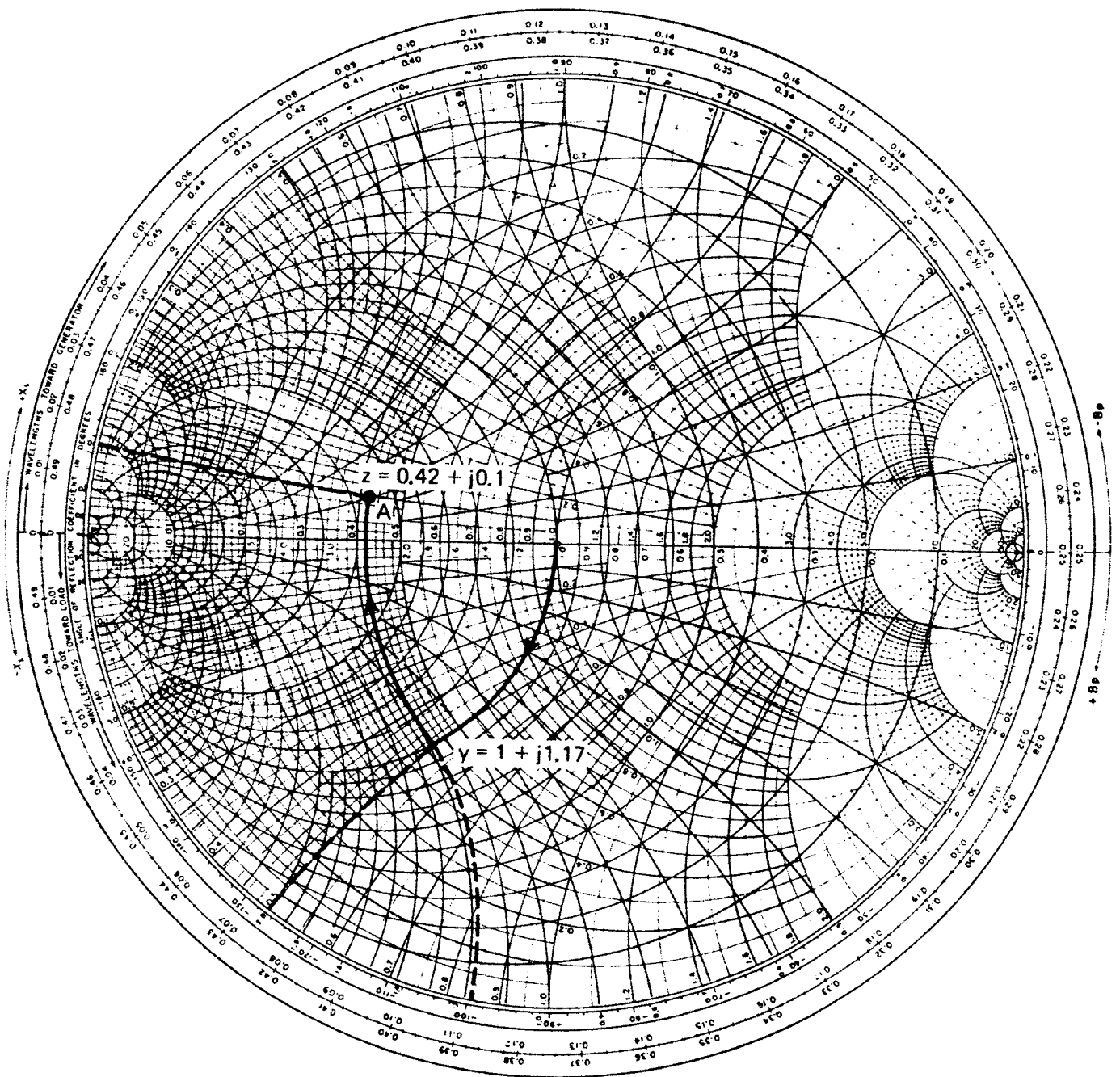
G_s (dB):	2	1	0	-1
G_s	1.59	1.26	1	0.79
g_s	0.743	0.588	0.467	0.369
d_s	0.629	0.55	0.476	0.406
R_s	0.274	0.384	0.476	0.559

(b)

Figure 3.4.2 (a) Constant-gain circles for $G_s = 2, 1, 0$, and -1 dB; (b) calculations of constant-gain circles.



(a)



(b)

Figure 3.4.3 Input matching network for $G_s = 2$ dB.

A typical construction is illustrated in Fig. 3.4.4, where the critical value of Γ_s (i.e., $\Gamma_{s,c} = 1/S_{11}$) and two constant-gain circles are shown.

Example 3.4.2

The S parameters of a GaAs FET measured at $V_{DS} = 5$ V, $I_{DS} = 10$ mA, and $f = 1$ GHz in a $50\text{-}\Omega$ system are

$$S_{11} = 2.27 \angle -120^\circ$$

$$S_{12} = 0$$

$$S_{21} = 4 \angle 50^\circ$$

$$S_{22} = 0.6 \angle -80^\circ$$

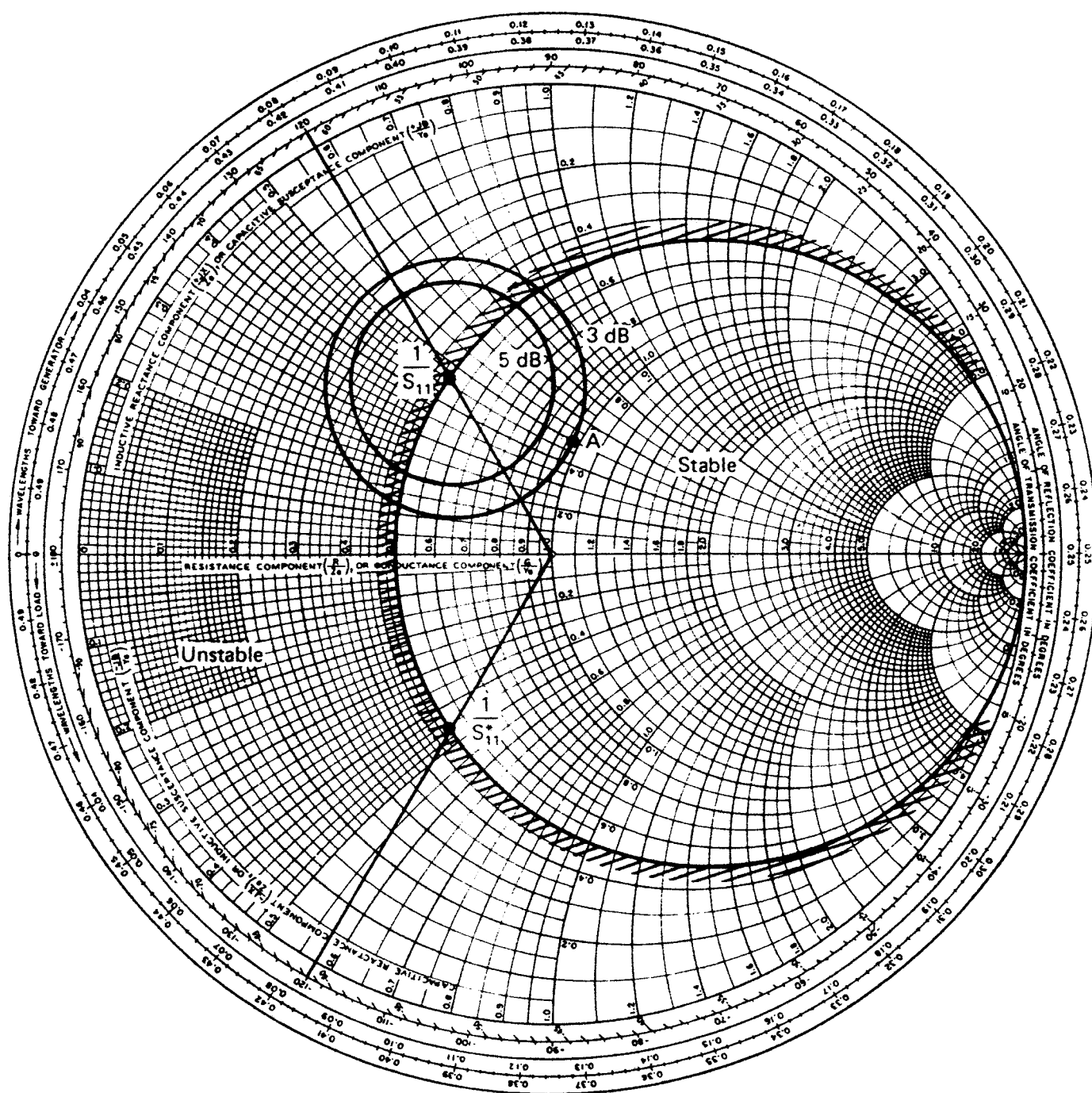


Figure 3.4.4 Stable and unstable regions, and G_s constant-gain circles for Example 3.4.2.

- Calculate the input impedance and the optimum output terminations.
- Determine the unstable region in the Smith chart and construct constant-gain circles for $G_s = 5$ dB and $G_s = 3$ dB.
- Design the input matching network for $G_s = 3$ dB with the greatest degree of stability.
- Determine G_{TU} in decibels.

Solution. (a) The input impedance is obtained from the Smith chart at the point $1/S_{11}^* = 0.44 \angle -120^\circ$ (see Fig. 3.4.4), namely

$$Z_{IN} = 50(-0.5 - j0.46) = -25 - j23 \Omega$$

The optimum termination for G_L is

$$\Gamma_L = S_{22}^* = 0.6 \angle 80^\circ$$

The impedance associated with Γ_L is obtained from the Smith chart as $Z_L = 50(0.56 + j1.03) = 28 + j51.5 \Omega$.

(b) The unstable region is where $\text{Re}(Z_s) < |\text{Re}(Z_{IN})|$. The unstable region is marked in Fig. 3.4.4.

In order to construct the constant-gain circle for $G_s = 5$ dB, we first locate the point $1/S_{11}$ in Fig. 3.4.4. Then, from (3.4.3), (3.4.7), and (3.4.8), we find that

$$g_s = 3.16[1 - (2.27)^2] = -13.123$$

$$R_s = \frac{\sqrt{1 + 13.123} [1 - (2.27)^2]}{1 - (2.27)^2(1 + 13.123)} = 0.217$$

and

$$d_s = \frac{-13.123(2.27)}{1 - (2.27)^2(1 + 13.123)} = 0.415$$

The $G_s = 5$ dB circle is drawn in Fig. 3.4.4. Similarly, for the $G_s = 3$ dB circle, we find that $g_s = -8.286$, $d_s = 0.401$, and $R_s = 0.27$.

(c) In order to obtain the greatest degree of stability we select Γ_s on the $G_s = 3$ dB circle such that it has the largest positive real part. That is, Γ_s is selected at point A in Fig. 3.4.4, namely

$$\Gamma_s = 0.245 \angle 79^\circ$$

or

$$Z_s = 50(0.97 + j0.5) = 48.5 + j25 \Omega$$

Since the input loop resistance is $48.5 - 25 = 23.5 \Omega$, the input port is stable.

(d) Since $G_s = 3$ dB,

$$G_{L,\max} = \frac{1}{1 - |S_{22}|^2} = \frac{1}{1 - (0.6)^2} = 1.562 \quad \text{or} \quad 1.94 \text{ dB}$$

and

$$G_o = |S_{21}|^2 = (4)^2 = 16 \quad \text{or} \quad 12.04 \text{ dB}$$

the unilateral transducer gain is

$$G_{TU} (\text{dB}) = 3 + 12.04 + 1.94 = 16.98 \text{ dB}$$

3.5 UNILATERAL FIGURE OF MERIT

When S_{12} can be set equal to zero, the design procedure is much simpler. In order to determine the error involved in assuming $S_{12} = 0$, we form the magnitude ratio of G_T and G_{TU} from (2.7.10) and (3.2.7), namely

$$\frac{G_T}{G_{TU}} = \frac{1}{|1 - X|^2} \quad (3.5.1)$$

where

$$X = \frac{S_{12} S_{21} \Gamma_s \Gamma_L}{(1 - S_{11} \Gamma_s)(1 - S_{22} \Gamma_L)}$$

From (3.5.1) the ratio of the transducer power gain to the unilateral transducer power gain is bounded by

$$\frac{1}{(1 + |X|)^2} < \frac{G_T}{G_{TU}} < \frac{1}{(1 - |X|)^2}$$

When $\Gamma_s = S_{11}^*$ and $\Gamma_L = S_{22}^*$, G_{TU} has a maximum value and, in this case, the maximum error introduced when using G_{TU} is bounded by

$$\frac{1}{(1 + U)^2} < \frac{G_T}{G_{TU}} < \frac{1}{(1 - U)^2} \quad (3.5.2)$$

where

$$U = \frac{|S_{12}| |S_{21}| |S_{11}| |S_{22}|}{(1 - |S_{11}|^2)(1 - |S_{22}|^2)} \quad (3.5.3)$$

is known as the *unilateral figure of merit*.

The value of U varies with frequency because of its dependence on the S parameters. A typical variation of U with frequency is shown in Fig. 3.5.1. In this case, the maximum value of U occurs at 100 MHz and 1 GHz, and is given by $U = -15$ dB or $U = 0.03$. Therefore, from (3.5.2),

$$\frac{1}{(1 + 0.03)^2} < \frac{G_T}{G_{TU}} < \frac{1}{(1 - 0.03)^2}$$

or in decibels,

$$-0.26 \text{ dB} < \frac{G_T}{G_{TU}} < 0.26 \text{ dB}$$

and the maximum error is ± 0.26 dB at 100 MHz and 1 GHz. In this case, the error is small enough to justify the unilateral assumption.

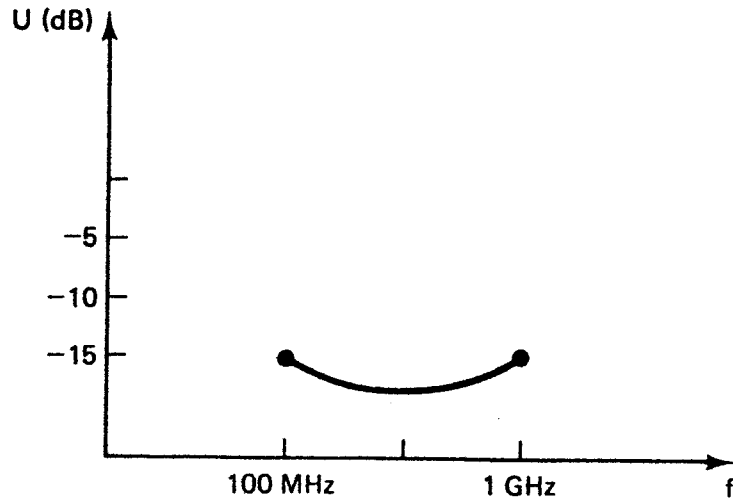


Figure 3.5.1 Frequency dependence of the unilateral figure of merit.

3.6 SIMULTANEOUS CONJUGATE MATCH— BILATERAL CASE

When $S_{12} \neq 0$, and the unilateral assumption cannot be made, the input and output reflection coefficients are given by (3.2.5) and (3.2.6), respectively. The conditions required to obtain maximum transducer power gain are

$$\Gamma_{IN} = \Gamma_s^* \quad (3.6.1)$$

and

$$\Gamma_{OUT} = \Gamma_L^* \quad (3.6.2)$$

These conditions are illustrated in Fig. 3.6.1.

From (3.2.5), (3.2.6), (3.6.1), and (3.6.2) we can write

$$\Gamma_s^* = S_{11} + \frac{S_{12} S_{21} \Gamma_L}{1 - S_{22} \Gamma_L} \quad (3.6.3)$$

and

$$\Gamma_L^* = S_{22} + \frac{S_{12} S_{21} \Gamma_s}{1 - S_{11} \Gamma_s} \quad (3.6.4)$$

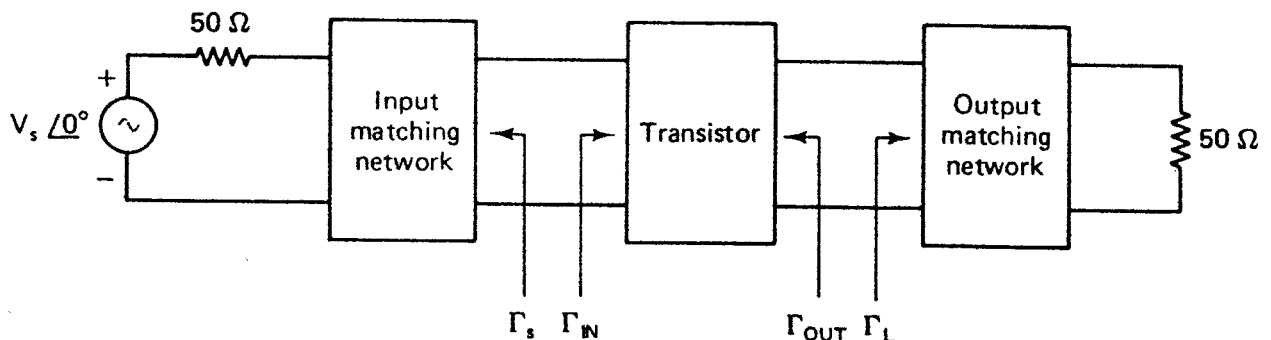


Figure 3.6.1 Simultaneous conjugate match exists when $\Gamma_{IN} = \Gamma_s^*$ and $\Gamma_{OUT} = \Gamma_L^*$.

Solving (3.6.3) and (3.6.4) simultaneously gives the values of Γ_s and Γ_L required for a simultaneous conjugate match. Calling these values Γ_{Ms} and Γ_{ML} , we obtain

$$\Gamma_{Ms} = \frac{B_1 \pm \sqrt{B_1^2 - 4|C_1|^2}}{2C_1} \quad (3.6.5)$$

$$\Gamma_{ML} = \frac{B_2 \pm \sqrt{B_2^2 - 4|C_2|^2}}{2C_2} \quad (3.6.6)$$

$$B_1 = 1 + |S_{11}|^2 - |S_{22}|^2 - |\Delta|^2 \quad (3.6.7)$$

$$B_2 = 1 + |S_{22}|^2 - |S_{11}|^2 - |\Delta|^2 \quad (3.6.8)$$

$$C_1 = S_{11} - \Delta S_{22}^*$$

$$C_2 = S_{22} - \Delta S_{11}^*$$

In what follows we will show that for an unconditionally stable two-port network, the solutions with a minus sign in (3.6.5) and (3.6.6) are the useful ones.

If $|B_1/2C_1| > 1$ and $B_1 > 0$ in (3.6.5), the solution with the minus sign produces $|\Gamma_{Ms}| < 1$ and the solution with the plus sign produces $|\Gamma_{Ms}| > 1$. If $|B_1/2C_1| > 1$ with $B_1 < 0$ in (3.6.5), the solution with the plus sign produces $|\Gamma_{Ms}| < 1$ and the solution with the minus sign produces $|\Gamma_{Ms}| > 1$. Similar considerations apply to (3.6.6).

Since it can be shown that $|B_i/2C_i|^2 > 1$ ($i = 1$ or 2) is similar to $K^2 > 1$, it follows that the condition $|B_i/2C_i| > 1$ is similar to $|K| > 1$ (see Problem 3.13).

Therefore, if $|K| > 1$ with K positive, one solution of (3.6.5) and (3.6.6) has a magnitude less than 1, and the other solution has magnitude greater than 1. In fact, in this case if $B_i > 0$ the solutions with the minus sign have magnitudes less than 1 (observe from Problem 3.5 that in this case B_1 and B_2 have the same sign). The analysis for $|K| > 1$ with K negative is left as an exercise (see Problem 3.13).

Associated with Γ_{Ms} and Γ_{ML} are a source and a load impedance. The real parts of these impedances are positive if $|\Gamma_{Ms}| < 1$ and $|\Gamma_{ML}| < 1$. From the previous considerations, we conclude that in terms of K , the condition that a two-port network can be simultaneously matched with $|\Gamma_{Ms}| < 1$ and $|\Gamma_{ML}| < 1$ is [3.1, 3.2]

$$K > 1$$

The condition $K > 1$ is only a necessary condition for unconditional stability. Therefore, a simultaneous conjugate match having unconditional stability is possible if $K > 1$ and $|\Delta| < 1$. Since $|\Delta| < 1$ implies that $B_1 > 0$ and $B_2 > 0$, the minus signs must be used in (3.6.5) and (3.6.6) when calculating the simultaneous conjugate match for an unconditionally stable two-port network.

In what follows any reference to a simultaneous conjugate match as-

sumes that the two-port network is unconditionally stable. In a potentially unstable situation the design procedure is best done in terms of G_p or G_A (see Section 3.8).

The maximum transducer power gain, under simultaneous conjugate match conditions, is obtained from (2.7.10) with $\Gamma_s = \Gamma_{Ms}$ and $\Gamma_L = \Gamma_{ML}$, namely

$$G_{T,\max} = \frac{(1 - |\Gamma_{Ms}|^2) |S_{21}|^2 (1 - |\Gamma_{ML}|^2)}{|(1 - S_{11}\Gamma_{Ms})(1 - S_{22}\Gamma_{ML}) - S_{12}S_{21}\Gamma_{ML}\Gamma_{Ms}|^2} \quad (3.6.9)$$

Substituting (3.6.5) and (3.6.6) into (3.6.9), and using (3.3.13) gives the relation

$$G_{T,\max} = \frac{|S_{21}|}{|S_{12}|} (K - \sqrt{K^2 - 1}) \quad (3.6.10)$$

The maximum stable gain is defined as the value of $G_{T,\max}$ when $K = 1$, namely

$$G_{MSG} = \frac{|S_{21}|}{|S_{12}|} \quad (3.6.11)$$

G_{MSG} is a figure of merit that represents the maximum value that $G_{T,\max}$ can have. It can be achieved by resistively loading the two-port (i.e., the transistor) to make $K = 1$, or by using feedback.

3.7 CONSTANT-GAIN CIRCLES—BILATERAL CASE

The bilateral case occurs when S_{12} cannot be neglected. Two different cases must be considered in the analysis: the unconditionally stable bilateral case and the potentially unstable bilateral case.

Unconditionally Stable Bilateral Case, $K > 1$ and $|\Delta| < 1$

This situation occurs when $K > 1$ and $|\Delta| < 1$, and any passive source and load terminations can be used. Of course, the terminations Γ_{Ms} and Γ_{ML} , given by (3.6.5) and (3.6.6), will produce a simultaneous conjugate match which results in the maximum value of the transducer power gain.

If the design calls for a transducer power gain different from the maximum, a constant-gain circle procedure based on (3.2.1) or (3.2.2) can be used. For example, a procedure based on (3.2.1) is as follows. Write (3.2.1) in the form

$$G_T = G'_s G_o G_L \quad (3.7.1)$$

where

$$G'_s = \frac{1 - |\Gamma_s|^2}{|1 - \Gamma_{IN} \Gamma_s|^2} \quad (3.7.2)$$

$$G_o = |S_{21}|^2$$

and

$$G_L = \frac{1 - |\Gamma_L|^2}{|1 - S_{22} \Gamma_L|^2} \quad (3.7.3)$$

Then the design procedure is as follows:

1. From (3.7.3), the constant-gain circles for G_L can be drawn using (3.4.3) and (3.4.7) to (3.4.9). Select the desired Γ_L for a given G_L gain.
2. Calculate Γ_{IN} from (3.2.5). Observe that Γ_{IN} depends on Γ_L ; therefore, G'_s depends on G_L .
3. From (3.7.2), the constant-gain circles for G'_s can be drawn using (3.4.3) and (3.4.7) to (3.4.9) (observing that Γ_{IN} replaces S_{ii}). Select the desired Γ_s for a given G'_s gain. The value of G'_s might not be satisfactory and will require the selection of another Γ_L and the procedure repeated.
4. Design the matching networks.

The procedure just outlined is not recommended for a practical design since Γ_{IN} is a function of Γ_L , making the G'_s function dependent of the G_L function. Furthermore, the centers of the gain circles do not give $G_{T,max}$. In fact, the graphical approach becomes tedious because of the iterative process required for obtaining the desired gain.

As shown in the next section, the design of a microwave transistor amplifier in the unconditional stable bilateral case, for a gain different from $G_{T,max}$, can be done using the operating power gain equation.

Example 3.7.1

Design a microwave amplifier using a GaAs FET to operate at $f = 6$ GHz with maximum transducer power gain. The transistor S parameters at the linear bias point, $V_{DS} = 4$ V and $I_{DS} = 0.5I_{DSS}$, are

$$S_{11} = 0.641 \angle -171.3^\circ$$

$$S_{12} = 0.057 \angle 16.3^\circ$$

$$S_{21} = 2.058 \angle 28.5^\circ$$

$$S_{22} = 0.572 \angle -95.7^\circ$$

Solution. From (3.3.13) and (3.3.17) we obtain $K = 1.504$ and $\Delta = 0.3014 \angle 109.88^\circ$. Since $K > 1$ and $|\Delta| < 1$, the GaAs FET is unconditionally stable.

Next, we must decide if the amplifier can be considered unilateral. From (3.5.3), $U = 0.1085$, and from (3.5.2),

$$-0.89 \text{ dB} < \frac{G_T}{G_{TU}} < 1 \text{ dB}$$

The inequality above shows that S_{12} cannot be neglected.

The reflection coefficients for a simultaneous conjugate match are calculated from (3.6.5) and (3.6.6) as follows:

$$B_1 = 0.9928$$

$$B_2 = 0.8255$$

$$C_1 = 0.4786 \angle 182.7^\circ$$

$$C_2 = 0.3911 \angle 256.1^\circ$$

$$\Gamma_{Ms} = 0.762 \angle 177.3^\circ$$

and

$$\Gamma_{ML} = 0.718 \angle 103.9^\circ$$

The maximum transducer power gain, from (3.6.10), is

$$G_{T,\max} = \frac{2.058}{0.057} (1.504 - \sqrt{(1.504)^2 - 1}) = 13.74 \quad \text{or} \quad 11.38 \text{ dB}$$

The design of the matching networks using microstrip lines is illustrated in Fig. 3.7.1, where the admittances associated with Γ_{Ms} and Γ_{ML} are

$$Y_{Ms} = \frac{7.2 - j1.23}{50} = (144 - j24.6) \times 10^{-3} \text{ S}$$

and

$$Y_{ML} = \frac{0.414 - j1.19}{50} = (8.28 - j23.8) \times 10^{-3} \text{ S}$$

The input matching network can be designed with an open shunt stub of length 0.185λ and a series transmission line of length 0.0615λ . The output matching network is designed with an open shunt stub of length 0.176λ and a series transmission line of length 0.169λ .

The ac amplifier schematic is shown in Fig. 3.7.2. Using Duroid ($\epsilon_r = 2.23$, $h = 0.7874 \text{ mm}$) for the board material, we find that $W = 2.41 \text{ mm}$ for a characteristic impedance of 50Ω , $\epsilon_{eff} = 1.9052$, and $\lambda = 0.7245\lambda_0$, where $\lambda_0 = 5 \text{ cm}$ at $f = 6 \text{ GHz}$. The microstrip lengths at $f = 6 \text{ GHz}$ are

$$0.185\lambda = 6.70 \text{ mm}$$

$$0.0615\lambda = 2.23 \text{ mm}$$

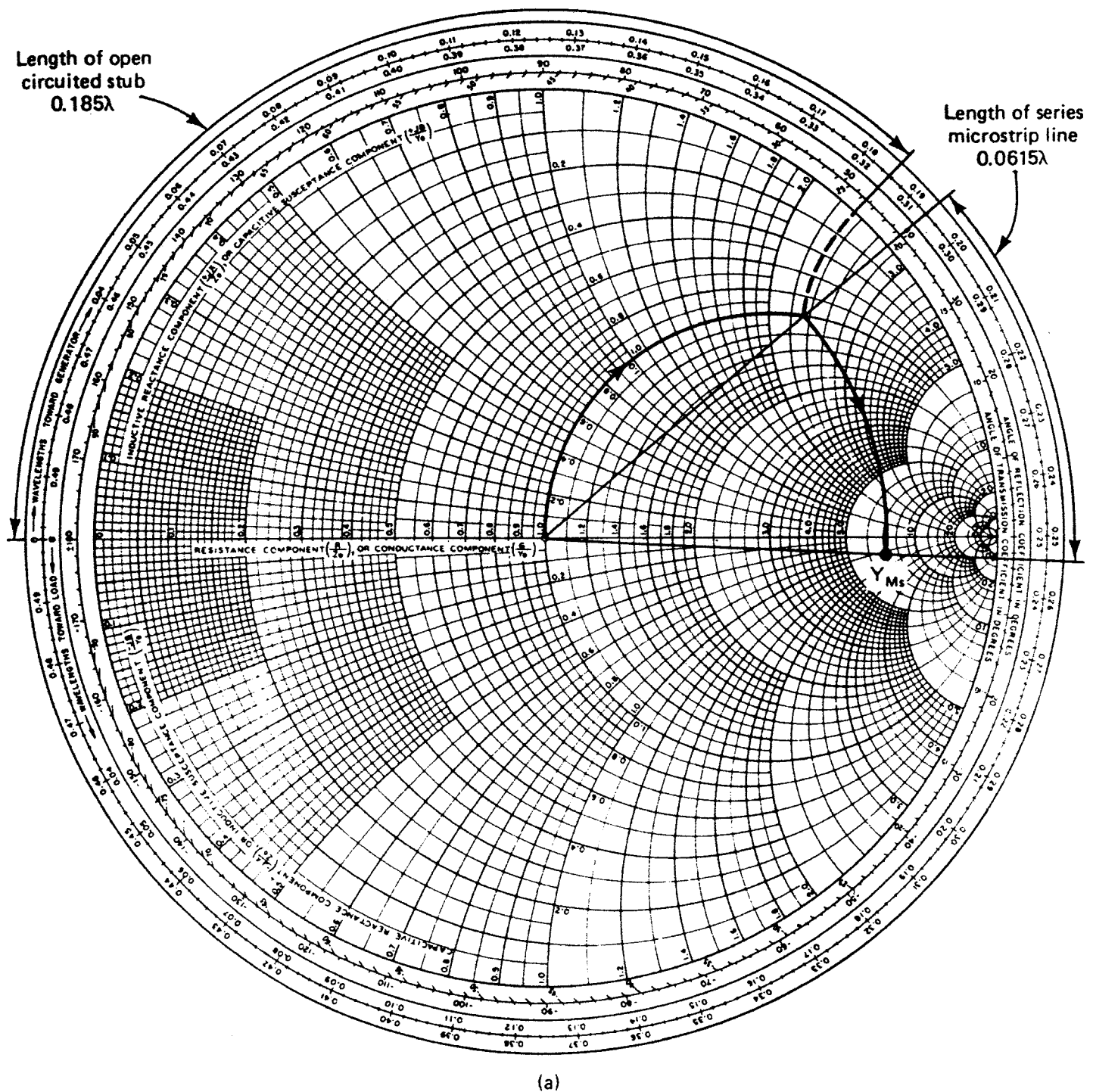


Figure 3.7.1 (a) Design of the input matching network; (b) design of the output matching network.

$$0.169\lambda = 6.12 \text{ mm}$$

$$0.176\lambda = 6.38 \text{ mm}$$

The design for $G_{T,\max}$ with Γ_{Ms} and Γ_{ML} , at 6 GHz, assures that the input and output VSWR are 1.

This example is revisited in Section 4.3, where noise considerations are included. Finally, we should point out that the stability must be checked at all frequencies, so that the reflection coefficients Γ_{Ms} and Γ_{ML} provide stable operation.

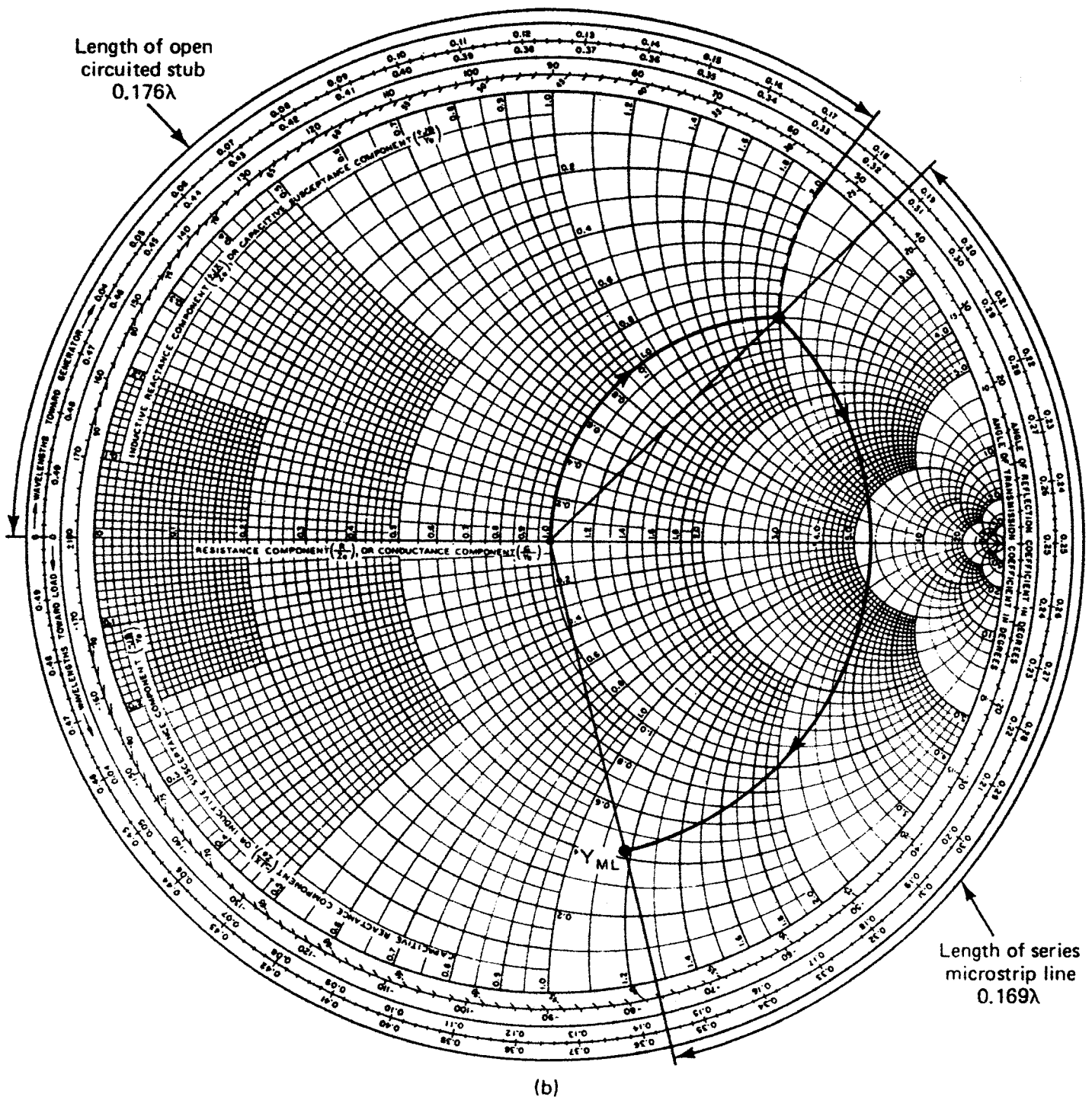


Figure 3.7.1 (continued)

Potentially Unstable Bilateral Case, $K < 1$ or $|\Delta| > 1$

A design procedure based on the expression for G_T in (3.2.1) or (3.2.2) is not recommended because it leads to a tedious iterative process. The process is somewhat similar to that given for the unconditionally stable bilateral case [i.e., (3.7.1) to (3.7.3)].

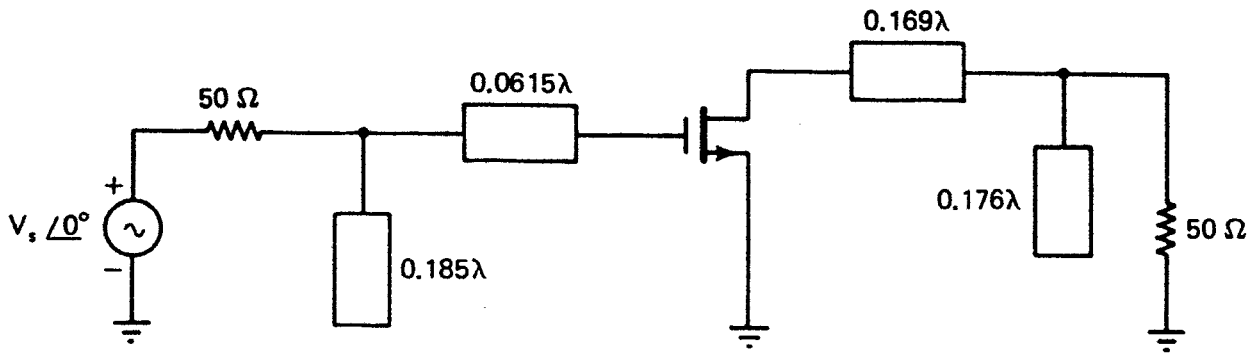


Figure 3.7.2 The ac schematic of a GaAs FET microwave amplifier. All microstrip lines have a characteristic impedance of $50\ \Omega$.

As shown in the next section, a design procedure for this case can be developed using the operating power gain equation.

In conclusion, when designing a microwave transistor amplifier where S_{12} cannot be neglected (i.e., bilateral case), a design procedure that calls for a transducer power gain different from $G_{T,\max}$ is tedious, and a simpler design procedure can be developed using the operating power gain equation. When the transistor is unconditionally stable, a simultaneous conjugate match can be found, and the design procedure is based on $G_{T,\max}$ or (as shown in the next section) on the operating power gain. In fact, in this case both procedures lead to the same results.

3.8 OPERATING AND AVAILABLE POWER GAIN CIRCLES

When S_{12} cannot be neglected, a design procedure based on the operating power gain G_p is commonly used. The operating power gain is independent of the source impedance; therefore, an operating power gain circle procedure for both unconditionally stable and potentially unstable transistors is simple and recommended for practical designs.

Again we must consider two cases, the unconditionally stable case and the potentially unstable case.

Unconditionally Stable Bilateral Case

To develop a design procedure with G_p , we write (3.2.3) in the form

$$G_p = \frac{|S_{21}|^2(1 - |\Gamma_L|^2)}{\left(1 - \left|\frac{S_{11} - \Delta\Gamma_L}{1 - S_{22}\Gamma_L}\right|^2\right) |1 - S_{22}\Gamma_L|^2}$$

$$= |S_{21}|^2 g_p \quad (3.8.1)$$

where

$$g_p = \frac{1 - |\Gamma_L|^2}{|1 - S_{22}\Gamma_L|^2 - |S_{11} - \Delta\Gamma_L|^2}$$

$$= \frac{1 - |\Gamma_L|^2}{1 - |S_{11}|^2 + |\Gamma_L|^2(|S_{22}|^2 - |\Delta|^2) - 2 \operatorname{Re}(\Gamma_L C_2)} \quad (3.8.2)$$

and

$$C_2 = S_{22} - \Delta S_{11}^* \quad (3.8.3)$$

Here G_p and g_p are functions of the device S parameters and Γ_L .

The constant operating power gain circles are obtained by letting $\Gamma_L = U_L + jV_L$ and substituting into (3.8.2). After some manipulations we obtain

$$\left[U_L - \frac{g_p \operatorname{Re}[C_2^*]}{1 + g_p(|S_{22}|^2 - |\Delta|^2)} \right]^2 + \left[V_L - \frac{g_p \operatorname{Im}[C_2^*]}{1 + g_p(|S_{22}|^2 - |\Delta|^2)} \right]^2$$

$$= \left[\frac{[1 - 2K|S_{12}S_{21}|g_p + |S_{12}S_{21}|^2g_p^2]^{1/2}}{1 + g_p(|S_{22}|^2 - |\Delta|^2)} \right]^2 \quad (3.8.4)$$

Equation (3.8.4) is recognized as a family of circles in the $U_L:V_L$ plane (i.e., the Smith chart) with g_p as a parameter. The centers of the circles are located at

$$U_p = \frac{g_p \operatorname{Re}[C_2^*]}{1 + g_p(|S_{22}|^2 - |\Delta|^2)}$$

and

$$V_p = \frac{g_p \operatorname{Im}[C_2^*]}{1 + g_p(|S_{22}|^2 - |\Delta|^2)}$$

The radii of the circles are given by

$$R_p = \frac{[1 - 2K|S_{12}S_{21}|g_p + |S_{12}S_{21}|^2g_p^2]^{1/2}}{|1 + g_p(|S_{22}|^2 - |\Delta|^2)|} \quad (3.8.5)$$

The distance from the origin of the Smith chart to the centers of the circles is given by

$$d_p = \sqrt{U_p^2 + V_p^2} = \frac{g_p |C_2^*|}{|1 + g_p(|S_{22}|^2 - |\Delta|^2)|}$$

Therefore, the centers of the circles C_p can be written as

$$C_p = \frac{g_p C_2^*}{1 + g_p(|S_{22}|^2 - |\Delta|^2)} \quad (3.8.6)$$

The maximum operating power gain occurs when $R_p = 0$. Therefore,

from (3.8.5) we can write

$$g_{p,\max}^2 |S_{12} S_{21}|^2 - 2K |S_{12} S_{21}| g_{p,\max} + 1 = 0 \quad (3.8.7)$$

where $g_{p,\max}$ is the maximum value of g_p . The solution to (3.8.7) for unconditional stability is

$$g_{p,\max} = \frac{1}{|S_{12} S_{21}|} (K - \sqrt{K^2 - 1}) \quad (3.8.8)$$

Therefore, substituting (3.8.8) into (3.8.1) gives

$$G_{p,\max} = \frac{|S_{21}|}{|S_{12}|} (K - \sqrt{K^2 - 1})$$

For a given G_p , Γ_L is selected from the constant operating power gain circles. $G_{p,\max}$ results when Γ_L is selected at the distance where $g_{p,\max} = G_{p,\max} / |S_{21}|^2$. The maximum output power results when a conjugate match is selected at the input (i.e., $\Gamma_s = \Gamma_{IN}^*$). It also follows that when $\Gamma_s = \Gamma_{IN}^*$ the input power is equal to the maximum available input power. Therefore, under these circumstances the maximum transducer power gain ($G_{T,\max}$) and the operating power gain are equal, and the values of Γ_s and Γ_L that result in $G_{p,\max}$ are identical to Γ_{Ms} and Γ_{ML} , respectively.

The procedure for drawing a constant operating power gain circle in the Z Smith chart is as follows:

1. For a given G_p , the radius and center of the constant operating power gain circle are given by (3.8.5) and (3.8.6).
2. Select the desired Γ_L .
3. For the given Γ_L , maximum output power is obtained with a conjugate match at the input, namely with $\Gamma_s = \Gamma_{IN}^*$, where Γ_{IN} is given by (3.2.5). This value of Γ_s produces the transducer power gain $G_T = G_p$.

Example 3.8.1

Design the amplifier in Example 3.7.1 to have an operating power gain of 9 dB instead of $G_{T,\max} = G_{p,\max} = 11.38$ dB.

Solution. Since

$$|S_{21}|^2 = (2.058)^2 = 4.235 \quad \text{or} \quad 6.27 \text{ dB}$$

then

$$g_p = \frac{G_p}{|S_{21}|^2} = \frac{7.94}{4.235} = 1.875$$

From the results in Example 3.7.1, $K = 1.504$, $|\Delta| = 0.3014$, and $C_2 = 0.3911 \angle 256.1^\circ$. Therefore, the radius and center of the 9-dB operating power gain circle, from (3.8.5) and (3.8.6), are $R_p = 0.431$ and $C_p = 0.508 \angle 103.9^\circ$.

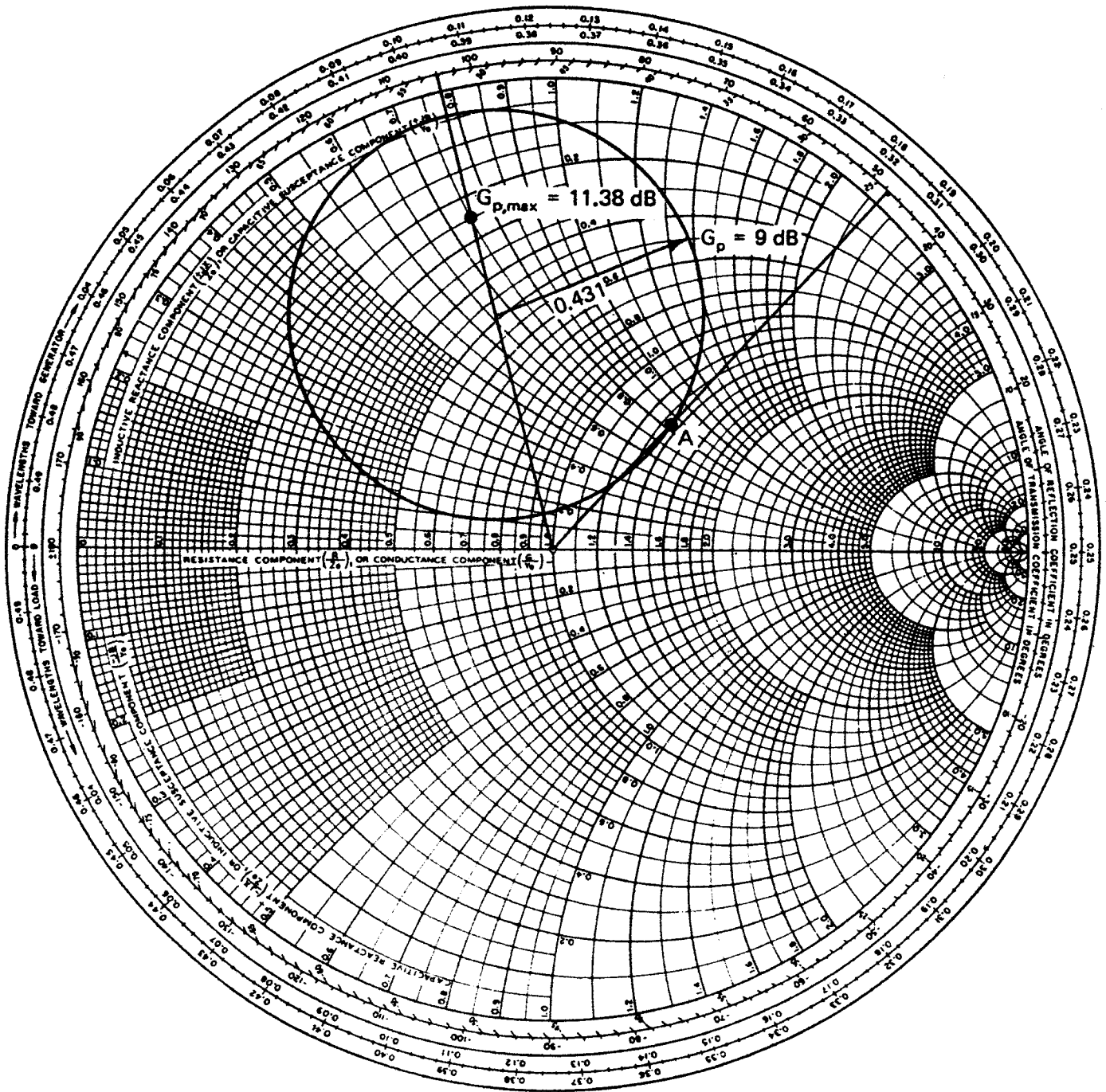


Figure 3.8.1 Operating power gain circle for $G_p = 9$ dB and location of $G_{p,max} = 11.38$ dB.

The graphical construction is shown in Fig. 3.8.1. The 9-dB operating power gain circle shows all loads that produce $G_p = 9$ dB. The load reflection coefficient can be selected at point A, namely $\Gamma_L = 0.36 \angle 47.5^\circ$. Then the required Γ_s for maximum output power is

$$\Gamma_s = \Gamma_{IN}^* = \left[S_{11} + \frac{S_{12} S_{21} \Gamma_L}{1 - S_{22} \Gamma_L} \right]^* = 0.629 \angle 175.51^\circ$$

The location of $G_{p,max} = 11.38$ dB can be found as follows:

$$g_{p,max} = \frac{G_{p,max}}{|S_{21}|^2} = \frac{13.74}{(2.058)^2} = 3.24$$

$$R_{p,max} = 0$$

and

$$C_{p,\max} = \frac{g_{p,\max} C_2^*}{1 + g_{p,\max} (|S_{22}|^2 - |\Delta|^2)} = 0.718 \angle 103.9^\circ$$

At the location of $G_{p,\max}$, we obtain from Fig. 3.8.1 $\Gamma_{L,\max} = 0.718 \angle 103.9^\circ$. This value of $\Gamma_{L,\max}$ is identical to the value Γ_{ML} found in Example 3.7.1. The associated Γ_s for maximum output power is

$$\Gamma_{s,\max} = \left[S_{11} + \frac{S_{12} S_{21} \Gamma_{L,\max}}{1 - S_{22} \Gamma_{L,\max}} \right]^* = 0.762 \angle 177.3^\circ$$

which is identical to the value of Γ_{Ms} in Example 3.7.1.

The derivation of the constant available power gain circles is similar to that of the operating power gain circles. It is simple to show that in the Γ_s plane the radius R_a and center C_a of a circle can be calculated using the relations

$$g_a = \frac{G_A}{|S_{21}|^2} \quad (3.8.9)$$

$$C_1 = S_{11} - \Delta S_{22}^* \quad (3.8.10)$$

$$R_a = \frac{[1 - 2K |S_{12} S_{21}| g_a + |S_{12} S_{21}|^2 g_a^2]^{1/2}}{|1 + g_a (|S_{11}|^2 - |\Delta|^2)|} \quad (3.8.11)$$

and

$$C_a = \frac{g_a C_1^*}{1 + g_a (|S_{11}|^2 - |\Delta|^2)} \quad (3.8.12)$$

For a given G_A , a constant available power gain circle can be plotted using (3.8.9) to (3.8.12). All Γ_s on this circle produce the given G_A . For the given G_A , maximum output power is obtained with $\Gamma_L = \Gamma_{OUT}^*$, where Γ_{OUT} is given by (3.2.6). This value of Γ_L produces the transducer power gain $G_T = G_A$.

Since the constant available power gain circles and the constant noise figure circles are functions of Γ_s , they can be plotted together on the Smith chart and the trade-offs that result between gain and noise figure can be analyzed.

Potentially Unstable Bilateral Case

With a potentially unstable transistor the design procedure for a given G_p is as follows:

1. For a given G_p , draw the constant operating power gain circle using (3.8.5) and (3.8.6), and also draw the output stability circle as discussed in Section 3.3 [i.e., see (3.3.7) and (3.3.8)]. Select a value of Γ_L that is in the stable region and not too close to the stability circle.

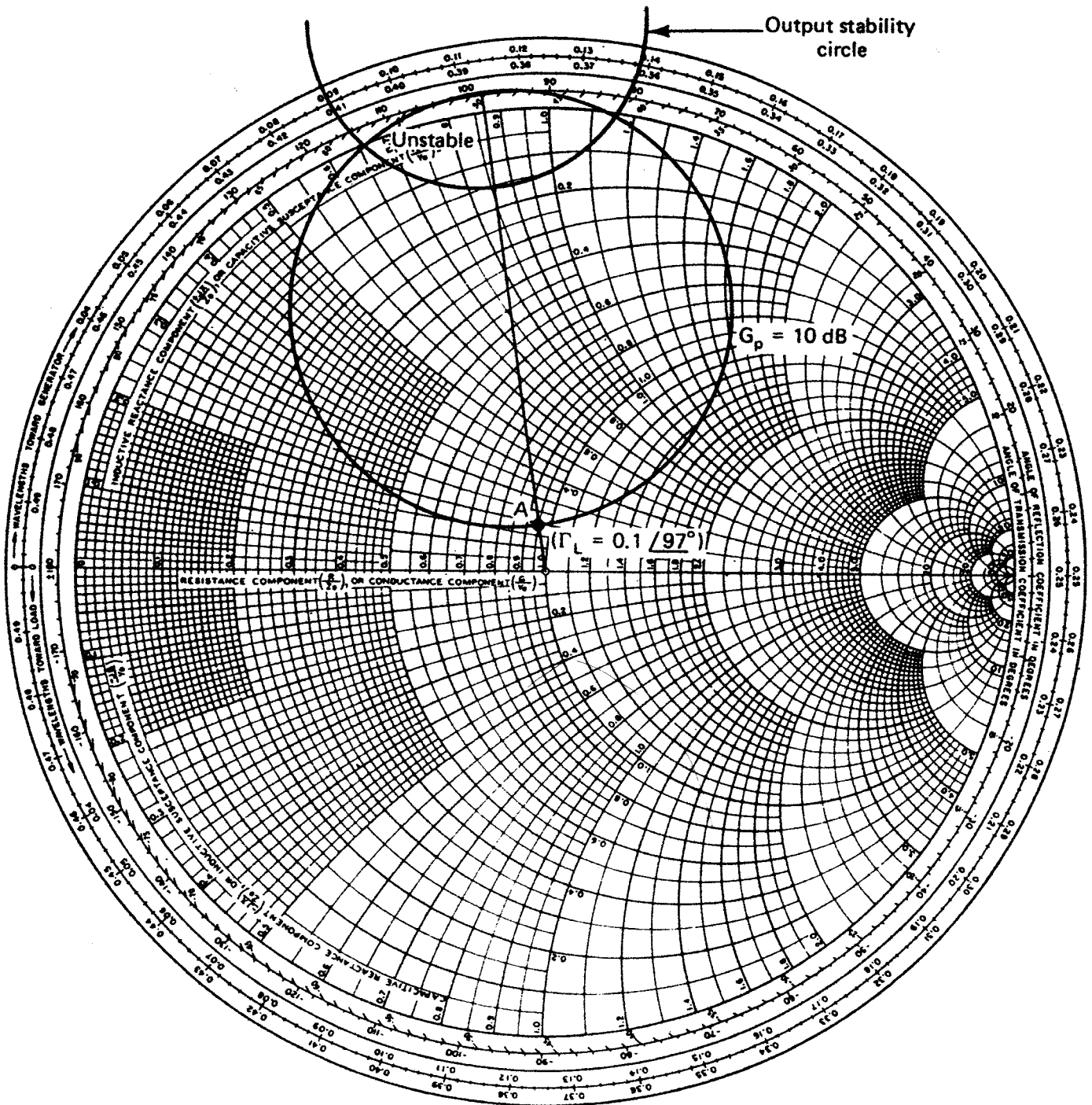


Figure 3.8.2 Power and stability circles construction for Example 3.8.2.

2. Calculate Γ_{IN} using (3.2.5) and determine if a conjugate match at the input is feasible. That is, draw the input stability circle as discussed in Section 3.3 [i.e., see (3.3.9) and (3.3.10)] and determine if $\Gamma_s = \Gamma_{IN}^*$ lies in the input stable region.
3. If $\Gamma_s = \Gamma_{IN}^*$ is not in the stable region, or in the stable region but very close to the input stability circle, the value of Γ_s can be selected arbitrarily or a new value of G_p selected. Of course, we must be careful when selecting Γ_s arbitrarily since the value of Γ_s affects the output power and the VSWR.

The values of Γ_L and Γ_s should not be too close to their respective

stability circles, because oscillations might occur when the input and output circuits are tuned.

Example 3.8.2

The S parameters of a GaAs FET at $I_D = 50\%I_{DSS}$, $I_{DSS} = 10$ mA, $V_{DS} = 5$ V, and $f = 8$ GHz are

$$S_{11} = 0.5 \angle -180^\circ$$

$$S_{12} = 0.08 \angle 30^\circ$$

$$S_{21} = 2.5 \angle 70^\circ$$

$$S_{22} = 0.8 \angle -100^\circ$$

Design an amplifier with $G_p = 10$ dB.

Solution. First we must check the stability of the transistor. From (3.3.13) and (3.3.17) we obtain $K = 0.4$ and $\Delta = 0.223 \angle 62.12^\circ$. Since $K < 1$, the GaAs FET is potentially unstable. The G_{MSG} given by (3.6.11) is $G_{MSG} = 2.5/0.08 = 31.25$ or 14.9 dB.

In order to design for $G_p = 10$ dB (4.9 dB less than the G_{MSG}), the 10-dB operating power gain circle and the output stability circle must be calculated. The radius and center of the 10-dB power gain circle, from (3.8.5) and (3.8.6), are $R_p = 0.473$ and $C_p = 0.572 \angle 97.2^\circ$. The radius and center of the output stability circle, from (3.3.7) and (3.3.8), are $r_L = 0.34$ and $C_L = 1.18 \angle 97.2^\circ$.

The Smith chart in Fig. 3.8.2 shows the construction of the 10-dB operating power gain circle and the output stability circle. Since $|S_{11}| < 1$, the stable region is the region outside the output stability circle. Γ_L is selected on the 10-dB power gain circle at location A, namely $\Gamma_L = 0.1 \angle 97^\circ$ or $Z_L = 50(0.96 + j0.19) \Omega$.

For a conjugate match at the input, Γ_s is given by $\Gamma_s = \Gamma_{IN}^* = 0.52 \angle 179.32^\circ$ and we must determine if the value of Γ_s is in the stable region. The radius and center of the input stability circle, from (3.3.9) and (3.3.10), are $r_s = 1.0$ and $C_s = 1.67 \angle 171^\circ$, where the stable region is the region outside the input stability circle. Therefore, Γ_s is a stable source reflection coefficient.

3.9 DC BIAS NETWORKS

It has been said that the least considered factor in microwave transistor amplifier design is the bias network [3.5]. While considerable effort is spent in designing for a given gain, noise figure, and bandwidth, little effort is spent in the dc bias network. The cost per decibel of microwave power gain or noise figure is high, and the designer cannot sacrifice the amplifier performance by having a poor dc bias design.

The purpose of a good dc bias design is to select the proper quiescent point and hold the quiescent point constant over variations in transistor parameters and temperature. A resistor bias network can be used with good results over moderate temperature changes. However, an active bias network is usually preferred for large temperature changes.

In the discussion that follows, we first consider the dc bias design for BJTs and then the bias design of GaAs FETs.

BJT Bias Networks

At low frequencies, a bypassed emitter resistor is an important contributor to the quiescent-point stability. At microwave frequencies, the bypass capacitor, which is in parallel with the emitter resistor, can produce oscillations by making the input port unstable at some frequencies. Furthermore, an emitter resistor will degrade the noise performance of the amplifier. Therefore, in most microwave transistor amplifiers, especially in the gigahertz region, the emitter lead of the transistor is grounded.

At microwave frequencies the transistor parameters that are affected most by temperature are I_{CBO} , h_{FE} , and V_{BE} . The conventional reverse current I_{CBO} (i.e., I_{CBO} at low frequencies) doubles every 10°C rise in temperature. That is,

$$I_{CBO,T_2} = I_{CBO,T_1} 2^{(T_2 - T_1)/10}$$

where I_{CBO,T_2} and I_{CBO,T_1} are the values of I_{CBO} at temperatures T_2 and T_1 , respectively. The temperature T_1 is usually the temperature at which the manufacturer measures I_{CBO} . This temperature is usually 25°C .

A microwave transistor has a more complicated reverse current flow. The reverse current flow of a microwave transistor is composed of two components; one is the conventional I_{CBO} and the other is a surface current, I_s , that flows across the top of the silicon lattice. The reverse current in a microwave transistor, which is referred to simply as I_{CBO} , increases at a rate much slower than the conventional I_{CBO} . A typical plot of the reverse current versus temperature for a microwave transistors is shown in Fig. 3.9.1. The conventional I_{CBO} slope is also shown in the figure for comparison.

The base-to-emitter voltage V_{BE} has a negative temperature coefficient, approximately given by

$$\frac{\Delta V_{BE}}{\Delta T} \approx -2 \times 10^{-3} \frac{\text{V}}{^\circ\text{C}}$$

The dc value of the current gain h_{FE} is defined as the value of the collector-to-base current at a constant value of V_{CE} . That is,

$$h_{FE} = \left. \frac{I_C}{I_B} \right|_{V_{CE} = \text{CONSTANT}}$$

The dc value of h_{FE} is typically found to increase linearly with temperature at the rate of $0.5\%/^\circ\text{C}$.

In order to find the change in collector current as a function of temperature in a dc bias network, we first find the expression for the collector current valid for any temperature. Then, observing that the temperature sensitive parameters are I_{CBO} , h_{FE} , and V_{BE} , we can write

$$I_C = f(I_{CBO}, h_{FE}, V_{BE})$$

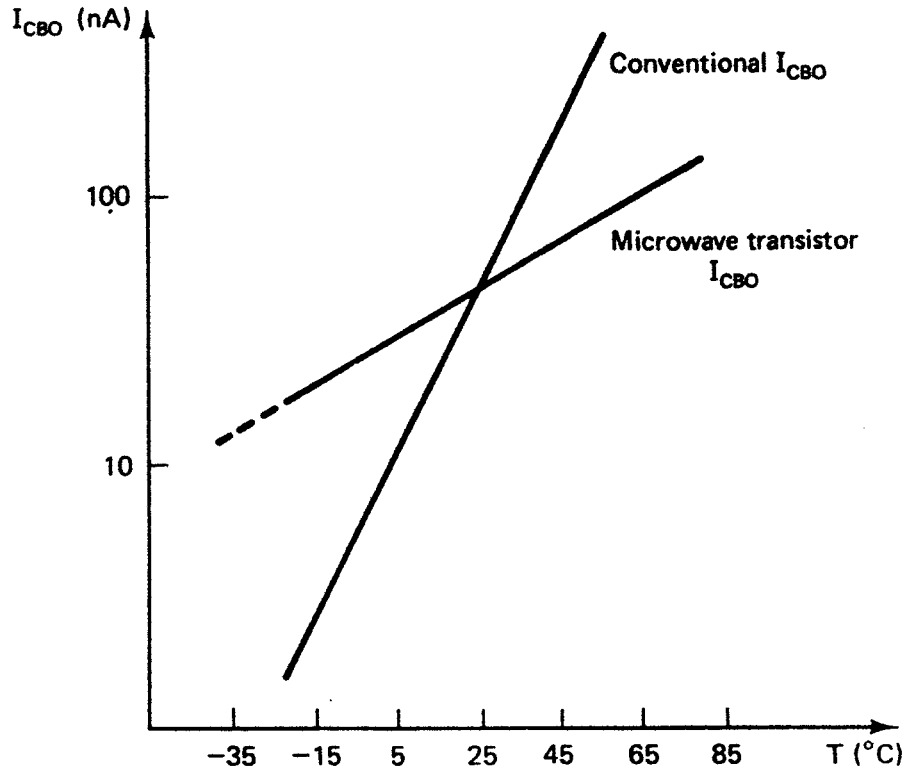


Figure 3.9.1 Typical reverse current versus temperature for a microwave transistor.

and

$$\Delta I_C = \left(\frac{\Delta I_C}{\Delta I_{CBO}} \right) \bigg|_{\substack{\Delta h_{FE}=0 \\ \Delta V_{BE}=0}} \Delta I_{CBO} + \left(\frac{\Delta I_C}{\Delta h_{FE}} \right) \bigg|_{\substack{\Delta I_{CBO}=0 \\ \Delta V_{BE}=0}} \Delta h_{FE} + \left(\frac{\Delta I_C}{\Delta V_{BE}} \right) \bigg|_{\substack{\Delta I_{CBO}=0 \\ \Delta h_{FE}=0}} \Delta V_{BE} \quad (3.9.1)$$

Defining the stability factors as

$$S_i = \frac{\Delta I_C}{\Delta I_{CBO}} \bigg|_{\substack{\Delta h_{FE}=0 \\ \Delta V_{BE}=0}}$$

$$S_{h_{FE}} = \frac{\Delta I_C}{\Delta h_{FE}} \bigg|_{\substack{\Delta I_{CBO}=0 \\ \Delta V_{BE}=0}}$$

and

$$S_{V_{BE}} = \frac{\Delta I_C}{\Delta V_{BE}} \bigg|_{\substack{\Delta I_{CBO}=0 \\ \Delta h_{FE}=0}}$$

we can write (3.9.1) in the form

$$\Delta I_C = S_i \Delta I_{CBO} + S_{h_{FE}} \Delta h_{FE} + S_{V_{BE}} \Delta V_{BE} \quad (3.9.2)$$

For a given dc bias network, the stability factors can be calculated and (3.9.2) can be used to predict the variations of I_C with temperature. In a design procedure, the maximum variation of I_C in a temperature range can be selected and (3.9.2) can be used to find the required stability factors. In turn, the

stability factors together with the Q -point location will fix the value of the resistors in the bias network.

Two grounded-emitter dc bias networks that can be used at microwave frequencies are shown in Fig. 3.9.2. The network in Fig. 3.9.2b produces lower values of resistance, and therefore is more compatible with thin- or thick-film resistor values.

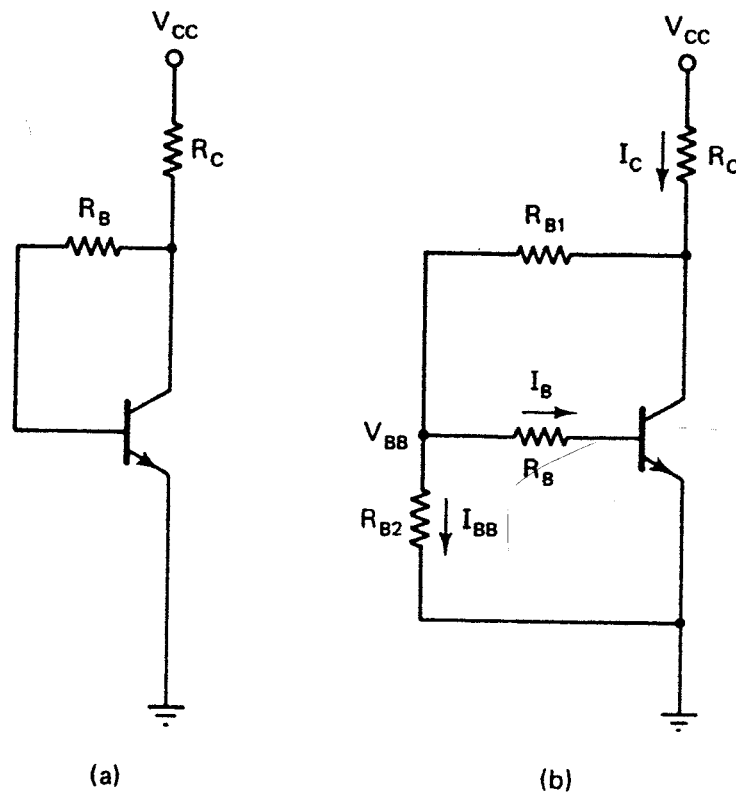


Figure 3.9.2 (a) Voltage feedback bias network; (b) voltage feedback bias network with constant-base current source.

Example 3.9.1

Design the dc bias network shown in Fig. 3.9.2b for $V_{CE} = 10$ V and $I_C = 10$ mA. Assume that $I_{CBO} = 0$, $V_{BE} = 0.7$ V, and $h_{FE} = 50$.

Solution. In this example we follow a procedure that results in good stability factors. Let the supply voltage V_{CC} be 20 V. The base current (I_B) is

$$I_B = \frac{I_C}{h_{FE}} = \frac{10 \times 10^{-3}}{50} = 200 \mu\text{A}$$

Assuming V_{BB} to be 2 V, we find that

$$R_B = \frac{V_{BB} - V_{BE}}{I_B} = \frac{2 - 0.7}{200 \times 10^{-6}} = 6.5 \text{ k}\Omega$$

R_{B2} is calculated assuming that $I_{BB} = 1$ mA (i.e., $I_{BB} = 5I_B$), namely

$$R_{B2} = \frac{V_{BB}}{I_{BB}} = \frac{2}{1 \times 10^{-3}} = 2 \text{ k}\Omega$$

R_{B1} is obtained from

$$R_{B1} = \frac{V_{CE} - V_{BB}}{I_{BB} + I_B} = \frac{10 - 2}{(1 + 0.2) \times 10^{-3}} = 6.66 \text{ k}\Omega$$

and R_C is obtained from

$$R_C = \frac{V_{CC} - V_{CE}}{I_C + I_{BB} + I_B} = \frac{20 - 10}{(10 + 1 + 0.2) \times 10^{-3}} = 893 \text{ }\Omega$$

The assumption $I_{BB} \gg I_B$ and $V_{BB} \approx 10\% V_{CC}$ produces good stability factors. It is left as an exercise to calculate the resulting stability factors.

At the lower microwave frequencies, the dc biasing network shown in Fig. 3.9.3, with a bypassed emitter resistor can be used. The bypassed emitter resistor provides excellent stability. For this network it is easy to show that

$$I_C = \frac{h_{FE}(V_{TH} - V_{BE})}{R_{TH} + (h_{FE} + 1)R_E} + \frac{(h_{FE} + 1)I_{CBO}(R_{TH} + R_E)}{R_{TH} + (h_{FE} + 1)R_E}$$

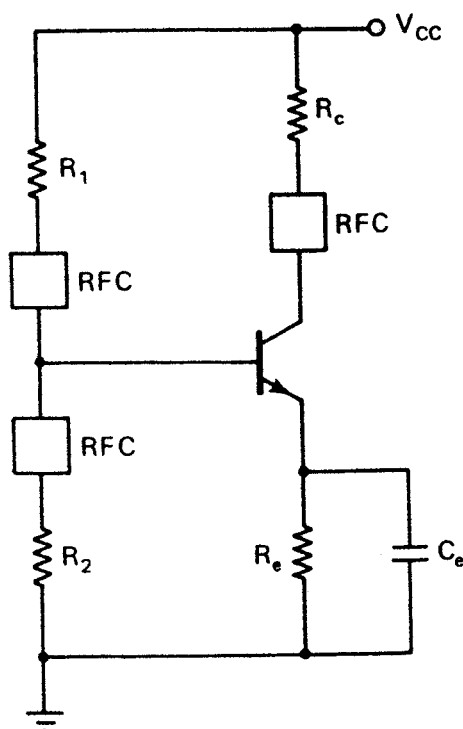


Figure 3.9.3 A dc bias network with a bypassed emitter resistor.

where

$$V_{TH} = \frac{V_{CC} R_2}{R_1 + R_2}$$

and

$$R_{TH} = \frac{R_1 R_2}{R_1 + R_2}$$

The stability factors are

$$S_i = \frac{(h_{FE} + 1)(R_{TH} + R_E)}{R_{TH} + (h_{FE} + 1)R_E}$$

$$S_{h_{FE}} \approx \frac{I_{C1}}{h_{FE}} \frac{S_{i2}}{h_{FE,2}} \quad (3.9.3)$$

and

$$S_{V_{BE}} = \frac{-h_{FE}}{R_{TH} + (h_{FE} + 1)R_E}$$

In (3.9.3), $\Delta h_{FE} = h_{FE,2} - h_{FE}$ and S_{i2} is the value of S_i with $h_{FE} = h_{FE,2}$.

An active dc biasing network is shown in Fig. 3.9.4. A *pnp* BJT is used to stabilize the operating point of the microwave transistor. The bypass capacitors C_1 and C_2 are typically 0.01- μ F disk capacitors. The radio frequency chokes (RFC) are typically made of two or three turns of No. 36 enameled wire on 0.1-in. air core. The operation of the network is as follows. If I_{C2} tends to increase, the current I_3 increases and the emitter-to-base voltage of Q_1 ($V_{EB,1}$) decreases. The decrease of $V_{EB,1}$ decreases I_{E1} , which in turn decreases I_{C2} and I_{B2} . The decrease in I_{B2} and I_{C2} produces the desired bias stability.

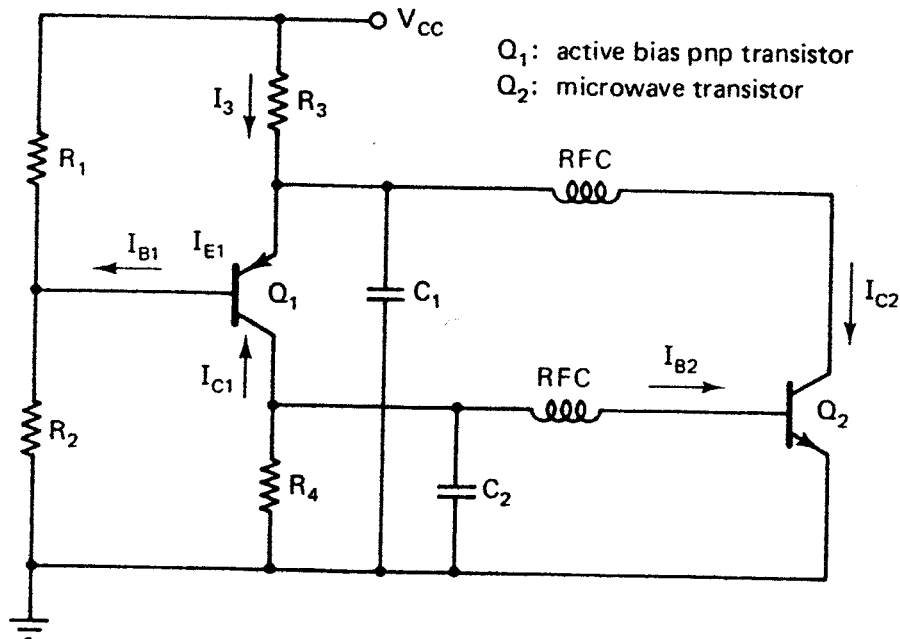


Figure 3.9.4 Active bias network for a BJT.

The selection of the dc quiescent point for a BJT depends on the particular application. For low-noise and low-power applications, the quiescent point A in Fig. 3.9.5 is recommended. At A, the BJT operates at low values of collector current. For low noise and higher power gain, the quiescent point at B is recommended. For high output power, in class A operation, the quiescent point at C is recommended. For higher output power and higher efficiency, the BJT is operated in class AB or B, using the quiescent point at D.

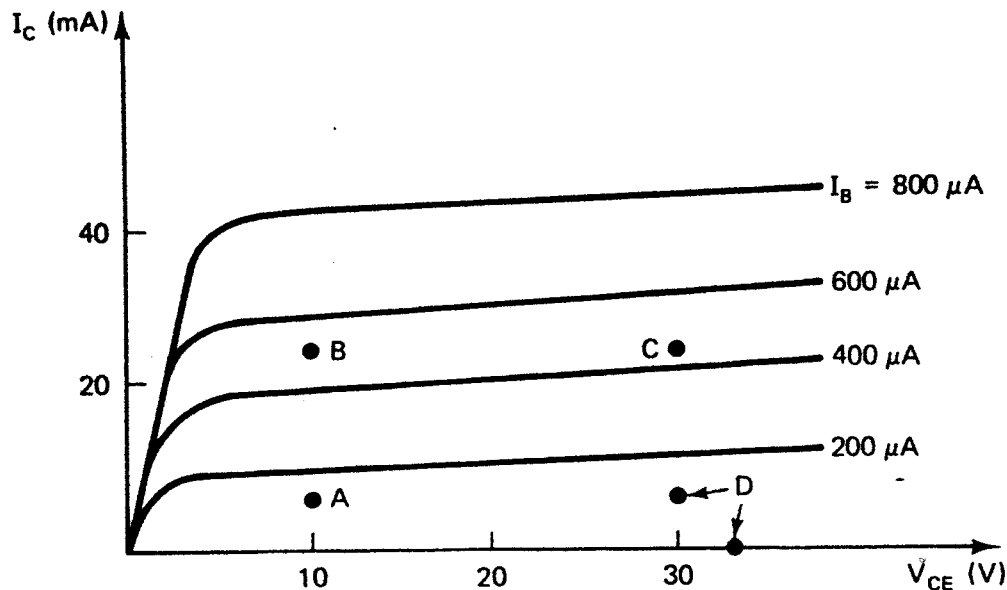


Figure 3.9.5 Selection of the dc operating point.

GaAs FET Bias Networks

The GaAs FETs can be biased in several ways. Five basic dc network configurations for GaAs FET amplifiers are shown in Fig. 3.9.6. [3.6]. The dc bias network in Fig. 3.9.6a requires a bipolar power source, while the networks in Figs. 3.9.6b to 3.9.6e require a unipolar supply. The column "How" in Fig. 3.9.6 indicates the polarity of the sources, as well as the sequence in which the voltages must be applied to prevent transient burnout of the GaAs FET device during turn-on. For example, in the dc bias network in Fig. 3.9.6a, if the drain is biased positive before the gate, the transistor will operate momentarily beyond its safe operating region. Therefore, the proper turn-on sequence is: first apply a negative bias to the gate (i.e., $V_G < 0$) and then apply the drain voltage ($V_D > 0$). One method to accomplish the previous turn-on procedure is to turn both sources at the same time and to include a long RC time constant network in the V_D supply and a short RC time constant network in the negative supply V_G .

The bias networks in Figs. 3.9.6d and 3.9.6e use a source resistor. The source resistor provides automatic transient protection. However, the source resistor will degrade the noise-figure performance, and the source bypass capacitor can cause low-frequency oscillations.

The decoupling capacitors shown in Fig. 3.9.6 are sometimes shunted with zener diodes. The zener diodes provide additional protection against transients, reverse biasing, and overvoltage.

The dc bias network of a GaAs FET must provide a stable quiescent point. It is not difficult to show that the negative feedback resistor R_s decreases the effect of variations of I_D with respect to temperature and I_{DSS} .

The selection of the dc quiescent point in a GaAs FET depends on the particular application. Figure 3.9.7 shows typical GaAs FET characteristics with four quiescent points located at A, B, C, and D.

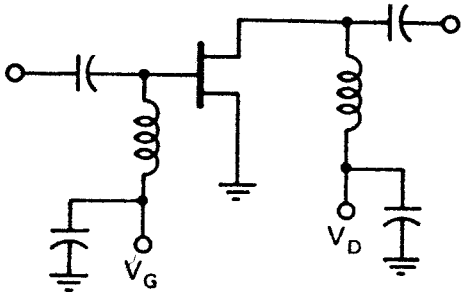
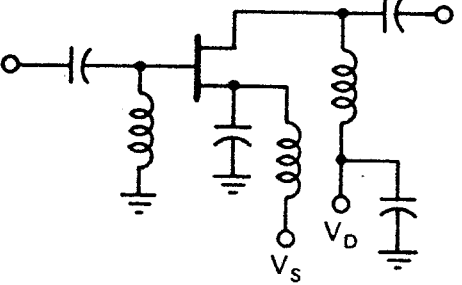
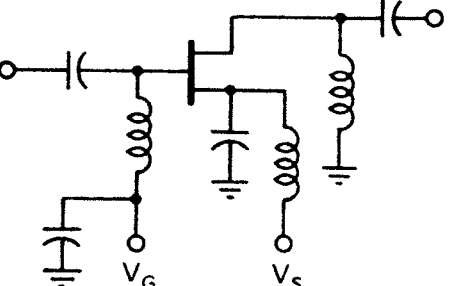
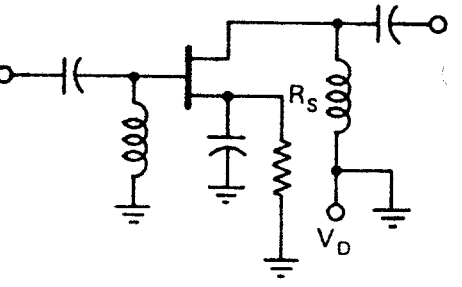
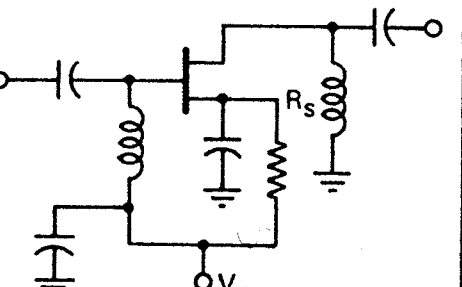
Figure	How	Amplifier characteristics	Power supply used
(a) $V_D = 5\text{ V}$ $V_G = -2\text{ V}$ 	Apply V_G , then V_D	Low noise High gain High power High efficiency	Bipolar: minimum source inductance
(b) $V_D = 7\text{ V}$ $V_S = 2\text{ V}$ 	Apply V_S , then V_D	[same as (a)]	Positive supply
(c) $V_G = -7\text{ V}$ $V_S = -5\text{ V}$ 	Apply V_S , then V_G	[same as (a)]	Negative supply
(d) $V_D = 7\text{ V}$ $V_S = 2\text{ V}$ $= I_{DS} R_S$ 	Apply V_D	Low noise High gain High power Lower efficiency Gain easily adjusted by varying R_S	Unipolar, incorporating R_S : automatic transient protection
(e) $V_G = -7\text{ V}$ $V_S = -5\text{ V}$ $= -I_{DS} R_S$ 	Apply V_G	[same as (d)]	Negative unipolar, incorporating R_S

Figure 3.9.6 Five basic dc bias networks. (From G. D. Vendelin [3.6]; reproduced with permission of Microwaves & RF.)

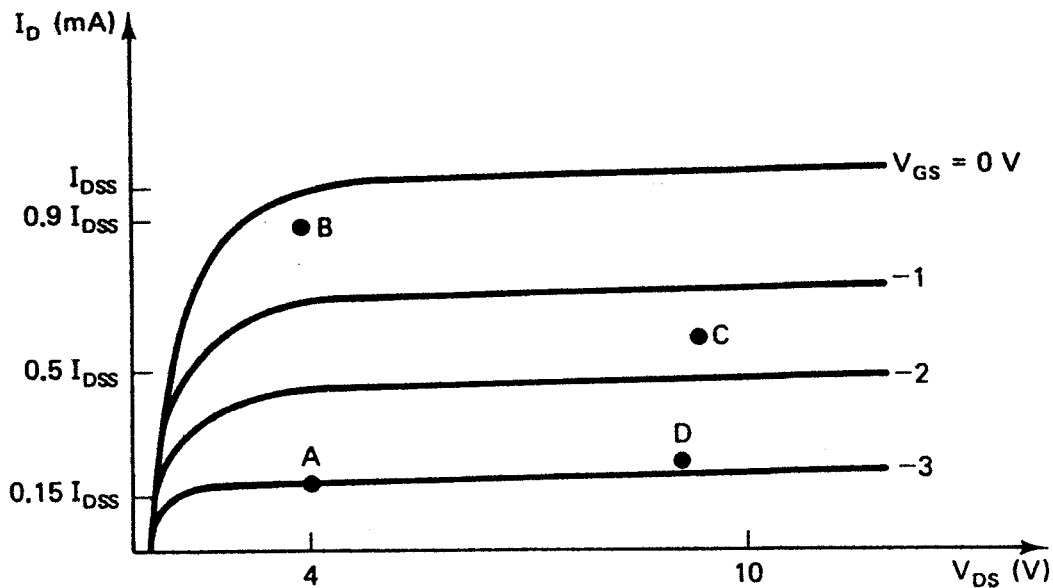


Figure 3.9.7 Typical GaAs FET characteristics and recommended quiescent points.

For low-noise, low-power application, the quiescent point *A* is recommended. At *A*, the FET operates at a low value of current (i.e., $I_{DS} \approx 0.15 I_{DSS}$).

For low noise and higher power gain, the recommended quiescent point is at *B*. The bias voltage remains the same as for point *A*, but the drain current is increased to $I_{DS} \approx 0.9 I_{DSS}$.

The GaAs FET output power level can be increased by selecting the quiescent point at *C* with $I_{DS} \approx 0.5 I_{DSS}$. The quiescent point at *C* maintains class A operation. For higher efficiency, or to operate the GaAs FET in class AB or B, the drain-to-source current must be decreased and the quiescent point *D* is recommended.

An active bias network for a common-source GaAs FET is shown in Fig. 3.9.8.

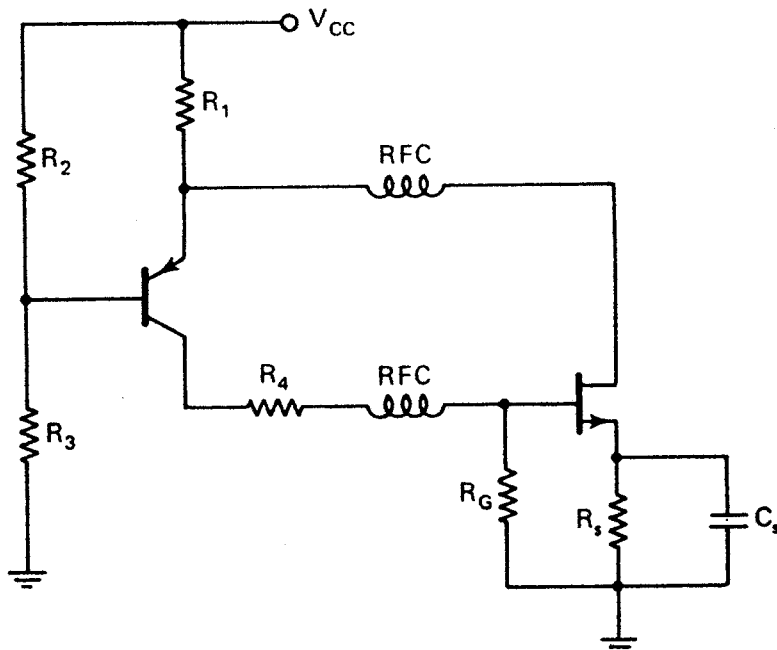


Figure 3.9.8 Active bias for a common-source GaAs FET.

PROBLEMS

- 3.1. Derive the expressions for G_p and G_A in (3.2.3) and (3.2.4) using Mason's rule.
- 3.2. (a) Show that $G_T \leq G_A$ and $G_T \leq G_p$. When is the equality sign satisfied?
 (b) Show that (3.2.3) can be obtained from (3.2.1) when $\Gamma_s = \Gamma_{IN}^*$, and (3.2.4) from (3.2.2) when $\Gamma_L = \Gamma_{OUT}^*$.
- 3.3. Prove that the maximum unilateral transducer power gain in (3.2.12) is obtained when $\Gamma_s = S_{11}^*$ and $\Gamma_L = S_{22}^*$.
- 3.4. Verify the stability circle equations in (3.3.5) and (3.3.6).
- 3.5. (a) Show that

$$|\Delta| \leq |S_{11}| |S_{22}| + |S_{12} S_{21}|$$

and

$$|S_{11}| |S_{22}| \leq |\Delta| + |S_{12} S_{21}|$$

Substitute these inequalities in (3.3.13) and verify that

$$(1 - |\Delta|)^2 > (|S_{11}|^2 - |S_{22}|^2)^2$$

Therefore, show that

$$B_1 B_2 > 0$$

and

$$B_1 + B_2 = 2(1 - |\Delta|^2)$$

where B_1 is given by (3.3.16) and

$$B_2 = 1 + |S_{22}|^2 - |S_{11}|^2 - |\Delta|^2$$

- (b) Show that the conditions $K > 1$ and $B_1 > 0$ are similar to $K > 1$ and $B_2 > 0$.
- (c) Show that the conditions $K > 1$ and $B_1 > 0$ are similar to the conditions $K > 1$ and $|\Delta| < 1$.
- (d) Verify that (3.3.14) and (3.3.15) are similar to $|\Delta| < 1$.
- 3.6. Prove that the necessary and sufficient conditions for unconditional stability are given by (3.3.13) to (3.3.15).
- 3.7. (a) Starting with (3.3.11) and (3.3.12), verify the conditions for unconditional stability.
- (b) The conditions for unconditional stability were analyzed by considering the values in the Γ_s and Γ_L plane that result in $|\Gamma_{IN}| < 1$ and $|\Gamma_{OUT}| < 1$. An alternative approach is to consider the values in the Γ_{IN} and Γ_{OUT} plane, where $|\Gamma_{IN}| < 1$ and $|\Gamma_{OUT}| < 1$, that results in $|\Gamma_s| < 1$ and $|\Gamma_L| < 1$. Using this approach, show that the plot of the $|\Gamma_s| = 1$ and $|\Gamma_L| = 1$ circles in the Γ_{IN} and Γ_{OUT} planes have radius given by

$$r_s = \frac{|S_{12} S_{21}|}{1 - |S_{11}|^2}$$

and

$$r_L = \frac{|S_{12} S_{21}|}{1 - |S_{22}|^2}$$

and centers given by

$$C_s = S_{22} + \frac{S_{12} S_{21} S_{11}^*}{1 - |S_{11}|^2}$$

and

$$C_L = S_{11} + \frac{S_{12} S_{21} S_{22}^*}{1 - |S_{22}|^2}$$

3.8. In each of the stability circle drawings shown in Fig. P3.8, indicate clearly the possible locations for a stable source reflection coefficient.

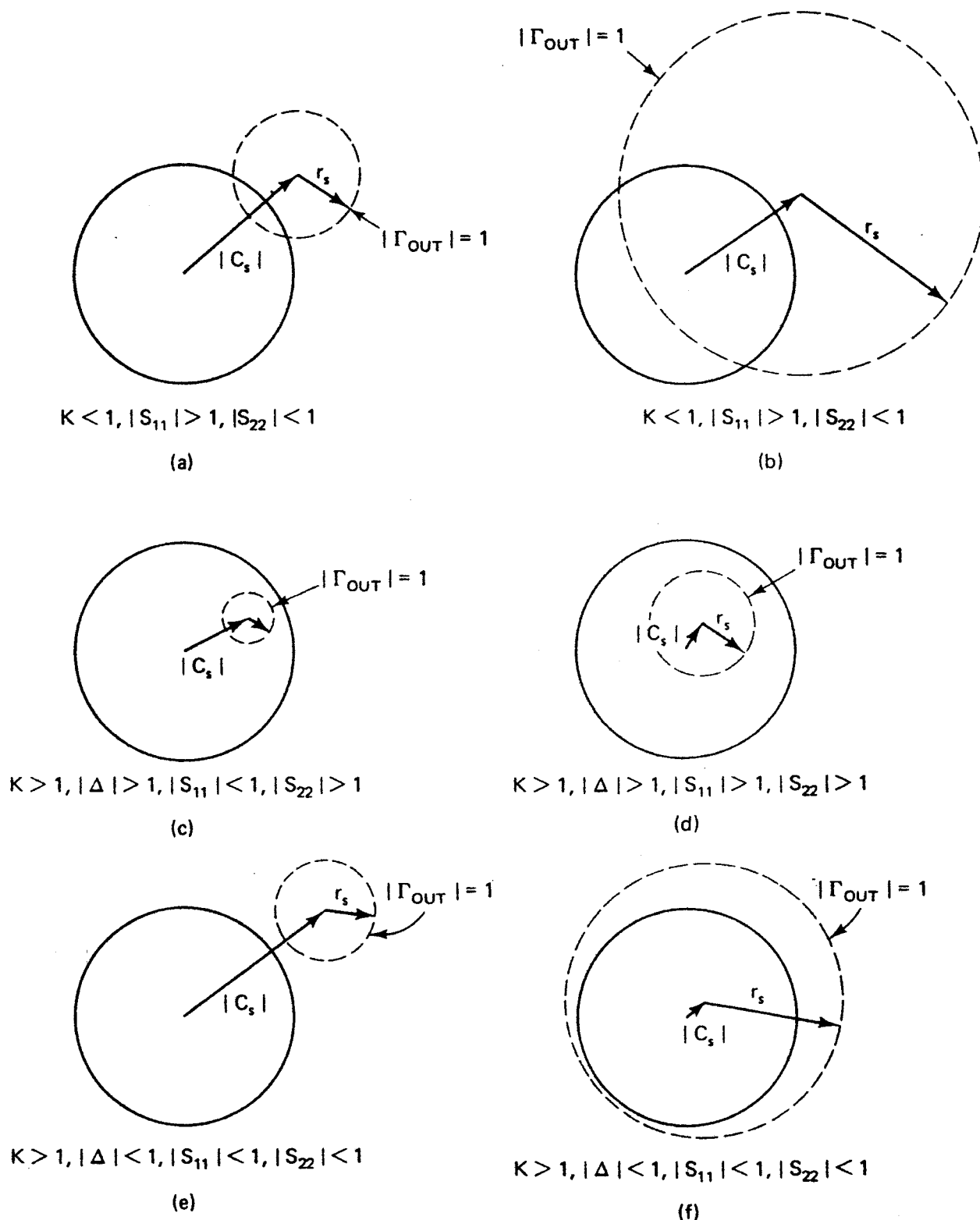


Figure P3.8

- 3.9. Verify the equation for the constant-gain circles in (3.4.6).
- 3.10. Show that the transducer power gain, when the input and output resistances to the transistor are Z_o , is given by $G_T = |S_{21}|^2$.
- 3.11. The scattering parameters for three different transistors are given below. Determine the stability in each case and in a potentially unstable case, draw the input and output stability circles.

(a) $S_{11} = 0.674 \angle -152^\circ$	(b) $S_{11} = 0.385 \angle -55^\circ$	(c) $S_{11} = 0.7 \angle -50^\circ$
$S_{12} = 0.075 \angle 6.2^\circ$	$S_{12} = 0.045 \angle 90^\circ$	$S_{12} = 0.27 \angle 75^\circ$
$S_{21} = 1.74 \angle 36.4^\circ$	$S_{21} = 2.7 \angle 78^\circ$	$S_{21} = 5 \angle 120^\circ$
$S_{22} = 0.6 \angle -92.6^\circ$	$S_{22} = 0.89 \angle -26.5^\circ$	$S_{22} = 0.6 \angle 80^\circ$

- 3.12. Verify the equations for a simultaneous conjugate match in (3.6.5) and (3.6.6).
- 3.13. (a) Show that $|B_i/2C_i|^2 > 1$ is similar to $K^2 > 1$, and therefore that $|B_i/2C_i| > 1$ is similar to $|K| > 1$.

Hint: Prove and use the identities

$$|C_1|^2 = |S_{11} - \Delta S_{22}^*|^2 = |S_{12} S_{21}|^2 + (1 - |S_{22}|^2)(|S_{11}|^2 - |\Delta|^2)$$

and

$$|C_2|^2 = |S_{22} - \Delta S_{11}^*|^2 = |S_{12} S_{21}|^2 + (1 - |S_{11}|^2)(|S_{22}|^2 - |\Delta|^2)$$

- (b) Analyze the solutions to (3.6.5) and (3.6.6) when $|K| > 1$ with K negative.

- 3.14. Verify the equation for $G_{T,\max}$ in (3.6.10).
- 3.15. Show that the unconditionally stable criteria $|\Delta| < 1$ implies that B_1 and B_2 in (3.6.7) and (3.6.8) are greater than zero.
- 3.16. Show that for small S_{12} , Γ_{Ms} and Γ_{ML} are close to S_{11}^* and S_{22}^* , respectively.
- 3.17. Verify the equation for the constant operating power gain circle in (3.8.4).
- 3.18. (a) Design a microwave transistor amplifier for $G_{TU,\max}$ using a BJT whose S parameters in a 50- Ω system at $V_{CE} = 10$ V, $I_C = 20$ mA, and $f = 1$ GHz are

$$S_{11} = 0.706 \angle -160^\circ$$

$$S_{12} = 0$$

$$S_{21} = 5.01 \angle 85^\circ$$

$$S_{22} = 0.508 \angle -20^\circ$$

- (b) Draw the constant-gain circles for $G_s = 2, 1, 0$, and -1 dB.

- 3.19. The scattering parameters of a GaAs FET in a 50- Ω system are

$$S_{11} = 2.3 \angle -135^\circ$$

$$S_{12} = 0$$

$$S_{21} = 4 \angle 60^\circ$$

$$S_{22} = 0.8 \angle -60^\circ$$

- (a) Determine the unstable region in the Smith chart and construct the constant-gain circle for $G_s = 4$ dB.
- (b) Design the input matching network for $G_s = 4$ dB with the greatest degree of stability.
- (c) Draw the complete ac amplifier schematic.

- 3.20. Design a microwave transistor amplifier for $G_{T,\max}$ using a BJT whose S parameters in a $50\text{-}\Omega$ system at $V_{CE} = 10\text{ V}$, $I_C = 4\text{ mA}$, and $f = 750\text{ MHz}$ are

$$S_{11} = 0.277 \angle -59^\circ$$

$$S_{12} = 0.078 \angle 93^\circ$$

$$S_{21} = 1.92 \angle 64^\circ$$

$$S_{22} = 0.848 \angle -31^\circ$$

(This problem is based on a design given in Ref. [3.7]).

- 3.21. Design a microwave transistor amplifier at $f = 750\text{ MHz}$ to have $G_p = 10\text{ dB}$ using the BJT in Problem 3.20. Also, determine the reflection coefficients for $G_{p,\max}$ and show that they are identical to Γ_{Ms} and Γ_{ML} in Problem 3.20.
- 3.22. At 2 GHz , a GaAs FET has the following S parameters:

$$S_{11} = 0.7 \angle -65^\circ$$

$$S_{12} = 0.03 \angle 60^\circ$$

$$S_{21} = 3.2 \angle 110^\circ$$

$$S_{22} = 0.8 \angle -30^\circ$$

Determine the stability and design an amplifier with $G_p = 10\text{ dB}$.

- 3.23. (a) Show that the available power gain can be expressed in the form

$$G_A = \frac{|S_{21}|^2(1 - |\Gamma_s|^2)}{1 - |S_{22}|^2 + |\Gamma_s|^2(|S_{11}|^2 - |\Delta|^2) - 2\text{Re}(C_1\Gamma_s)}$$

- (b) Verify the constant available power gain circle equations in (3.8.9) to (3.8.12).
- (c) Discuss the design procedure for a given G_A in a potentially unstable bilateral case.
- 3.24. (a) Derive the stability factors for the dc bias networks in Fig. 3.9.2.
- (b) Calculate the stability factors for the dc bias network in Example 3.9.1. If h_{FE} changes from 50 to 150, what happens to the quiescent point?
- 3.25. Design the dc bias network shown in Fig. 3.9.3 for $V_{CE} = 6\text{ V}$, $I_C = 1\text{ mA}$, and $S_i = 5$. Assume that $h_{FE} = 100$, and $I_{CBO} = 1\text{ }\mu\text{A}$ at 25°C . Calculate the resulting stability factors and find what happens to the operating point if the temperature increases to 75°C .
- 3.26. (a) In the network shown in Fig. 3.9.4, derive the expression for I_C as a function of the network parameters.
- (b) If $R_1 = 100\text{ k}\Omega$, $R_2 = 200\text{ k}\Omega$ (potentiometer), $R_3 = 5\text{ k}\Omega$ (potentiometer), and $R_4 = 2.6\text{ k}\Omega$, find the typical operating point of Q_2 .

REFERENCES

- [3.1] K. Kurokawa, "Power Waves and the Scattering Matrix," *IEEE Transactions on Microwave Theory and Techniques*, March 1965.
- [3.2] G. E. Bodway, "Two Port Power Flow Analysis Using Generalized Scattering Parameters," *Microwave Journal*, May 1967.

- [3.3] D. Woods, "Reappraisal of the Unconditional Stability Criteria for Active 2-Port Networks in Terms of S Parameters," *IEEE Transactions on Circuits and Systems*, February 1976.
- [3.4] T. T. Ha, *Solid State Microwave Amplifier Design*, Wiley-Interscience, New York, 1981.
- [3.5] "Microwave Transistor Bias Considerations," Hewlett-Packard Application Note 944-1, April 1975.
- [3.6] G. D. Vendelin, "Five Basic Bias Designs for GaAs FET Amplifiers," *Microwaves*, February 1978.
- [3.7] W. H. Froehner, "Quick Amplifier Design with Scattering Parameters," *Electronics*, October 1967.

NOISE, BROADBAND, AND HIGH-POWER DESIGN METHODS

4.1 INTRODUCTION

In Chapter 3, design methods for given stability and gain criteria were discussed. This chapter presents the basic principles involved in the design of low-noise, broadband, and high-power transistor amplifiers.

In some applications the design objective is for a minimum noise figure. Since a minimum noise figure and maximum power gain cannot be obtained simultaneously, constant noise figure circles, together with constant available power gain circles, can be drawn on the Smith chart, and reflection coefficients can be selected that compromise between the noise figure and gain performance. The trade-offs that result from noise considerations, stability, and gain are discussed in this chapter.

The noise performance of the GaAs FET is superior to that of the BJT above 4 GHz. A minimum noise figure in both BJTs and GaAs FETs is obtained at low collector or drain current.

The design philosophy in a broadband amplifier is to obtain flat gain over the prescribed range of frequencies. This can be obtained by the use of compensated matching networks, negative feedback, or balance amplifiers.

The small-signal S parameters can be used in the design of microwave transistor amplifiers with linear power output (i.e., class A operation). However, the small-signal S parameters are not useful in the design of large-output power amplifiers. In this case, large-signal impedance or reflection coefficient data as a function of output power and gain are needed.

4.2 NOISE IN TWO-PORT NETWORKS

In a microwave amplifier, even when there is no input signal, a small output voltage can be measured. We refer to this small output power as the *amplifier noise power*. The total noise output power is composed of the amplified noise input power plus the noise output power produced by the amplifier.

The model of a noisy two-port microwave amplifier is shown in Fig. 4.2.1. The noise input power can be modeled by a noisy resistor that produces thermal or Johnson noise. This noise is produced by the random fluctuations of the electrons due to thermal agitation. The rms value of the noise voltage V_N , produced by the noisy resistor R_N over a frequency range $f_H - f_L$, is given by

$$V_N = \sqrt{4kTBR_N} \quad (4.2.1)$$

where k is Boltzmann's constant (i.e., $k = 1.374 \times 10^{-23}$ J/°K), T is the resistor noise temperature, and B is the noise bandwidth (i.e., $B = f_H - f_L$).

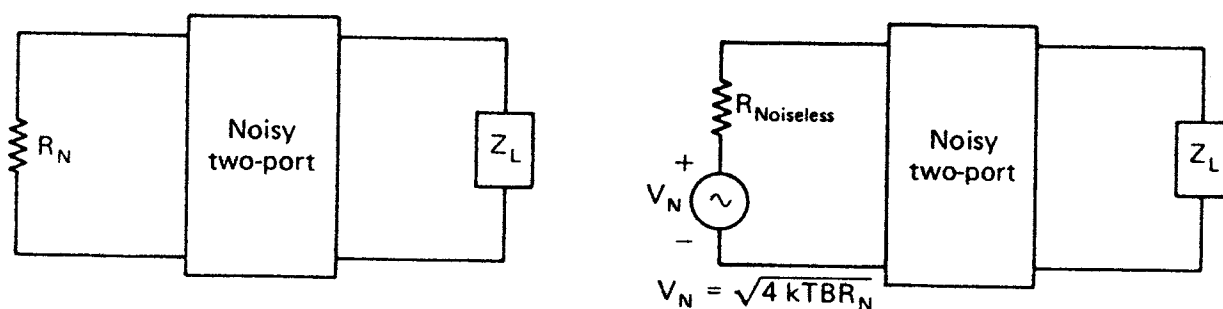


Figure 4.2.1 Model of a noisy microwave amplifier.

Equation (4.2.1) shows that the thermal noise power depends on the bandwidth and not on a given center frequency. Such a distribution of noise is called *white noise*.

The maximum available noise power from R_N is

$$P_N = \frac{V_N^2}{4R_N} = kTB \quad (4.2.2)$$

Example 4.2.1

Calculate the noise voltage and maximum available noise power produced by a 2-M Ω resistor at a standard temperature ($T = 290^\circ\text{K}$) in a 5-kHz bandwidth.

Solution. Using (4.2.1) and (4.2.2), the noise voltage and maximum available noise power are

$$V_N = \sqrt{4(1.374 \times 10^{-23})(290)(5 \times 10^3)(2 \times 10^6)} = 12.6 \mu\text{V}$$

and

$$P_N = \frac{(12.6 \times 10^{-6})^2}{4(2 \times 10^6)} = 19.9 \times 10^{-18} \text{ W}$$

The noise figure (F) describes quantitatively the performance of a noisy microwave amplifier. The noise figure of a microwave amplifier is defined as the ratio of the total available noise power at the output of the amplifier to the available noise power at the output due to thermal noise from R_N . The noise figure can be expressed in the form

$$F = \frac{P_{N_o}}{P_{N_i} G_A} \quad (4.2.3)$$

where P_{N_o} is the total available noise power at the output of the amplifier, $P_{N_i} = kTB$ is the available noise power due to R_N in a bandwidth B , and G_A is the available power gain.

Since G_A can be expressed in the form

$$G_A = \frac{P_{S_o}}{P_{S_i}}$$

where P_{S_o} is the available signal power at the output and P_{S_i} is the available signal power at the input, then (4.2.3) can be written as

$$F = \frac{P_{S_i}/P_{N_i}}{P_{S_o}/P_{N_o}}$$

In other words, F can also be defined as the ratio of the available signal-to-noise power ratio at the input to the available signal-to-noise power ratio at the output. A minimum noise figure is obtained by properly selecting the source reflection coefficient of the amplifier.

A model for the calculation of the noise figure of a two-stage amplifier is shown in Fig. 4.2.2. P_{N_i} is the available input noise power, G_{A1} and G_{A2} are the available power gains of each stage, and P_{n1} and P_{n2} represent the noise power appearing at the output of amplifiers 1 and 2, respectively, due to the internal amplifier noise.

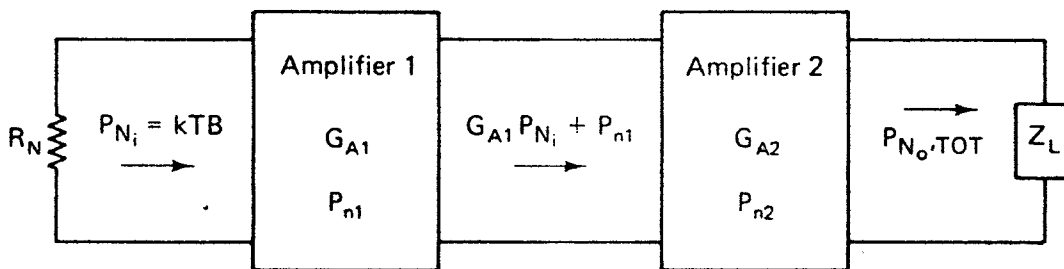


Figure 4.2.2 Noise figure model of a two-stage amplifier.

The total available noise power at the output ($P_{N_o, \text{TOT}}$) is given by

$$P_{N_o, \text{TOT}} = G_{A2} (G_{A1} P_{N_i} + P_{n1}) + P_{n2}$$

Therefore, from (4.2.3) the noise figure of the two-stage amplifier is given by

$$F = \frac{P_{N_o, \text{TOT}}}{P_{N_i} G_{A1} G_{A2}} = 1 + \frac{P_{n1}}{P_{N_i} G_{A1}} + \frac{P_{n2}}{P_{N_i} G_{A1} G_{A2}}$$

or

$$F = F_1 + \frac{F_2 - 1}{G_{A1}} \quad (4.2.4)$$

where

$$F_1 = 1 + \frac{P_{n1}}{P_{N_i} G_{A1}}$$

and

$$F_2 = 1 + \frac{P_{n2}}{P_{N_i} G_{A2}}$$

F_1 and F_2 are recognized as the individual noise figures of the first and second stages, respectively.

Equation (4.2.4) shows that the noise figure of the second stage is reduced by G_{A1} . Therefore, the noise contribution from the second stage is small if G_{A1} is large, and can be significant if the gain G_{A1} is low. It is not always important to minimize the first-stage noise if the gain reduction is too large. In fact, we can select a higher gain, even if F_1 is higher than the minimum noise figure of the first stage, such that a low value of F is obtained. In a design, a trade-off between gain and noise figure is usually made.

4.3 CONSTANT NOISE FIGURE CIRCLES

The noise figure of a two-port amplifier is given by [4.1]

$$F = F_{\min} + \frac{r_n}{g_s} |Y_s - Y_o|^2 \quad (4.3.1)$$

where r_n is the equivalent normalized noise resistance of the two-port (i.e., $r_n = R_N/Z_o$), $Y_s = g_s + jb_s$ represents the source admittance, and $Y_o = g_o + jb_o$ represents that source admittance which results in the minimum noise figure, called F_{\min} .

We can express Y_s and Y_o in terms of the reflection coefficients Γ_s and Γ_o , namely

$$Y_s = \frac{1 - \Gamma_s}{1 + \Gamma_s} \quad (4.3.2)$$

and

$$Y_o = \frac{1 - \Gamma_o}{1 + \Gamma_o} \quad (4.3.3)$$

Substituting (4.3.2) and (4.3.3) into (4.3.1) results in the relation

$$F = F_{\min} + \frac{4r_n |\Gamma_s - \Gamma_o|^2}{(1 - |\Gamma_s|^2) |1 + \Gamma_o|^2} \quad (4.3.4)$$

Equation (4.3.4) depends on F_{\min} , r_n , and Γ_o . These quantities are known as the *noise parameters* and are given by the manufacturer of the transistor or can be determined experimentally. The source reflection coefficient can be varied until a minimum noise figure is read in a noise figure meter. The value of F_{\min} , which occurs when $\Gamma_s = \Gamma_o$, can be read from the meter, and the source reflection coefficient that produces F_{\min} can be determined accurately using a network analyzer. The noise resistance r_n can be measured by reading the noise figure when $\Gamma_s = 0$, called $F_{\Gamma_s=0}$. Then, using (4.3.4) we obtain

$$r_n = (F_{\Gamma_s=0} - F_{\min}) \frac{|1 + \Gamma_o|^2}{4|\Gamma_o|^2}$$

F_{\min} is a function of the device operating current and frequency, and there is one value of Γ_o associated with each F_{\min} . A typical plot of F_{\min} versus current for a BJT is illustrated in Fig. 4.3.1.

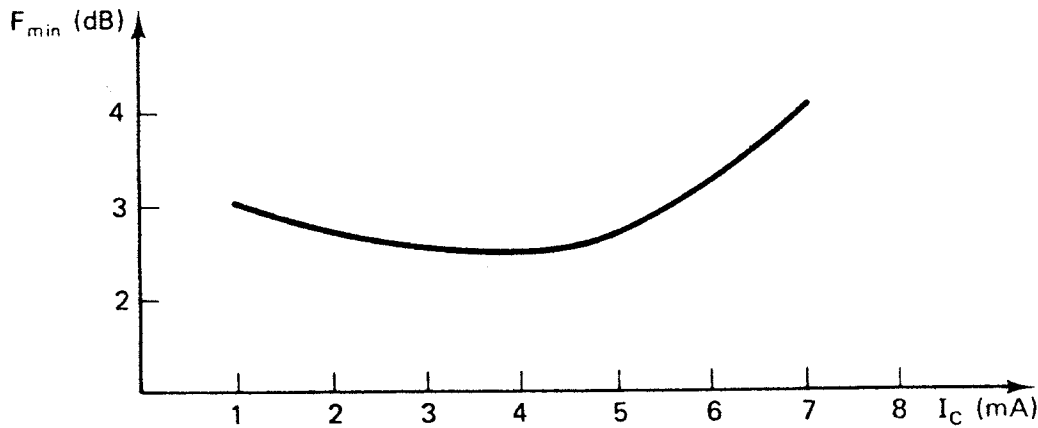


Figure 4.3.1 Typical F_{\min} versus collector current measured at $V_{CE} = 10$ V and $f = 4$ GHz.

Equation (4.3.4) can be used to design Γ_s for a given noise figure. For a given noise figure F_i , we define a noise figure parameter, called N_i , as

$$N_i = \frac{|\Gamma_s - \Gamma_o|^2}{1 - |\Gamma_s|^2} = \frac{F_i - F_{\min}}{4r_n} |1 + \Gamma_o|^2 \quad (4.3.5)$$

Equation (4.3.5) can be written as

$$(\Gamma_s - \Gamma_o)(\Gamma_s^* - \Gamma_o^*) = N_i - N_i |\Gamma_s|^2$$

or

$$|\Gamma_s|^2(1 + N_i) + |\Gamma_o|^2 - 2 \operatorname{Re}(\Gamma_s \Gamma_o^*) = N_i$$

If we now multiply both sides by $1 + N_i$, we obtain

$$|\Gamma_s|^2(1 + N_i)^2 + |\Gamma_o|^2 - 2(1 + N_i) \operatorname{Re}(\Gamma_s \Gamma_o^*) = N_i^2 + N_i(1 - |\Gamma_o|^2)$$

or

$$\left| \Gamma_s - \frac{\Gamma_o}{1 + N_i} \right|^2 = \frac{N_i^2 + N_i(1 - |\Gamma_o|^2)}{(1 + N_i)^2} \quad (4.3.6)$$

Equation (4.3.6) is recognized as a family of circles with N_i as a parameter. The circles are centered at

$$C_{Fi} = \frac{\Gamma_o}{1 + N_i} \quad (4.3.7)$$

with radii

$$R_{Fi} = \frac{1}{1 + N_i} \sqrt{N_i^2 + N_i(1 - |\Gamma_o|^2)} \quad (4.3.8)$$

Equations (4.3.5), (4.3.7), and (4.3.8) show that when $F_i = F_{\min}$, then $N_i = 0$, $C_{F_{\min}} = \Gamma_o$, and $R_{F_{\min}} = 0$. That is, the center of the F_{\min} circle is located at Γ_o with zero radius. From (4.3.7), the centers of the other noise figure circles are located along the Γ_o vector.

A typical set of constant noise figure circles is shown in Fig. 4.3.2. This set of curves show that $F_{\min} = 3$ dB is obtained when $\Gamma_s = \Gamma_o = 0.58 \angle 138^\circ$ and at point A, $\Gamma_s = 0.38 \angle 119^\circ$ produces $F_i = 4$ dB.

In a design there is always a difference between the designed noise figure and the measured noise figure of the final amplifier. This occurs because of the loss associated with the matching elements and the transistor noise figure variations from unit to unit. Typically, the noise figure difference can be from a fraction of a decibel to 1 dB in a narrowband design.

In the unilateral case, a set of G_s constant-gain circles can be drawn in the Smith chart containing the noise figure circles. A typical plot for a GaAs FET is illustrated in Fig. 4.3.3. This plot shows the trade-offs that can be made between gain and noise figure in a design. Maximum gain and minimum noise figure cannot, in general, be obtained simultaneously. In Fig. 4.3.3, the maximum G_s gain of 3 dB, obtained with $\Gamma_s = 0.7 \angle 110^\circ$, results in a noise figure of $F_i \approx 4$ dB; and the minimum noise figure $F_{\min} = 0.8$ dB, obtained with $\Gamma_s = 0.6 \angle 40^\circ$, results in a gain $G_s \approx -1$ dB.

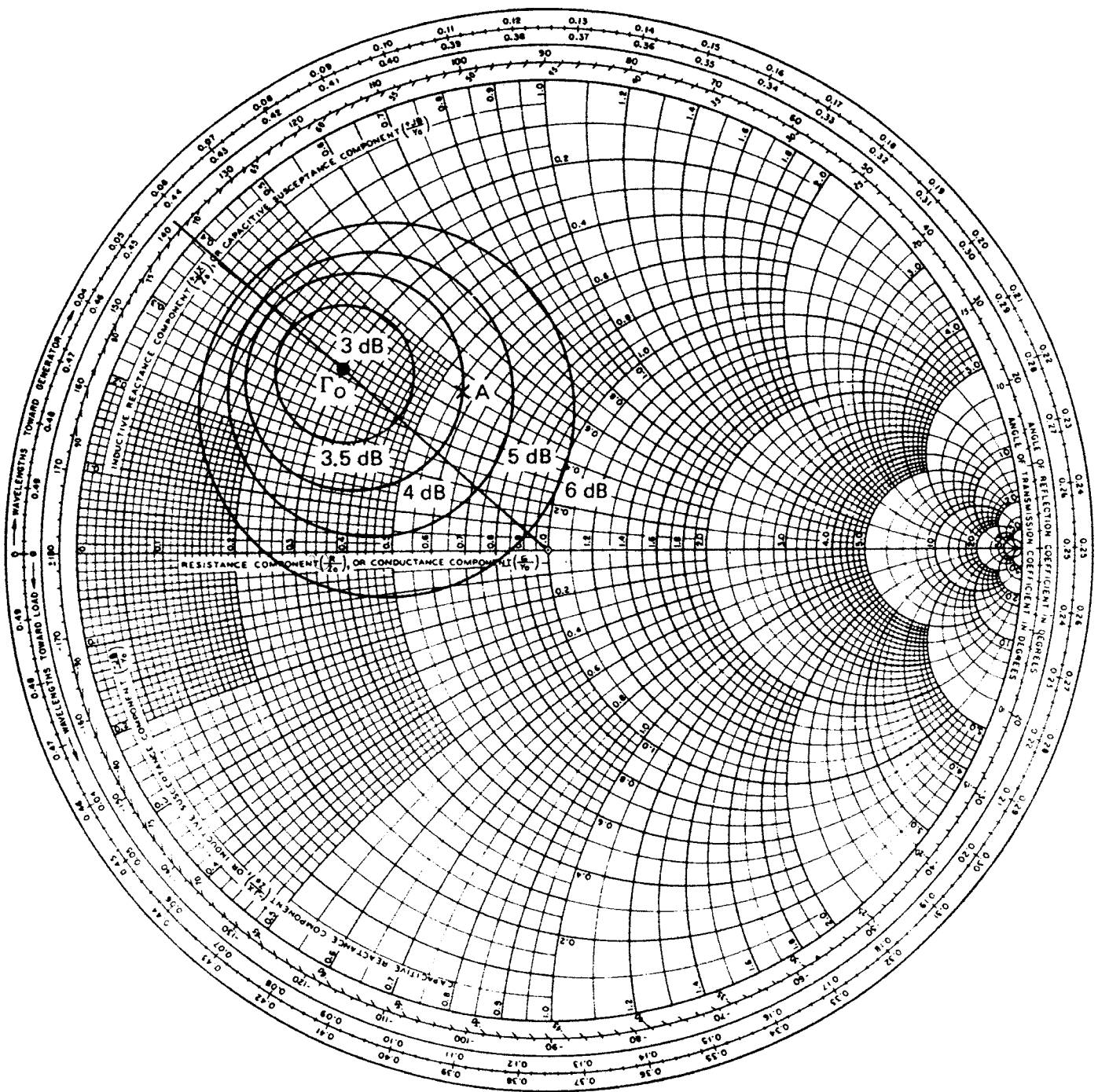


Figure 4.3.2 Typical constant noise figure circles in the Γ_s plane.

Example 4.3.1

The scattering and noise parameters of a BJT measured at a bias point for low-noise operation ($V_{CE} = 10$ V, $I_C = 4$ mA) at $f = 4$ GHz are

$$S_{11} = 0.552 \angle 169^\circ$$

$$S_{12} = 0.049 \angle 23^\circ$$

$$S_{21} = 1.681 \angle 26^\circ$$

$$S_{22} = 0.839 \angle -67^\circ$$

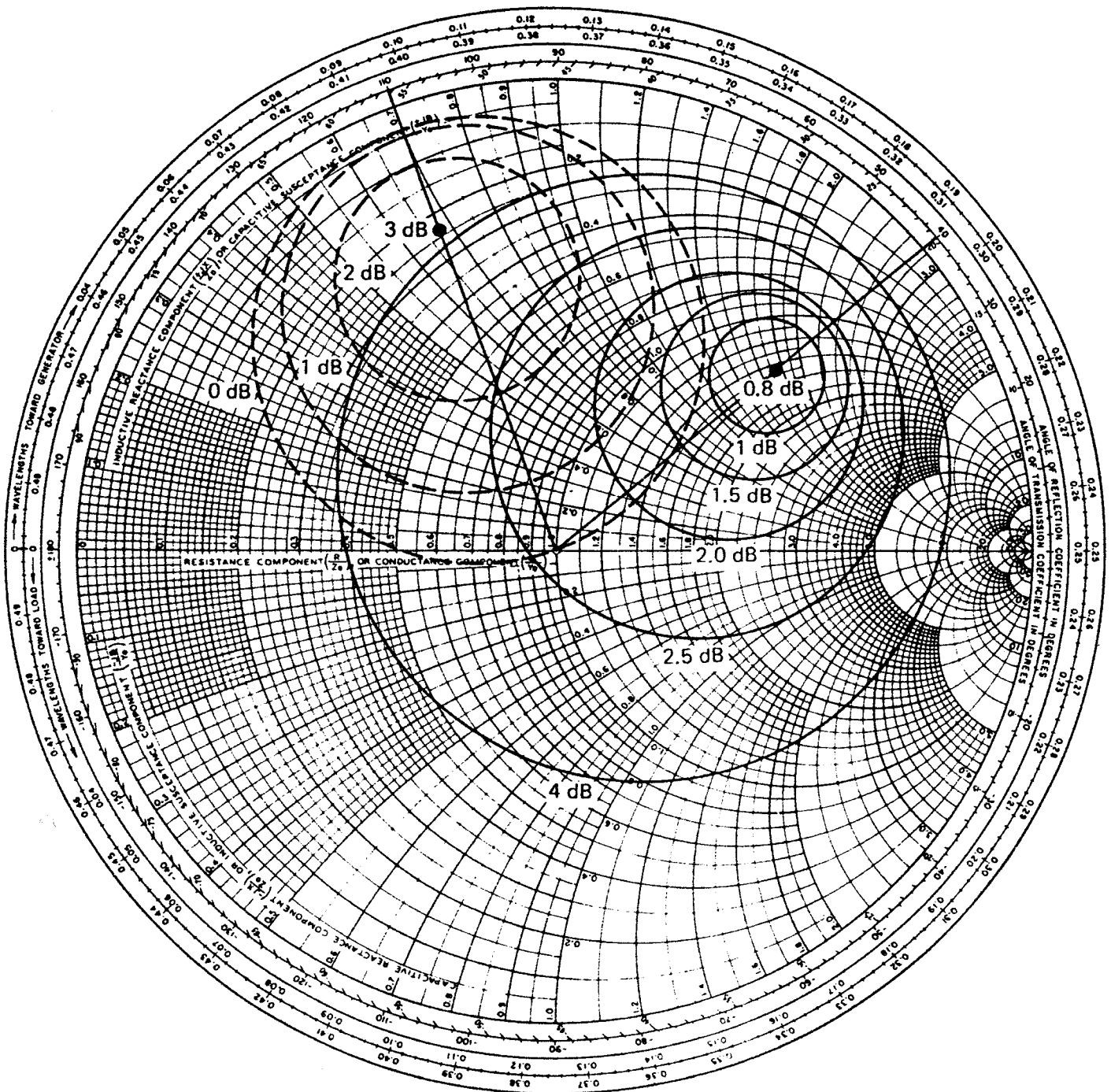


Figure 4.3.3 Noise figure circles (solid curves) and G_s constant-gain circles (dashed curves). The transistor is a GaAs FET with $V_{DS} = 4$ V, $I_{DS} = 12$ mA, and $f = 6$ GHz.

and

$$F_{\min} = 2.5 \text{ dB}$$

$$\Gamma_o = 0.475 \angle 166^\circ$$

$$R_N = 3.5 \Omega$$

Design a microwave transistor amplifier to have a minimum noise figure. (This example is based on a design from Hewlett-Packard Application Note 967 [4.2].)

Solution. The transistor is unconditionally stable at 4 GHz. A minimum noise figure of 2.5 dB is obtained with $\Gamma_s = \Gamma_o = 0.475 \angle 166^\circ$. The constant noise figure circles in Fig. 4.3.4 for $F_i = 2.5$ to 3 dB were calculated using (4.3.5), (4.3.7), and (4.3.8). For example, the $F_i = 2.8$ -dB circle was obtained as follows:

$$N_i = \frac{1.905 - 1.778}{4(3.5/50)} |1 + 0.475 \angle 166^\circ|^2 = 0.1378$$

$$C_{F_i} = \frac{0.475 \angle 166^\circ}{1 + 0.1378} = 0.417 \angle 166^\circ$$

and

$$R_{F_i} = \frac{1}{1 + 0.1378} \sqrt{(0.1378)^2 + 0.1378[1 - (0.475)^2]} = 0.312$$

Figure 4.3.4 shows that for this transistor F_{\min} is not very sensitive to small variations in Γ_s around Γ_o . In fact, the 2.6-dB constant-noise circle (i.e., a 0.1-dB increase in noise figure) results when Γ_s changes in magnitude by 0.2 from its value at Γ_o .

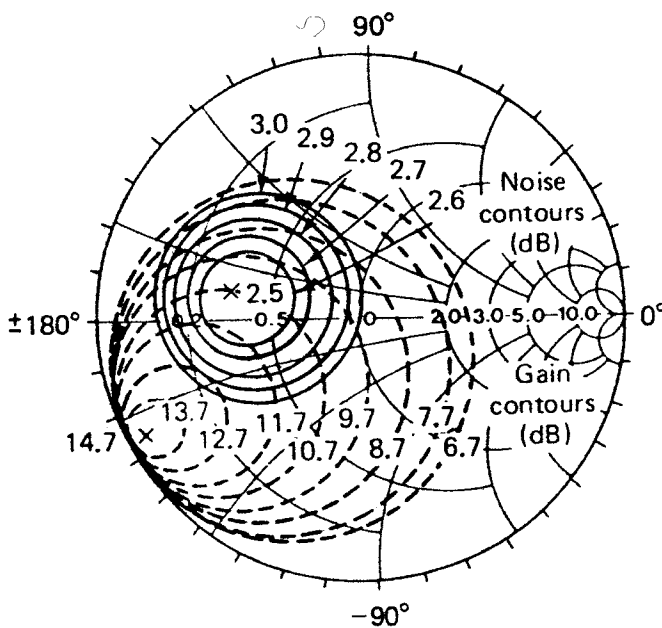


Figure 4.3.4 Constant noise figure circles and available power gain circles. (From Ref. [4.2]; courtesy of Hewlett-Packard.)

The load reflection coefficient is selected to provide maximum gain for the lowest noise figure (i.e., with $\Gamma_s = \Gamma_o$) and, of course, for optimum VSWR at the output. Therefore,

$$\Gamma_L = \left(S_{22} + \frac{S_{12} S_{21} \Gamma_o}{1 - S_{11} \Gamma_o} \right)^* = 0.844 \angle 70.4^\circ$$

and the resulting gains are $G_T = G_A = 11$ dB and $G_p = 12.7$ dB.

The amplifier was designed, built, and tested by Hewlett-Packard [4.2]. The ac amplifier schematic is shown in Fig. 4.3.5. The input matching network was designed with a short-circuited stub and a quarter-wave transformer with $Z_o = 31.1 \Omega$. The output matching network was designed with a 0.61-cm microstrip line to provide soldering area, followed by a $\lambda/8$ short-circuited stub to tune out most of the susceptance component of $Y_1 = 1/Z_1$. Then, another series microstrip line followed by an

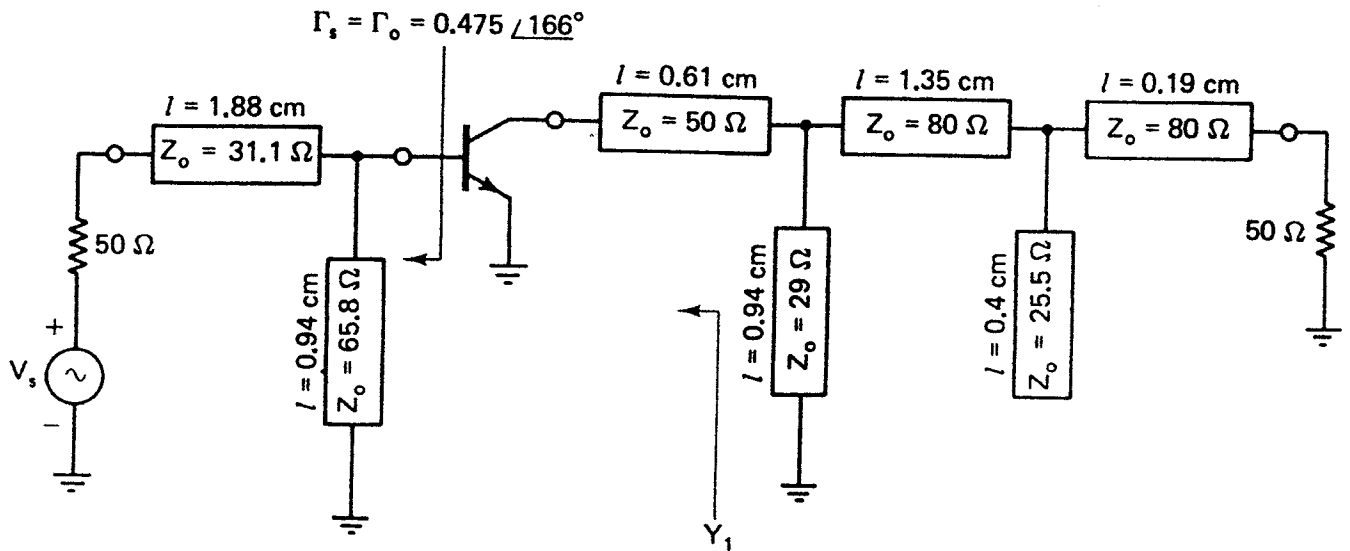


Figure 4.3.5 Amplifier schematic. The microstrip lengths are given for $\epsilon_{ff} = 1$ at $f = 4$ GHz. (From Ref. [4.2]; courtesy of Hewlett-Packard.)

open stub that provides some tuning capabilities was used. A final series microstrip line was used to obtain the match to 50 Ω .

Of course, the output matching network could have been designed differently. The form selected (see Fig. 4.3.5) provides flexibility for tuning by adjusting the lengths of the series lines (i.e., the $l = 1.35$ -cm and $l = 0.19$ -cm lines), by changing the width (i.e., the characteristic impedance) of the open-circuited stub and by modifying the lengths of the short-circuited stub.

The complete amplifier schematic and the microstrip board layout are shown in Fig. 4.3.6. The board material is Duroid ($\epsilon_r = 2.23$, $h = 0.031$ in.).

The measured characteristics of the amplifier are shown in Fig. 4.3.7. Figure 4.3.7 shows that the amplifier performance is very good in the frequency range 3.7 to 4.2 GHz. The 3-dB bandwidth (see Fig. 4.3.7e) is 850 MHz, which corresponds to a 21% bandwidth.

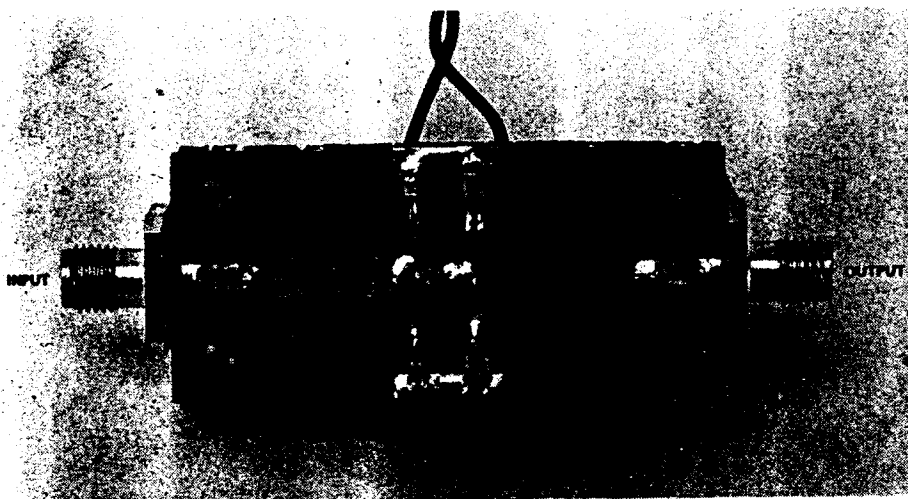
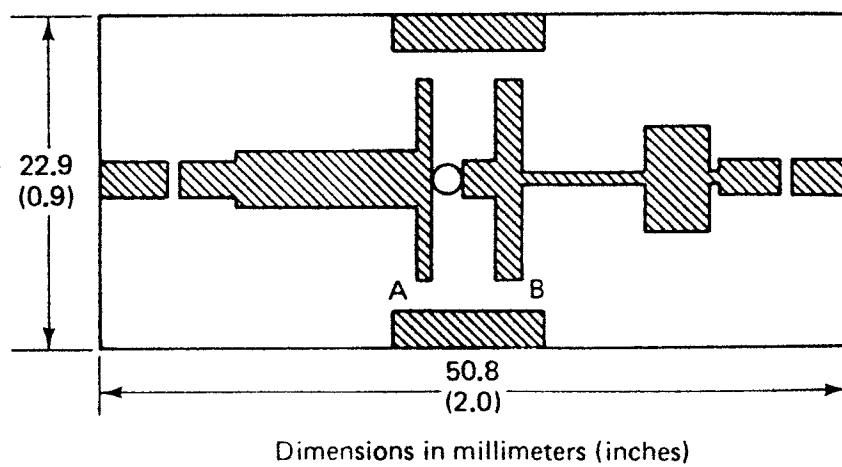
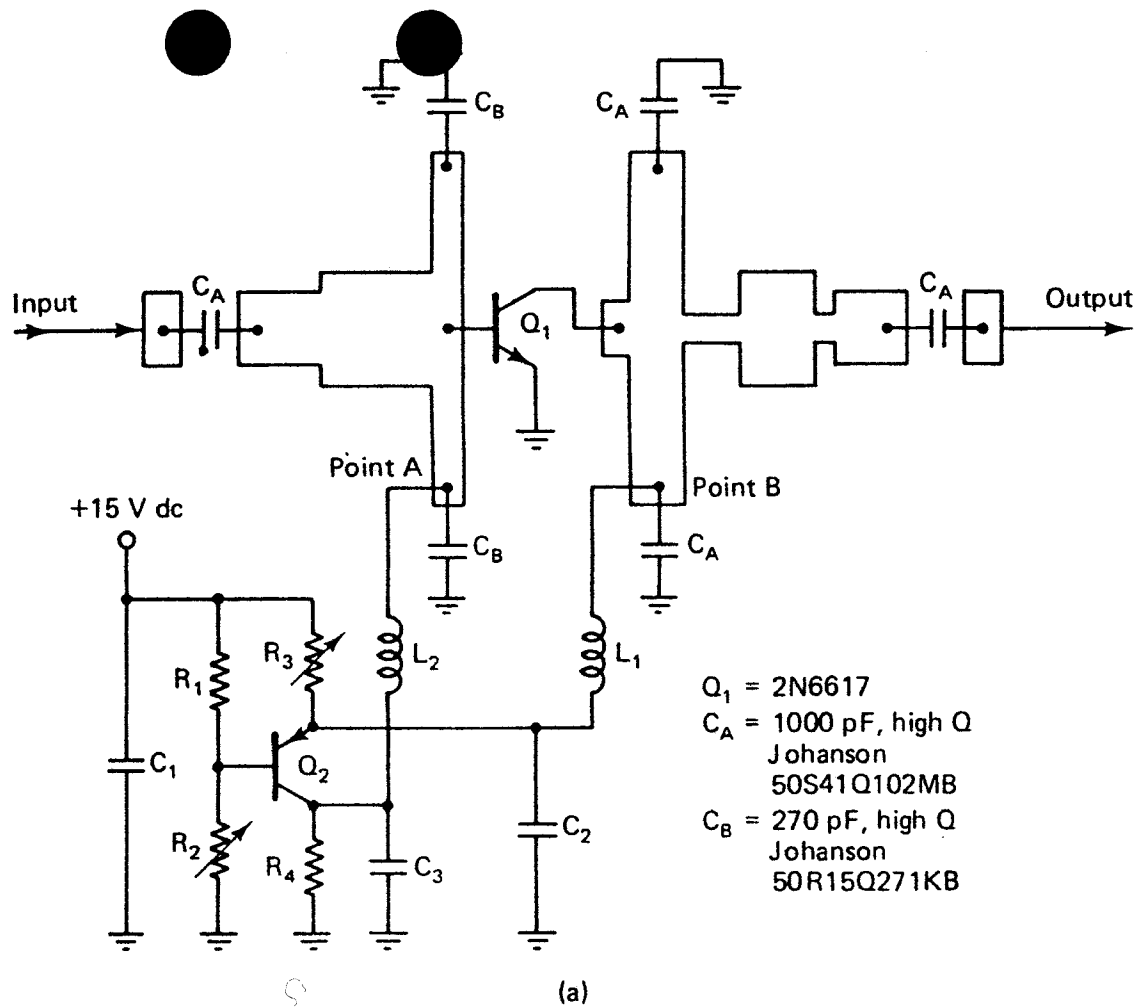
It is easy to show that for this BJT, $K = 1.012$, $\Delta = 0.419 \angle 111.04^\circ$, $G_{T,\max} = G_{A,\max} = 14.7$ dB, $\Gamma_{Ms} = 0.941 \angle -154^\circ$, and $\Gamma_{ML} = 0.979 \angle 70^\circ$. Since the available power gain with $\Gamma_s = \Gamma_o$ is $G_A = 11$ dB, a sacrifice in gain was needed to obtain optimum noise performance.

Example 4.3.2

The scattering and noise parameters of a GaAs FET measured at three different optimum bias settings at $f = 6$ GHz are:

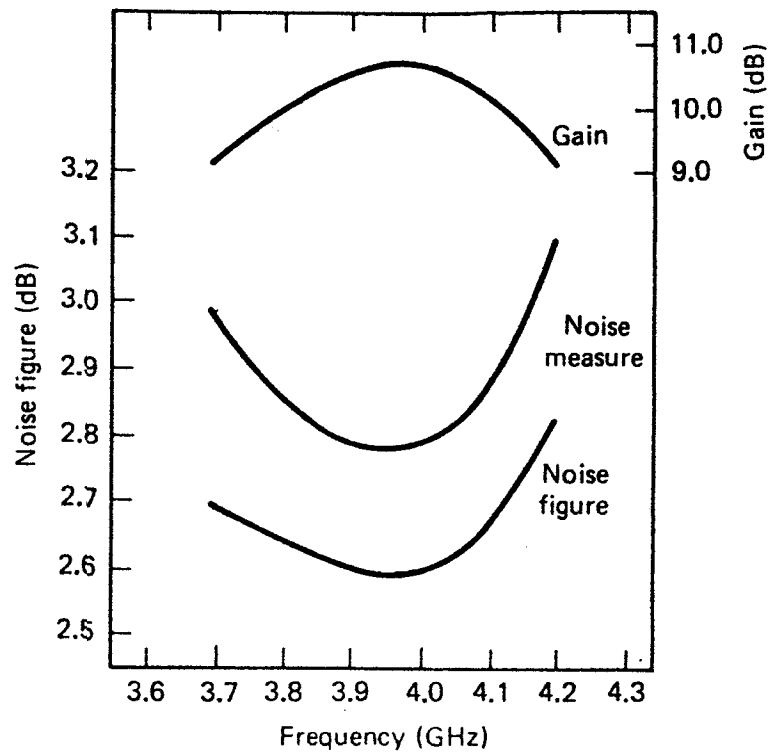
Minimum Noise Figure ($V_{DS} = 3.5$ V, $I_{DS} = 15\%I_{DSS}$):

$$\begin{aligned} S_{11} &= 0.674 \angle -152^\circ & F_{\min} &= 2.2 \text{ dB} \\ S_{12} &= 0.075 \angle 6.2^\circ & \Gamma_o &= 0.575 \angle 138^\circ \\ S_{21} &= 1.74 \angle 36.4^\circ & R_N &= 6.64 \Omega \\ S_{22} &= 0.6 \angle -92.6^\circ \end{aligned}$$

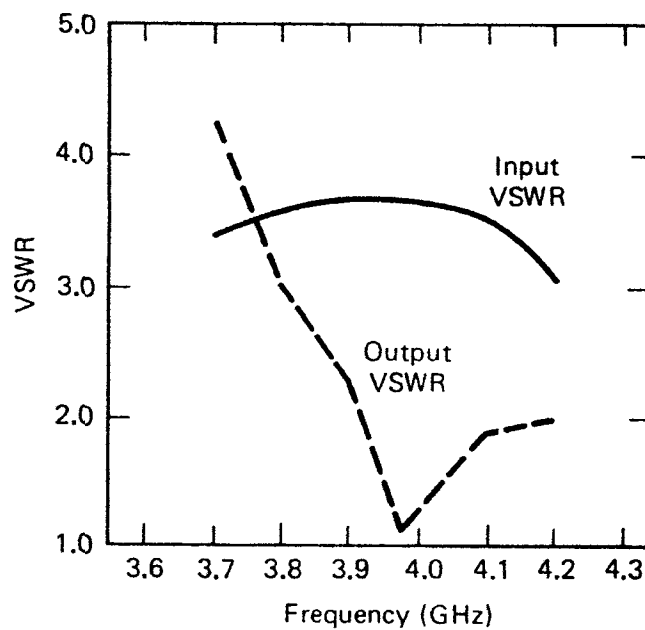


(b)

Figure 4.3.6 (a) Complete amplifier schematic; (b) microstrip board layout. (From Ref. [4.2]; courtesy of Hewlett-Packard.)



(a)



(b)

Figure 4.3.7 Measured amplifier characteristics: (a) noise and gain performance; (b) input-output VSWR performance; (c) power output performance; (d) temperature performance at 4 GHz; (e) wideband gain performance. (From Ref. [4.2]; courtesy of Hewlett-Packard.)

Linear Power Output ($V_{DS} = 4\text{ V}$, $I_{DS} = 50\%I_{DSS}$):

$$S_{11} = 0.641 \angle -171.3^\circ \quad F_{\min} = 2.9\text{ dB}$$

$$S_{12} = 0.057 \angle 16.3^\circ \quad \Gamma_o = 0.542 \angle 141^\circ$$

$$S_{21} = 2.058 \angle 28.5^\circ \quad R_N = 9.42\ \Omega$$

$$S_{22} = 0.572 \angle -95.7^\circ$$

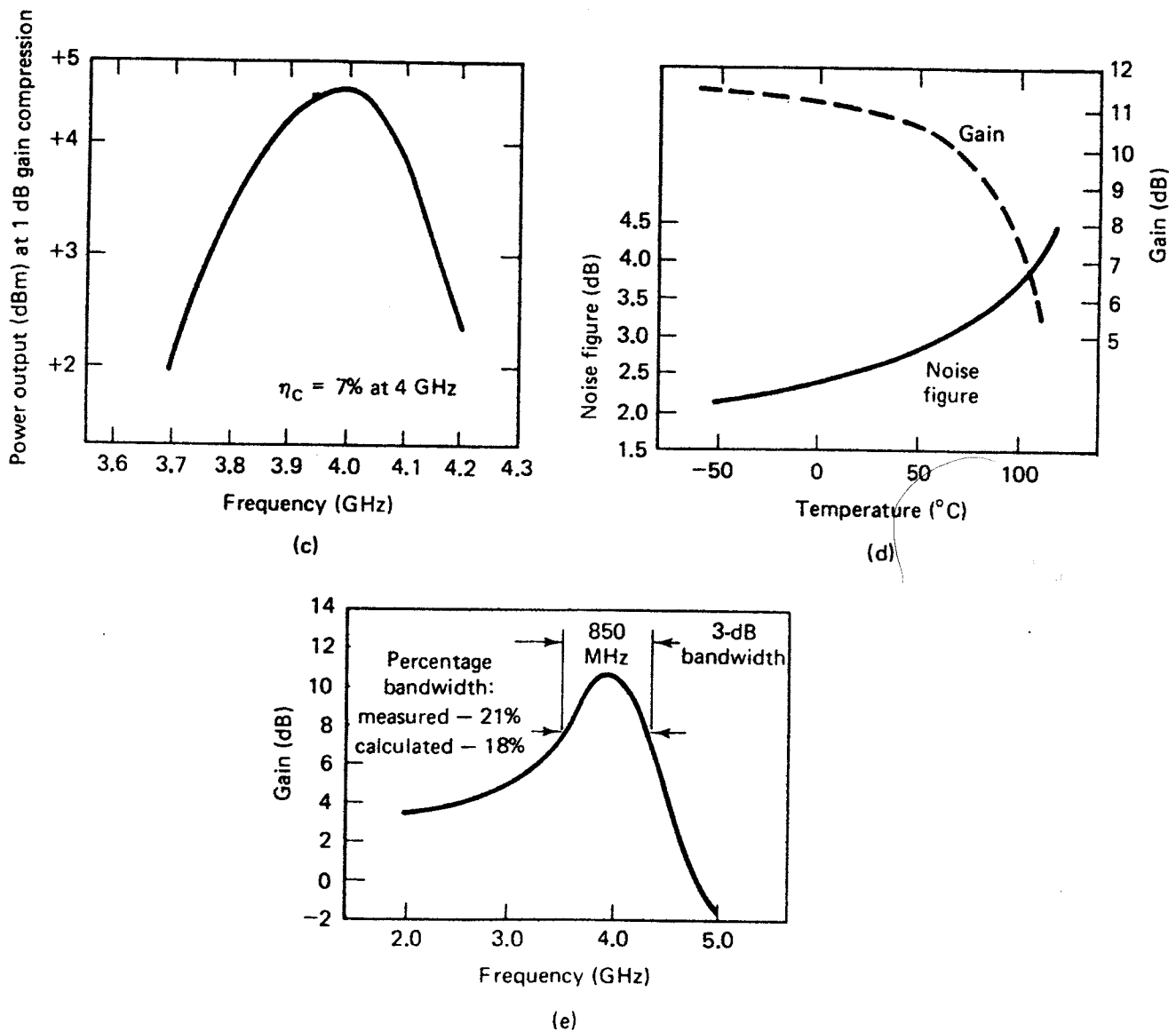


Figure 4.3.7 (continued)

Maximum Gain ($V_{DS} = 4\text{ V}$, $I_{DS} = 100\%I_{DSS}$):

$$S_{11} = 0.614 \angle -167.4^{\circ}$$

$$S_{12} = 0.046 \angle 65^{\circ}$$

$$S_{21} = 2.187 \angle 32.4^{\circ}$$

$$S_{22} = 0.716 \angle -83^{\circ}$$

Design a microwave transistor amplifier to have good ac performance. (This example is based on a design from Hewlett-Packard Application Note 970 [4.3].)

Solution. There are four ac performances that must be considered: noise figure, power gain, power output, and input and output VSWR. The linear power-output bias point ($V_{DS} = 4\text{ V}$, $I_{DS} = 50\%I_{DSS}$) provides a good compromise between the minimum noise figure and maximum gain. At this bias point Fig. 4.3.8 gives the noise, gain, and power parameters. The output power performance, measured at the 1-dB compression point, was experimentally measured and it is given in the figure. (See Section 4.7 for the definition of the 1-dB compression point.) The data for the output power were taken with an input power drive of 8.3 dBm.

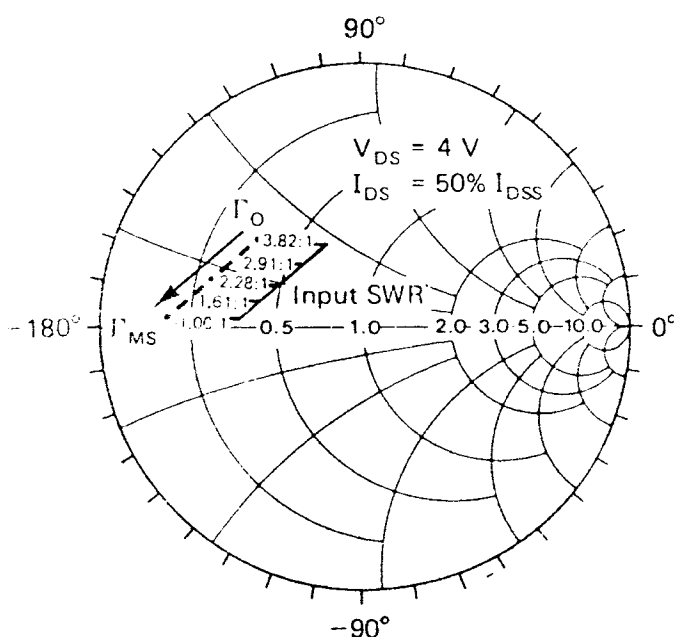
Noise Parameters	Gain Parameters	Power Parameters
$\Gamma_o = 0.542 \angle 141^\circ$	$\Gamma_{Ms} = 0.762 \angle 177.3^\circ$	$\Gamma_{PS} = 0.729 \angle 166^\circ$
$\Gamma_L = 0.575 \angle 104.5^\circ$	$\Gamma_{ML} = 0.718 \angle 103.9^\circ$	$\Gamma_{PL} = 0.489 \angle 101^\circ$
$F_{\min} = 2.9 \text{ dB}$	$F = 4.44 \text{ dB}$	$F = 3.69 \text{ dB}$
$G_A = 9.33 \text{ dB}$	$G_{A, \max} = 11.38 \text{ dB}$	$G_p = 8.2 \text{ dB}$
$P_{1\text{dB}} = 9.3 \text{ dBm}$	$P_{1\text{dB}} = 13.4 \text{ dBm}$	$P_{1\text{dB}} = 15.5 \text{ dBm}$

Figure 4.3.8 Noise, gain, and power parameters at the linear power output bias ($V_{DS} = 4 \text{ V}$, $I_D = 50\% I_{DSS}$).

The input VSWR with $\Gamma_s = \Gamma_{Ms}$ is 1, and the VSWR = 3.82 with $\Gamma_s = \Gamma_o$. In order to calculate the VSWR, we obtained $|\Gamma_a|$ (see Fig. 4.3.10a) and used (1.3.11), namely

$$\text{VSWR} = \frac{1 + |\Gamma_a|}{1 - |\Gamma_a|}$$

Other relations for calculating $|\Gamma_a|$ are given in Problem 4.6.



Γ_s	Mag./Ang.	Γ_L Mag./Ang.	F (dB)	G_A (dB)	Input VSWR	Output VSWR
Γ_o —	$0.542 \angle 141^\circ$	$0.575 \angle 104^\circ$	2.90	9.33	3.82:1	1.00:1
	$0.572 \angle 152^\circ$	$0.601 \angle 105^\circ$	2.97	10.04	2.91:1	1.00:1
	$0.614 \angle 160^\circ$	$0.627 \angle 106^\circ$	3.14	10.55	2.28:1	1.00:1
	$0.678 \angle 169^\circ$	$0.667 \angle 105^\circ$	3.57	11.10	1.61:1	1.00:1
Γ_{Ms} —	$0.762 \angle 177^\circ$	$0.718 \angle 104^\circ$	4.44	11.38	1.00:1	1.00:1

Figure 4.3.9 Trade-offs between noise figure, power gain, and VSWR. (From Ref. [4.3]; courtesy of Hewlett-Packard.)

Figure 4.3.9 shows the noise figure, G_A and input and output VSWR as the reflection coefficient is varied from Γ_o to Γ_{Ms} , along a straight line, in the Smith chart. Figure 4.3.9 shows that a good compromise between noise figure, G_A , and VSWR is to use $\Gamma_s = 0.614 \angle 160^\circ$ and $\Gamma_L = 0.627 \angle 106^\circ$. The noise figure is increased by 0.24 dB from the minimum noise, but G_A is increased by 1.22 dB and the input VSWR is improved by 40% (i.e., VSWR = 2.28). The ac schematic of the amplifier for the selected values of Γ_s and Γ_L is shown in Fig. 4.3.10a and the microstrip board layout is shown in Fig. 4.3.10b. The board material is Duroid ($\epsilon_r = 2.23$, $h = 0.031$ in.). The measured characteristics of the amplifier are shown in Fig. 4.3.11.

In the last two examples the transistors were unconditionally stable. In a potentially unstable situation, we must check that the optimum noise reflection coefficient $\Gamma_s = \Gamma_o$ is in the stable region of the source stability circle. Once Γ_s is selected, Γ_L is selected for maximum gain (i.e., $\Gamma_L = \Gamma_{OUT}^*$), and again we must check that the value of Γ_L is in the stable region of the load stability circle.

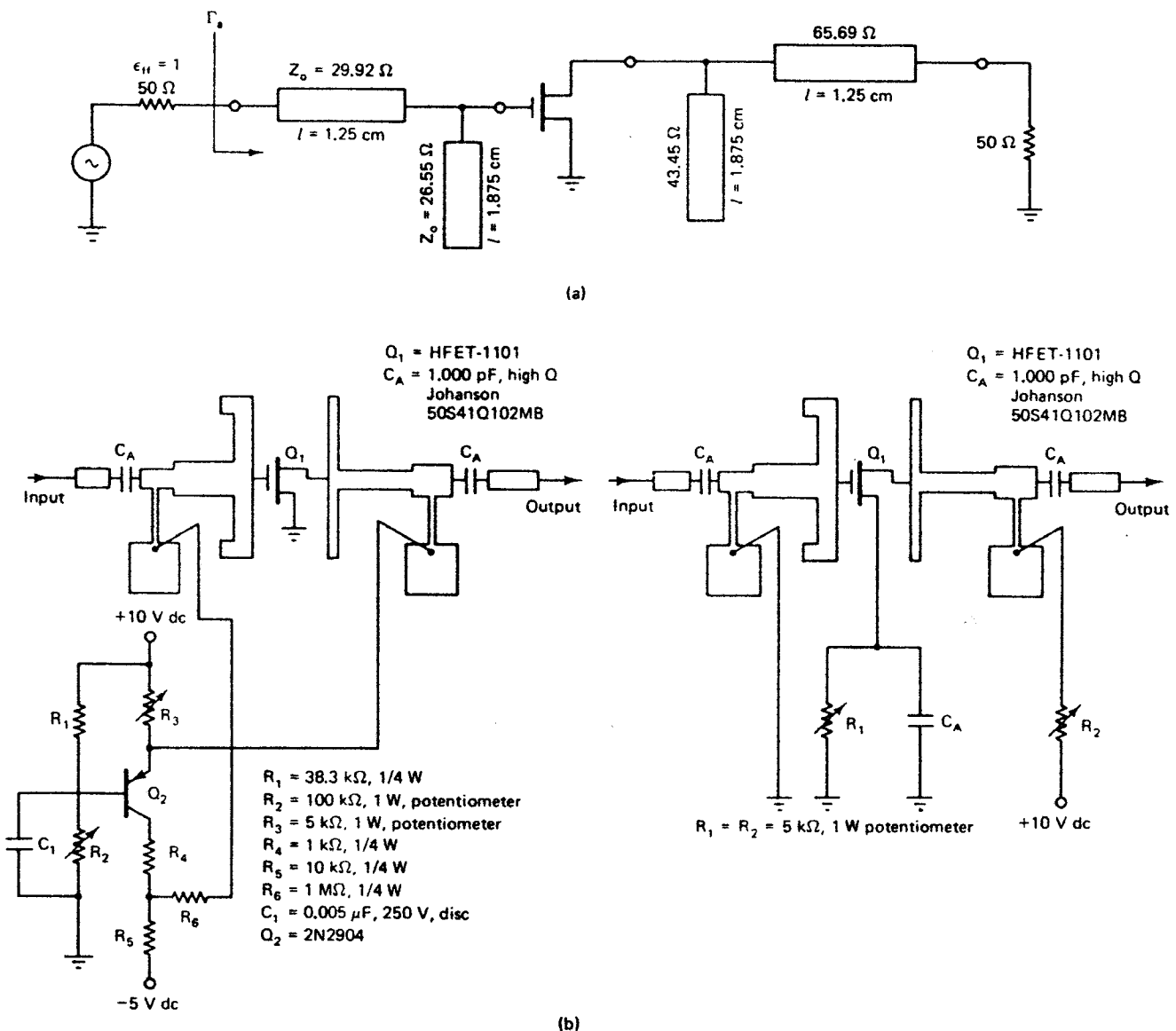


Figure 4.3.10 (a) The ac schematic of the amplifier with $\epsilon_{ff} = 1$; (b) microstrip layout with two different dc bias networks. (From Ref. [4.3]; courtesy of Hewlett-Packard.)

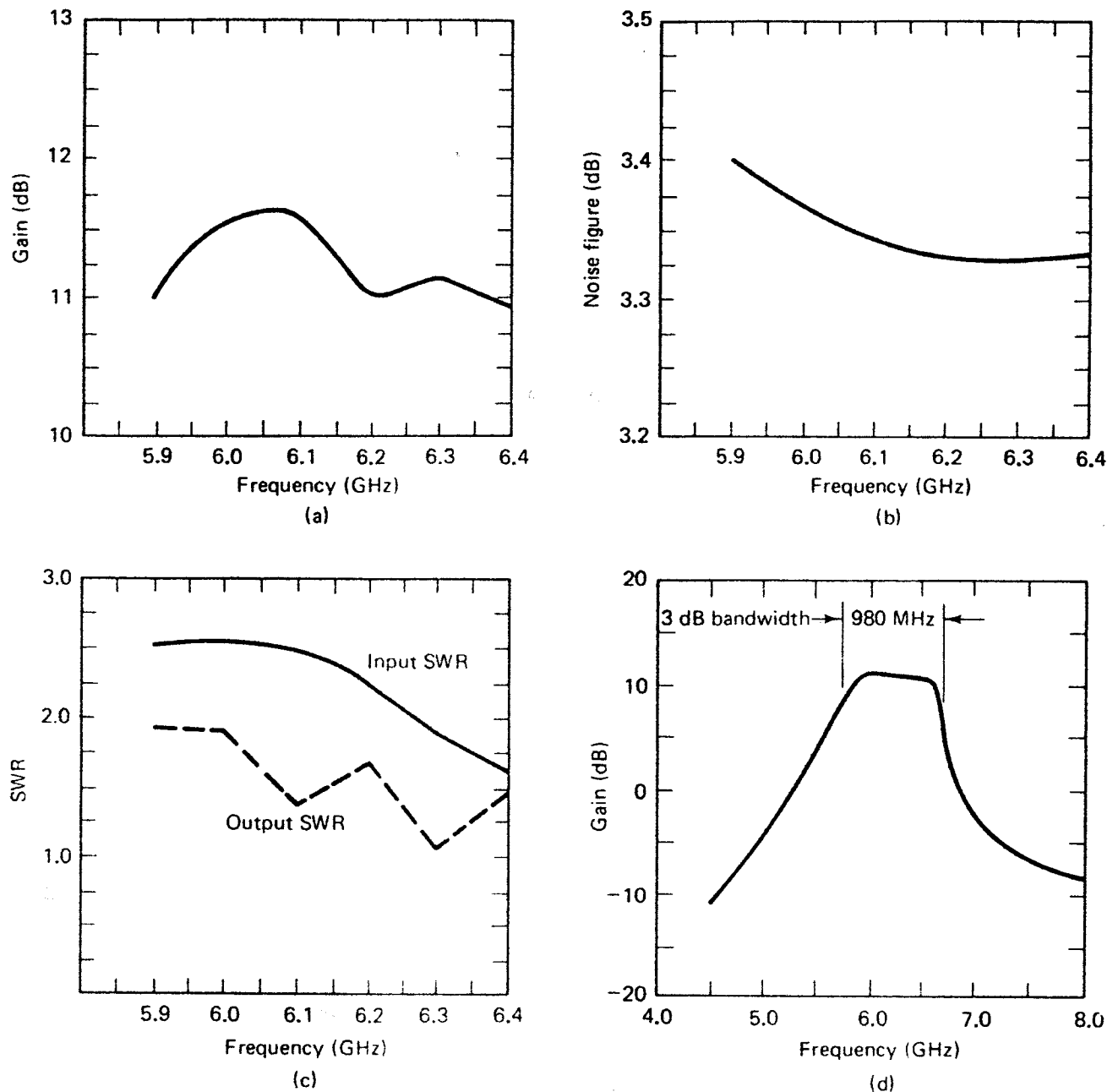


Figure 4.3.11 Measured characteristics of the amplifier: (a) gain performance; (b) noise performance; (c) input-output VSWR performance; (d) wideband gain performance. (From Ref. [4.3]; courtesy of Hewlett-Packard.

4.4 BROADBAND AMPLIFIER DESIGN

The design of broadband amplifiers introduces new difficulties which require careful considerations. Basically, the design of a constant-gain amplifier over a broad frequency range is a matter of properly designing the matching networks, or the feedback network, in order to compensate for the variations of $|S_{21}|$ with frequency. The design specifications might require the use of rather sophisticated synthesis procedures in the design of the matching networks.

Some of the difficulties encountered in the design of a broadband amplifier are:

1. The variations of $|S_{21}|$ and $|S_{12}|$ with frequency. Typically, $|S_{21}|$ decreases with frequency at the rate of 6 dB/octave and $|S_{12}|$ increases with frequency at the same rate. Typical variations of $|S_{21}|$, $|S_{12}|$, and $|S_{12}S_{21}|$ with frequency are illustrated in Fig. 1.9.7. The variations of $|S_{12}S_{21}|$ with frequency is important since the stability of the circuit depends on this quantity. It is in the flat region that we have to check the amplifier stability.
2. The scattering parameters S_{11} and S_{22} are also frequency dependent and their variations are significant over a broad range of frequencies.
3. There is a degradation of the noise figure and VSWR in some frequency range of the broadband amplifier.

Two techniques that are commonly used to design broadband amplifiers are (1) the use of compensated matching networks and (2) the use of negative feedback.

The technique of compensated matching networks involves mismatching the input and output matching networks to compensate for the changes with frequency of $|S_{21}|$. The matching networks are designed to give the best input and output VSWR. However, because of the broad bandwidth the VSWR will be optimum around certain frequencies, and a balanced amplifier design may be required.

The design of compensated matching networks can be done in analytical form with the help of the Smith chart. However, the use of a computer is usually required because of the complex analytical procedures. Of course, the use of a proper analytical procedure produces a starting design which can be optimized using computer-aided design (CAD) methods.

The matching networks can also be designed using network synthesis techniques. Passive network synthesis for the design of networks using lumped elements is well developed, and the techniques to implement the filter with microwave components are also well known [4.4, 4.5]. The microwave filters, typically, operate between two different impedances and must provide a prescribed insertion loss and bandwidth.

Insertion-loss synthesis techniques can be used to design impedance matching networks with prescribed responses. The synthesis process is a powerful tool when used in a CAD program. A good commercially available program is AMPSYN [4.6]. AMPSYN is a user-oriented interactive program for obtaining impedance matching networks with a desired frequency characteristic. AMPSYN synthesizes lumped elements matching networks and provides for transformations of the lumped design to approximate transmission-line equivalents.

An interesting method for broadband amplifier design suitable to CAD has been developed by Mellor [4.7]. The broadband design involves the use of an interstage matching network. The amplifier schematic is shown in Fig. 4.4.1.

Transistors Q_1 and Q_2 have a gain that decreases with increasing fre-

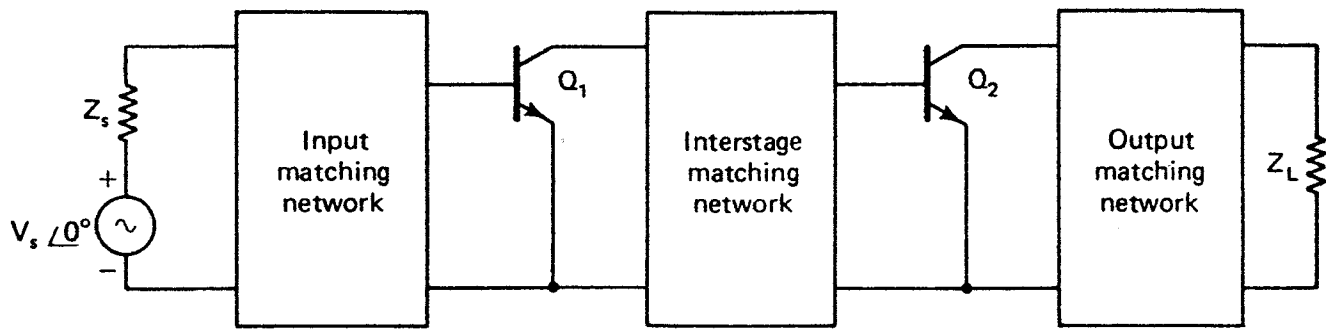


Figure 4.4.1 Broadband amplifier schematic.

quency. The specifications for a good input and output match will require that the input and output matching networks have a constant gain over the frequency range of the amplifier (i.e., a flat frequency response). The interstage matching network must provide a gain having a positive slope with increasing frequency to compensate for the transistor roll-off and, therefore, to give an overall flat frequency response. The synthesis approach involves modeling the transistors with lumped elements and using an insertion-loss method to obtain the matching networks. The design of a broadband amplifier for a specific gain and noise figure requires, in general, the use of CAD techniques.

Example 4.4.1

The S parameters of a BJT are given in Fig. 4.4.2. Design a broadband amplifier with a transducer power gain of 10 dB in the frequency range 300 to 700 MHz. (This example is based on a design from Hewlett-Packard Application Note 95-1 [4.8].)

f (MHz)	S_{11}	S_{21}	S_{22}
300	$0.3 \angle -45^\circ$	$4.47 \angle 40^\circ$	$0.86 \angle -5^\circ$
450	$0.27 \angle -70^\circ$	$3.16 \angle 35^\circ$	$0.855 \angle -14^\circ$
700	$0.2 \angle -95^\circ$	$2.0 \angle 30^\circ$	$0.85 \angle -22^\circ$

Figure 4.4.2 Scattering parameters of a BJT.

Solution. The values in Fig. 4.4.2 show that

$$\begin{aligned}
 |S_{21}|^2 &= 13 \text{ dB} && \text{at } 300 \text{ MHz} \\
 &= 10 \text{ dB} && \text{at } 450 \text{ MHz} \\
 &= 6 \text{ dB} && \text{at } 700 \text{ MHz}
 \end{aligned}$$

Therefore, in order to compensate for the variations of $|S_{21}|$, the matching networks must decrease the gain by 3 dB at 300 MHz, 0 dB at 450 MHz, and increase the gain by 4 dB at 700 MHz.

For this transistor

$$G_{s,\max} = \frac{1}{1 - |S_{11}|^2} = \begin{cases} 0.409 \text{ dB} & \text{at } 300 \text{ MHz} \\ 0.329 \text{ dB} & \text{at } 450 \text{ MHz} \\ 0.177 \text{ dB} & \text{at } 700 \text{ MHz} \end{cases}$$

and little is to be gained by matching the source. Therefore, only the output matching network needs to be designed. Observe that $|S_{22}| \approx 0.85$ over the frequency range. Therefore,

$$G_{L,\max} = \frac{1}{1 - |S_{22}|^2} = 5.6 \text{ dB}$$

and the gain of 4 dB from G_L at 700 MHz is possible.

The output matching network is designed by plotting the constant-gain circles for $G_L = -3$ dB at 300 MHz, $G_L = 0$ dB at 450 MHz, and $G_L = 4$ dB at 700 MHz (see Fig. 4.4.3). The matching networks must transform the 50- Ω load to some point on the -3 -dB circle at 300 MHz, to some point on the 0-dB circle at 450 MHz, and to some point on the 4-dB gain circle at 700 MHz. Of course, there are many matching networks that can perform the required transformation. The matching network selected is an ell network consisting of a shunt and series inductor combination (see Fig. 4.4.4).

The shunt inductor susceptance decreases with frequency and transforms the 50- Ω load along the constant-conductance circle as shown in Fig. 4.4.3. The series inductor reactance increases with frequency and transforms the parallel combination of 50 Ω and shunt inductance along a constant-resistance circle as shown in Fig. 4.4.3. Optimizing the values of L_1 and L_2 is a trial-and-error procedure. The graphical construction is illustrated in Fig. 4.4.3 and the final ac schematic of the amplifier is shown in Fig. 4.4.4.

The value of L_1 is obtained at 300 MHz (i.e., the lowest frequency), from Fig. 4.4.3, as

$$\frac{50}{j\omega L_1} = -j1.2$$

or

$$L_1 = 22.1 \text{ nH}$$

and the value of L_2 is obtained at 700 MHz (i.e., the highest frequency), from Fig. 4.4.3, as

$$\frac{j\omega L_2}{50} = j(3.2 - 0.4)$$

or

$$L_2 = 31.8 \text{ nH}$$

At the input, the direct connection of the 50- Ω source resistor to the base of the transistor results in $G_s = 0$ dB and an input VSWR smaller than 1.86 [i.e.,

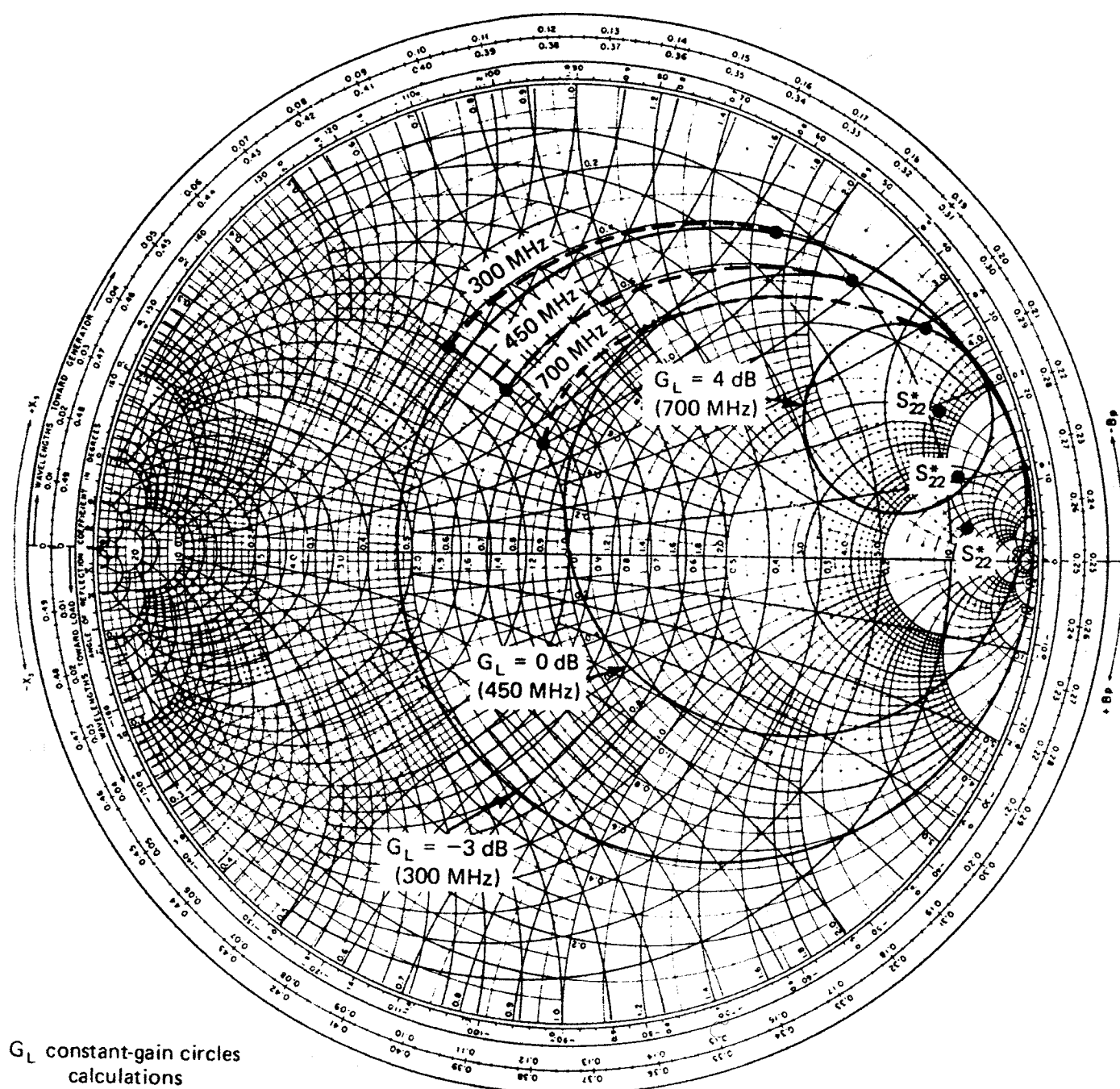


Figure 4.4.3 Broadband design in the Smith chart.

$(1 + 0.3)/(1 - 0.3) = 1.86]$. The VSWR can be improved by matching the $50\text{-}\Omega$ source to S_{11} over the frequency band. The corresponding improvement in gain is small since $G_{s,\max} = 0.409\text{ dB}$ at $f = 300\text{ MHz}$.

The design of compensated matching networks to obtain gain flatness results in impedance mismatching that can significantly degrade the input and output VSWR. The use of balanced amplifiers is a practical method for obtaining a broadband amplifier with flat gain and good input and output

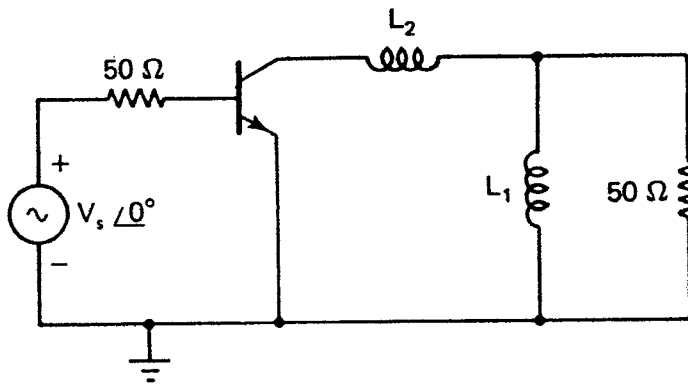


Figure 4.4.4 The ac schematic of the broadband amplifier.

VSWR. The most popular arrangement of a balanced amplifier, shown in Fig. 4.4.5, uses two 3-dB hybrid couplers. A microstrip realization, shown in Fig. 4.4.6, uses an interdigitated structure which is known as the 3-dB *Lange coupler* [4.9].

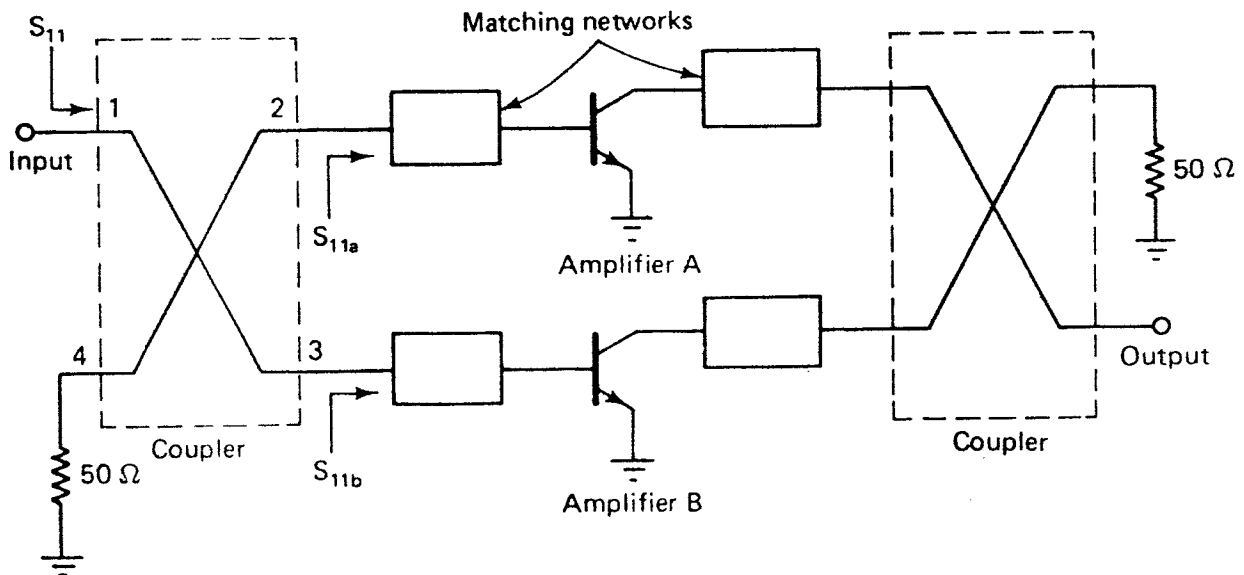


Figure 4.4.5 Balanced amplifier configuration.

The input 3-dB coupler divides the input power equally between ports 2 and 3, and the output 3-dB coupler recombines the output signals from the amplifiers. The reflected signals at the input and output due to mismatching are coupled to the 50- Ω loads. It can be shown that the S parameters of the $\lambda/4$, 3-dB Lange coupler are given by

$$|S_{11}| = 0.5 |S_{11a} - S_{11b}|$$

$$|S_{21}| = 0.5 |S_{21a} + S_{21b}|$$

$$|S_{12}| = 0.5 |S_{12a} + S_{12b}|$$

$$|S_{22}| = 0.5 |S_{22a} - S_{22b}|$$

If the two amplifiers are identical, then $S_{11} = 0$ and $S_{22} = 0$ and the gain S_{21} (and also S_{12}) is equal to the gain of one side of the coupler. The bandwidth of

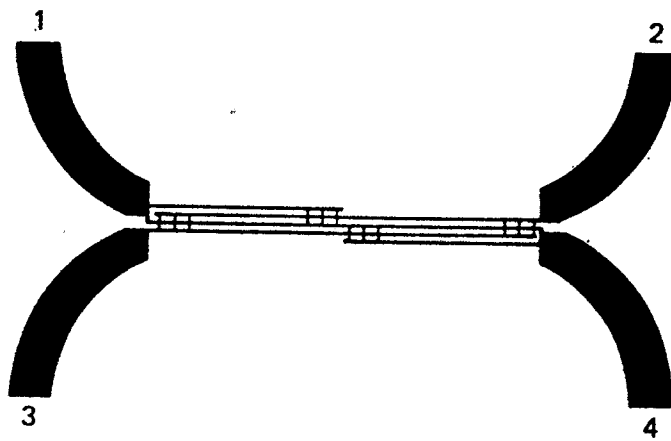


Figure 4.4.6 A 3-dB Lange coupler. (From J. Lange [4.9]; copyright 1969, IEEE; reproduced with permission of IEEE.)

the balanced amplifier is limited by the bandwidth of the coupler (about 2 octaves).

The advantages of the balanced amplifier configuration are many:

1. The individual amplifiers can be designed for flat gain, noise figure, and so on (even if the individual amplifier VSWR is high), with the balanced amplifier input and output VSWR dependent on the coupler (i.e., ideally the VSWR is 1 if the amplifiers are identical).
2. A high degree of stability.
3. The output power is twice that obtained from the single amplifier.
4. If one of the amplifiers fails, the balanced amplifier unit will still operate with reduced gain.
5. Balanced amplifier units are easy to cascade with other units, since each unit is isolated by the coupler.

The disadvantages of the balanced amplifier configuration are that the unit uses two amplifiers, consumes more dc power, and is larger.

Negative feedback can be used in broadband amplifiers to provide a flat gain response and to reduce the input and output VSWR. It also controls the amplifier performance due to variations in the S parameters from transistor to transistor. As the bandwidth requirements of the amplifier approach a decade of frequency, gain compensation based on matching networks only is very difficult, and negative feedback techniques are used. In fact, a microwave transistor amplifier using negative feedback can be designed to have very wide bandwidths (greater than 2 decades) with small gain variations (tenths of a decibel). On the minus side, negative feedback will degrade the noise figure and reduce the maximum power gain available from a transistor.

The most common methods of applying negative feedback are by the series and shunt resistor feedback configurations shown in Fig. 4.4.7. The coupling capacitors and the dc bias network have been omitted.

The following simple analysis illustrates the use of negative feedback. The BJT and GaAs FET can be represented by the equivalent circuit shown in Fig. 4.4.8 when the parasitic elements can be neglected (i.e., at low frequencies).

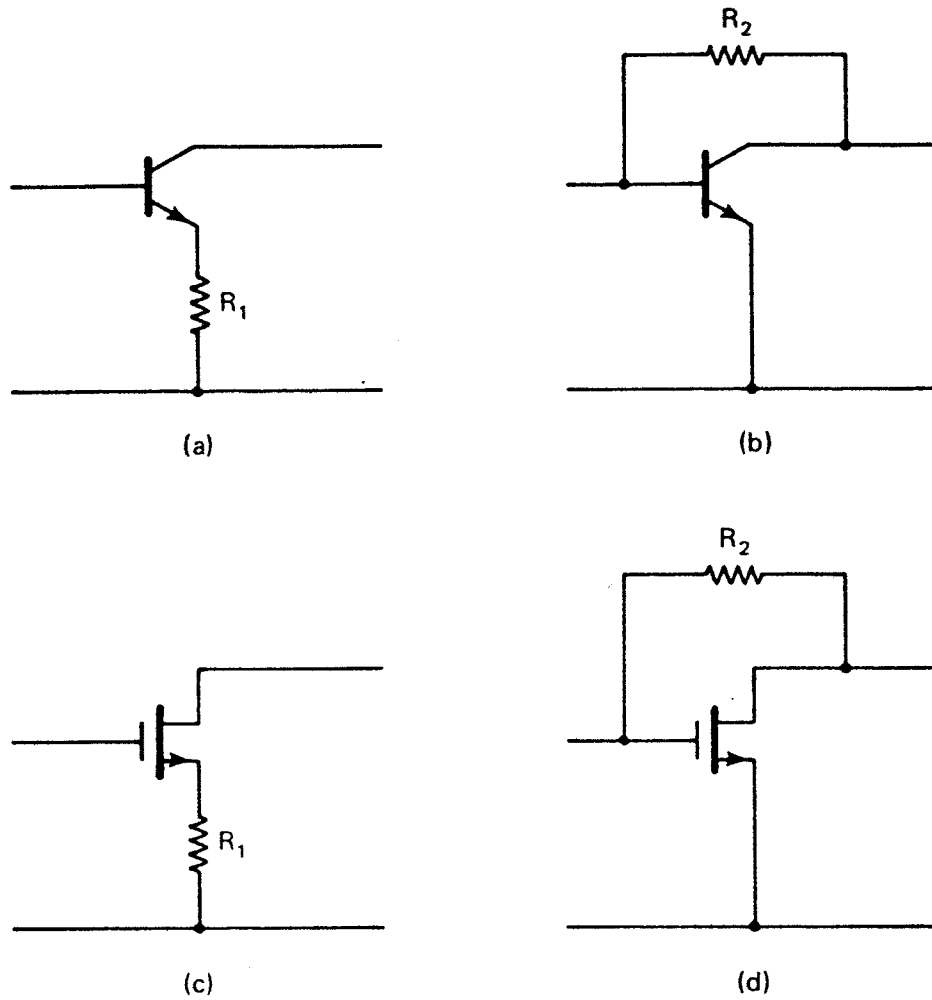


Figure 4.4.7 (a) BJT with series feedback resistor; (b) BJT with shunt feedback resistor; (c) GaAs FET with series feedback resistor; (d) GaAs FET with shunt feedback resistor.

The resulting negative-feedback equivalent networks, including both series and shunt feedback, are shown in Fig. 4.4.9.

The admittance matrix for the network shown in Fig. 4.4.9b can be written in the form

$$\begin{bmatrix} i_1 \\ i_2 \end{bmatrix} = \begin{bmatrix} \frac{1}{R_2} & -\frac{1}{R_2} \\ \frac{g_m}{1 + g_m R_1} - \frac{1}{R_2} & \frac{1}{R_2} \end{bmatrix} \begin{bmatrix} v_1 \\ v_2 \end{bmatrix}$$

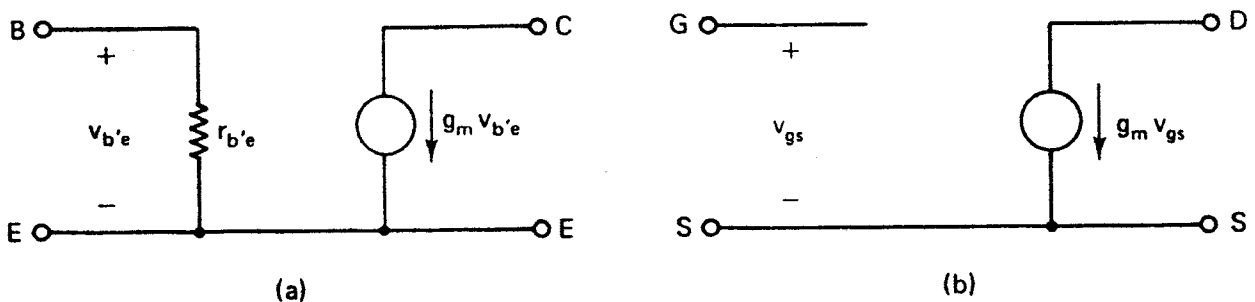


Figure 4.4.8 (a) BJT equivalent network; (b) GaAs FET equivalent network.

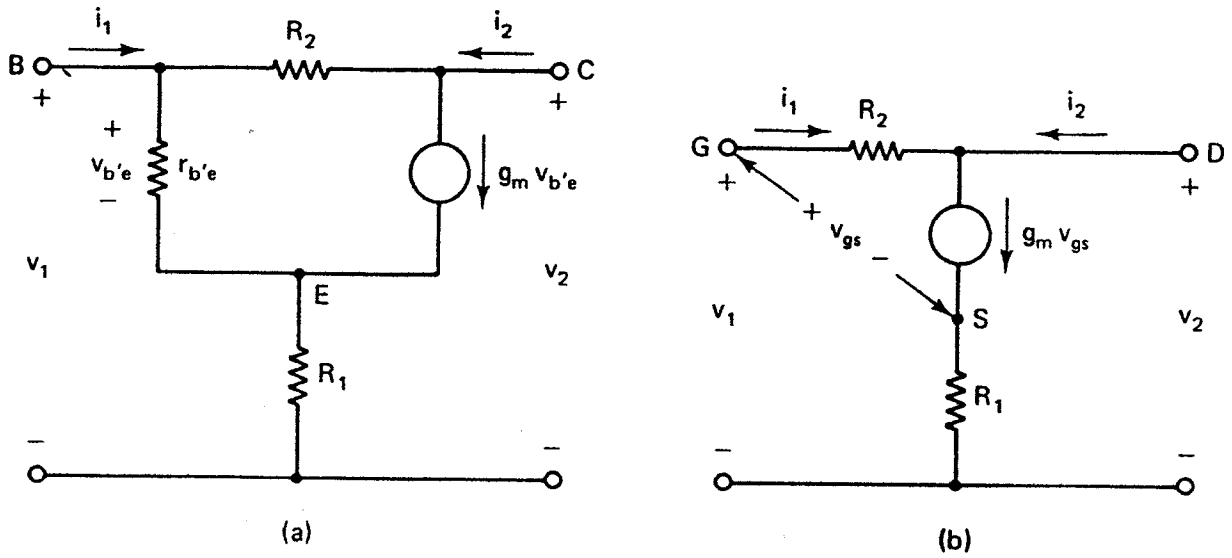


Figure 4.4.9 (a) BJT negative-feedback model; (b) GaAs FET negative-feedback model.

and a similar matrix can be written for Fig. 4.4.9a. Using Fig. 1.8.1 to convert from y parameters to S parameters gives

$$S_{11} = S_{22} = \frac{1}{D} \left[1 - \frac{g_m Z_o^2}{R_2(1 + g_m R_1)} \right] \quad (4.4.1)$$

$$S_{21} = \frac{1}{D} \left(\frac{-2g_m Z_o}{1 + g_m R_1} + \frac{2Z_o}{R_2} \right) \quad (4.4.2)$$

and

$$S_{12} = \frac{2Z_o}{DR_2} \quad (4.4.3)$$

where

$$D = 1 + \frac{2Z_o}{R_2} + \frac{g_m Z_o^2}{R_2(1 + g_m R_1)}$$

From (4.4.1) the conditions $S_{11} = S_{22} = 0$ (i.e., input and output VSWR = 1) are satisfied when

$$1 + g_m R_1 = \frac{g_m Z_o^2}{R_2}$$

or

$$R_1 = \frac{Z_o^2}{R_2} - \frac{1}{g_m} \quad (4.4.4)$$

Substituting (4.4.4) into (4.4.2) and (4.4.3) gives

$$S_{21} = \frac{Z_o - R_2}{Z_o} \quad (4.4.5)$$

and

$$S_{12} = \frac{Z_o}{R_2 + Z_o}$$

Equation (4.4.4) shows that $S_{11} = S_{22} = 0$ can be satisfied, with positive values of R_1 , if the transconductance is large.

A range of values that satisfies $S_{11} = S_{22} = 0$ can be found. The minimum transconductance [called $g_{m(\min)}$] occurs when $R_1 = 0$ [i.e., $g_{m(\min)} = R_2/Z_o^2$] and it follows from (4.4.5) that

$$g_{m(\min)} = \frac{1 - S_{21}}{Z_o}$$

For example, if an amplifier has $|S_{21}|^2 = 10$ dB in a 50- Ω system, the minimum transconductance required is

$$g_{m(\min)} = \frac{1 - (-3.16)}{50} = 83 \text{ mS}$$

and the required shunt feedback resistor is

$$R_2 = 83 \times 10^{-3}(50)^2 = 208 \text{ } \Omega$$

Observe that (4.4.5) shows that

$$R_2 = Z_o(1 + |S_{21}|) \quad (4.4.6)$$

which is a well-known relation in feedback amplifiers.

When both R_1 and R_2 are used and g_m has a high value, (4.4.4) shows that the minimum input and output VSWR is obtained when $R_1 R_2 \approx Z_o^2$. The high value of g_m in a BJT makes them suitable for negative-feedback applications. However, most GaAs FETs have low values of g_m and one must be careful when using them in negative-feedback configurations. Equation (4.4.5) shows that S_{21} depends only on R_2 and not on the transistor parameters. Therefore, gain flattening can be achieved with negative feedback.

An important consideration in negative-feedback design is the phase of S_{21} . At low frequencies the phase of S_{21} is close to 180°, and as the frequency increases (above f_β) the phase of S_{21} varies rapidly. At some frequency the phase of S_{21} is such that a portion of the output voltage is in phase with the input voltage (i.e., positive feedback). This problem can be solved by decreasing the feedback when the phase shift of S_{21} approaches 90°. For example, in the case of shunt negative feedback (see Fig. 4.4.7), an inductor can be connected in series with R_2 such that after a certain frequency the negative feedback decreases in proportion to the S_{21} roll-off.

The previous analysis, although based on a simplified model, can be used in a preliminary design. Then CAD methods can be used to calculate the S parameters of the transistor with the feedback network connected, and to obtain the required Γ_s and Γ_L for optimum performance.

Example 4.4.2

Perform a preliminary analysis in the design of a BJT broadband amplifier having a transducer power gain of 10 dB from 10 to 1500 MHz. The S parameters of the transistor (in a 50- Ω system) at 10 V, 4 mA, the associated K factors, and $|S_{21}|^2$ in decibels (i.e., the transducer power gain in a 50- Ω system) are given in Fig. 4.4.10. (This example is based on a design from Ref. [4.10].)

F (MHz)	S_{11}		S_{21}		S_{12}		S_{22}		$ S_{21} ^2$ (dB)	K
	Mag.	Ang.	Mag.	Ang.	Mag.	Ang.	Mag.	Ang.		
10	0.95	-2°	7.35	174.6°	0.003	84.3°	1.01	-1°	17.3	0.11
100	0.92	-11°	7.15	168.0°	0.007	79.0°	0.99	-4°	17.1	0.18
250	0.87	-28°	6.83	154.5°	0.015	69.2°	0.96	-10°	16.7	0.29
500	0.78	-54°	6.28	135.0°	0.026	54.0°	0.90	-18°	16.0	0.42
750	0.69	-78°	5.67	123.0°	0.033	41.4°	0.84	-25°	15.1	0.53
1000	0.63	-98°	5.04	113.0°	0.037	33.0°	0.79	-30°	14.1	0.67
1250	0.60	-114°	4.42	99.9°	0.038	29.3°	0.77	-33°	13.0	0.81
1500	0.60	-127°	3.88	87.0°	0.039	28.0°	0.76	-35°	11.8	0.91

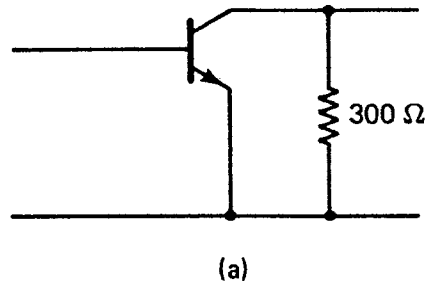
Figure 4.4.10 S parameters of the transistor, K factors, and $|S_{21}|^2$ in decibels.

Solution. The transistor is certainly capable of providing a transducer power gain of 10 dB. However, since $K < 1$, the transistor is potentially unstable and a stability analysis must be performed. Also, observe that above 1250 MHz the phase of S_{21} is less than 90° , and a portion of the output voltage is in phase with the input.

The input and output stability circles are given in Fig. 4.4.11. The analysis of the output stability circles show that a shunt resistor of 300 Ω at the output of the transistor provides stability. The resulting S parameters for the network shown in Fig. 4.4.12a are given in Fig. 4.4.12b. The stability of the network in Fig. 4.4.12a is much improved.

F (MHz)	C_s				C_L			
	Mag.	Ang.	r_s	Stable Region	Mag.	Ang.	r_L	Stable Region
10	1.27	-43°	0.90	Inside	1.05	13°	0.24	Outside
100	30.53	88°	30.34	Outside	1.13	21°	0.37	Outside
250	4.61	89°	4.24	Outside	1.26	32°	0.54	Outside
500	3.61	103°	3.08	Outside	1.40	39°	0.64	Outside
750	2.63	117°	1.96	Outside	1.39	42°	0.58	Outside
1000	2.26	129°	1.46	Outside	1.41	44°	0.53	Outside
1250	2.14	140°	1.24	Outside	1.40	44°	0.46	Outside
1500	1.99	150°	1.04	Outside	1.39	45°	0.42	Outside

Figure 4.4.11 Stability circles locations.



F (MHz)	S_{11}		S_{21}		S_{12}		S_{22}		$ S_{21} ^2$ (dB)	K	$ \Delta $
	Mag.	Ang.	Mag.	Ang.	Mag.	Ang.	Mag.	Ang.			
10	0.95	-2°	6.30	174.7°	0.003	84.4°	0.72	-1°	15.98	1.4	0.69
100	0.92	-11°	6.13	168.3°	0.006	79.3°	0.71	-4°	15.75	1.1	0.66
250	0.87	-28°	5.88	155.2°	0.013	69.9°	0.69	-10°	15.38	0.94	0.61
500	0.79	-53°	5.44	136.1°	0.023	55.1°	0.65	-19°	14.71	1.0	0.54
750	0.70	-77°	4.94	124.5°	0.029	42.9°	0.61	-26°	13.88	1.2	0.45
1000	0.64	-97°	4.42	114.7°	0.032	34.7°	0.57	-32°	12.90	1.4	0.37
1250	0.61	-113°	3.89	101.7°	0.033	31.1°	0.56	-35°	11.79	1.6	0.34
1500	0.60	-126°	3.42	88.8°	0.034	29.8°	0.55	-38°	10.67	1.9	0.33

(b)

 Figure 4.4.12 (a) Stabilized transistor network; (b) the resulting S parameters.

The gain $|S_{21}|^2$ is reduced because the 300- Ω resistor dissipates some of the output power. Still, the network in Fig. 4.2.12a can easily provide the transducer power gain of 10 dB. The S_{11} and S_{22} parameters are large, showing that the input and output VSWR are poor. The phase of S_{21} above 1250 MHz remains less than 90° .

The shunt negative-feedback resistor-inductor combination, shown in Fig. 4.4.13, can now be designed to provide a flat gain of 10 dB (i.e., $|S_{21}|^2 = 10$ dB or $|S_{21}| = 3.16$) with 50- Ω input and output impedances. The value of R_2 is calculated using (4.4.6), namely

$$R_2 = 50(1 + 3.16) = 208 \, \Omega$$

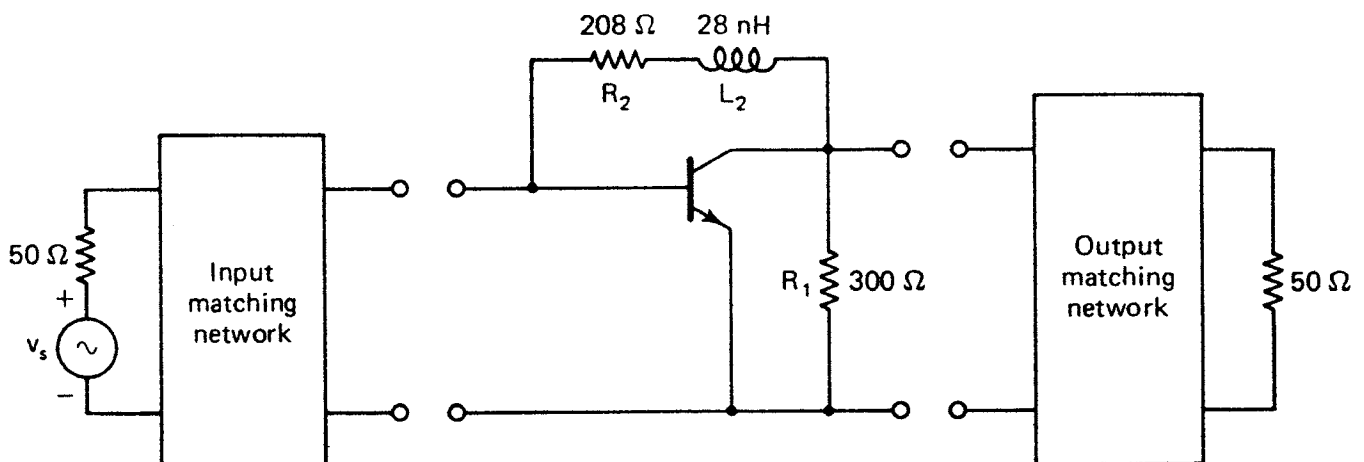


Figure 4.4.13 The feedback network and the matching networks.

Equation (4.4.7) expresses the fact that the area under the curve $\ln |1/\Gamma|$ cannot be greater than π/RC . Therefore, if matching is required over a certain bandwidth, it can be obtained at the expense of less power transfer.

The best utilization of the area under the curve $\ln |1/\Gamma|$ is obtained when $|\Gamma|$ is constant over the frequency range ω_a to ω_b and equal to 1 outside that range. This situation is illustrated in Fig. 4.4.16, and it follows from (4.4.7) that

$$|\Gamma| = \Gamma_x = e^{-\pi/(\omega_b - \omega_a)RC}$$

or

$$\Gamma_x = e^{-\pi(Q_2/Q_1)} \quad (4.4.8)$$

where

$$Q_1 = \frac{R}{X_c}$$

and

$$Q_2 = \frac{\omega_o}{\omega_b - \omega_a}$$

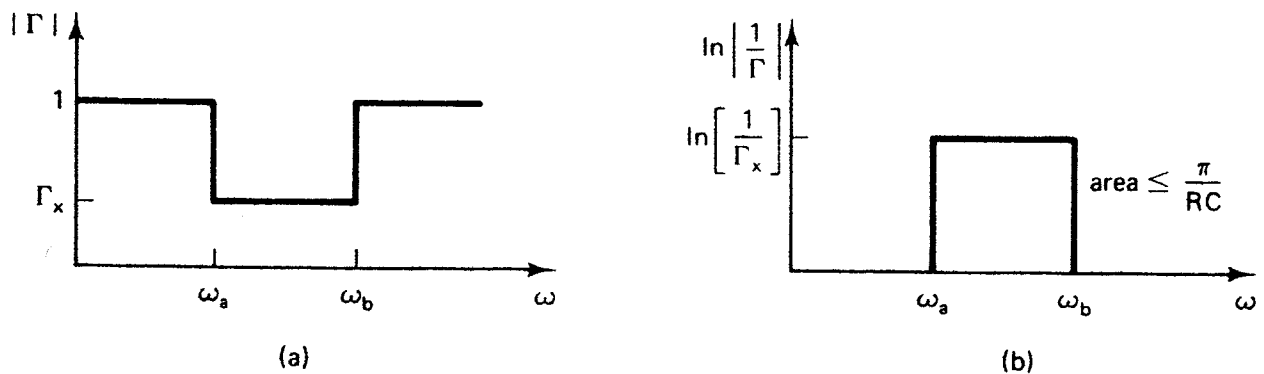


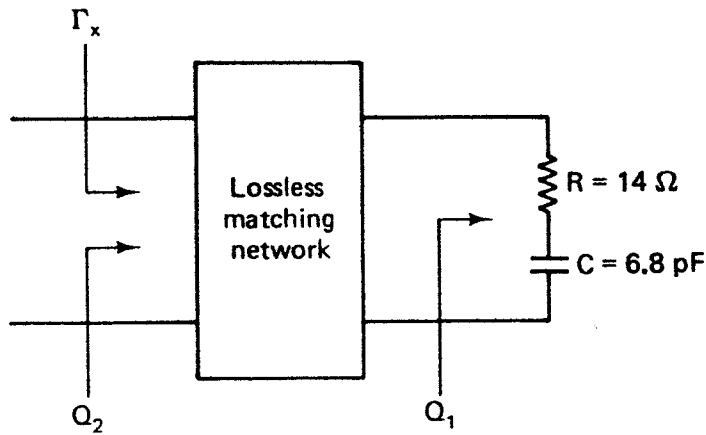
Figure 4.4.16 Optimum values of $|\Gamma|$.

Equation (4.4.8) gives the best ideally achievable Γ_x that can be obtained in the band ω_a to ω_b with no power transfer outside the band. Although a matching network satisfying the requirements above cannot be obtained in practice, the relation (4.4.8) can be used as a guideline for the best Γ_x .

The expression (4.4.8) can also be used for the networks shown in Figs. 4.4.15b to 4.4.15d when the appropriate definition of Q_1 and Q_2 are used. These are given in the figures.

Example 4.4.3

Over the frequency range $f_a = 500$ MHz to $f_b = 900$ MHz, find the best Γ_x that can be achieved in the network shown in Fig. 4.4.17.


 Figure 4.4.17 Calculation of Γ_x .

Solution. At $f_o = 700$ MHz we obtain

$$Q_1 = \frac{1}{\omega_o RC} = \frac{1}{2\pi(700 \times 10^6)14(6.8 \times 10^{-12})} = 2.39$$

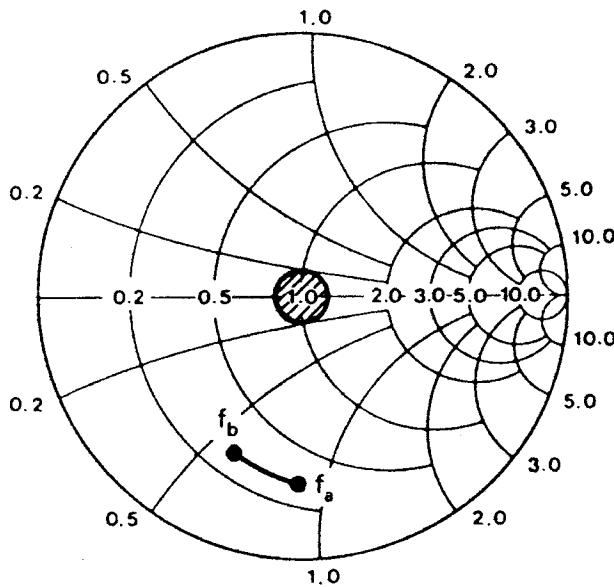
and

$$Q_2 = \frac{7}{4} = 1.75$$

Then, from (4.4.8), the value of Γ_x is

$$\Gamma_x = e^{-\pi(1.75/2.39)} = 0.1$$

The normalized load impedance of the network in Fig. 4.4.17 (i.e., $z = 0.28 - j468 \times 10^6/f$) is plotted in Fig. 4.4.18 over the frequency range f_a to f_b . Also, the region $\Gamma_x < 0.1$ for the ideally achievable match is shown shaded.


 Figure 4.4.18 Best achievable match Γ_x .

4.5 AMPLIFIER TUNING

The input reflection coefficient in the bilateral case is a function of the output reflection coefficient, and vice versa. Therefore, Γ_{IN} varies with output tuning and Γ_{OUT} varies with input tuning.

After an amplifier is built, tuning or alignment is necessary in order for the amplifier to provide optimum performance. The tuning is usually done by performing minor changes and adjusting the components of the matching networks.

An amplifier is easy to tune when the ratios of the fractional changes in Γ_{IN} due to Γ_L , and Γ_{OUT} due to Γ_s , are small.

The input reflection tuning factor δ_{IN} is defined as

$$\delta_{IN} = \left| \frac{d\Gamma_{IN}/\Gamma_{IN}}{d\Gamma_L/\Gamma_L} \right|$$

which in terms of the two-port network S parameters can be written as

$$\delta_{IN} = \frac{|S_{21}| |S_{12}| |\Gamma_L|}{|1 - S_{22}\Gamma_L| |S_{11} - \Delta\Gamma_L|} \quad (4.5.1)$$

In practice, a value of $\delta_{IN} < 0.3$ produces good tunability. Equation (4.5.1) shows that δ_{IN} can be zero under some circumstances. That is, $\delta_{IN} = 0$ when $S_{12} = 0$, which occurs when the unilateral assumption can be made. In this case, the output tuning does not affect the input. Also, $\delta_{IN} = 0$ when $\Gamma_L = 0$, which is a very specific value of Γ_L that probably degrades the gain and noise performance of the amplifier. Of course, $\delta_{IN} = 0$ when $S_{21} = 0$, that is, when there is no power gain. The derivation for the output tunability factor δ_{OUT} is left as an exercise.

Equation (4.5.1) can be solved for Γ_L in terms of δ_{IN} , namely

$$|\Gamma_L| = \left| \alpha \pm \left| \alpha^2 - \frac{S_{11}}{S_{22}\Delta} \right|^{1/2} \right| \quad (4.5.2)$$

where

$$\alpha = \frac{\Delta + S_{11}S_{22} + S_{12}S_{21}\delta_{IN}^{-1}}{2S_{22}\Delta} \quad (4.5.3)$$

The value of $|\Gamma_L|$ obtained from (4.5.2) and (4.5.3) for a given δ_{IN} is, in general, different from the value that produces maximum power gain or optimum noise performance. Therefore, this value of Γ_L produces good tunability but mismatches the amplifier.

4.6 BANDWIDTH ANALYSIS

The conditions for a conjugate match at the input and output ports are satisfied at one frequency. One reason the output power varies with frequency is the frequency dependence of the matching networks. However, the most important factor that limits the frequency response is the variations of the transistor S parameters with frequency.

The input port, under conjugate matched conditions, is shown in Fig. 4.6.1a. A conjugate match means that $\Gamma_s = \Gamma_{IN}^*$ or $Y_s = Y_{IN}^*$. With

$$Y_{IN} = G_{s,M} + jB_{s,M}$$

and

$$Y_s = G_{s,M} - jB_{s,M}$$

the network in Fig. 4.6.1a can be represented by the *RLC* network shown in Fig. 4.6.1b. The values $G_{s,M}$ and $B_{s,M}$ represent the conductance and susceptance obtained under conjugate match conditions.

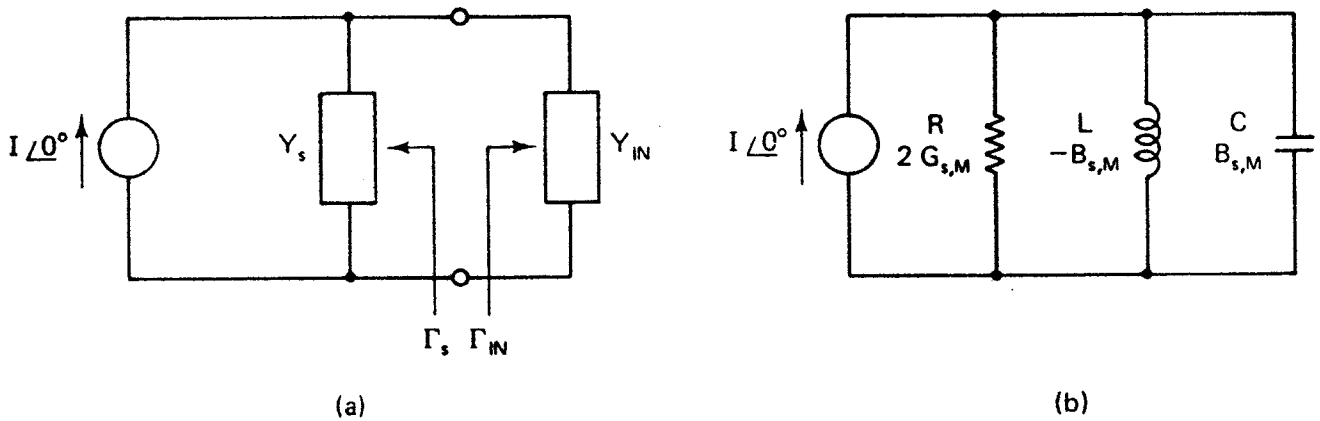


Figure 4.6.1 Equivalent networks of the input port under conjugate match conditions.

The input inherent bandwidth, $(BW)_{IN}^i$, is the bandwidth obtained under conjugate matched conditions where the matched terminations are determined by the *S* parameters of the two-port device. The input inherent bandwidth is given by

$$(BW)_{IN}^i = \frac{f_o}{Q_{IN}} \quad \text{Hz} \quad (4.6.1)$$

where f_o is the frequency at which the conjugate matched values were obtained and Q_{IN} is the “que” of the equivalent input network. The value of Q_{IN} , for the network in Fig. 4.6.1b, can be expressed in different forms, namely

$$Q_{IN} = \omega_o RC = \frac{R}{\omega_o L} \quad (4.6.2)$$

where $\omega_o = 2\pi f_o = 1/\sqrt{LC}$. Substituting (4.6.2) into (4.6.1), we obtain

$$(BW)_{IN}^i = \frac{2f_o G_{s,M}}{|B_{s,M}|} \quad (4.6.3)$$

where $R = 1/2G_{s,M}$ and $|B_{s,M}| = \omega_o C = 1/\omega_o L$. Similarly, the output inherent bandwidth is given by

$$(\text{BW})_{\text{OUT}}^i = \frac{2f_o G_{s,M}}{|B_{L,M}|} \quad (4.6.4)$$

where $Y_L = Y_{\text{OUT}}^*$.

Example 4.6.1

In the microwave transistor amplifier of Example 3.7.1 we found that for a simultaneous conjugate match at $f = 6$ GHz, $\Gamma_{Ms} = 0.762 \angle 177.3^\circ$, and $\Gamma_{ML} = 0.718 \angle 103.9^\circ$. Calculate the amplifier bandwidth limitation due to the matching networks.

Solution. The admittances $Y_{\text{IN}} = Y_s^*$ and $Y_{\text{OUT}} = Y_L^*$ associated with Γ_{Ms} and Γ_{ML} are

$$Y_{\text{IN}} = (144 + j24.6) \times 10^{-3} \text{ S}$$

and

$$Y_{\text{OUT}} = (8.28 + j23.8) \times 10^{-3} \text{ S}$$

The equivalent network at the input port is illustrated in Fig. 4.6.1. The equivalent network for the output port is similar. From Y_{IN} and Y_{OUT} , it follows that $G_{s,M} = 144 \times 10^{-3}$, $B_{s,M} = 24.6 \times 10^{-3}$, $G_{L,M} = 8.28 \times 10^{-3}$, and $B_{L,M} = 23.8 \times 10^{-3}$. Therefore, from (4.6.3) and (4.6.4),

$$(\text{BW})_{\text{IN}}^i = \frac{2(6 \times 10^9)144 \times 10^{-3}}{24.6 \times 10^{-3}} = 70.2 \text{ GHz}$$

and

$$(\text{BW})_{\text{OUT}}^i = \frac{2(6 \times 10^9)8.28 \times 10^{-3}}{23.8 \times 10^{-3}} = 4.17 \text{ GHz}$$

Since $(\text{BW})_{\text{IN}}^i \gg (\text{BW})_{\text{OUT}}^i$, the bandwidth limitations due to the matching networks are determined by $(\text{BW})_{\text{OUT}}^i$.

The broad bandwidth $(\text{BW})_{\text{OUT}}^i$ cannot be obtained in practice because of the transistor S -parameter variations with frequency. In fact, the overall bandwidth of the amplifier, as shown in Fig. 4.3.11d, is 980 MHz.

The inherent bandwidth of either the input or output port can be decreased by increasing the Q of the network. From (4.6.2), we can increase Q by increasing the capacitance or decreasing the inductance of the network. When Y_{IN} has a capacitive susceptance, the bandwidth is decreased by adding capacitance, and when Y_{IN} has an inductive susceptance, the bandwidth is decreased by adding inductance.

Consider the case where Y_{IN} has a capacitive susceptance. The admittance Y_{IN} is given by

$$Y_{\text{IN}} = G_{\text{IN},M} + jB_{\text{IN},M}$$

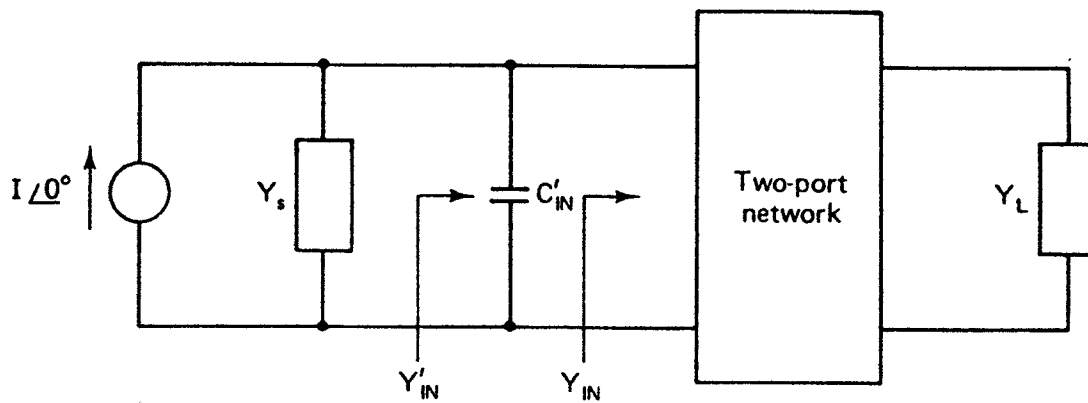


Figure 4.6.2 Increasing Q by adding the capacitance C'_{IN} .

If we add to the input port the capacitor C'_{IN} , shown in Fig. 4.6.2, the admittance Y'_{IN} is given by

$$Y'_{IN} = Y_{IN} + j\omega_o C'_{IN}$$

and a conjugate match requires that $Y_s = (Y'_{IN})^*$. Therefore,

$$G_{s,M} = G_{IN,M}$$

and

$$B_{s,M} = -(B_{IN,M} + \omega_o C'_{IN})$$

The input port bandwidth is

$$(BW)_{IN} = \frac{2f_o G_{s,M}}{B_{IN,M} + \omega_o C'_{IN}}$$

which can be solved for C'_{IN} , to obtain

$$C'_{IN} = \frac{B_{IN,M}}{\omega_o} \left[\frac{(BW)_{IN}^i}{(BW)_{IN}} - 1 \right] \quad (4.6.5)$$

where (4.6.3.) was used.

Equation (4.6.5) gives the value of the additional capacitance required to obtain the bandwidth $(BW)_{IN}$. Similarly, for the output network the capacitance required to produce a bandwidth $(BW)_{OUT}$ is

$$C'_{OUT} = \frac{B_{OUT,M}}{\omega_o} \left[\frac{(BW)_{OUT}^i}{(BW)_{OUT}} - 1 \right]$$

When Y_{IN} has an inductive susceptance, the bandwidth is decreased by adding the inductor L'_{IN} shown in Fig. 4.6.3. It follows that the value of inductance required to obtain the bandwidth $(BW)_{IN}$ is

$$L'_{IN} = \frac{1}{\omega_o |B_{IN,M}| \left[\frac{(BW)_{IN}^i}{(BW)_{IN}} - 1 \right]}$$

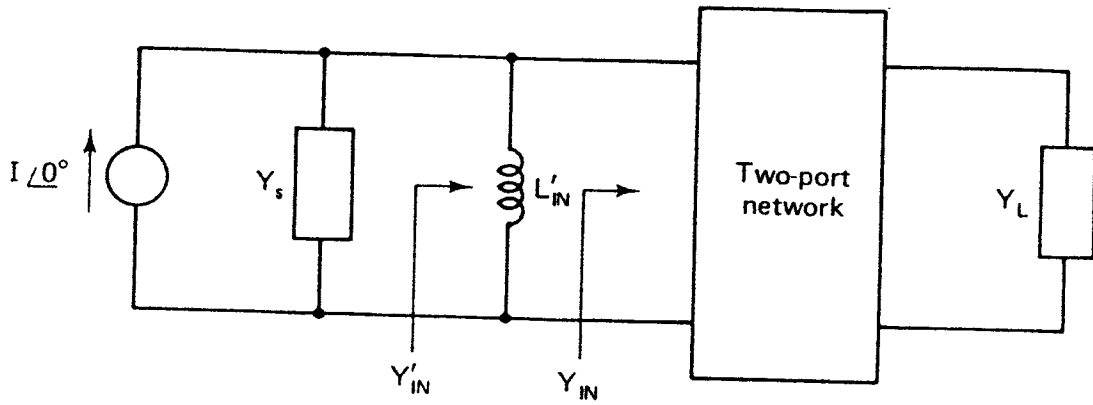


Figure 4.6.3 Increasing Q by adding the inductance L'_{IN} .

In the output port, the value of inductance required to obtain $(BW)_{OUT}$ is

$$L'_{OUT} = \frac{1}{\omega_o |B_{OUT,M}| \left[\frac{(BW)_{OUT}^i}{(BW)_{OUT}} - 1 \right]}$$

The previous methods of adding capacitance or inductance to narrowband the amplifier response does not affect the original simultaneous conjugate matched calculations.

The overall bandwidth of n identical single tuned networks is related to the bandwidth of one stage, $(BW)_1$, by the relation

$$(BW)_n = (BW)_1 \sqrt{2^{1/n} - 1} \quad (4.6.6)$$

The factor

$$\sqrt{2^{1/n} - 1}$$

is called the *bandwidth reduction factor*. In the case of two single tuned networks (i.e., $n = 2$), (4.6.6) gives

$$(BW)_2 = (BW)_1 (0.644)$$

4.7 HIGH-POWER AMPLIFIER DESIGN

Thus far we have presented design techniques, based on the small-signal S parameters of transistors, for maximum or arbitrary power gain, low noise, and broadband amplifiers. The small-signal S parameters are not useful for power amplifier design because power amplifiers usually operate in nonlinear regions. The small-signal S parameters can be used in large-signal amplifiers operating in class A (i.e., linear output power). However, for class AB, B, or C the small-signal S parameters are not suitable for design purposes.

A set of large-signal S parameters is needed to characterize the transistor for power applications. Unfortunately, the measurement of large-signal S parameters is difficult and is not properly defined. Therefore, an alternative set of

large-signal parameters is needed to characterize the transistor. This can be done by providing information of source and load reflection coefficients as a function of output power and gain, especially the measurement of the source and load reflection coefficients, together with the output power, when the transistor is operated at its 1-dB gain compression point. The listing of the 1-dB compression point data is used to specify the power-handling capabilities of the transistor.

The 1-dB gain compression point (called $G_{1\text{dB}}$) is defined as the power gain where the nonlinearities of the transistor reduces the power gain by 1 dB over the small-signal linear power gain. That is,

$$G_{1\text{dB}}(\text{dB}) = G_o(\text{dB}) - 1 \quad (4.7.1)$$

where $G_o(\text{dB})$ is the small-signal linear power gain in decibels. Since the power gain is defined as

$$G_p = \frac{P_{\text{OUT}}}{P_{\text{IN}}}$$

or

$$P_{\text{OUT}}(\text{dBm}) = G_p(\text{dB}) + P_{\text{IN}}(\text{dBm})$$

we can write the output power at the 1-dB gain compression point, called $P_{1\text{dB}}$, as

$$P_{1\text{dB}}(\text{dBm}) = G_{1\text{dB}}(\text{dB}) + P_{\text{IN}}(\text{dBm}) \quad (4.7.2)$$

Substituting (4.7.1) into (4.7.2) gives

$$P_{1\text{dB}}(\text{dBm}) - P_{\text{IN}}(\text{dBm}) = G_o(\text{dB}) - 1 \quad (4.7.3)$$

Equation (4.7.3) shows that the 1-dB gain compression point is that point at which the output power minus the input power in dBm is equal to the small-signal power gain minus 1 dB.

A typical plot of P_{OUT} versus P_{IN} which illustrates the 1-dB gain compression point is shown in Fig. 4.7.1. Observe the linear output power characteristics for power levels between the minimum detectable signal output power ($P_{o,\text{mds}}$) and $P_{1\text{dB}}$. The dynamic range (DR), shown in Fig. 4.7.1, is that range where the amplifier has a linear power gain. The dynamic range is limited at low power levels by the noise level. An input signal ($P_{i,\text{mds}}$) is detectable only if its output power level ($P_{o,\text{mds}}$) is above the noise power level.

The thermal noise power level of a two-port, with noise figure F , is given by

$$P_{N_o} = kTBG_A F$$

Observing that $kT = -174 \text{ dBm}$ (or $kTB = -114 \text{ dBm/MHz}$ at $T = 290^\circ\text{K}$) and assuming that the minimum detectable input signal is X decibels above

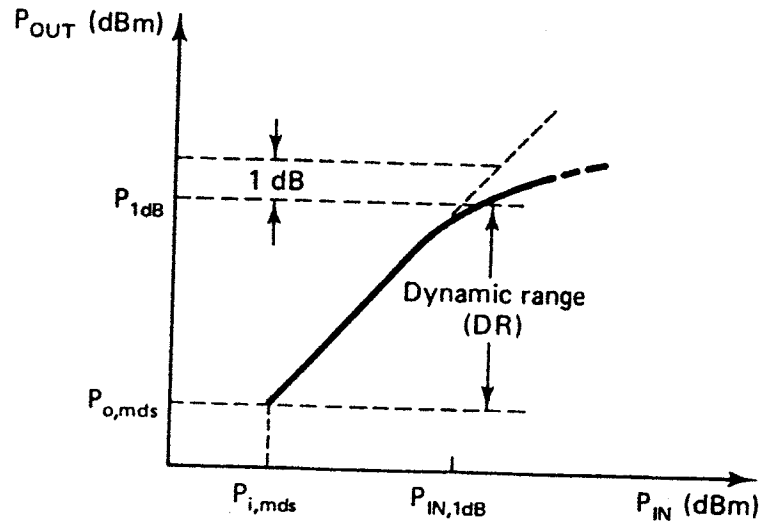


Figure 4.7.1 The 1-dB gain compression point and the dynamic range of microwave amplifiers.

thermal noise, we can write

$$P_{i,mds} = -174 \text{ dBm} + 10 \log B + F(\text{dB}) + X(\text{dB}) \quad (4.7.4)$$

and

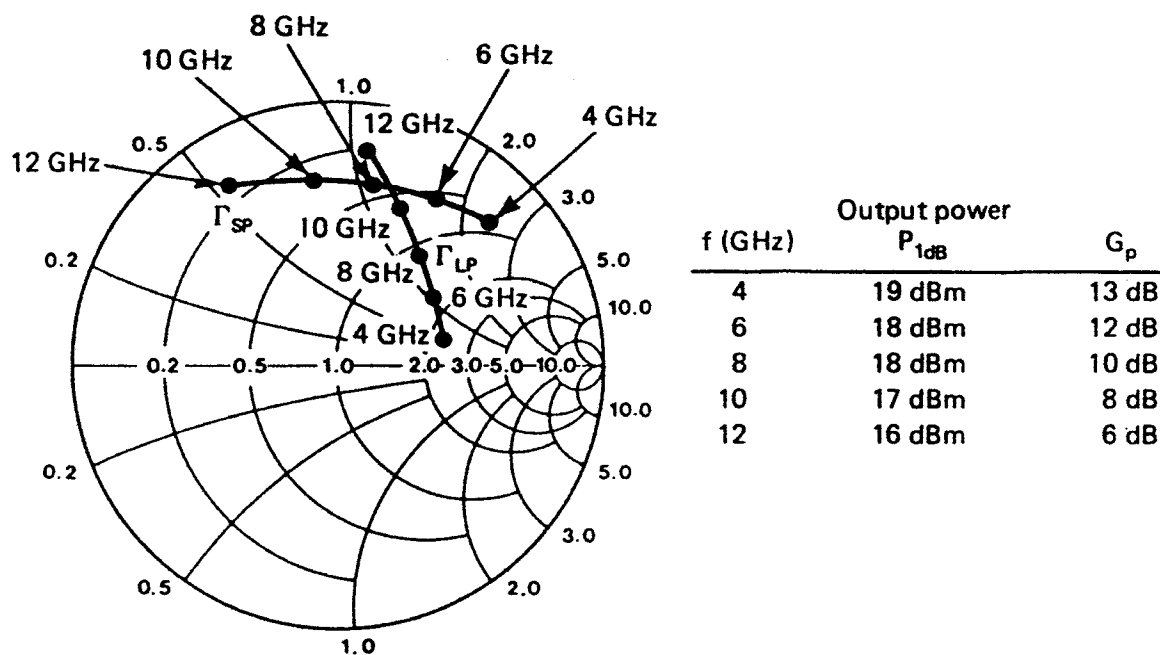
$$P_{o,mds} = -174 \text{ dBm} + 10 \log B + F(\text{dB}) + X(\text{dB}) + G_A(\text{dB}) \quad (4.7.5)$$

A typical value of $X(\text{dB})$ is 3 dB.

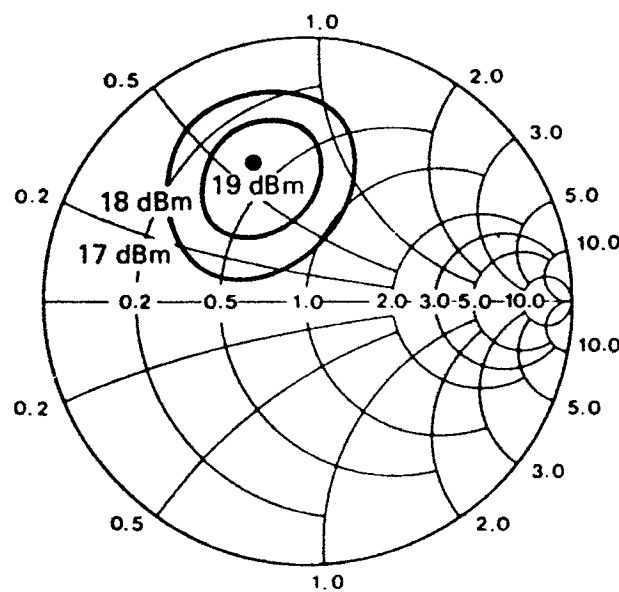
As previously discussed, a power transistor can be described in terms of the large-signal source and load reflection coefficients required to produce a given output power and gain. Of course, these parameters are functions of frequency and bias conditions. For example, in a GaAs FET the 1-dB gain compression point is usually measured at a drain-to-source voltage and gate-to-source voltage that optimizes the output power. From Fig. 3.9.7, this is usually at $I_{DS} = 50\% I_{DSS}$.

A typical set of power reflection coefficients is shown in Fig. 4.7.2a. The values of Γ_{SP} and Γ_{LP} denoted by points are the source and load power reflection coefficients for maximum output power. The values of Γ_{SP} and Γ_{LP} are given for $f = 4 \text{ GHz}$ to $f = 12 \text{ GHz}$. Figure 4.7.2b illustrates typical output power contours as a function of the load reflection coefficient. For this transistor $P_{1dB} = 19 \text{ dBm}$ and $G_{1dB} = 6 \text{ dB}$. The 18-dBm and 17-dBm output power contours are also shown. The input was conjugately matched at all times.

A typical measuring system for large-signal parameters is illustrated in Fig. 4.7.3. The transistor under test is placed in a measuring setup where the dc bias and ac input signal level can be varied. The output tuning stubs are adjusted until the power meter C measures a given power level and the input tuning stubs are adjusted for zero reflected power (read at power meter B). The power meter A reads the incident power, and the power gain (at given output power level) can be obtained. Since there is no reflected power, the input port is conjugately matched, and the output impedance is that impedance required to produce the output power read at power meter C.



(a)



(b)

Figure 4.7.2 (a) Typical large-signal reflection coefficients. (b) Typical output power contours as a function of Γ_{LP} for a GaAs FET at $f = 10$ GHz, $V_{DS} = 10$ V, and $I_D = 50\%I_{DSS}$. For this transistor the optimum output power is 19 dBm at 1-dB gain compression and $G_{1dB} = 6$ dB.

The transistor can then be disconnected from the test setup and the impedance at the reference planes A and B is measured with a network analyzer. These measurements produce the values of Γ_{SP} and Γ_{LP} for a given output power and gain. Of course, Γ_{SP} and Γ_{LP} are functions of output power level, frequency, and bias conditions.

A source of distortion in power amplifiers is that caused by intermodulation products. When two or more sinusoidal frequencies are applied to a nonlinear amplifier, the output contains additional frequency components

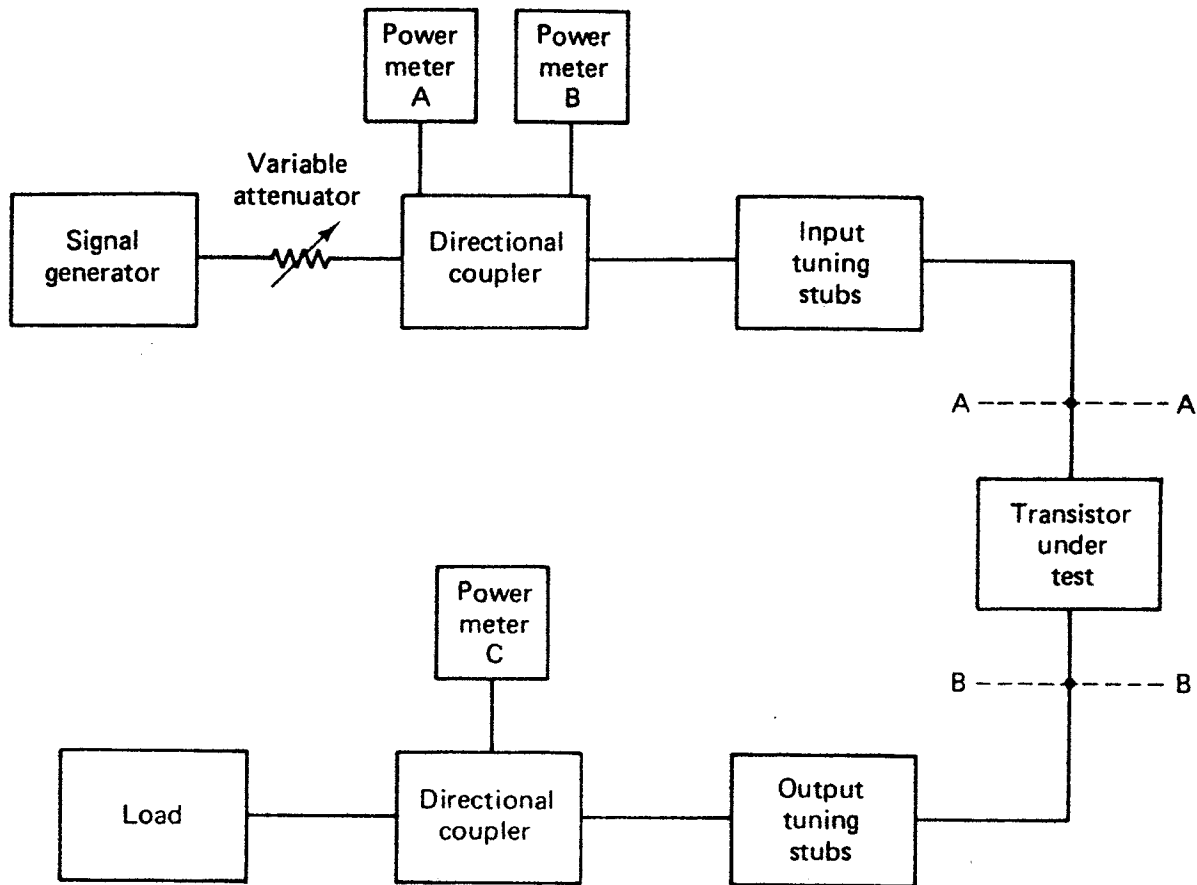


Figure 4.7.3 Measuring system for large-signal parameters.

called *intermodulation products*. For example, if two sinusoidal signals

$$v(t) = A \cos 2\pi f_1 t + A \cos 2\pi f_2 t \quad (4.7.6)$$

are applied to a nonlinear amplifier whose output voltage can be represented by the power series

$$v_o(t) = \alpha_1 v(t) + \alpha_2 v^2(t) + \alpha_3 v^3(t) \quad (4.7.7)$$

the output signal will contain frequency components at dc, f_1 , f_2 , $2f_1$, $2f_2$, $3f_1$, $3f_2$, $f_1 \pm f_2$, $2f_1 \pm f_2$, and $2f_2 \pm f_1$. The frequencies $2f_1$ and $2f_2$ are the second harmonics, $3f_1$ and $3f_2$ are the third harmonics, $f_1 \pm f_2$ are the second-order intermodulation products (since the sum of the f_1 and f_2 coefficients is 2), and $2f_1 \pm f_2$ and $2f_2 \pm f_1$ are the third-order intermodulation products (since the sum of the f_1 and f_2 coefficients is 3). The input and output power spectra, from (4.7.6) and (4.7.7), are shown in Fig. 4.7.4.

Figure 4.7.4 shows that the third-order intermodulation products at $2f_1 - f_2$ and $2f_2 - f_1$ are very close to the fundamental frequencies f_1 and f_2 and fall within the amplifier bandwidth, producing distortion in the output.

If we measure the third-order intermodulation product output power ($P_{2f_1-f_2}$) versus the input power at f_1 (P_{f_1}), the graph shown in Fig. 4.7.5 results. The third-order intercept point (called P_{IP}) is defined as the point where P_{f_1} and $P_{2f_1-f_2}$ intercept, when the two-port is assumed to be linear. Observe that the slope of P_{f_1} is 1 and that of $P_{2f_1-f_2}$ is 3. This occurs because

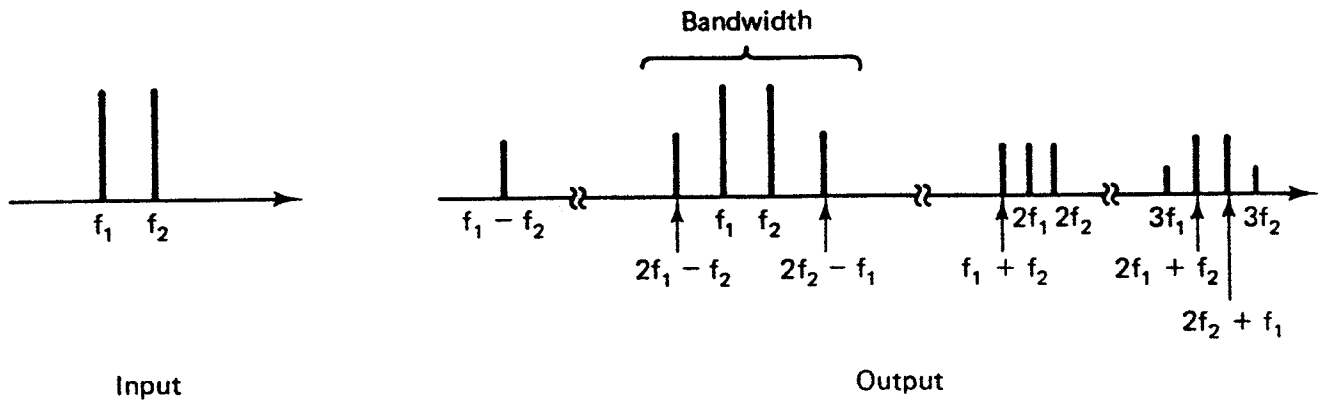


Figure 4.7.4 Input and output power spectrum.

for the assumed $v_o(t)$ in (4.7.7) the power of the third-order intermodulation product is proportional to the cube of the input signal amplitude A . The power P_{IP} is a theoretical level. However, it is a useful quantity to estimate the third-order intermodulation products at different power levels.

For the three-term series in (4.7.7), it can be shown analytically and experimentally that the third-order intercept point is approximately 10 dB above the 1-dB gain compression point. That is,

$$P_{IP}(\text{dBm}) = P_{1\text{dB}}(\text{dBm}) + 10 \text{ dB} \quad (4.7.8)$$

Also, it can be shown that

$$2P_{2f_1-f_2} = 3P_{f_1} - 2P_{IP}$$

or

$$P_{f_1} - P_{2f_1-f_2} = \frac{2}{3}(P_{IP} - P_{2f_1-f_2}) \quad (4.7.9)$$

The spurious free dynamic range (DR_f) of an amplifier (see Fig. 4.7.5) is defined as the range $P_{f_1} - P_{2f_1-f_2}$, when $P_{2f_1-f_2}$ is equal to the minimum detectable output signal. Therefore, from (4.7.5) and (4.7.9),

$$\begin{aligned} DR_f &= \frac{2}{3}(P_{IP} - P_{o,\text{mds}}) \\ &= \frac{2}{3}[P_{IP} + 174 \text{ dBm} - 10 \log B - F(\text{dB}) - X(\text{dB}) - G_A(\text{dB})] \end{aligned}$$

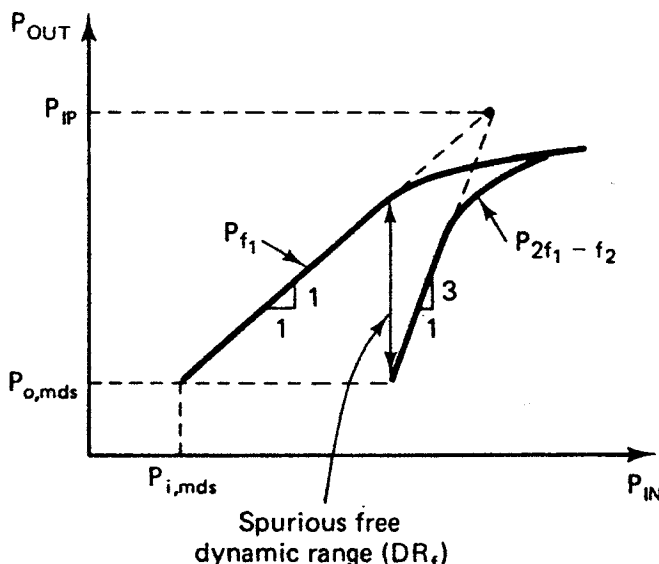


Figure 4.7.5 Third-order intercept point.

Example 4.7.1

An amplifier has an available power gain of 40 dB, 500-MHz bandwidth, noise figure of 7 dB, and a 1-dB gain compression point of 25 dBm. Calculate DR and DR_f .

Solution. The minimum detectable input and output signals, from (4.7.4) and (4.7.5), assuming that $X = 3$ dB, are

$$P_{i,mds} = -174 \text{ dBm} + 10 \log (500 \times 10^6) \text{ dB} + 7 \text{ dB} + 3 \text{ dB} = -77 \text{ dBm}$$

and

$$P_{o,mds} = -77 \text{ dBm} + 40 \text{ dB} = -37 \text{ dBm}$$

Therefore,

$$DR = P_{1dB} - P_{o,mds} = 25 \text{ dBm} + 37 \text{ dBm} = 62 \text{ dB}$$

The third-order intercept point, from (4.7.8), is

$$P_{IP} = 25 \text{ dBm} + 10 \text{ dB} = 35 \text{ dBm}$$

and

$$DR_f = \frac{2}{3}(25 \text{ dBm} + 37 \text{ dBm}) = 48 \text{ dB}$$

Another source of signal distortion is caused by a nonlinear phase characteristic. For a signal to be amplified with no distortion, the magnitude of the power gain transfer function must be constant as a function of frequency and the phase must be a linear function of frequency. A linear phase shift produces a constant time delay to signal frequencies, and a nonlinear phase shift produces different time delays to different frequencies.

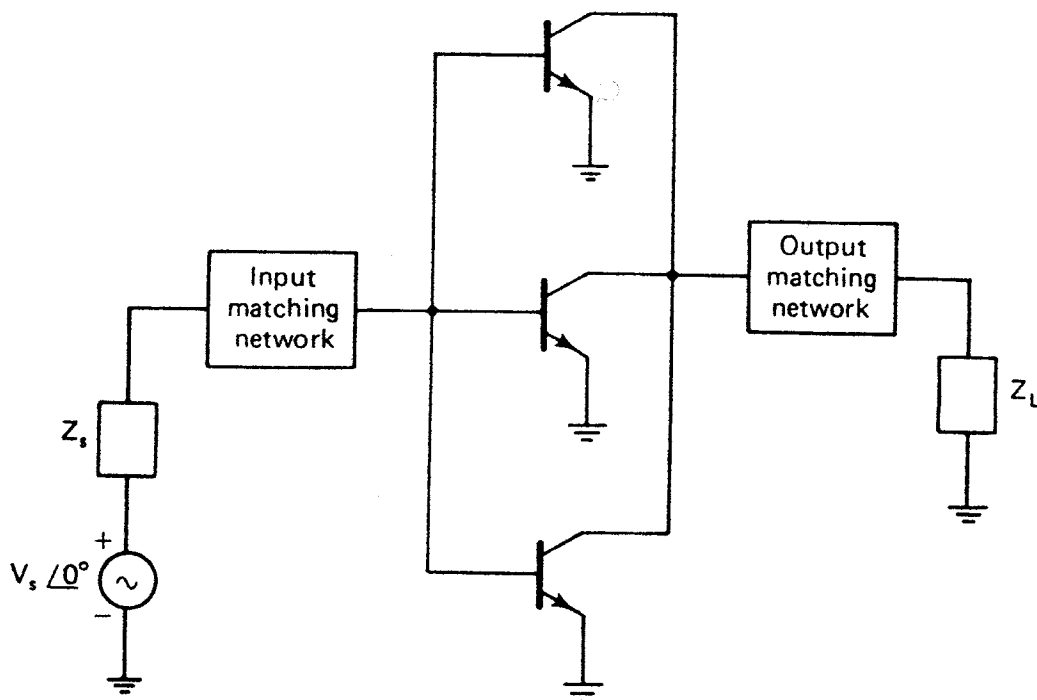


Figure 4.7.6 Method for paralleling transistors.

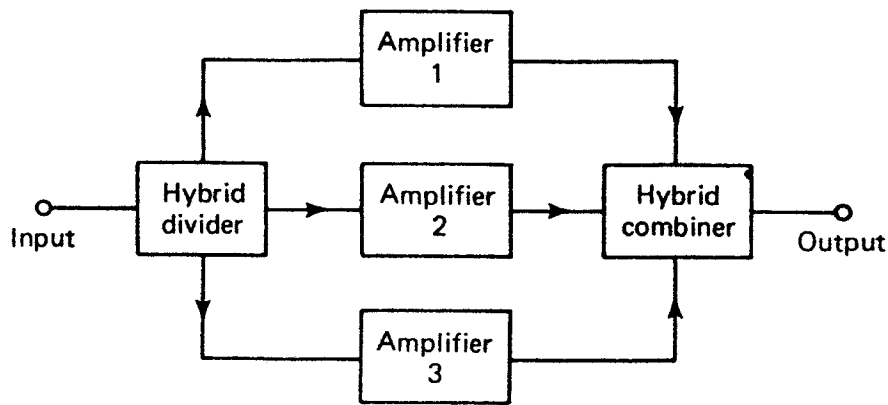


Figure 4.7.7 A hybrid combiner/divider.

A phase distortion called *AM-to-PM conversion* occurs when an AM signal is transmitted through a power amplifier. The phase shift becomes a function of the instantaneous amplitude of the signal, and the output phase consists of a mean value with a small ripple. The AM-to-PM conversion is defined as the change in output phase for a 1-dB increment of the input power.

Power transistors are provided with flanges or studs for proper mounting and heat dissipation. The maximum junction temperature for a BJT is around 200°C and the maximum channel temperature for a GaAs FET is around 175°C .

When more power is required than can be provided by a single microwave transistor amplifier, power-combining techniques are used. One can use a method of paralleling several transistors, as shown in Fig. 4.7.6. However, this method is not recommended, for several reasons:

1. The input and output impedance levels can be of the same order as the losses in the input and output matching networks. For example, a 0.1-nH inductor having a Q of 150, at $f = 400$ MHz, has a resistance loss of $R = \omega L/Q = 1.6 \Omega$, which can be similar to the input resistance of sev-

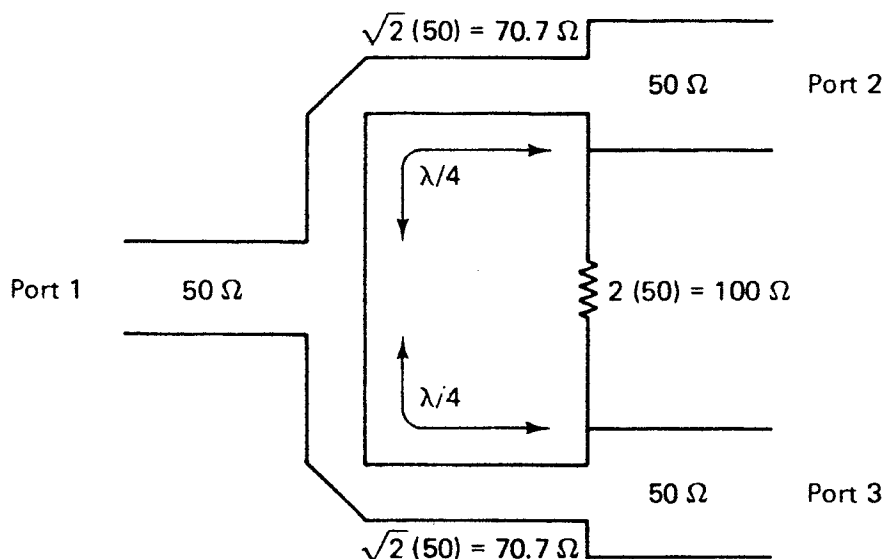


Figure 4.7.8 The Wilkinson coupler.

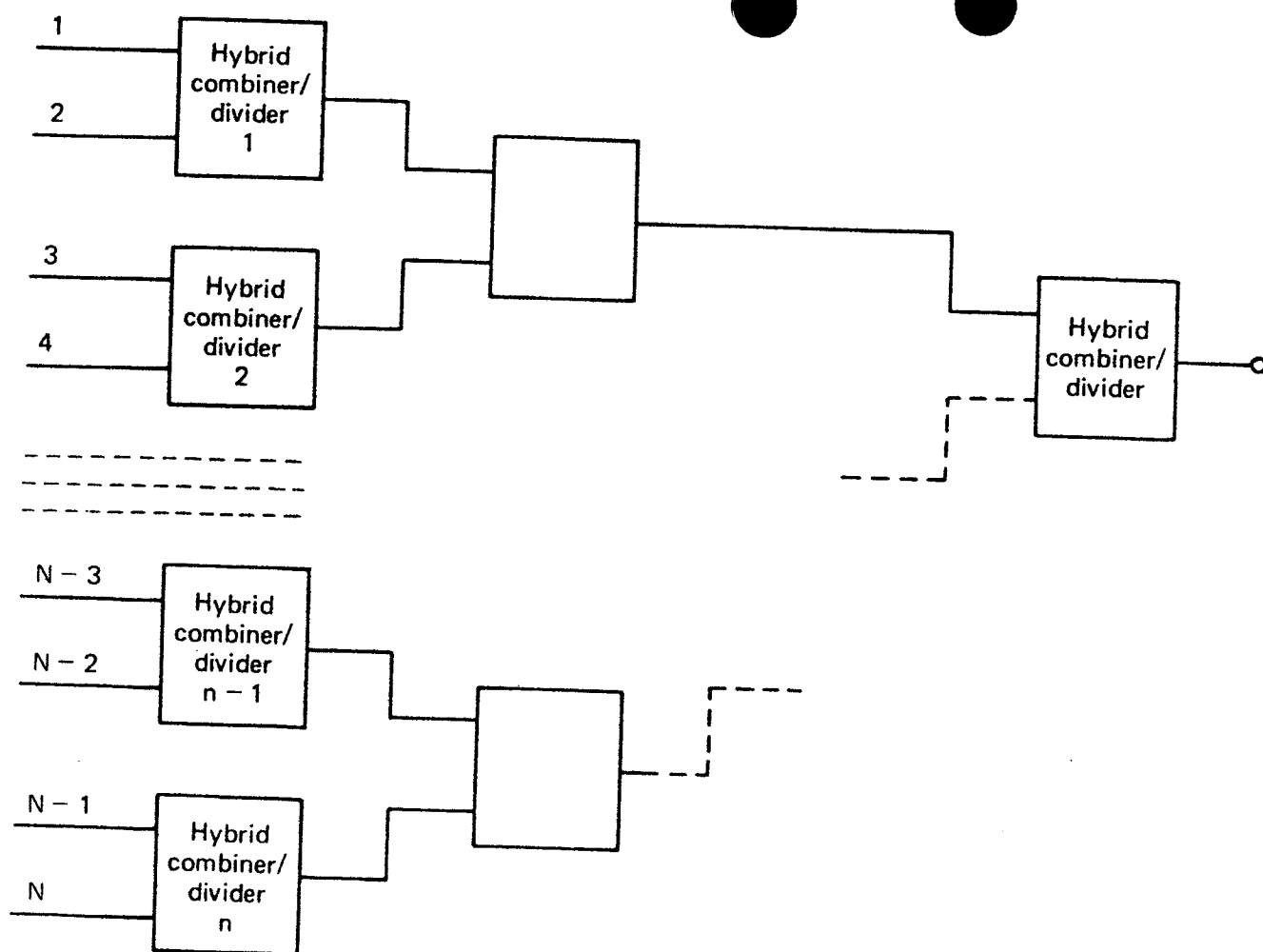


Figure 4.7.9 An n -way hybrid combiner/divider.

eral paralleled transistors. Therefore, the total power output that can be obtained from several paralleled transistors is less than the theoretical total output power because the efficiency decreases as the number of transistors increases.

2. If one transistor fails, the complete amplifier network fails.

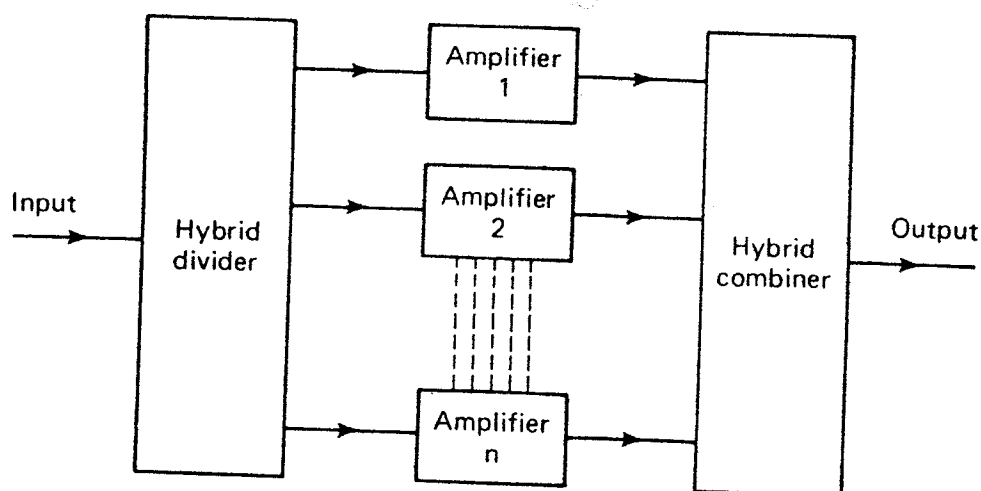


Figure 4.7.10 An n -way power amplifier.

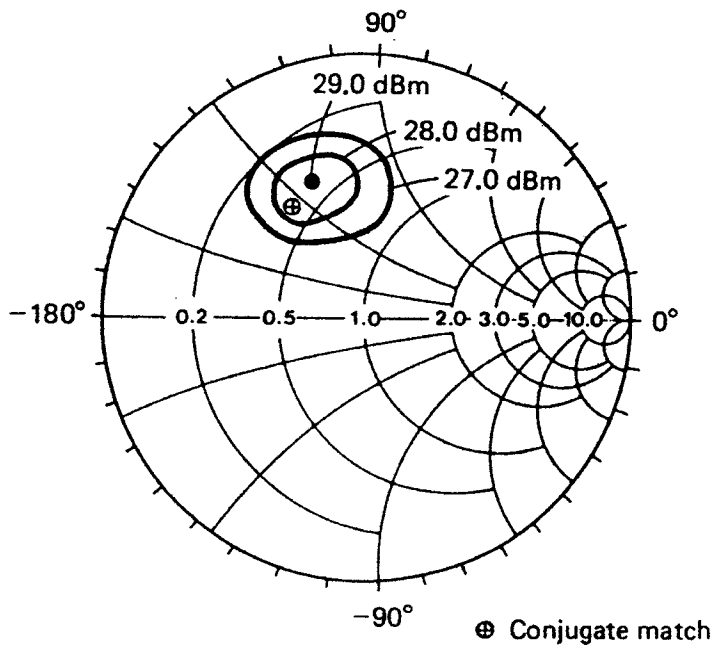


Figure 4.7.11 Output power contours at 2 GHz, $V_{CE} = 18$ V, and $I_C = 110$ mA. (From Ref. [4.12]; courtesy of Hewlett-Packard.)

3. All transistors must be well matched for power output and gain in order to obtain good load sharing.

A method that avoids the problem of paralleling power transistors is shown in Fig. 4.7.7. It uses a hybrid divider and a hybrid combiner to divide the input power equally to several amplifiers, and to combine the output power of each amplifier. The failure of one amplifier does not cause failure of the complete unit. The complete unit will continue to operate with reduced output power.

A popular two-way hybrid divider known as the *Wilkinson coupler* is shown in Fig. 4.7.8. It consists of two $\lambda/4$ transmission lines with characteristic impedances of $Z_o = \sqrt{2} (50) = 70.7 \Omega$. The input signal is connected to port 1 and divides equally, both in amplitude and phase, when ports 2 and 3 are equally terminated. No power is dissipated in the $100\text{-}\Omega$ resistor when equal loads are connected to ports 2 and 3. If ports 2 and 3 are terminated in 50Ω , the input impedance of port 1 is the parallel combination of the two $50\text{-}\Omega$ loads, after each is transformed by the $\lambda/4$ line with $Z_o = 70.7 \Omega$. That is, each $50\text{-}\Omega$ load transforms to 100Ω , and port 1 sees a $50\text{-}\Omega$ matched input impedance. When a mismatch occurs at port 2 or 3, the reflected signals split through the two transmission lines, travel to the input port, split again, and travel back to the output ports. That is, the reflected wave returns to the output port in two parts, each 180° out of phase from each other. The value of the resistor $2Z_o = 100 \Omega$ was selected so that the two parts of the reflected wave have equal amplitude and, therefore, perfect cancellation results.

Of course, the two-way hybrid divider in Fig. 4.7.8 can be used as a two-way combiner by applying the input signals at ports 2 and 3 and taking the output at port 1.

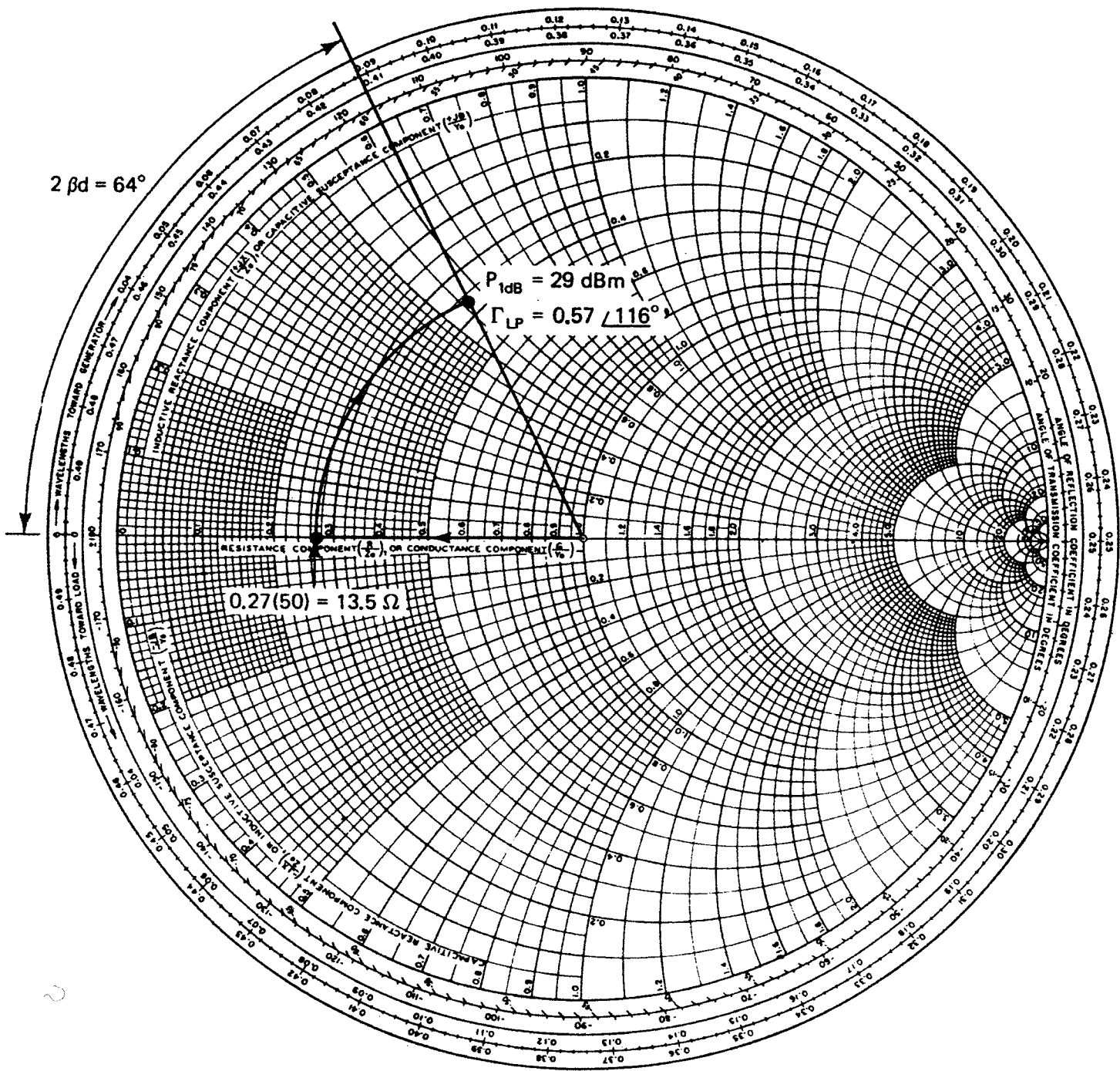


Figure 4.7.12 Design of the output matching network.

Figure 4.7.9 shows the block diagram of an n -way power combiner/divider. The insertion losses of the coupler limit the overall efficiency. The block diagram of an n -way amplifier is shown in Fig. 4.7.10.

Example 4.7.2

Design a power amplifier at 2 GHz using a BJT. The S parameters of the transistor and power characteristics at 2 GHz are

$$S_{11} = 0.64 \angle 153^\circ$$

$$S_{21} = 2.32 \angle 10^\circ$$

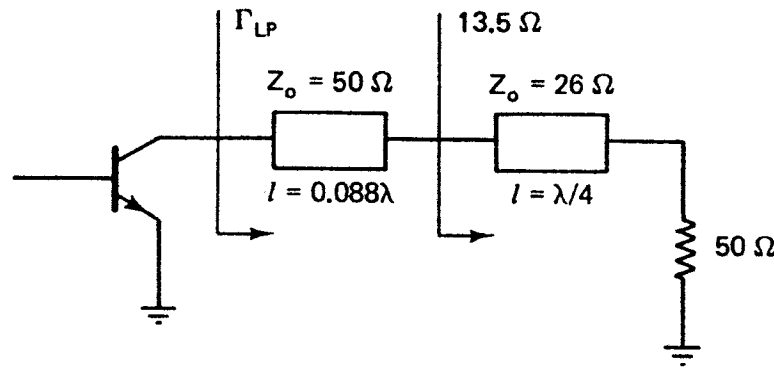


Figure 4.7.13 Output network for the 2-GHz amplifier.

$$S_{12} = 0.07 \angle -8^\circ$$

$$S_{22} = 0.51 \angle -119^\circ$$

$$P_{1\text{dB}} = 29 \text{ dBm}$$

$$G_{1\text{dB}} = 11.5 \text{ dB}$$

Output power contours are shown in Fig. 4.7.11. This figure shows the loci of equal $P_{1\text{dB}}$ for different output loading. The input was conjugately matched at all times. The $P_{1\text{dB}}$ point and the output conjugate match point were close. (This example is based on a design from Hewlett-Packard Application Note 972 [4.12].)

Solution. The transistor is unconditionally stable at 2 GHz since $K = 1.15$ and $\Delta = 0.207 \angle 58.5^\circ$. The output network is designed to provide the output power $P_{1\text{dB}} = 29 \text{ dBm}$. The output matching network design is shown in Fig. 4.7.12. The 50-Ω load was transformed to a resistance of 13.5 Ω using a quarter-wave transformer with characteristic impedance Z_o given by

$$Z_o = \sqrt{50(13.5)} = 26 \Omega$$

A transmission line of length $\beta d = 32^\circ$ (i.e., 0.088λ) was used to complete the match. The output network schematic is shown in Fig. 4.7.13.

In order to obtain an output power of 29 dBm, the input must be conjugately matched. The input conjugate match is calculated using (3.2.5), namely

$$\begin{aligned} \Gamma_{SP} = (\Gamma_{IN})^* &= \left[0.64 \angle 153^\circ + \frac{(0.07 \angle -8^\circ)(2.32 \angle 10^\circ)(0.57 \angle 116^\circ)}{1 - (0.51 \angle -119^\circ)(0.57 \angle 116^\circ)} \right]^* \\ &= 0.749 \angle -147.1^\circ \end{aligned}$$

The small-signal S parameters were used to calculate Γ_s , since, for this transistor, at $P_{1\text{dB}}$ the behavior can be assumed to be linear.

The design of the input matching network is illustrated in Fig. 4.7.14. An open-circuited shunt stub of length 0.185λ ($Z_o = 50 \Omega$), followed by a 50-Ω series transmission line of length 3.5° (0.0097λ), were used to obtain the match. The complete ac schematic is shown in Fig. 4.7.15.

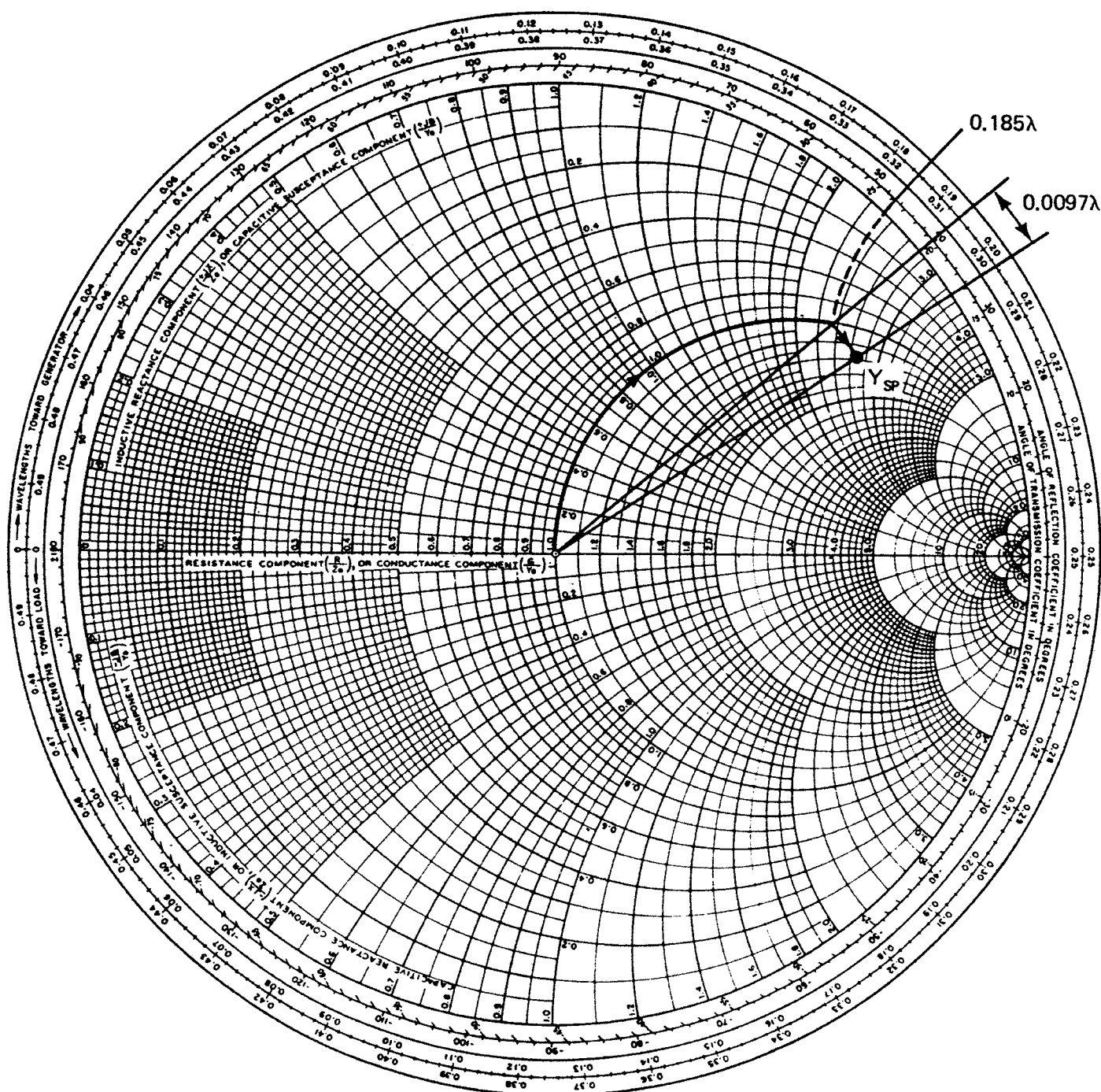


Figure 4.7.14 Design of the input matching network.

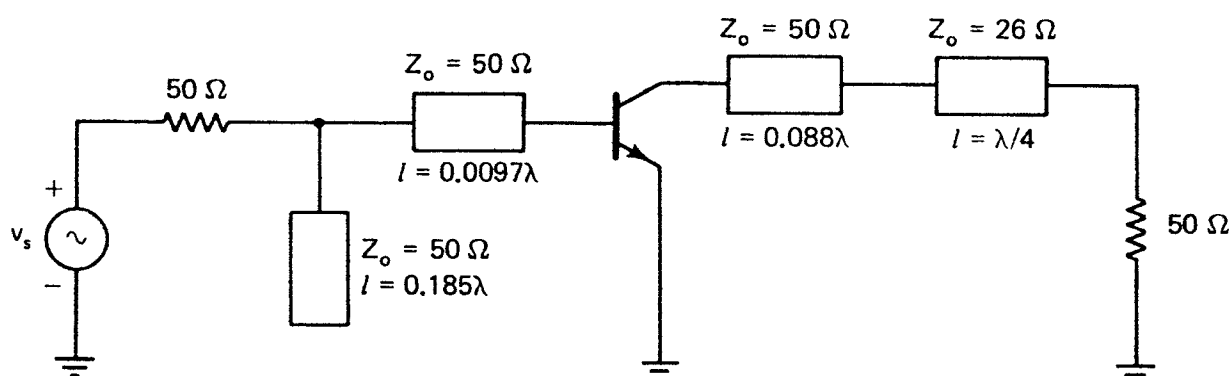


Figure 4.7.15 Schematic of the power amplifier.

4.8 TWO-STAGE AMPLIFIER DESIGN

The configuration of a two-stage microwave transistor amplifier is shown in Fig. 4.8.1. The design of a two-stage amplifier usually consists in the optimization of one of the following requirements: (1) overall high gain, (2) overall low noise figure, or (3) overall high power. In a two-stage amplifier the stability of the individual stages, as well as the overall stability, must be checked.

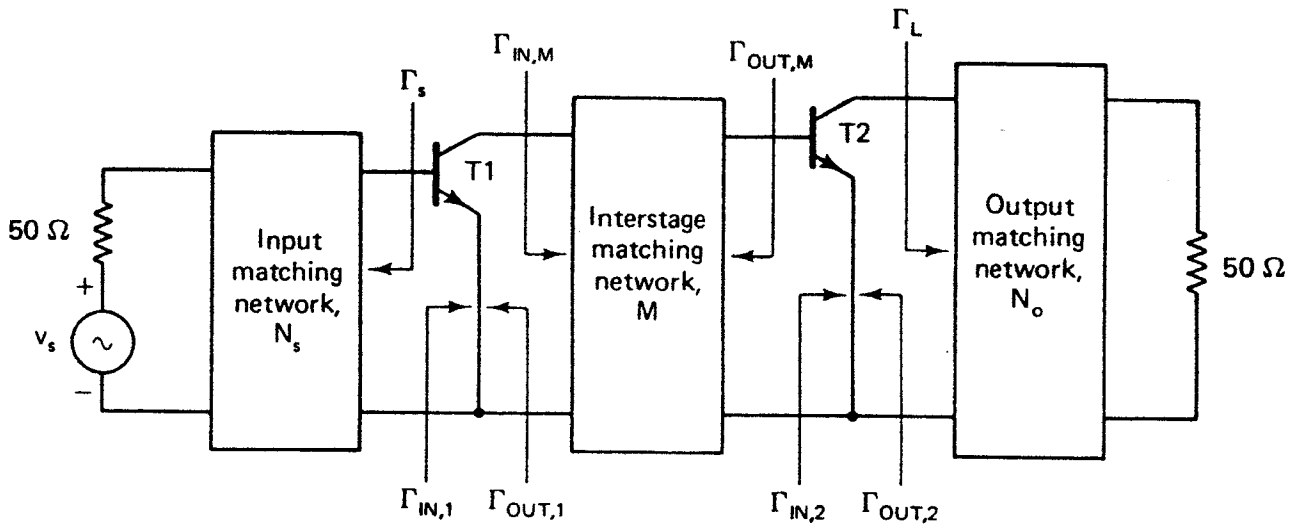


Figure 4.8.1 Diagram of a two-stage amplifier.

In a design requiring overall high gain, the reflection coefficients are selected as follows:

$$\begin{aligned}\Gamma_s &= (\Gamma_{IN,1})^* \\ \Gamma_{IN,M} &= (\Gamma_{OUT,1})^* \\ \Gamma_{OUT,M} &= (\Gamma_{IN,2})^* \\ \Gamma_L &= (\Gamma_{OUT,2})^*\end{aligned}$$

In a design requiring high power the reflection coefficients are selected as follows:

$$\begin{aligned}\Gamma_s &= (\Gamma_{IN,1})^* \\ \Gamma_{IN,M} &= \Gamma_{LP,1} \\ \Gamma_{OUT,M} &= (\Gamma_{IN,2})^* \\ \Gamma_L &= \Gamma_{LP,2}\end{aligned}$$

where $\Gamma_{LP,1}$ and $\Gamma_{LP,2}$ are the large-signal load reflection coefficients of $T1$ and $T2$. In other words, the design of N_o results in $\Gamma_L = \Gamma_{LP,2}$ and the design of M is for a conjugate match at its output [i.e., $\Gamma_{OUT,M} = (\Gamma_{IN,2})^*$] and at its input $\Gamma_{IN,M} = \Gamma_{LP,1}$ (i.e., to present $\Gamma_{LP,1}$ to transistor $T1$). The network N_s presents a conjugate match at the input of transistor $T1$.

In a low-noise design, the reflection coefficients are selected as follows:

$$\begin{aligned}\Gamma_s &= \Gamma_{o,1} \\ \Gamma_{IN,M} &= (\Gamma_{OUT,1})^* \\ \Gamma_{OUT,M} &= \Gamma_{o,2} \\ \Gamma_L &= (\Gamma_{OUT,2})^*\end{aligned}$$

where $\Gamma_{o,1}$ and $\Gamma_{o,2}$ are the optimum noise source reflection coefficients for stages 1 and 2, respectively.

From (4.2.4), the overall noise figure of a two-stage amplifier depends on F_1 , F_2 , and G_{A1} . The transistor of the first stage is usually selected to have low noise figure and a higher noise figure is permitted in the second stage. Although some trade-offs between noise figure and gain are possible, usually the optimum noise match with $\Gamma_{o,1}$ and $\Gamma_{o,2}$ is used.

PROBLEMS

4.1. (a) Show that the noise figure for a three-stage amplifier is given by

$$F = F_1 + \frac{F_2 - 1}{G_{A1}} + \frac{F_3 - 1}{G_{A1}G_{A2}}$$

where F_1 , F_2 , and F_3 are the noise figures of the first, second, and third stages; and G_{A1} and G_{A2} are the available power gains of the first and second stages.

- (b) Two cascade amplifiers have noise figures of $F_1 = 1$ dB and $F_2 = 3$ dB, and a gain of $G_{A1} = 10$ dB and $G_{A2} = 16$ dB. Calculate the overall noise figure.
- 4.2. The scattering and noise parameters of a GaAs FET measured at a low-noise bias point ($V_{DS} = 5$ V, $I_D = 15\%I_{DSS} = 10$ mA) at $f = 12$ GHz are

$$\begin{aligned}S_{11} &= 0.75 \angle -116^\circ & F_{\min} &= 2.2 \text{ dB} \\ S_{12} &= 0.01 \angle 67^\circ & \Gamma_o &= 0.65 \angle 120^\circ \\ S_{21} &= 3.5 \angle 64^\circ & R_N &= 10 \Omega \\ S_{22} &= 0.77 \angle -65^\circ\end{aligned}$$

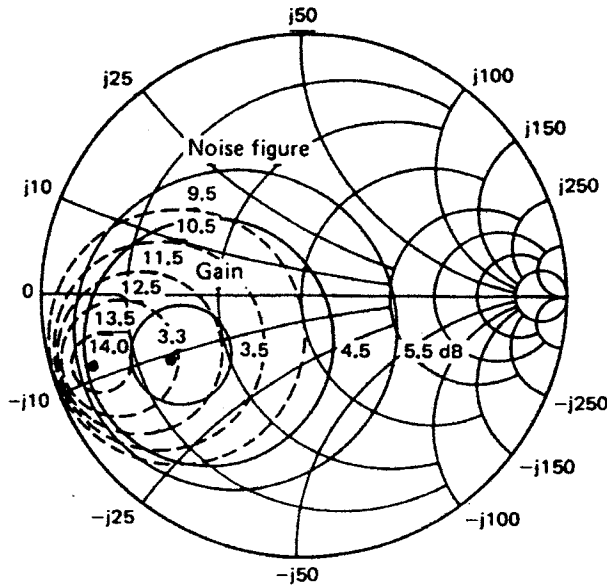
Design a microwave transistor amplifier to have a minimum noise figure.

- 4.3. The scattering and noise parameters of a GaAs FET measured at a low-noise bias point ($V_{DS} = 3.5$ V, $I_D = 15\%I_{DSS} = 12$ mA) at $f = 2$ GHz are

$$\begin{aligned}S_{11} &= 0.8 \angle -51.9^\circ & F_{\min} &= 1.25 \text{ dB} \\ S_{12} &= 0.045 \angle 54.6^\circ & \Gamma_o &= 0.73 \angle 60^\circ \\ S_{21} &= 2.15 \angle 128.3^\circ & R_N &= 19.4 \Omega \\ S_{22} &= 0.73 \angle -30.5^\circ\end{aligned}$$

Design a microwave transistor amplifier to have a minimum noise figure.

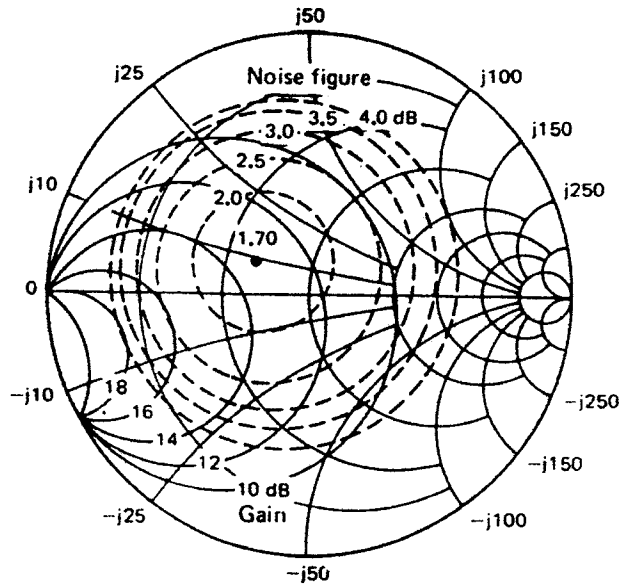
- 4.4. (a) A manufacturer provides the information shown in Fig. P4.4 for two microwave transistors. Evaluate the noise parameters for each transistor. Are the constant-gain circles given for G_T , G_A , or G_p ?
- (b) Verify the location of the $G_A = 10.7$ dB constant-gain circle in Fig. 4.3.4.



Frequency = 2 GHz, 10 V, 5 mA

$$\begin{aligned} S_{11} &= 0.655 \angle 162.1^\circ & S_{21} &= 2.286 \angle 45.8^\circ \\ S_{12} &= 0.064 \angle 23.7^\circ & S_{22} &= 0.569 \angle -54.6^\circ \end{aligned}$$

(a)



Frequency = 2 GHz, 10 V, 5 mA

$$\begin{aligned} S_{11} &= 0.646 \angle 172^\circ & S_{21} &= 3.042 \angle 47.9^\circ \\ S_{12} &= 0.051 \angle 13.5^\circ & S_{22} &= 0.642 \angle -64^\circ \end{aligned}$$

(b)

Figure P4.4 Two microwave transistors. (From Avantek Transistor Designers Catalog; courtesy of Avantek.)

- 4.5. (a) Design a microwave transistor amplifier at 2 GHz to have a minimum noise figure using the transistor in Fig. P4.4a. Specify the resulting G_T , G_A , and G_p .
- (b) Design a microwave transistor amplifier at 2 GHz to have $F_i = 2.5$ dB using the transistor in Fig. P4.4b. Specify the resulting G_T , G_A , and G_p .
- 4.6. (a) In the network shown in Fig. P4.6, verify that $|\Gamma_a| = |\Gamma_{IN}|$, where

$$|\Gamma_a| = \left| \frac{Z_a - Z_o}{Z_a + Z_o} \right|$$

and

$$|\Gamma_{IN}| = \left| \frac{Z_{IN} - Z_s^*}{Z_{IN} + Z_s} \right|$$

- (b) Show that $|\Gamma_a|$ can also be expressed in the form

$$|\Gamma_a| = \left| \frac{\Gamma_{IN} - \Gamma_s^*}{1 - \Gamma_{IN} \Gamma_s} \right|$$

- 4.7. Verify (4.4.1), (4.4.2), and (4.4.3).

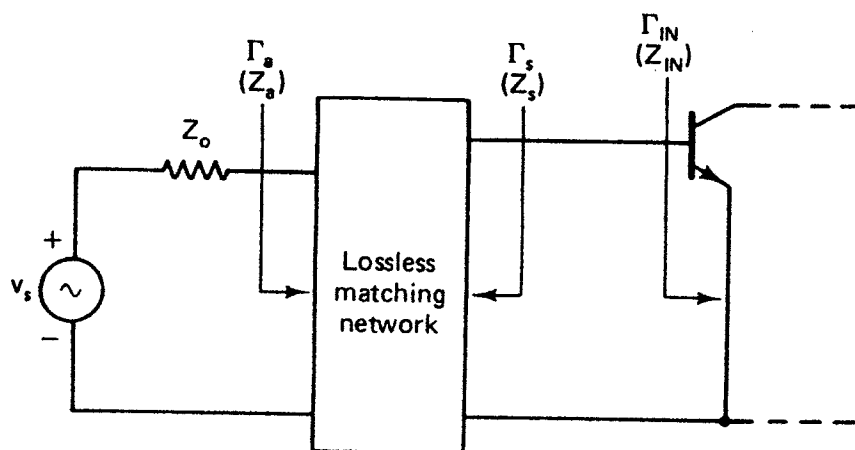


Figure P4.6

- 4.8. Design a broadband microwave BJT amplifier to have $G_{TU} = 12$ dB from 150 to 400 MHz. The transistor S parameters are as follows:

f (MHz)	S_{11}	S_{21}	S_{22}
150	$0.31 \angle -36^\circ$	5	$0.91 \angle -6^\circ$
250	$0.29 \angle -55^\circ$	4	$0.86 \angle -15^\circ$
400	$0.25 \angle -76^\circ$	2.82	$0.81 \angle -26^\circ$

(This problem is based on an example given in Ref. [4.13].)

Hint: G_s will be small and only G_L should be used to compensate for the variations of $|S_{21}|$ with frequency. G_s should be designed to provide a good VSWR at the input. The output matching network can be designed as in Fig. 4.4.4, or for a better match at the three frequencies an extra inductor in series with the 50- Ω load can be added.

- 4.9. Design a broadband microwave BJT amplifier with $G_{TU} = 10$ dB from 1 to 2 GHz with a noise figure of less than 4 dB. For this transistor S_{12} can be neglected and the scattering and noise parameters are as follows:

f (GHz)	S_{11}	S_{21}	S_{22}	Γ_o	R_N	F_{\min} (dB)
1	$0.64 \angle -98^\circ$	$5.04 \angle 113^\circ$	$0.79 \angle -30^\circ$	$0.48 \angle 23^\circ$	23.3	1.45
1.5	$0.60 \angle -127^\circ$	$3.90 \angle 87^\circ$	$0.76 \angle -35^\circ$	$0.45 \angle 61^\circ$	15.6	1.49
2	$0.59 \angle -149^\circ$	$3.15 \angle 71^\circ$	$0.75 \angle -43^\circ$	$0.41 \angle 88^\circ$	15.7	1.61

In this problem, design the input and output matching networks so that $G_{TU} = 10$ dB at the band edges only, and calculate the resulting gain at 1.5 GHz. The noise figure over the band must be less than 4 dB.

- 4.10. (a) In the network shown in Fig. P4.10a, what is the best Γ_x that can be achieved in the frequency range 400 to 600 MHz?
 (b) In the network shown in Fig. P4.10b, what is the best Γ_x that can be obtained in the range 6 to 12 GHz?
- 4.11. For the networks in Fig. 4.4.15b, c, and d, the gain-bandwidth restrictions are

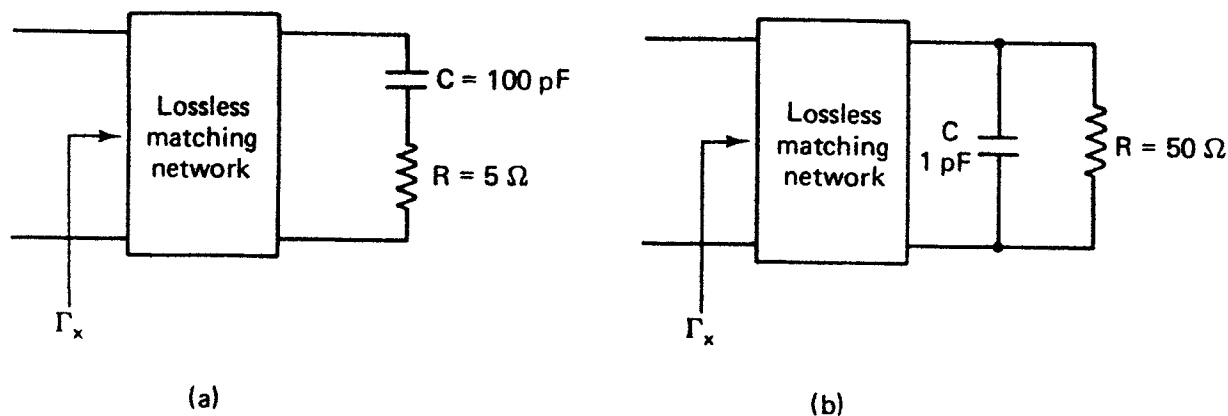


Figure P4.10

given by

$$\int_0^\infty \frac{1}{\omega^2} \ln \left| \frac{1}{\Gamma} \right| d\omega \leq \pi RC \quad (\text{for Fig. 4.4.15b})$$

$$\int_0^\infty \frac{1}{\omega^2} \ln \left| \frac{1}{\Gamma} \right| d\omega \leq \frac{\pi L}{R} \quad (\text{for Fig. 4.4.15c})$$

$$\int_0^\infty \ln \left| \frac{1}{\Gamma} \right| d\omega \leq \frac{\pi R}{L} \quad (\text{for Fig. 4.4.15d})$$

Show that Γ_x can be expressed in the form given in (4.4.8) when the appropriate definitions of Q_1 and Q_2 are used. These are given in Fig. 4.4.15.

- 4.12. (a) Verify the equation for δ_{IN} in (4.5.1).
 (b) Verify the relation between δ_{IN} and Γ_L in (4.5.2).
 (c) Derive a relation for δ_{OUT} .
- 4.13. (a) Show that K for the balance amplifier, using a 3-dB Lange coupler, is given by

$$K = \frac{1 + P^2}{2P}$$

where

$$P = |S_{21} S_{12}|$$

Show that K has a minimum value of 1 when $P = 1$ (i.e., when $|S_{21} S_{12}| = 1$) and $K > 1$ for all other values of P .

- (b) The S parameters of a transistor at 2.1 GHz are

$$S_{11} = -0.699 - j0.348$$

$$S_{21} = -10.9 + j7.895$$

$$S_{22} = 0.309 + j0.459$$

$$S_{12} = 0.009 + j0.015$$

and the resulting K , $K = 0.48$, shows that the transistor is potentially unstable. If the transistor is used in a balanced amplifier configuration, calculate the resulting S parameters and K .

4.14. The S parameters of a transistor at 8 GHz are

$$S_{11} = 0.75 \angle -100^\circ$$

$$S_{21} = 2.5 \angle 93^\circ$$

$$S_{12} = 0$$

$$S_{22} = 0.7 \angle -50^\circ$$

Determine

- The terminations for $G_{TU, \max}$.
 - The inherent bandwidths and Q of the input and output networks.
 - The additional elements (C or L) that must be added to the input and/or output networks to make the bandwidth 20% of the inherent bandwidth.
 - The optimum terminations for part (c) and the resulting G_{TU} .
- 4.15. In a microwave transistor amplifier it is found that $\Gamma_{Ms} = 0.476 \angle 166^\circ$ and $\Gamma_{ML} = 0.846 \angle 72^\circ$ at $f = 4$ GHz. Calculate the amplifier input and output intrinsic bandwidths. If the bandwidth is to be limited to 400 MHz, find the value of C_{OUT} or L_{OUT} that must be added to the output network.
- 4.16. Analyze the Wilkinson coupler shown in Fig. 4.7.8.
- 4.17. An amplifier has a transducer power gain of 30 dB, 800-MHz bandwidth, and a noise figure of 5 dB. The 1-dB gain compression point is given as 28 dBm. Calculate DR, DR_f , and the maximum output power for no third-order intermodulation distortion.
- 4.18. The specifications for two power GaAs FETs at 4 GHz are as follows:

	P_{1dB} (dBm)	G_{1dB} (dB)	G_p (dB)
FET 1	25	6	7
FET 2	20	8	9

Show that the two-way power amplifier shown in Fig. P4.18 can be used to deliver $P_{OUT} = 27.7$ dBm, at 1 dB compression, with $P_{IN} = 6.3$ dBm. The loss of the two-way combiner/divider is -0.3 dB. Specify the FET that must be used in each stage, and indicate the power and gain levels at all points.

Hint: The power at the output of the divider is 19.0 dBm.

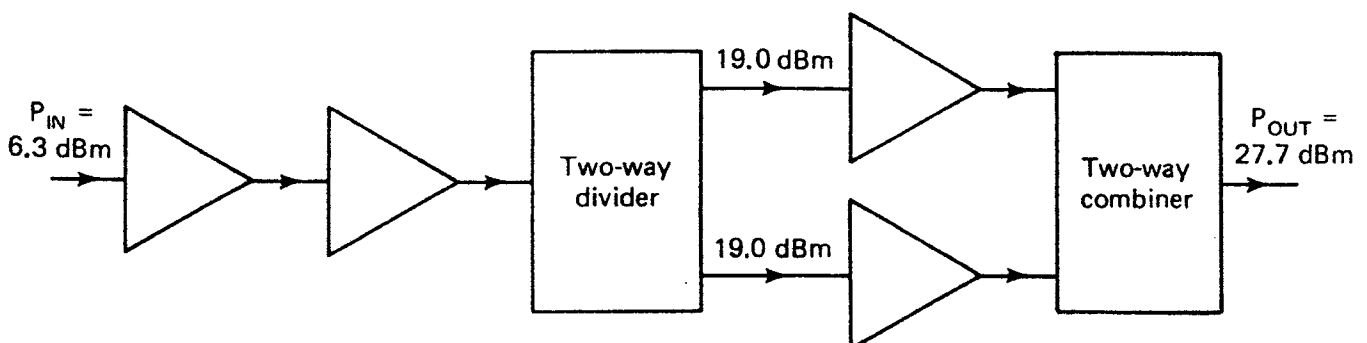


Figure P4.18

4.19. Design a power amplifier at 4 GHz using a BJT. The S parameters of the transistor and power characteristics at 4 GHz are

$$S_{11} = 0.32 \angle -145^\circ$$

$$S_{21} = 1.38 \angle -113^\circ$$

$$S_{12} = 0.08 \angle -98^\circ$$

$$S_{22} = 0.8 \angle -177^\circ$$

$$P_{1\text{dB}} = 27.5 \text{ dBm}$$

$$G_{1\text{dB}} = 7 \text{ dB}$$

$$\Gamma_{LP} = 0.1 \angle 0^\circ$$

4.20. In the two-stage amplifier shown in Fig. 4.8.1, transistors $T1$ and $T2$ are potentially unstable. Can the overall amplifier be unconditionally stable?

REFERENCES

- [4.1] H. A. Haus (chairman), "Representation of Noise in Linear Two Ports," IRE Subcommittee 7.9 on Noise, *Proceedings of the IEEE*, January 1960.
- [4.2] "A Low Noise 4 GHz Transistor Amplifier Using the HXTR-6101 Silicon Bipolar Transistor," Hewlett-Packard Application Note 967, May 1975.
- [4.3] "A 6 GHz Amplifier Using the HFET-1101 GaAs FET," Hewlett-Packard Application Note 970, February 1978.
- [4.4] T. T. Ha, *Solid State Microwave Amplifier Design*, Wiley-Interscience, New York, 1981.
- [4.5] G. Matthaei, L. Young, and E. M. T. Jones, *Microwave Filters, Impedance-Matching Networks, and Coupling Structures*, Artech House, Inc., Dedham, MA., 1980.
- [4.6] AMPSYN (computer program), Compact Software, Inc., 1131 San Antonio Road, Palo Alto, CA 94303.
- [4.7] D. J. Mellor and J. G. Linvill, "Synthesis of Interstage Networks of Prescribed Gain versus Frequency Slopes," *IEEE Transactions on Microwave Theory and Techniques*, December 1975.
- [4.8] R. W. Anderson, "S Parameter Techniques for Faster, More Accurate Network Design," Hewlett-Packard Application Note 95-1 (or *Hewlett-Packard Journal*), February 1967.
- [4.9] J. Lange, "Integrated Stripline Quadrature Hybrids," *IEEE Transactions on Microwave Theory and Techniques*, December 1969.
- [4.10] L. Besser, "Microwave Circuit Design," *Electronic Engineering*, October 1980.
- [4.11] R. M. Fano, "Theoretical Limitations on the Broadband Matching of Arbitrary Impedances," *Journal of the Franklin Institute*, January 1950.
- [4.12] "Two Telecommunications Power Amplifiers for 2 and 4 GHz Using the HXTR-5102 Silicon Bipolar Power Transistor," Hewlett-Packard Application Note 972, 1980.
- [4.13] R. S. Carson, *High-Frequency Amplifiers*, Wiley-Interscience, New York, 1975.

MICROWAVE TRANSISTOR OSCILLATOR DESIGN

5.1 INTRODUCTION

In this chapter the analytical techniques that are used in the design of negative-resistance oscillators are discussed. The small- and large-signal S parameters provide all the information needed to design negative-resistance oscillators.

In a negative-resistance oscillator we refer to the matching networks at the two ports as the terminating and the load (or resonant) matching networks. The load-matching network is the network that determines the frequency of oscillation, and the terminating network is used to provide the proper matching.

The design of the terminating and load matching networks must be done carefully. For example, the condition $|\Gamma_{IN}| > 1$ is necessary for oscillation. A short circuit at the terminating port can produce $|\Gamma_{IN}| > 1$. However, no power is delivered to a short-circuited termination.

In the low range of microwave frequencies, the lumped-element Colpitts, Hartley, and Clapp oscillators are commonly used.

5.2 ONE-PORT NEGATIVE-RESISTANCE OSCILLATORS

A general schematic diagram for one-port negative-resistance oscillators is shown in Fig. 5.2.1. The negative-resistance device is represented by the amplitude and frequency-dependent impedance

$$Z_{IN}(V, \omega) = R_{IN}(V, \omega) + jX_{IN}(V, \omega)$$

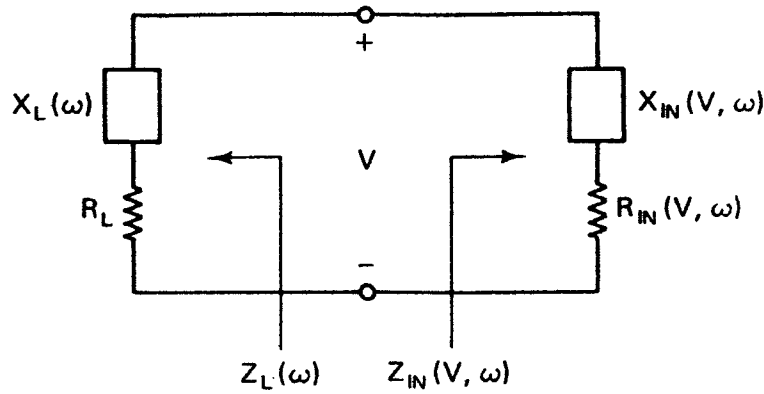


Figure 5.2.1 Schematic diagram for one-port negative-resistance oscillators.

where

$$R_{IN}(V, \omega) < 0$$

The oscillator is constructed by connecting the device to a passive load impedance, called

$$Z_L(\omega) = R_L + jX_L(\omega)$$

The discussion in Section 3.3 showed that the one-port network in Fig. 5.2.1 is stable if

$$\text{Re} [Z_{IN}(V, \omega) + Z_L(\omega)] > 0$$

and the network will oscillate when

$$\Gamma_{IN}(V, \omega)\Gamma_L(\omega) = 1$$

The oscillation conditions can be expressed in the form

$$R_{IN}(V, \omega) + R_L = 0 \quad (5.2.1)$$

and

$$X_{IN}(V, \omega) + X_L(\omega) = 0$$

To be specific, the device is defined to be unstable over some frequency range $\omega_1 < \omega < \omega_2$ if $R_{IN}(V, \omega) < 0$. The one-port network is unstable for some ω_o in the range if the net resistance of the network is negative, that is, when

$$|R_{IN}(V, \omega_o)| > R_L \quad (5.2.2)$$

Any transient excitation due to noise in the circuit will initiate an oscillation at the frequency ω_o , for which the net reactance of the network is equal to zero, namely

$$X_L(\omega_o) = -X_{IN}(V, \omega_o) \quad (5.2.3)$$

At ω_o a growing sinusoidal current will flow through the circuit, and the oscillation will continue to build up as long as the resistance is negative. The

amplitude of the voltage must eventually reach a steady-state value, called V_o , which occurs when the loop resistance is zero. To satisfy the conditions (5.2.1) and (5.2.2), the impedance $Z_{IN}(V, \omega)$ must be amplitude dependent and, therefore, at $V = V_o$ we can write

$$R_{IN}(V_o, \omega_o) + R_L = 0 \quad (5.2.4)$$

The frequency of oscillation determined by (5.2.3) is not stable since $X_{IN}(V, \omega_o)$ is amplitude dependent. That is,

$$X_{IN}(V_1, \omega_o) \neq X_{IN}(V_o, \omega_o)$$

where V_1 is an arbitrary voltage. Therefore, it is necessary to find another condition to guarantee a stable oscillation. If the frequency dependence of $Z_{IN}(V, \omega)$ can be neglected for small variations around ω_o , Kurokawa [5.1] has shown that the condition for a stable oscillation is

$$\left. \frac{\partial R_{IN}(V, \omega)}{\partial V} \right|_{V=V_o} \left. \frac{dX_L(\omega)}{d\omega} \right|_{\omega=\omega_o} - \left. \frac{\partial X_{IN}(V, \omega)}{\partial V} \right|_{V=V_o} \left. \frac{dR_L(\omega)}{d\omega} \right|_{\omega=\omega_o} > 0 \quad (5.2.5)$$

In other words, the frequency of oscillation determined by (5.2.3) and (5.2.4) is stable only if (5.2.5) is satisfied. In most cases

$$\frac{dR_L(\omega)}{d\omega} = 0$$

(i.e., R_L is a constant) and (5.2.5) simplifies accordingly.

Example 5.2.1

A negative-resistance device can be modeled by the parallel combination of a capacitor and a negative conductance, as shown in Fig. 5.2.2a. The amplitude dependence of the negative conductance, shown in Fig. 5.2.2b, is given by

$$G(V) = G_M \left(1 - \frac{V}{V_M} \right) \quad (5.2.6)$$

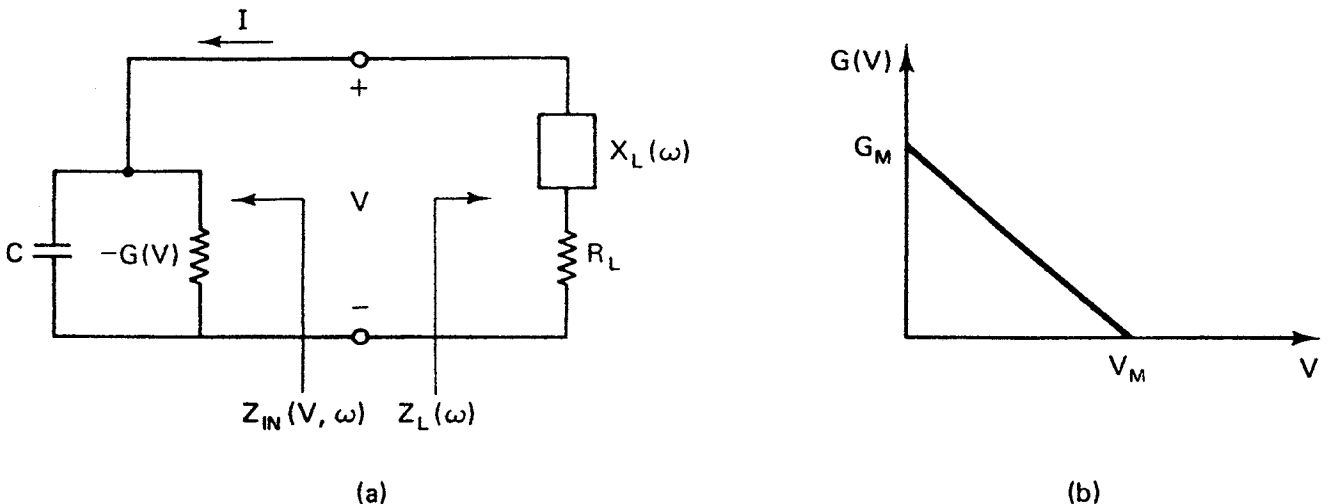


Figure 5.2.2 (a) Negative-resistance device; (b) amplitude variations of $G(V)$.

Design a load circuit, Z_L , to provide oscillation at ω_o and calculate the output power.

Solution. The device impedance is

$$Z_{IN}(V, \omega) = R_{IN}(V, \omega) + jX_{IN}(V, \omega) = \frac{-G(V)}{G^2(V) + \omega^2 C^2} + j \frac{-\omega C}{G^2(V) + \omega^2 C^2} \quad (5.2.7)$$

From (5.2.3) to (5.2.5) a stable oscillation at $\omega = \omega_o$ occurs when

$$R_L = \left. \frac{G(V)}{G^2(V) + \omega^2 C^2} \right|_{\omega = \omega_o, V = V_o} \quad (5.2.8)$$

$$X_L(\omega) = \left. \frac{\omega C}{G^2(V) + \omega^2 C^2} \right|_{\omega = \omega_o, V = V_o} \quad (5.2.9)$$

and

$$\left. \frac{\partial R_{IN}}{\partial V} \right|_{V = V_o} \left. \frac{dX_L}{d\omega} \right|_{\omega = \omega_o} > 0 \quad (5.2.10)$$

where V_o is the oscillation voltage level at the frequency of oscillation ω_o .

Substituting (5.2.6) into (5.2.7) gives for R_{IN} ,

$$R_{IN} = \frac{-(1/G_M)(1 - V/V_M)}{(1 - V/V_M)^2 + \omega^2 C^2/G_M^2} \quad (5.2.11)$$

Differentiating (5.2.11) with respect to V gives

$$\frac{\partial R_{IN}}{\partial V} = \frac{-1 + 2(V/V_M) - V^2/V_M^2 + \omega^2 C^2/G_M^2}{G_M V_M [(1 - V/V_M)^2 + (\omega^2 C^2/G_M^2)]^2} \quad (5.2.12)$$

and substituting (5.2.12) into (5.2.10) produces the relation

$$\left. \frac{dX_L}{d\omega} \right|_{\omega = \omega_o} \left[-1 + 2 \frac{V}{V_M} - \frac{V^2}{V_M^2} + \frac{\omega^2 C^2}{G_M^2} \right] \bigg|_{V = V_o} > 0 \quad (5.2.13)$$

There is no direct way to solve for R_L and X_L from (5.2.8), (5.2.9), and (5.2.13). Therefore, another design consideration such as maximizing the power delivered to R_L must be introduced.

The current in the circuit is given by

$$I = V(-G(V) + j\omega C)$$

and the output power is given by

$$P = \frac{1}{2} |I|^2 R_L = \frac{1}{2} |V|^2 R_L (G^2(V) + \omega^2 C^2) \quad (5.2.14)$$

Substituting (5.2.6) and (5.2.8) into (5.2.14) gives

$$P = \frac{1}{2} V_M^2 \left(1 - \frac{G(V)}{G_M} \right)^2 G(V) \quad (5.2.15)$$

The expression (5.2.15) can be maximized for G as follows:

$$\frac{\partial P}{\partial G(V)} = \frac{1}{2} V_M^2 \left[1 - 4 \frac{G(V)}{G_M} + 3 \frac{G^2(V)}{G_M^2} \right] = 0$$

or

$$\frac{G(V)}{G_M} = \frac{1}{3} \quad (5.2.16)$$

Substituting (5.2.16) into (5.2.6) gives

$$\frac{V}{V_M} = \frac{2}{3} \quad (5.2.17)$$

which is the output voltage when maximum output power is delivered to R_L . If (5.2.17) is evaluated at $V = V_o$ and substituted back into (5.2.13), the following result is obtained:

$$\left. \frac{dX_L}{d\omega} \right|_{\omega=\omega_o} \left(\frac{\omega_o^2 C^2}{G_M^2} - \frac{1}{9} \right) > 0 \quad (5.2.18)$$

The only unknown in (5.2.18) is X_L , so the frequency dependence of X_L can easily be determined around ω_o .

From (5.2.16), (5.2.8), and (5.2.9) the values of R_L and $X_L(\omega)$ that maximize the power delivered to R_L at ω_o are

$$R_L = \frac{G_M/3}{(G_M/3)^2 + \omega_o^2 C^2} \quad (5.2.19)$$

and

$$X_L(\omega_o) = \frac{\omega_o C}{(G_M/3)^2 + \omega_o^2 C^2} \quad (5.2.20)$$

At this point, it is necessary to check if R_L satisfies the condition (5.2.2) when the amplitude level is zero (i.e., the starting oscillation condition). Therefore, using (5.2.11) and (5.2.19), we have that

$$|R_{IN}(V, \omega_o)| \Big|_{V=0} > R_L$$

when

$$\frac{\omega_o C}{G_M} > \frac{1}{\sqrt{3}}$$

If we examine the ratio of R_L to $|R_{IN}(0, \omega_o)|$, we obtain

$$\frac{R_L}{|R_{IN}(0, \omega_o)|} = 3 \frac{1 + (\omega_o C/G_M)^2}{1 + 9(\omega_o C/G_M)^2} \quad (5.2.21)$$

If $\omega_o C/G_M$ is large, (5.2.21) can be approximated by

$$\frac{R_L}{|R_{IN}(0, \omega_o)|} \approx \frac{1}{3} \quad (5.2.22)$$

The relation (5.2.22) provides a good design guideline for selecting R_L . That is, let

$$R_L = \frac{1}{3} |R_{IN}(0, \omega_o)| \quad (5.2.23)$$

From (5.2.20), the frequency of oscillation ω_o is

$$X_L(\omega_o) \approx \frac{1}{\omega_o C} \quad (5.2.24)$$

and from (5.2.18),

$$\left. \frac{dX_L}{d\omega} \right|_{\omega=\omega_o} > 0 \quad (5.2.25)$$

Obviously, an inductor ($X_L = \omega L$) satisfies (5.2.24) and (5.2.25), and ω_o is given by

$$\omega_o \approx \frac{1}{\sqrt{LC}}$$

5.3 TWO-PORT NEGATIVE-RESISTANCE OSCILLATORS

A two-port network configuration is shown in Fig. 5.3.1. The two-port network is characterized by the S parameters of the transistor, the terminating impedance Z_T , and the load impedance Z_L .

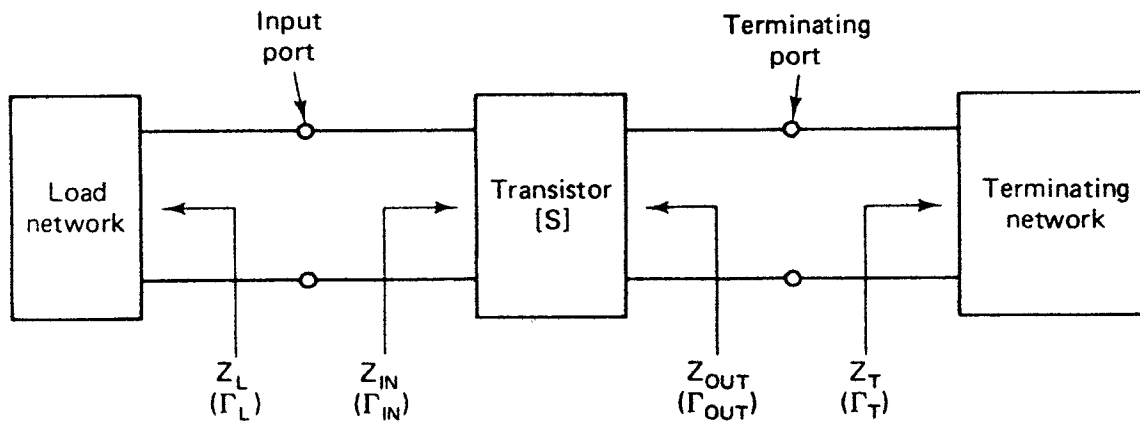


Figure 5.3.1 Two-port oscillator model.

When the two-port is potentially unstable, an appropriate Z_T permits the two-port to be represented as a one-port negative-resistance device with input impedance Z_{IN} , as shown in Fig. 5.2.1. The conditions for a stable oscillation are given by (5.2.3) to (5.2.5).

The negative resistance of Z_{IN} is a function of voltage and as the oscillation power increases, the negative resistance can decrease to a value lower than the load resistance, at which point the oscillation stops. This problem is eliminated by designing the magnitude of the negative resistance, at $V = 0$, to be larger than the load. The value given in (5.2.23) [i.e., $|R_{IN}(0, \omega_o)| = 3R_L$] is commonly used in practice.

When the input port is made to oscillate, the terminating port also oscillates. The fact that both ports are oscillating can be proved as follows.

The input port is oscillating when

$$\Gamma_{IN} \Gamma_L = 1 \quad (5.3.1)$$

and from (3.2.5) and (5.3.1),

$$\Gamma_L = \frac{1}{\Gamma_{IN}} = \frac{1 - S_{22} \Gamma_T}{S_{11} - \Delta \Gamma_T}$$

or

$$\Gamma_T = \frac{1 - S_{11} \Gamma_L}{S_{22} - \Delta \Gamma_L} \quad (5.3.2)$$

Also, from (3.2.6),

$$\Gamma_{OUT} = \frac{S_{22} - \Delta \Gamma_L}{1 - S_{11} \Gamma_L} \quad (5.3.3)$$

and from (5.3.2) and (5.3.3) it follows that

$$\Gamma_{OUT} \Gamma_T = 1$$

which shows that the terminating port is also oscillating.

A design procedure for a two-port oscillator is as follows:

1. Use a potentially unstable transistor at the frequency of oscillation ω_o .
2. Design the terminating network to make $|\Gamma_{IN}| > 1$. Series or shunt feedback can be used to increase $|\Gamma_{IN}|$.
3. Design the load network to resonate Z_{IN} . That is, let

$$X_L(\omega_o) = -X_{IN}(\omega_o) \quad (5.3.4)$$

and

$$R_L = \frac{|R_{IN}(0, \omega_o)|}{3} \quad (5.3.5)$$

This design procedure is popular due to its high rate of success. However, the frequency of oscillation will shift somewhat from its designed value at ω_o . This occurs because the oscillation power increases until the negative resistance is equal to the load resistance and X_{IN} varies as a function of V (i.e., as a function of the oscillation power). Also, there is no assurance that the oscillator is providing optimum power.

Example 5.3.1

Design an 8-GHz GaAs FET oscillator using the reverse-channel configuration shown in Fig. 5.5.4. The S parameters of the transistor, in the reverse-channel configuration, at 8 GHz are

$$S_{11} = 0.98 \angle 163^\circ$$

$$S_{21} = 0.675 \angle -161^\circ$$

$$S_{12} = 0.39 \angle -54^\circ$$

$$S_{22} = 0.465 \angle 120^\circ$$

(This example is based on a design from Refs. [5.2] and [5.3].)

Solution. The transistor is potentially unstable at 8 GHz (i.e., $K = 0.529$) and the stability circle at the gate-to-drain port is shown in Fig. 5.3.2. In the notation of Fig. 5.3.1, the gate-to-drain port is the terminating port.

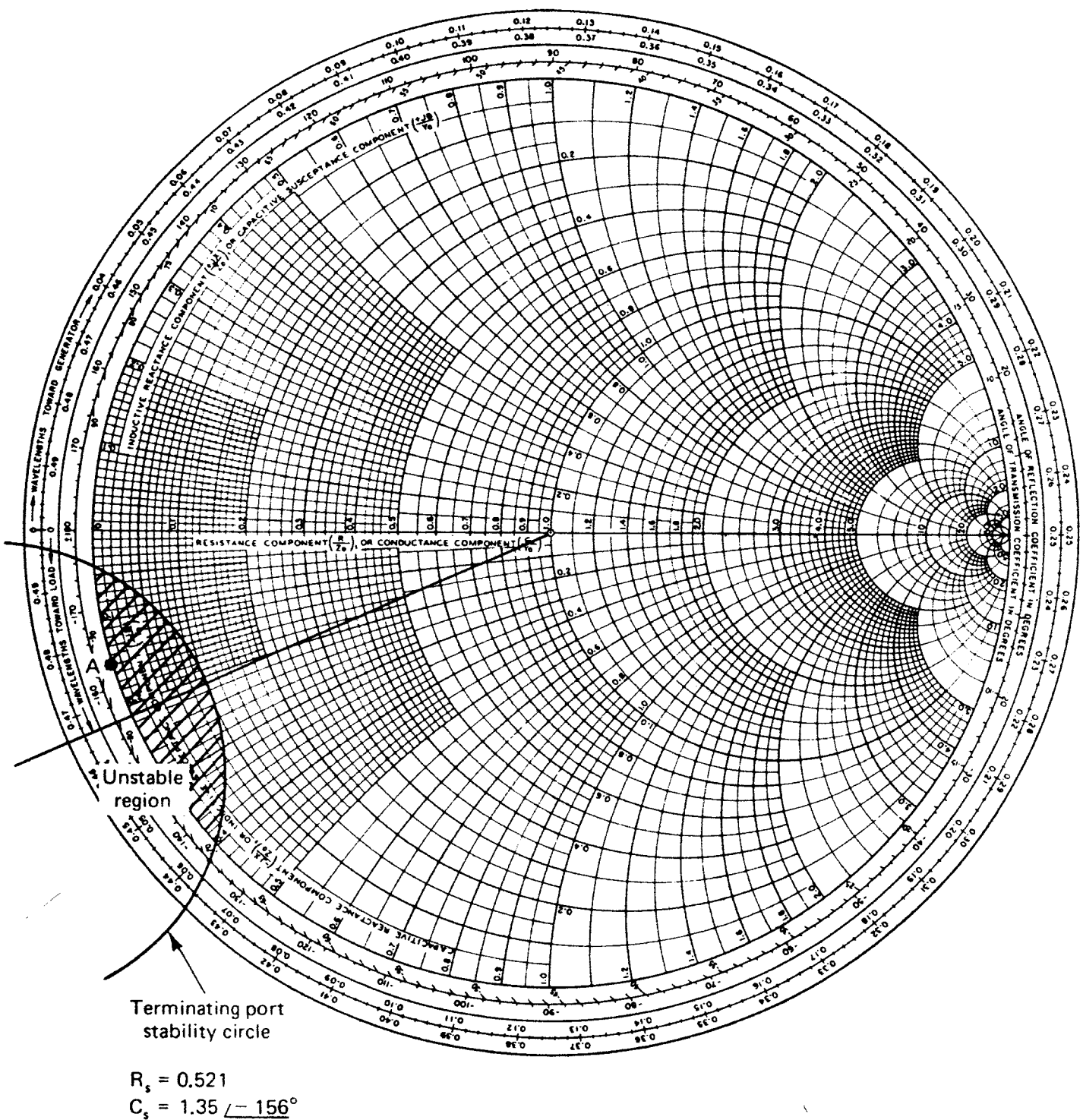


Figure 5.3.2 Terminating port stability circle.

As shown in Fig. 5.3.2, any Γ_T in the shaded region produces $|\Gamma_{IN}| > 1$ (i.e., a negative resistance at the input port). Selecting Γ_T at point A in Fig. 5.3.2 (i.e., $\Gamma_T = 1 \angle -163^\circ$), the associated impedance is $Z_T = -j7.5 \Omega$. This reactance can be implemented by an open-circuited 50- Ω line of length 0.226λ . With Z_T connected, the input reflection coefficient is found to be $\Gamma_{IN} = 12.8 \angle -16.6^\circ$, and the associated impedance is $Z_{IN} = -58 - j2.6 \Omega$. The load matching network is designed using (5.3.4) and (5.3.5), that is, $Z_L = 19 + j2.6 \Omega$ at $f_o = 8$ GHz.

As reported in Refs. [5.2] and [5.3], the oscillator was constructed and oscillated readily at frequencies between 7.5 and 7.8 GHz, with output power between 680 and 940 mW at $V_{DS} = 9$ V. Some tuning was necessary to move the oscillation frequency to 8 GHz.

Example 5.3.2

Design a 2.75-GHz oscillator using a BJT in a common-base configuration. The transistor S parameters at 2.75 GHz are

$$S_{11} = 0.9 \angle 150^\circ$$

$$S_{21} = 1.7 \angle -80^\circ$$

$$S_{12} = 0.07 \angle 120^\circ$$

$$S_{22} = 1.08 \angle -56^\circ$$

(This example is based on a design from Ref. [5.4].)

Solution. The transistor is potentially unstable at 2.75 GHz ($K = -0.64$). The instability of the transistor can be increased using external feedback. For the common-base configuration (and also for the common-gate configuration) a common lead inductance from base to ground (as shown in Fig. 5.3.3) is commonly used.

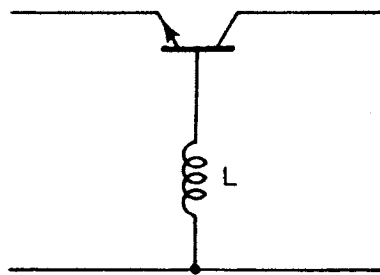


Figure 5.3.3 BJT with external feedback to increase instability.

Varying L from 0.5 nH to 15 nH shows that the instability at the input and output are optimized with $L = 1.45$ nH. With $L = 1.45$ nH, the resulting S parameters for the network in Fig. 5.3.3 are

$$S_{11} = 1.72 \angle 100^\circ$$

$$S_{21} = 2.08 \angle -136^\circ$$

$$S_{12} = 0.712 \angle 94^\circ$$

$$S_{22} = 1.16 \angle -102^\circ$$

and $K = -0.56$.

The common lead inductance has been used to raise $|S_{11}|$ and $|S_{22}|$ to large values. Since $|S_{11}| > |S_{22}|$, it appears that the emitter-to-ground port is the best place for the load network (i.e., the tuning network). Of course, these values are obtained with 50- Ω terminations, and 50- Ω terminations are not necessarily used for the matching networks.

The terminating network can be designed to present an impedance to the collector having a real part smaller than 50 Ω , and to couple the oscillator to a 50- Ω termination. A design for the terminating network is illustrated in Fig. 5.3.4. With the values shown in Fig. 5.3.4, $\Gamma_{IN} = 2.21 \angle 119^\circ$ ($Z_{IN} = -24 + j24.2 \Omega$). From (5.3.4) and (5.3.5) the impedance of the load matching network should be $Z_L = 8 - j24.2 \Omega$.

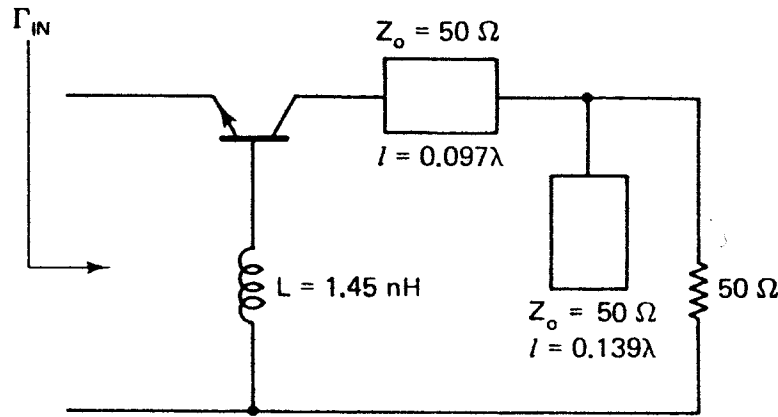


Figure 5.3.4 Terminating network design.

5.4 OSCILLATOR DESIGN USING LARGE-SIGNAL MEASUREMENTS

In this section a two-step method based on large-signal measurements is developed for oscillator design [5.5]. Basically, the method consists in designing the terminating network so that the two-port presents a large (i.e., optimum) negative resistance at the input port. The resulting one-port negative-resistance network can be placed in a nonoscillating circuit and the optimum load impedance as a function of power (i.e., large-signal measurements) can be measured.

The reflection coefficient Γ_{IN} for the network in Fig. 5.3.1 is given by

$$\Gamma_{IN} = \frac{S_{11} - \Delta \Gamma_T}{1 - S_{22} \Gamma_T}$$

which can be manipulated into the form

$$\begin{aligned} \Gamma_{IN} &= \frac{S_{11} - \Delta S_{22}^*}{1 - |S_{22}|^2} + \frac{S_{12} S_{21}}{1 - |S_{22}|^2} \frac{\Gamma_T - S_{22}^*}{1 - S_{22} \Gamma_T} \\ &= \Gamma_{IN,o} + \alpha \Gamma'_T \end{aligned} \quad (5.4.1)$$

where

$$\Gamma_{IN,o} = \frac{S_{11} - \Delta S_{22}^*}{1 - |S_{22}|^2} \quad (5.4.2)$$

$$\alpha = \frac{S_{12} S_{21}}{1 - |S_{22}|^2} \frac{1 - S_{22}^*}{1 - S_{22}} \quad (5.4.3)$$

and

$$\Gamma'_T = \frac{Z_T - Z_{22}^*}{Z_T + Z_{22}} \quad (5.4.4)$$

Z_{22} is the impedance associated with S_{22} .

A simple graphical method can be developed to relate Γ_T to Γ_{IN} . The transformation in (5.4.1) shows that the magnitude of Γ'_T (i.e., the Γ'_T plane normalized to Z_{22}) is multiplied by $|\alpha|$ and the phase of Γ'_T is rotated by $\angle \alpha$. Since $\Gamma_{IN,o}$ is a constant in the Γ_{IN} plane, its contribution is to shift the center of Γ'_T . A typical transformation is illustrated in Fig. 5.4.1. Any Γ'_T in the shaded area will cause oscillations.

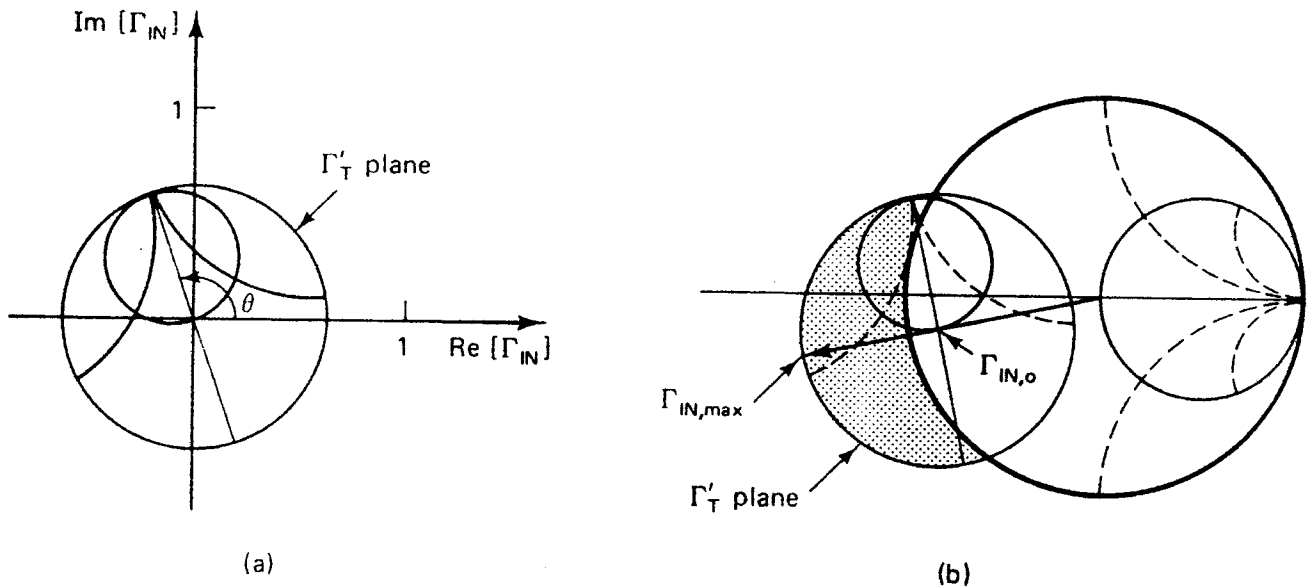


Figure 5.4.1 (a) Γ'_T plane scaled by α , where $\theta = \arg(\alpha)$; (b) typical mapping from Γ'_T plane to Γ_{IN} according to (5.4.1).

From (5.4.1), $|\Gamma_{IN}|$ is a maximum when $|\Gamma'_T| = 1$ and $\alpha\Gamma'_T$ is in the direction of $\Gamma_{IN,o}$. That is,

$$\Gamma_{IN,max} = \Gamma_{IN,o} + |\alpha| \hat{u}_{IN,o} \quad (5.4.5)$$

where $\hat{u}_{IN,o}$ is a unit vector in the direction of $\Gamma_{IN,o}$. The value of $\Gamma_{IN,max}$ is illustrated in Fig. 5.4.1b.

The value of Γ_T that maximizes Γ_{IN} , called $\Gamma_{T,o}$, is given by

$$\Gamma_{T,o} = \frac{1 + (\hat{u}_{12}/\hat{u}_{IN,o})S_{22}^*}{(\hat{u}_{12}/\hat{u}_{IN,o}) + S_{22}} \quad (5.4.6)$$

where \hat{u}_{12} is a unit vector in the direction of $S_{12} S_{21}$. The associated input and

terminating impedances are

$$Z_{IN,max} = \frac{1 + \Gamma_{IN,max}}{1 - \Gamma_{IN,max}} \quad (5.4.7)$$

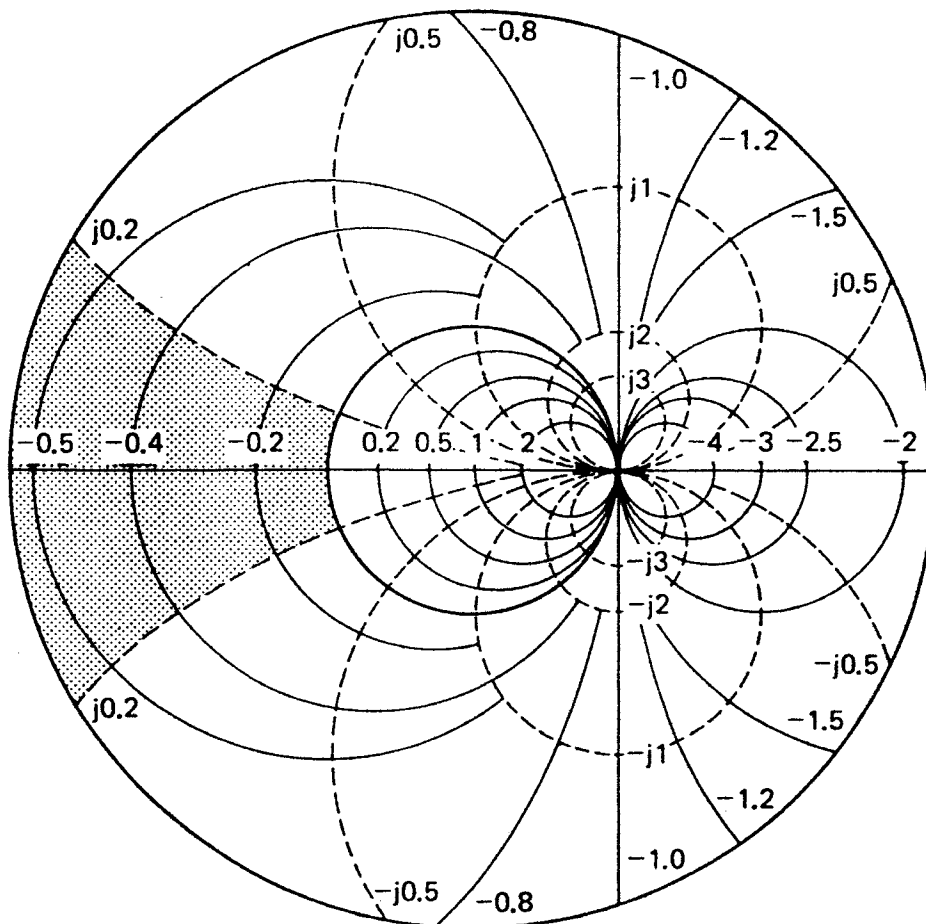
and

$$Z_{T,o} = \frac{1 + \Gamma_{T,o}}{1 - \Gamma_{T,o}} \quad (5.4.8)$$

The value of $\Gamma_{T,o}$ in (5.4.6) produces an optimum Γ_{IN} (i.e., $\Gamma_{IN,max}$). In other words, the two-port network has been reduced to an optimum negative-resistance one-port by maximizing the small-signal input reflection coefficient of the transistor. Thus far, only the small-signal S parameters of the transistor were used since the optimized Γ_{IN} is the amplitude-independent small-signal input reflection coefficient.

The one-port negative-resistance oscillator can now be characterized by measuring the input impedance as a function of input power at the frequency ω_o . This is a large-signal characterization of the one-port which is also called a *device-line characterization*.

It is a good idea to place $\Gamma_{IN,max}$ within the range shown in Fig. 5.4.2. In this range the associated $|R_{IN,max}|$ is less than 50Ω and $X_{IN,max}$ is small. The reason for this selection is that in the design procedure that follows we need to take some measurements at the input port with a $50\text{-}\Omega$ source impedance. Also, the larger the ratio $|R_{IN,max}|/X_{IN,max}$, the larger the Q .



The method described establishes the terminating impedance that reduces the two-port to an optimum negative-resistance one-port. The one-port can now be characterized by large-signal measurements.

The large-signal characterization is achieved by measuring, in the circuit shown in Fig. 5.4.3, the current I_D and the impedance $Z_{IN}(I_D, \omega_o)$, as V_s is varied. The measurements are made at the desired frequency of oscillation ω_o , and the source resistance is typically $50\ \Omega$. With $|R_{IN, \max}|$ selected in the range shown in Fig. 5.4.2, the circuit in Fig. 5.4.3 is stable.

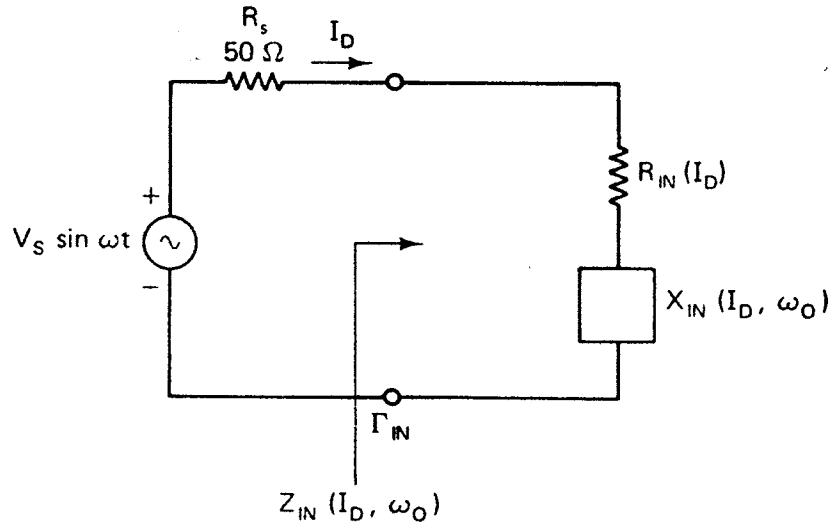


Figure 5.4.3 Large-signal measuring circuit.

In the circuit shown in Fig. 5.4.3, the current I_D is given by

$$I_D = \frac{V_s}{R_s + R_{IN}(I_D) + jX_{IN}(I_D, \omega_o)} \quad (5.4.9)$$

and the power delivered by the negative resistance $R_{IN}(I_D)$ is

$$P_D(\omega_o) = \frac{1}{2} |I_D|^2 |R_{IN}(I_D)|$$

The measurement of P_D versus $Z_{IN}(I_D, \omega_o)$ generates the large-signal characteristics of the one-port network. If the one-port is now terminated in the load impedance (see Fig. 5.2.1),

$$Z_L(\omega_o) = -Z_{IN}(I_D, \omega_o)$$

the power delivered to Z_L is given by $P_L(\omega_o) = P_D(\omega_o)$.

Obviously, the measurement of I_D at microwave frequencies is difficult. Therefore, in practice the reflection coefficient Γ_{IN} as a function of the available power from the source is measured. The available power from the source

is given by

$$P_{\text{AVS}} = \frac{V_s^2}{8R_s}$$

The power added P_{ADD} (i.e., the reflected minus the available input power) is given by

$$P_{\text{ADD}} = P_{\text{AVS}}(|\Gamma_{\text{IN}}|^2 - 1)$$

and can be expressed in the form

$$P_{\text{ADD}} = \frac{V_s^2 |R_{\text{IN}}|}{2[(R_{\text{IN}} + R_s)^2 + X_{\text{IN}}^2]} \quad (5.4.10)$$

Substituting (5.4.9) into (5.4.10) gives

$$P_{\text{ADD}} = \frac{|I_D|^2}{2} |R_{\text{IN}}|$$

which shows that the added power is the power that the one-port will deliver to the load $Z_L(\omega_o) = -Z_{\text{IN}}(I_D, \omega_o)$.

The large-signal characterizations of the one-port are generated by measuring Γ_{IN} and P_{AVS} , and calculating P_{ADD} versus Z_{IN} as a function of I_D at the desired frequency of oscillation ω_o .

There are several ways of implementing the load impedance $Z_L(\omega_o)$ and, of course, not all of them will give us a stable oscillation. For a stable oscillation we have to check that $Z_L(\omega_o)$ satisfies the condition given in (5.2.5). This can be achieved easily since the amplitude dependence of $R_{\text{IN}}(I_D)$ can be obtained from the measured data, and the required impedance variation (i.e., $dX_L/d\omega \geq 0$) can be determined.

In conclusion, the design procedure uses the small-signal S parameters to establish the terminating impedance that results in an optimum negative-resistance one-port network. Then the one-port oscillator performance is described by the measured large-signal characteristics.

Example 5.4.1

Design an oscillator using a GaAs FET whose S parameters at 10 GHz are

$$S_{11} = 0.9 \angle 180^\circ$$

$$S_{12} = 0.79 \angle -98^\circ$$

$$S_{21} = 0.89 \angle -163^\circ$$

$$S_{22} = 0.2 \angle 180^\circ$$

(This example is based on a design from Ref. [5.5].)

Solution. For this transistor $K = 0.51$, showing that the device is potentially unstable. $\Gamma_{T,o}$ and $\Gamma_{\text{IN},\text{max}}$ and the associated $Z_{T,o}$ and $Z_{\text{IN},\text{max}}$ can be determined from (5.4.2) to

(5.4.8), namely

$$\Gamma_{IN,o} = 0.89 \angle -171^\circ$$

$$\alpha = 0.76 \angle 99^\circ$$

$$\Gamma_{T,o} = 1 \angle 114^\circ$$

$$Z_{T,o} = j0.66$$

$$\Gamma_{IN,max} = 1.65 \angle -171^\circ$$

$$Z_{IN,max} = -0.247 - j0.074$$

The complete mapping of the Γ_T plane into the Γ_{IN} plane is illustrated in Fig. 5.4.4. Observe the locations of $\Gamma_{IN,o}$ and $\Gamma_{IN,max}$.

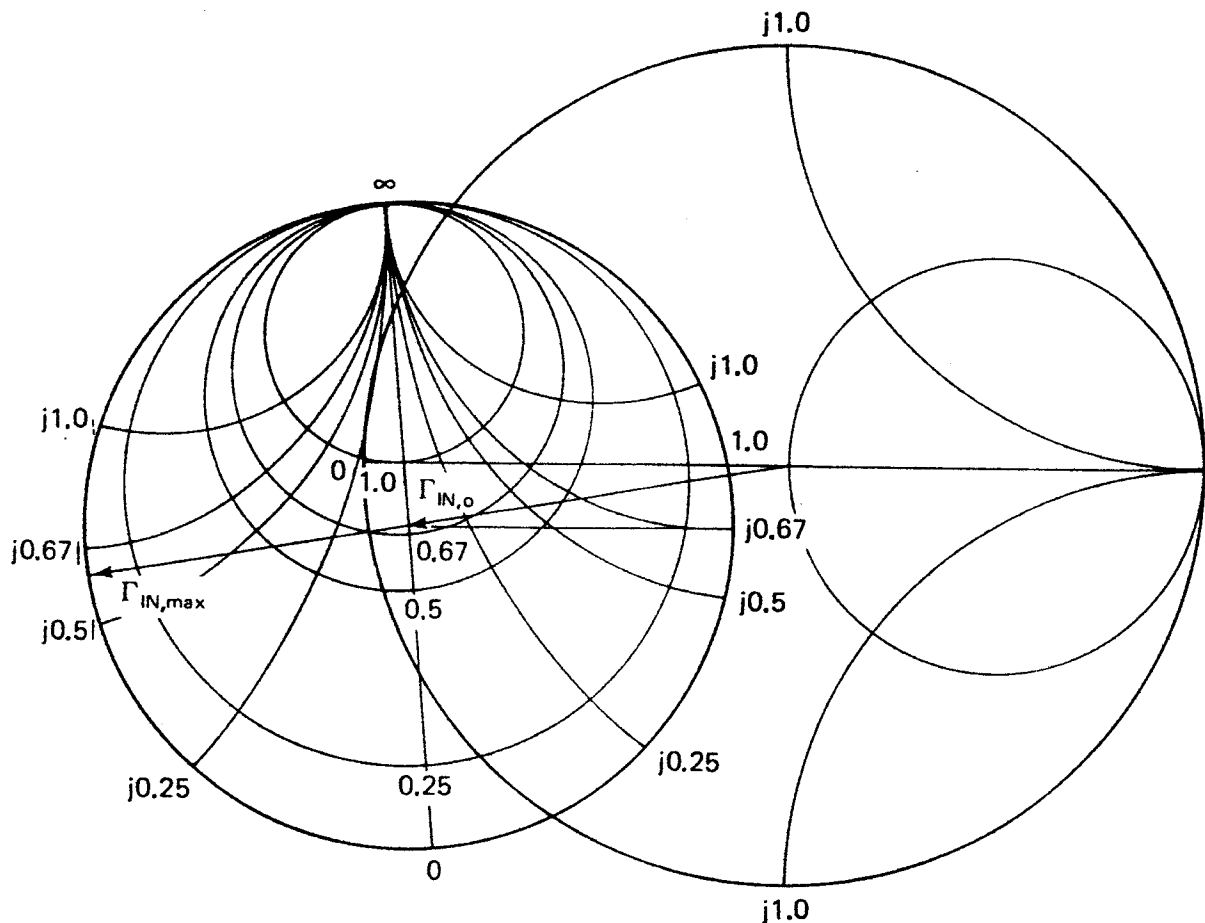


Figure 5.4.4 Mapping of Γ_T plane into the Γ_{IN} plane. (From W. Wagner [5.5]; reproduced with permission of *Microwave Journal*.)

With the termination $Z_{T,o} = j0.66$, the transistor large-signal characteristics are now measured. The results from the large-signal measurements are given in Fig. 5.4.5. It is observed that the maximum power added is 45 mW when $Z_L = 4 - j7.5 \Omega$.

5.5 OSCILLATOR CONFIGURATIONS

At the low end of the microwave frequency range, lumped-element oscillators are commonly used. Three basic oscillator configurations used are the Colpitts, Hartley, and Clapp oscillators. They are shown in Fig. 5.5.1 in a

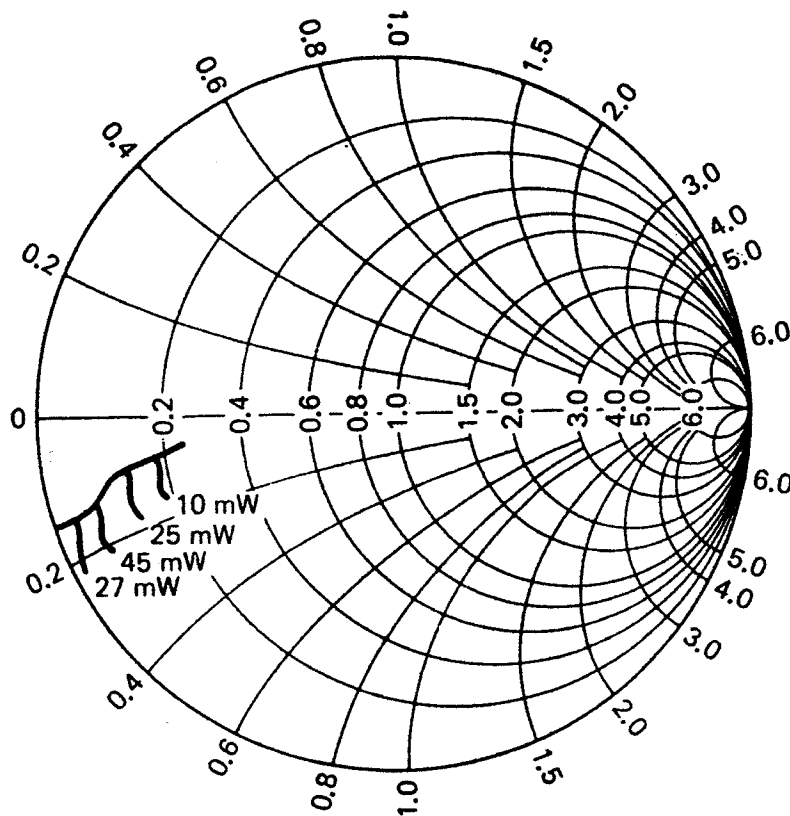


Figure 5.4.5 Large-signal characteristic at 10 GHz with $Z_{T,o} = j0.66$. (From W. Wagner [5.5]; reproduced with permission of *Microwave Journal*.)

common-base transistor configuration. The Colpitts network uses a capacitor voltage divider in the tuned circuit to provide the correct feedback. The Hartley network uses a tapped inductor tuned circuit, and the Clapp network is similar to the Colpitts network but with an extra capacitor in series with the inductor to improve the frequency stability.

The high- Q tapped inductor required in the Hartley's oscillator is difficult to build. Therefore, the Colpitts and Clapp oscillators are usually preferred.

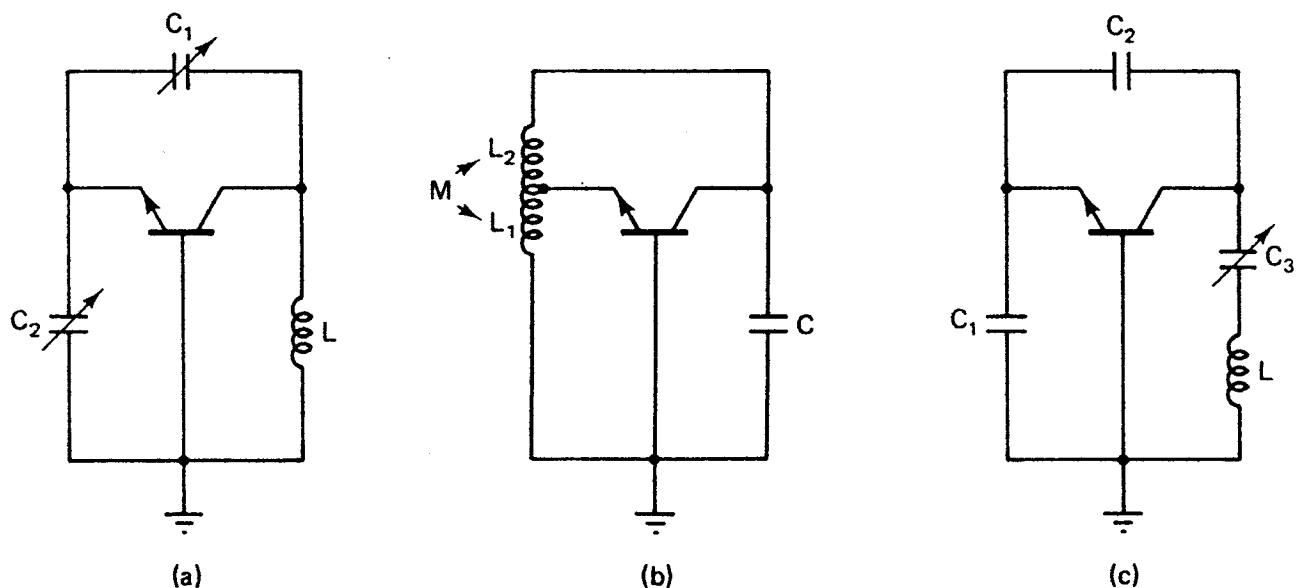


Figure 5.5.1 Three types of common-base transistor configurations: (a) Colpitts; (b) Hartley; (c) Clapp.

At higher microwave frequencies (i.e., in the gigahertz range), the parasitic capacitances of the packaged transistors provide some or all the feedback needed for oscillation. In this range the negative-resistance design procedure is used, since the S parameters provide all the needed design information. The negative-resistance design procedure basically consists of selecting a transistor in an oscillator topology that provides the required output power. The transistor in the configuration selected must be potentially unstable at the desired frequency of oscillation. Feedback can be added to increase the negative resistance associated with Γ_{IN} or Γ_{OUT} . The terminating and load matching networks must be designed to provide the proper resonance conditions.

For a BJT negative-resistance oscillator the most effective network topology is the common-base configuration. This configuration, illustrated in Fig. 5.5.2, is used in low-power oscillator circuits, and it is easy to tune. The inductor feedback element is used to increase $|\Gamma_{IN}|$ and $|\Gamma_{OUT}|$. Common-emitter and common-collector configurations have also been used in microwave oscillators.

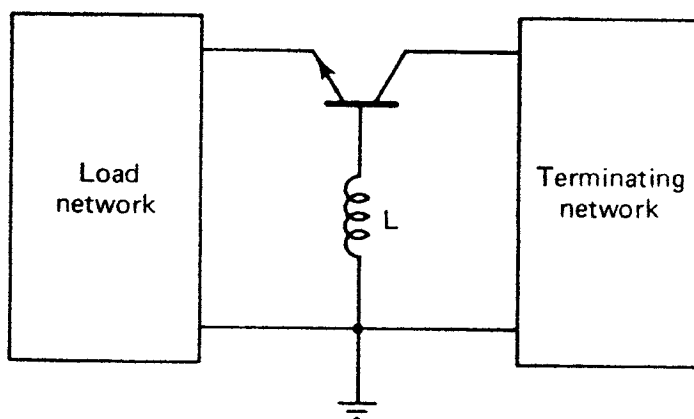


Figure 5.5.2 Common-base configuration.

The two common network configurations for GaAs FETs oscillators are shown in Fig. 5.5.3. The common-gate configuration is used in low-power oscillator circuits since it is easy to tune. A series inductive feedback is usually required to improve $|\Gamma_{IN}|$ and $|\Gamma_{OUT}|$. The common-source configuration is used for higher oscillator output power and the feedback network is usually a capacitor. The common-drain configuration is not popular because the oscillator implementation is difficult.

A GaAs FET oscillator can also be built using the reverse-channel configuration shown in Fig. 5.5.4. A reverse-channel configuration uses a symmetrical GaAs FET with a negative voltage applied to the drain terminal. The transistor becomes a noninverting device, making the common lead inductance regenerative. The S parameters in this reverse-channel configuration show that $|S_{12}|$ increases markedly with frequency and $|S_{11}|$ is greater than unity in a large frequency range.

Vendelin [5.6] shows some configurations, and discusses some design procedures, for low-noise oscillators and buffered oscillators.

The load tuning elements are not limited to lossless or RLC networks.

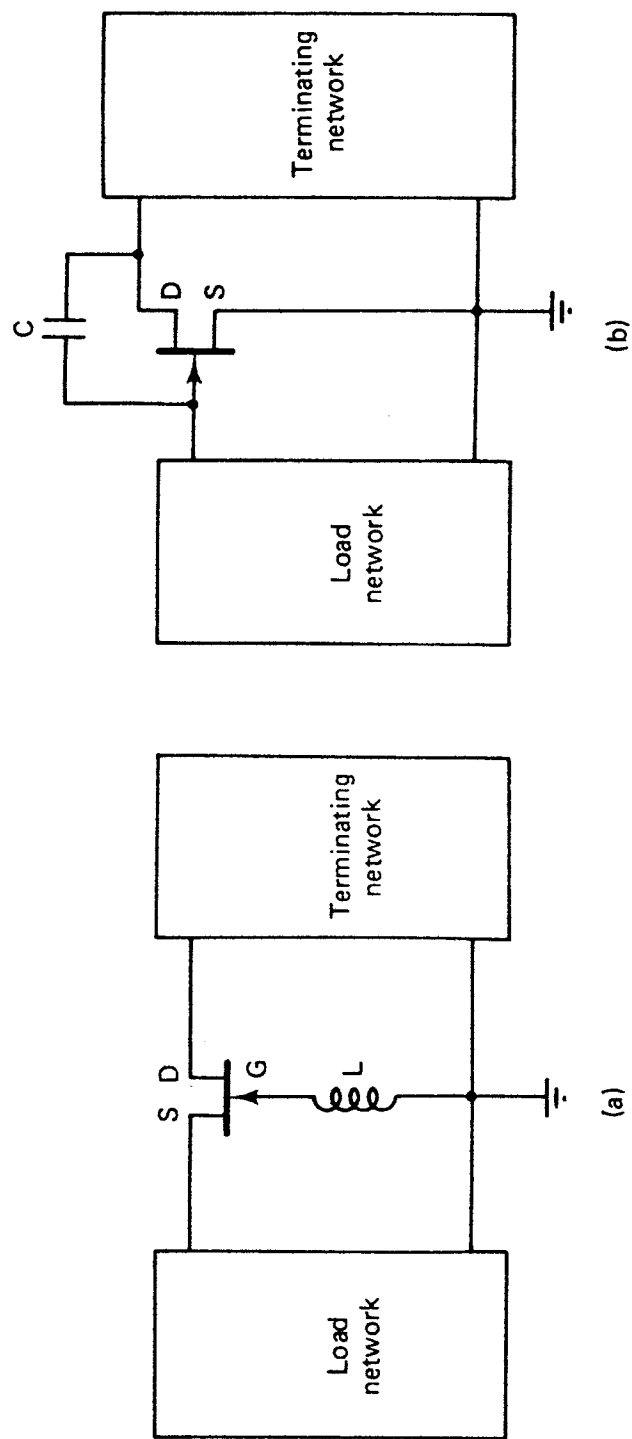


Figure 5.5.3 (a) Common-gate configuration; (b) common-source configuration.

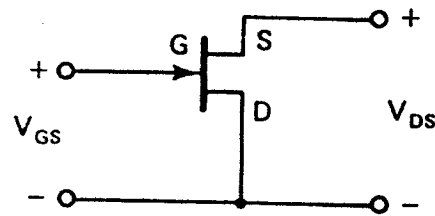


Figure 5.5.4 Reverse-channel GaAs FET.

Load tuning networks can be designed using YIG (yttrium iron garnet) resonators, varactor diodes, and so on.

A YIG resonator consists of a ferrimagnetic material which can be modeled by a parallel RLC resonant circuit. The value of the elements depend on the magnetization, coupling, and resonance linewidth of the YIG sphere, and on the applied dc magnetic field. The uniform dc magnetic field is applied with an electromagnet with a single gap. The gap design is important since a nonuniform dc magnetic field results in a tuning hysteresis and spurious responses. A common-gate GaAs FET oscillator using a YIG resonator is shown in Fig. 5.5.5.

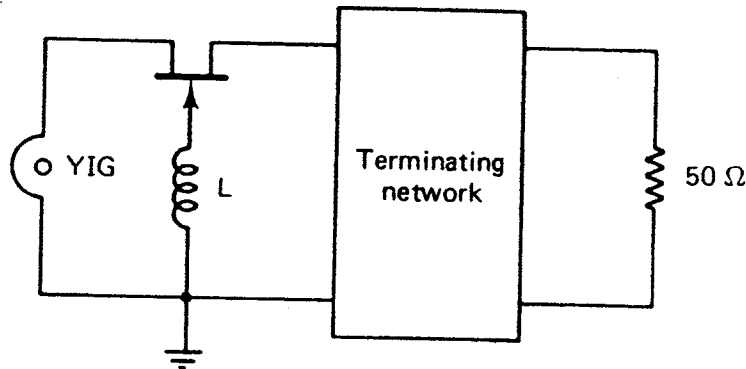


Figure 5.5.5 YIG-tuned oscillator.

The YIG sphere is strongly coupled to the transmission line that connects to the active device. Assuming that the YIG sphere is always magnetically saturated and that the sphere diameter is $\ll \lambda/4$, the YIG device can be modeled by a parallel resonant circuit, as shown in Fig. 5.5.6. The element values are given by [5.7]

$$G_o = \frac{d^2}{\mu_o V \omega_m Q_U} + G_L$$

$$L_o = \frac{\mu_o V \omega_m}{\omega_o d^2}$$

$$C_o = \frac{1}{\omega_o^2 L_o}$$

where

$$\omega_m = \gamma 8 \pi^2 M_s$$

$$Q_U = \frac{H_o - 4 \pi M_s / 3}{\Delta H}$$

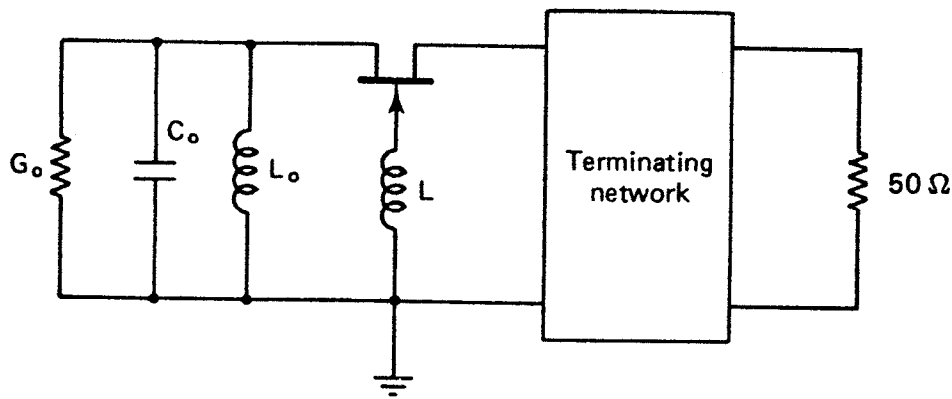


Figure 5.5.6 Equivalent network of a YIG sphere in a YIG-tuned oscillator.

Here $4\pi M_s$ is the saturation magnetization of the sphere, $\mu_o = 4\pi(10^{-7})$ henrys per meter, V is the volume of the sphere, d the coupling loop diameter, γ the gyromagnetic ratio (2.8 MHz/Oe), H_o the applied dc magnetic field, Q_U the unloaded Q , ΔH the resonance line width (approximately 0.2 Oe), and ω_o the center frequency of resonance. The frequency ω_o can be expressed as

$$\omega_o = 2\pi\gamma H_o$$

A varactor-tuned oscillator uses the voltage-controlled capacitance of a varactor diode to accomplish the electronic tuning. A basic schematic of a varactor-tuned oscillator is shown in Fig. 5.5.7.

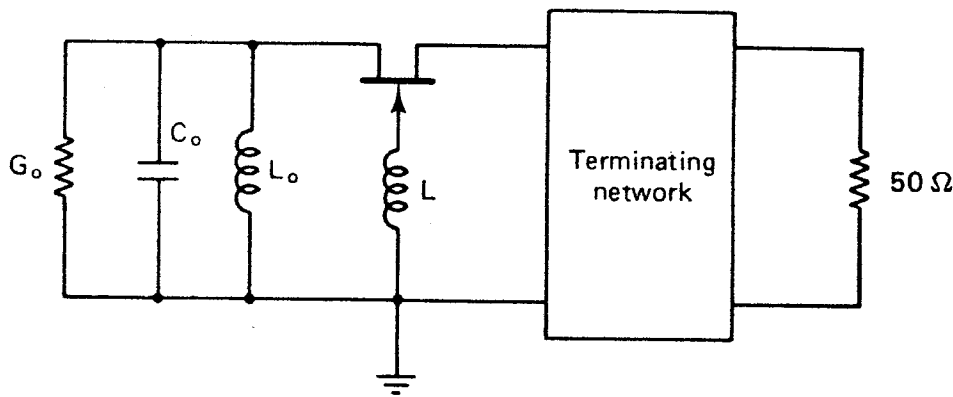


Figure 5.5.7 Varactor-tuned oscillator.

Varactor diodes of different types having a wide range of capacitances are available. In the varactor circuit model shown in Fig. 5.5.8, the varactor diode capacitance (C_v), for Schottky-type devices, is given by the formula

$$C_v = \frac{C_o}{(1 + V/\phi)^{1/2}}$$

where C_o is the value of capacitance at zero voltage, V the reverse bias voltage, and ϕ the junction contact potential ($\phi \approx 0.7$ V). The resistance R_s represents the series resistance of the diode, and the reverse diode resistance R_r is large and therefore can be neglected.

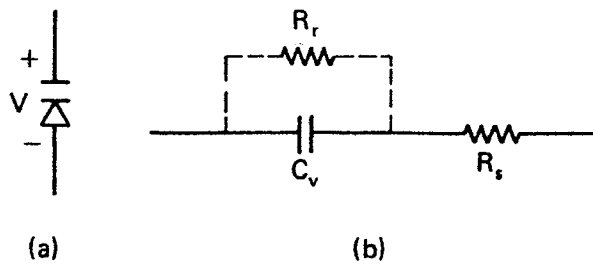


Figure 5.5.8 (a) Varactor diode circuit symbol; (b) model.

PROBLEMS

- 5.1. Design a 2-GHz oscillator using a BJT with external feedback as shown in Fig. 5.3.3. The S parameters of the network at 2 GHz are as follows:

	$L = 0 \text{ H}$	$L = 0.5 \text{ nH}$
S_{11}	$0.94 \angle 174^\circ$	$1.04 \angle 173^\circ$
S_{21}	$1.90 \angle -28^\circ$	$2.00 \angle -30^\circ$
S_{12}	$0.013 \angle 98^\circ$	$0.043 \angle 153^\circ$
S_{22}	$1.01 \angle -17^\circ$	$1.05 \angle -18^\circ$

(This problem is based on a design from Ref. [5.6].)

- 5.2. In Problem 5.1 implement the input tuning network using a YIG sphere. Specify the characteristics of the YIG sphere.
- 5.3. Design the input tuning network for the oscillator in Example 5.3.1.
- 5.4. Design a 10-GHz oscillator using a common-gate GaAs FET. The S parameters of the transistor at 10 GHz, $V_{DS} = 6 \text{ V}$, $I_{DS} = 150 \text{ mA}$, are

$$S_{11} = 0.85 \angle -36^\circ$$

$$S_{21} = 0.53 \angle 96^\circ$$

$$S_{12} = 0.22 \angle -36^\circ$$

$$S_{22} = 1.125 \angle 171^\circ$$

Show the dc bias network.

- 5.5. Implement the input tuning network of Example 5.3.2 using a varactor diode. Specify the diode characteristics.
- 5.6. Verify the relations (5.4.1) to (5.4.6).
- 5.7. Design an 8-GHz GaAs FET oscillator using the large-signal method discussed in Section 5.4. The S parameters of the transistor at 8 GHz are

$$S_{11} = 0.8 \angle 140^\circ$$

$$S_{12} = 0.2 \angle -70^\circ$$

$$S_{21} = 0.8 \angle 140^\circ$$

$$S_{22} = 0.9 \angle 170^\circ$$

The large-signal characteristics with the termination $Z_{T,o}$ are shown in Fig. P5.5.

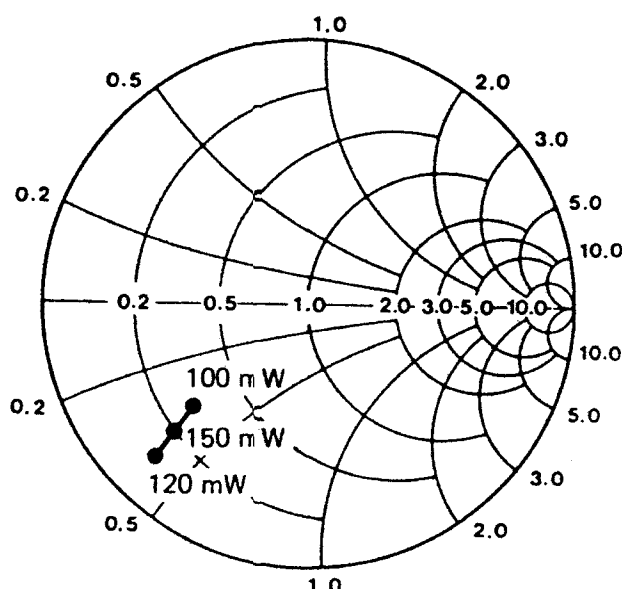


Figure P5.5

- 5.8. (a) Johnson [5.8] shows that the output power of an oscillator can be approximated with the equation

$$P_{\text{OUT}} = P_{\text{sat}} (1 - e^{-G_o P_{\text{IN}} / P_{\text{sat}}})$$

where P_{sat} is the saturated output power of the amplifier, P_{IN} is the input power, and G_o is the small-signal power gain. Show that the maximum oscillator power [$P_{\text{osc}}(\text{max})$] is given by

$$P_{\text{osc}}(\text{max}) = P_{\text{sat}} \left(1 - \frac{1}{G_o} - \frac{\ln G_o}{G_o} \right)$$

and the maximum efficient gain, defined by

$$G_{\text{ME}} = \frac{P_{\text{OUT}} - P_{\text{sat}}}{P_{\text{IN}}}$$

is given by

$$G_{\text{ME}}(\text{max. oscillator power}) = \frac{G_o - 1}{\ln G_o}$$

Hint: The maximum oscillator power occurs at the point of maximum $P_{\text{OUT}} - P_{\text{IN}}$, or where

$$\frac{\partial P_{\text{OUT}}}{\partial P_{\text{IN}}} = 1$$

- (b) A GaAs FET has $G_o = 7.5$ dB with $P_{\text{sat}} = 1$ W. Calculate the maximum oscillator power and the corresponding maximum gain.
- (c) Draw typical $P_{\text{osc}}/P_{\text{sat}}$ versus G_o , and G_{ME} (maximum oscillator power) versus G_o plots.
- 5.9. The conductance of a two-terminal negative-resistance device used in a YIG-tuned oscillator has a dependence on RF voltage amplitude A given by $-G = (15 - 2A) \times 10^{-3}$ S, where $A < 7.5$ V. Assuming an equivalent circuit of the form shown in Fig. P5.9 plot the power variation of the oscillator when the dc magnetic field is increased from 3000 to 4500 Oe. Use $V = 0.75 \times 10^{-6} \text{ m}^3$, $d = 2$ mm, $4\pi M_s = 1750$ G, $G_L = 10$ mS, $l = 10$ mm, $Z_o = 200 \Omega$, and $\Delta H = 0.5$ Oe.

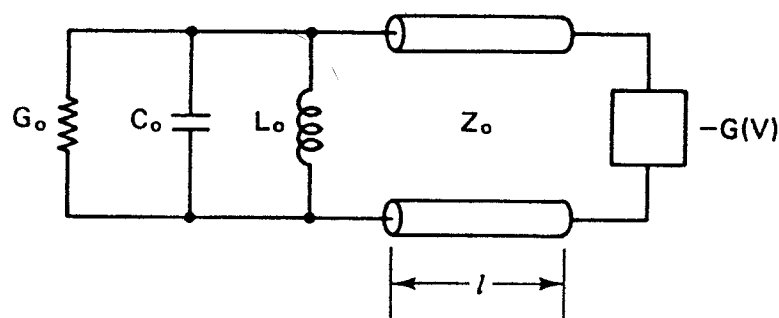


Figure P5.9

REFERENCES

- [5.1] K. Kurokawa, "Some Basic Characteristics of Broadband Negative Resistance Oscillator Circuits," *The Bell System Technical Journal*, July 1969.
- [5.2] P. C. Wade, "Novel FET Power Oscillators," *Electronics Letters*, September 1978.
- [5.3] P. C. Wade, "Say Hello to Power FET Oscillators," *Microwaves*, April 1979.
- [5.4] COMPACT reference manual, Compact Software, Inc., 1131 San Antonio Road, Palo Alto, CA 94303.
- [5.5] W. Wagner, "Oscillator Design by Device Line Measurement," *Microwave Journal*, February 1979.
- [5.6] G. D. Vendelin, *Design of Amplifiers and Oscillators by the S Parameter Method*, Wiley-Interscience, New York, 1982.
- [5.7] D. V. Morgan and M. J. Howes, editors, *Microwave Solid State Devices and Applications*, Peter Peregrinus Ltd., New York, 1980.
- [5.8] K. M. Johnson, "Large Signal GaAs MESFET Oscillator Design," *IEEE Transactions on Microwave Theory and Techniques*, March 1979.

APPENDIX A

COMPUTER-AIDED DESIGN: COMPACT AND SUPER-COMPACT*

The use of computer analysis and optimization programs is of great importance in the design of microwave transistor amplifiers. In some designs, straightforward calculations are a tedious process, and a CAD program is a must. In fact, CAD methods are extremely valuable when used in conjunction with good engineering principles.

In this appendix, some of the capabilities of the programs COMPACT and SUPER-COMPACT [A.1] are described first, followed by an example. Although the program COMPACT is now considered to be an "old" program, the example is worked using both COMPACT and SUPER-COMPACT. These large-scale CAD programs are very powerful, providing a wide range of capabilities.

Among the features of COMPACT are: circuit analysis, stability analysis, sensitivity analysis, optimization (up to 15 variables), a Monte Carlo analysis that permits the designer to evaluate component tolerances, and so on. SUPER-COMPACT, introduced in 1980, provides all the features of COMPACT, plus a host of new capabilities. Some of the new capabilities of SUPER-COMPACT are an efficient circuit interconnection feature, total file flexibility, interactive graphics, better optimization, new circuit elements, and so on. The interactive graphics plots polar or rectangular charts of S parameters, constant-noise circles, constant-gain and stability circles, and so on. The reader should refer to Ref. [A.1] for the full range of capabilities of these programs.

The following example illustrates the use of the large-scale CAD programs COMPACT and SUPER-COMPACT in the analysis, design, and optimization of a microwave transistor amplifier.

*COMPACT and SUPER-COMPACT are trademarks of Compact Software, Inc. [A.1].

> 1

ENTER GAIN IN DBS -- START,STOP,STEP

> 9 10 2

***** OPERATING POWER GAIN CIRCLES *****

9.0000000 DB GAIN CIRCLE . RADIUS= .43090543
CENTER.MAG = .50827681 CENTER.ANG = 103.93965

ENTER 1 FOR OPERATING GAIN CIRCLES.
2 FOR AVAILABLE GAIN CIRCLES.
3 FOR EXIT

> 3

MENU SELECTION

> 7

ENTER 1 FOR INPUT REFLECTION COEFFICIENT
2 FOR OUTPUT REFLECTION COEFFICIENT
3 TO EXIT

> 1

ENTER GAMMA TERMINATION (MAG,ANG)

> .36 47.5

***** THE INPUT REFLECTION COEFFICIENT *****
GAMMA.MAG = .62902135 GAMMA.ANG = -175.51289

@FIN

INDEX

ABCD parameters, 2-4, 24-25

matrix, 1-3

Active bias:

BJT, 130

GaAs FET, 133

Added power, 207

Admittance coordinates Smith chart (see Smith chart)

Admittance parameters, 2-4, 24-26

matrix, 2

AM to PM conversion, 181

Amplifier:

balanced, 159-60

bandwidth, 170-74

broadband, 154-69

feedback, 102, 155, 160-66

high-power, 174-87

low-noise, 140-54

stability (see Stability)

tuning, 169-70

two-stage, 187-88

AMPSYN, 156, 193

Attenuation constant, 5

Available noise power, 141

Available power, 15-18, 21, 85-86, 92, 206-7

Available power gain (see also Power gain):

circles (see Constant-gain circles)

maximum, 32

Average power, 14

Balanced amplifier, 159-60

Balanced shunt stubs, 75-76, 78-79

Bandwidth:

analysis, 170-74

inherent, 171-72

reduction factor, 174

Beta cutoff frequency, 28-29, 33

Bias circuit (see dc bias)

BJT:

bias (see dc bias)

characteristics, 31-34, 139

figure of merit, 32

junction temperature, 181

model, 31-32

Boltzman constant, 140

Broadband design, 154-69

CAD, 155, 166, 217-40

Capacitor:

bypass, 130

chip, 75

coupling, 75

Cascade, 3-4, 11

Chain parameters, 2

matrix, 2-3

Chain scattering parameters, 11

matrix, 8, 11-12

Characteristic impedance:

complex, 5

microstrip, 68-69

real, 13

transmission line, 5, 7, 13

Chip, 23, 27-28

- Class:
 - A operation, 130, 133, 139
 - AB operation, 130, 133
 - B operation, 130, 133
- COMPACT, 217–22
- Compensated matching networks, 155, 158
- Complex propagation constant, 5
- Compressed Smith chart (*see* Smith chart)
- Compression point (*see* Gain compression point)
- Computer-aided design (*see* CAD)
- Conduction loss, 72
- Conjugate match:
 - maximum gain, 112–14
 - simultaneous (*see* Simultaneous conjugate match)
- Constant-conductance circles, 46
- Constant-gain circles:
 - available power gain, 123
 - potentially unstable, 123–25
 - unconditionally stable, 123
- operating power gain, 119–25
 - potentially unstable, 123–25
 - unconditionally stable, 119–23
- transducer power gain, 102–10, 114–19
 - bilateral case, 114–19
 - potentially unstable, 118–19
 - unconditionally stable, 114–15
 - unilateral case, 102–10
 - potentially unstable, 106–10
 - unconditionally stable, 103–6
- Constant-reactance circles, 44, 46
- Constant-resistance circles, 44, 46
- Constant-susceptance circles, 46
- Contact potential, 213
 - resistance, 27
- Conversions, 23–26
- Coupler, 159
- dc bias:
 - BJT, 125–30
 - GaAs FET, 131–33
 - networks, 128–33
 - operating point, 130–31, 133
 - stability, 126–27
- Device-line characterization, 205
- Dielectric constant:
 - effective, 68
 - relative, 67
- Dielectric loss, 72
- Dielectric substrate, 67
- Dispersion, 71–72
- Distortion, 177, 180
- Dynamic range, 175, 180
 - free spurious, 179–80
- Ell matching sections, 55–56
- Error function, 219–20, 225
- Fano, 167
- Feedback:
 - negative (*see* Negative feedback)
 - series, 161
 - shunt, 161
- Figure of merit, 32, 114
- Flow graph (*see* Signal flow graphs)
- GaAs FET:
 - bias (*see* dc bias)
 - characteristics, 34–36, 139
 - junction temperature, 181
 - model, 34–36
- Gain-bandwidth, 32
- Gain circles (*see* Constant-gain circles)
- Gain compression point, 175
- Gate length, 35
- Gyromagnetic ratio, 213
- h* parameters (*see* Hybrid parameters)
- h_{FE} , 32, 126–27
- Hybrid combiner/divider, 181–82
- Hybrid parameters, 2, 4, 24–25
 - matrix, 2
- Hybrid- π model, 31
- I_{CBO} , 126–27
- IGFET, 34
- Impedance coordinates Smith chart (*see* Smith chart)
- Impedance matching networks (*see* Matching)
- Impedance parameters, 1–4, 24–25
 - matrix, 2
- Incident:
 - power, 14
 - voltage, 14
 - wave, 5, 9–10, 14, 20
- Incoming wave, 5
- Indefinite scattering matrix, 29
- Input reflection coefficient (*see* Reflection coefficient)
- Input stability circle, 96
- Insulated-gate field-effect transistor (*see* IGFET)
- Interdigitated, 159
- Intermodulation distortion:
 - products, 178–79
 - third-order, 178
- Interstage design, 155–56, 187
- JFET, 34
- Junction field-effect transistor (*see* JFET)
- Lange coupler, 159–60
- Large signal:
 - characterization, 174–75
- Electrical length, 5, 13
- Electron transit time, 35
 - saturation drift velocity, 35

- measurements, 176–78, 203–8
- scattering parameters, 174–78
- Low-noise amplifier (*see* Amplifier)
- Mason's rule, 83–86**
- Matched line, 8
 - impedance, 16
 - load, 85–86
 - termination, 10, 21
- Matching:
 - network, 55–56
 - network design, 55–67, 74–80, 116–19, 147–49, 157–59, 185–86, 203
- Maximum available gain (*see* Power gain)
- Maximum available noise power, 140
- Maximum frequency of oscillation (f_{\max}), 32–35
- Maximum power gain (*see* Power gain)
- Maximum stable gain, 114
- MESFET, 34
- Metal oxide semiconductor field-effect transistor (*see* MOSFET)
- Metal semiconductor field-effect transistor (*see* MESFET)
- Microstrip:
 - attenuation, 72–73
 - capacitance, 68
 - characteristic impedance, 68–69
 - definition, 67
 - dispersion, 71–72
 - effective dielectric, 68
 - effective width, 71
 - field configuration, 67
 - geometry, 67
 - losses, 72–73
 - matching network design, 74–80, 116–19 (*see also* Matching)
 - phase velocity, 68
 - quality factor, 73–74
 - radiation factor, 74
 - wavelength, 68–70
- Microwave amplifier:
 - block diagram, 55
 - schematic, 78–80
 - signal flow graph, 83
- Microwave transistor:
 - BJT, 31–33
 - characteristics, 31–36
 - GaAs FET, 34–36
- Minimum noise figure (*see* Noise)
- MOSFET, 34
- Negative feedback, 102, 155, 160–66**
- Negative resistance, 48–49
- Negative resistance oscillators (*see* Oscillators)
- Nepers, 5
- Noise:
 - bandwidth, 140
 - extrinsic, 36
 - figure, 141–44, 151–54
 - figure circles, 142–47
 - figure parameters, 143
 - intervalley, 36
 - intrinsic, 36
 - Johnson, 140
 - measurement, 143
 - minimum, 141–54
 - parameters, 143, 145, 148, 152
 - power, 140, 175
 - resistance, 142
 - resistor, 140
 - shot, 34
 - temperature, 140
 - thermal, 140, 175
 - two-stage amplifier, 141–42
 - voltage, 140
 - white, 140
- Normalizing impedance, 15–22
 - admittance, 46
 - resistance, 15, 22
- n -port network, 19–22
- n -way amplifier, 182–84
- n -way hybrid combiner/divider, 182–84
- Open-circuited line, 8**
 - shunt stub, 75, 78, 116–19, 148, 185
- Operating point (*see* dc bias)
- Operating power gain (*see* Power gain)
 - circles (*see* Constant-gain circles)
- Optimization, 217–28
- Optimum:
 - noise figure, 142
 - terminations, 103, 105
- Oscillation conditions, 195–96
- Oscillators:
 - BJT, 210, 213
 - Clapps, 209
 - Colpitts, 209
 - configurations, 208–14
 - design procedure, 200
 - GaAs FET, 210–13
 - Hartley, 209
 - large-signal measurements, 203–9
 - maximum power, 197–98
 - negative resistance, 194–208, 210
 - one-port, 194–99
 - reverse channel, 200, 210–12
 - terminating network, 199–203
 - two-port, 199–203
 - varactor tuned, 213–14
 - YIG tuned, 212–13
- Outgoing wave, 5
- Output reflection coefficient (*see* Reflection coefficient)
- Output stability circle, 96, 124–25
- Packaged, 23, 27–28**
- Packaged capacitance, 27
- inductance, 27

- Paralleling, 180–81
- Parameters conversions, 23–26
- Parasitics, 32
- Phase velocity, 5, 7
- Phasor, 4
- Potentially unstable:
 - bilateral, 118–19, 123–25
 - unilateral, 106–10
- Power amplifier, 174–86
- Power combiners and dividers:
 - hybrid, 181–82
 - n -way, 182–84
 - Wilkinson, 181–83
- Power delivered to the load, 16–17, 85–86, 92
- Power gain:
 - available, 92, 123
 - maximum available, 32, 121, 141
 - maximum operating, 120–21
 - maximum stable, 114
 - maximum transducer, 114, 121
 - maximum unilateral transducer, 94, 106
 - operating, 92, 119–21
 - transducer, 17, 22, 32, 86, 114
 - unilateral transducer, 93–94, 102
- Propagation constant, 5
- Q**, 168–69, 171
- Quarter-wave transformer, 8, 78, 147, 185
- Quasi-TEM, 67–68, 71
- Quiescent point, 130–33
- Radiation factor**, 74
- Radio frequency choke (RFC), 129–30
- Reference:
 - impedance (*see* Normalizing impedance)
 - plane, 12–13
 - resistance (*see* Normalizing resistance)
- Reflected:
 - power, 16–17, 21
 - voltage, 14
 - wave, 5–6, 9–10, 14, 20
- Reflection coefficient:
 - definition, 5, 9
 - input, 10, 22, 84–85
 - load, 5, 9
 - noise, 142–44, 188
 - output, 10, 85
 - plane, 43
 - power, 176–77, 187
 - simultaneous conjugate match, 112–14
 - transmission line, 5–6, 8
 - two-stage design, 187–88
- Resonance line width, 213
- Reverse channel, 200, 210–12
- definitions, 10, 16–18
- generalized, 19–22
- indefinite, 29
- large-signal, 174–78
- matrix, 8, 10, 23
- measurement, 10–11
- n -port, 20
- properties, 13–18
- transistors, 23, 26–31
- Scattering transfer parameters (*see* Chain scattering parameters)
- Schottky, 34, 213
- Shifting reference planes, 12–13
- Short-circuit current gain (*see* h_{FE})
- Short-circuited line, 8
 - shunt stub, 75–78, 147–48
- Shot noise, 34
- Signal flow graphs:
 - applications, 84–87
 - branch, 80–81
 - generator, 81–82
 - input reflection coefficient, 84–85
 - load, 82–83
 - loops, 84
 - microwave amplifier, 83
 - output reflection coefficient, 85
 - path, 83
 - theory, 80–87
 - two-port, 81
- Simultaneous conjugate match, 112–14
- Smith chart:
 - admittance or Y chart, 45–47
 - compressed, 48
 - design, 55–66
 - gain circles (*see* Constant-gain circles)
 - impedance calculation, 49–51
 - impedance or Z chart, 45–47
 - negative resistance, 48–49
 - network characteristics, 53–54
 - normalized impedance and admittance or ZY chart, 51–54, 55–66
 - theory, 43–51
- Stability:
 - analysis, 95–100, 164–65
 - circles, 96–98, 101, 124–25, 201
 - conditions, 98–100
 - potentially unstable, 95–96, 99–100
 - unconditionally stable, 95–100
- Stability factors, 127
- Standard temperature, 140
- Standing wave ratio (*see* VSWR)
- Strip conductor, 67
- Stub (*see* Short- or open-circuited line)
- Substrate, 67
- SUPER-COMPACT, 222–28
- TEM mode**, 67
- Terminating matching network, 199–203
- Thermal noise, 34
- Thévenin, 16–17, 20
- Scattering matrix, 8, 10, 23
- Scattering parameters:
 - conversions, 24–25

Index

- Third-order intercept point, 178–79
- Three-port, 29, 31
- Transconductance, 163
- Transducer cutoff frequency, 28
- Transducer power gain, 17, 22, 32, 86 (*see also* Constant-gain circles)
- Transfer or *T* parameters (*see* Chain scattering parameters)
- Transmission coefficient:
 - forward, 10, 17, 28
 - reverse, 10, 28
- Transmission line, 4–8
 - input impedance, 6–7, 49–50
 - lossless, 7, 13–14
 - matched, 8
 - open-circuited, 8
 - quarter-wave, 8
 - short-circuited, 8
 - uniform, 5, 36
- Traveling waves, 4–7, 9, 13
- Tuning factor, 170
- Two-port network:
 - cascade, 11
 - noise, 140–42
 - parameters conversions, 22–25
 - representations, 1–4, 9, 13
- Two-stage amplifier:
 - design, 187–88
 - high-gain, 187
 - high-power, 187
 - low-noise, 188
- UM-MAAD, 230–40
- Unconditionally stable:
 - bilateral, 114–23
 - conditions, 98–100
 - unilateral, 103–6
- Unilateral figure of merit, 111–12
- Unilateral transducer power gain (*see* Power gain)
- Unit diagonal matrix, 23
- Unstable two-port (*see* Stability)
- Varactor diode, 213–14
- Voltage gain, 87
- Voltage standing-wave ratio (*see* VSWR)
- VSWR, 7–8, 50–51
- Wavelength:
 - free space, 68
 - microstrip, 68
- Wilkinson's coupler, 181–83
- y* parameters (*see* Admittance parameters)
- YIG sphere, 212–13
- z* parameters (*see* Impedance parameters)